

**Dismounted Pelvic Blast Injury:
Mechanisms of Injury, Associated Injuries and
Mitigation Strategies**

Iain Alexander Rankin

Dissertation submitted in fulfilment of the requirements for the degree of:

Doctor of Philosophy

Department of Bioengineering, Imperial College London

February 2021

Declaration of Originality

The work presented within this thesis is my own and all else is appropriately referenced.

Copyright Declaration

The copyright of this thesis rests with the author and is made available under a Creative Commons Attribution Non-Commercial No Derivatives Licence. Researchers are free to copy, distribute or transmit the contents of the thesis on the condition that they attribute it, that they do not use it for commercial purposes, and that they do not alter, transform, or build upon it. For any reuse or redistribution, researchers must make clear to the others the licence terms of this work.

Acknowledgements

The research to follow within this thesis would not have been possible without the help and support of a number of people, to whom I would like to express my gratitude.

First and foremost, I would like to thank my supervisors, Dr Spyros Masouros and Professor Jon Clasper, for their support and guidance over the past three years. I thank them for the opportunity they gave me to explore the world of bioengineering. Without their continuous support and enthusiasm for this project, I would never have achieved what I have been able to do. I will always be indebted to their guidance, support, and encouragement.

I would like to give a special thanks to Dr Thuy-Tien Nguyen for her assistance and friendship throughout this research; her engineering knowledge and skills have proved invaluable. I would also like to thank my other academic colleagues and friends, both fellow PhD students and post docs, whose thoughts and discussions have helped guide this work. Thanks to Dr Dilen Carpanen, Dr Louise McMenemy, Dr Sarah Stewart, Dr Alastair Darwood, and Dr Kirstie Edwards.

I am exceptionally grateful to my parents, Fiona and Robin, whose continuous, unwavering, and unconditional support has helped me at every stage of my career, both before and during the research of this PhD. I would like to thank them for always being there, for helping guide me through any challenges I have faced, and for always listening; they are my role models as parents and I hope to one day match their support to my future children.

Finally, I would like to thank my wife, Georgie, to whom this thesis is dedicated. Her support, kindness, and determination to help me achieve, through (perhaps feigned) excitement and enthusiasm for my work, discussing my ideas and encouraging me to always give it my all, has helped me strive to make this research the best it could be. Thank you.

Abstract

Explosive blast has been the most common cause of wounding and death in recent military conflicts. Where blast resulted in injury to the pelvis of an on-foot casualty, the mortality rate was high. The mechanism of injury by which this occurs is not known. The research presented in this thesis sought to understand the pattern and mechanism of this devastating injury, in order to develop protective strategies.

An analysis was performed of battlefield data which identified pelvic vascular injury as the cause of death in these casualties. Furthermore, it showed displaced pelvic fractures, perineal wounding, and traumatic amputation to be associated with this lethal injury.

Hypothesised mechanisms of injury were investigated using cadaveric animal models of blast. These investigations showed rapid outward movement of the lower limbs ('limb flail'), caused by the blast wave, to be necessary for displaced pelvic fractures with vascular injury to occur. High velocity sand ejecta, as propagated by blast ('sand blast'), showed correlation with increasing velocity and injury patterns of worsening severity across the trauma range. This included the associated injuries of perineal wounding and traumatic amputation. Following this research, lower limb flail and high velocity sand blast were identified as the mechanisms of injury of blast to the pelvis.

Novel pelvic protective equipment was developed to limit lower limb flail in a cadaveric animal model of blast. This resulted in a reduction of pelvic fractures and elimination of pelvic vascular injury. Protective silk shorts were subsequently examined in a human cadaveric model and shown to markedly reduce the severity of injury from high velocity sand blast.

Implementation of the protective strategies described in this thesis is suggested to reduce the severe injury burden and mortality rate associated with blast injury to the pelvis.

Awards, Publications and Presentations

Awards

US Department of Defense Research Highlight:

Selected by the US Department of Defense Blast Injury Research Program

Coordinating Office as the highlight publication of the month (August 2020) for

'significant research in the area of blast injury prevention, mitigation, and treatment.'

https://blastinjuryresearch.amedd.army.mil/index.cfm/news_and_highlights/research_highlights/FY20/pelvic_injuries

Publications

Rankin IA, Nguyen T-T, Carpanen D, Darwood A, Clasper JC, Masouros SD. Pelvic Protection Limiting Lower Limb Flail Reduces Mortality. *J Biomech Eng.* 2020;20(1156). doi:10.1115/1.4048078. PMID: 32793978

Rankin IA, Nguyen T-T, Carpanen D, Clasper JC, Masouros SD. A New Understanding of the Mechanism of Injury to the Pelvis and Lower Limbs in Blast. *Front Bioeng Biotechnol.* 2020;8:960. doi:10.3389/fbioe.2020.00960. PMCID: PMC7438440

Rankin IA, Webster CE, Gibb I, Clasper JC, Masouros SD. Pelvic injury patterns in blast: morbidity and mortality. *J Trauma Acute Care Surg.* 2020;88(6):832-838. doi:10.1097/ta.0000000000002659. PMID: 32176176

Rankin IA, Ramasamy A, Cooper J. Blast injuries to the pelvis: essential lessons learned. *Journal of Trauma and Orthopaedics*. 2019;7(4):52-54

Rankin IA, Nguyen TT, Carpanen D, Clasper JC, Masouros SD. Restricting Lower Limb Flail is Key to Preventing Fatal Pelvic Blast Injury. *Ann. Biomed. Eng.* 1–9 (2019). doi: 10.1007/s10439-019-02296-z. PMID 31147806

Presentations

Rankin IA, Pelvic Protection Limiting Lower Limb Flail Reduces Mortality. Society of Military Orthopaedic Surgeons 62nd Annual Meeting December 2020

Rankin IA, High-Velocity Sand Blast is a Significant Injury Mechanism Implicated in Blast Trauma. Society of Military Orthopaedic Surgeons 62nd Annual Meeting December 2020

Rankin IA, Tier 1 Pelvic Protective Equipment Reduces Injury from High Velocity Sand Blast. Society of Military Orthopaedic Surgeons 62nd Annual Meeting December 2020

Rankin IA, Reinforced Pelvic Protection Mitigates the Effects of Dismounted Pelvic Blast Injury. Military Health System Research Symposium August 2019

Rankin IA, Restricting Lower Limb Flail is Key to Preventing Fatal Pelvic Blast Injury. Military Health System Research Symposium August 2019, Blast Injury Conference July 2019, Combined Services Orthopaedic Symposium May 2019

Rankin IA, Dismounted Pelvic Blast Injury. Blast Injury Conference November 2018

Contents

Chapter 1	Introduction.....	22
1.1	Scope of the chapter	22
1.2	Introduction	23
1.3	Aims	25
1.4	Thesis structure	25
Chapter 2	Blast Injury and the Pelvis.....	28
2.1	Scope of the chapter	28
2.2	Explosive devices in modern warfare	29
2.2.1	Blast physics	30
2.2.2	Mechanisms of blast injury	33
2.3	Pelvic anatomy	36
2.4	Pelvic injury classifications.....	40
2.4.1	Civilian pelvic injury classification systems.....	40
2.4.2	Military pelvic fracture classification systems	44
2.5	Military pelvic fracture patterns of injury	45
2.6	Conclusion.....	47
Chapter 3	Dismounted Pelvic Blast Injury: Battlefield Data.....	49
3.1	Scope of the chapter	49
3.2	Dismounted blast injury	50
3.3	Dismounted Pelvic Blast injury: morbidity and mortality	51
3.3.1	Results.....	57
3.3.2	Discussion	64
3.3.3	Conclusion	68
3.4	Chapter conclusion.....	68
Chapter 4	Dismounted Pelvic Blast Injury: Management and Mitigation.....	69
4.1	Scope of the chapter	69

4.2	Management of the pelvic blast injury casualty	70
4.2.1	Initial resuscitation and haemorrhage control	70
4.2.2	Orthopaedic injuries	72
4.2.3	Associated injuries	75
4.3	Mitigation strategies	77
4.4	Hypothesised mechanisms of injury	81
4.4.1	Axial load hypothesis	81
4.4.2	Flail Mechanism hypothesis	82
4.4.3	Sand Blast Hypothesis	84
4.5	Conclusion	84
Chapter 5 Dismounted Pelvic Blast Injury: Experimental Platforms and Models		85
5.1	Scope of the chapter	85
5.2	Platforms to investigate blast injury	86
5.2.1	Shock Tube	86
5.2.2	Gas Gun	89
5.2.3	Free-field blast testing	92
5.2.4	Solid-blast injury platforms	93
5.2.5	Miscellaneous	95
5.2.6	Computational modelling	95
5.2.7	Experimental platforms conclusion	96
5.3	Animal models	97
5.3.1	The small animal quadruped pelvis	100
5.4	Injury risk evaluation	104
5.4.1	Scaling of animal models	106
5.5	Chapter Conclusion	107
Chapter 6 Mechanisms of injury: Lower Limb Flail in the Mouse Model		108
6.1	Scope of the chapter	108
6.2	Introduction	109
6.3	Methods	110

6.4	Results	116
6.5	Discussion	122
6.6	Conclusion.....	128
Chapter 7 Mechanisms of Injury: High Velocity Sand Blast.....		130
7.1	Scope of the chapter	130
7.2	Introduction	131
7.3	Methods.....	133
7.4	Results	141
7.5	Discussion	147
7.6	Conclusion.....	154
Chapter 8 Mitigation Strategies: Pelvic Personal Protective Equipment.....		155
8.1	Scope of the chapter	155
8.2	Introduction	156
8.3	Methods.....	157
8.4	Results	163
8.5	Discussion	168
8.6	Conclusion.....	177
Chapter 9 The Mechanism of Injury of Traumatic Amputation		178
9.1	Scope of the chapter	178
9.2	Introduction	179
9.3	Methods.....	182
9.4	Results	188
9.5	Discussion	194
9.6	Conclusion.....	199
Chapter 10 Mitigation of High-Velocity Sand Blast		200
10.1	Scope of the chapter	200
10.2	Introduction	201
10.3	Methods.....	203

10.4	Results	209
10.5	Discussion	213
10.6	Conclusion.....	215
Chapter 11	Summary, Future Research and Conclusions	217
11.1	Scope of the chapter	217
11.2	Thesis Summary.....	218
11.3	Future Research.....	221
11.4	Conclusion.....	224
Bibliography	225

List of Figures

Figure 1: Intra-operative photograph showing a pelvic blast injury. The soldier sustained bilateral traumatic proximal femoral amputations in addition to his pelvic injuries. (Ramasamy <i>et al.</i> , 2012, figure reproduced with permission).....	24
Figure 2: Friedlander wave form in a simple free field explosion (Edwards and Clasper, 2016, figure reproduced with permission)	31
Figure 3: Pressure wave form of (a) a simple free field explosion and (b) a semi-confined blast (Edwards and Clasper, 2016, figure reproduced with permission)	32
Figure 4: Morbidity and mortality as a function of distance from explosive (Champion <i>et al.</i> , 2009, figure reproduced with permission)	34
Figure 5: The bony pelvis (Gray, 1918).....	36
Figure 6: The pubic symphysis (Gray, 1918).....	37
Figure 7: Pelvic ligamentous structures (Gray, 1918)	38
Figure 8: Pelvic arterial vasculature (Gray, 1918)	39
Figure 9: AO/OTA Classification (AO Foundaton, 2018, figure reproduced with open access)	41
Figure 10: Tile classification. (Milenković and Mitković, 2020, figure reproduced with open access).....	42
Figure 11: Young-Burgess Classification (Alton and Gee, 2014, figure reproduced with permission).....	43
Figure 12: Differences in incidence of injury patterns in the mounted and dismounted casualty (Singleton <i>et al.</i> , 2013, figure reproduced with permission)	46
Figure 13: Quantifying pelvic disruption on CT. (a, top) superior-inferior, (b, middle) anterior-posterior, and (c, bottom) lateral.	55

Figure 14: ROC curve analysis for lateral displacement distance of the sacroiliac joints as predictive of pelvic vascular injury (AUROC 0.73, 95% CI 0.63 – 0.83, $p < 0.001$). 62

Figure 15: ROC curve analysis for lateral displacement distance of the sacroiliac joints as predictive of mortality (AUROC 0.70 (95% CI 0.59 – 0.80, $p < 0.01$). 63

Figure 16: Tier 1 pelvic protection (left) (Lewis *et al.*, 2013) and Tier 2 (right) (Saunders and Carr 2018) (Figures reproduced with permission)..... 78

Figure 17: Tier 3 pelvic protection being worn over combat trousers (Lewis *et al.*, 2013, figure reproduced with permission) 79

Figure 18: (a, top) Schematic of the Imperial College London shock tube, with adaptors for use with cell, tissue, or small animal research. (b, bottom) Examples of different blast wave pressure profiles with varying peak pressure, duration and impulse (Nguyen *et al.*, 2018, figure reproduced with permission). 88

Figure 19: Schematic of the Imperial College London gas gun, with sabot adapted for delivery of a small, metallic fragment simulating projectile (FSP) (Nguyen *et al.*, 2018, figure reproduced with permission)..... 91

Figure 20: Aerial photograph of 5000 kg trinitrotoluene (TNT) detonated to investigate blast effects (TNO Defence Security and Safety, 2020, figure reproduced with permission). 92

Figure 21: (a, left) Schematic of Imperial College London drop tower. (b, right) Typical force-time response curve (Nguyen *et al.*, 2018, figure reproduced with permission). 93

Figure 22: Schematic of an under-body blast simulator. (Bailey, Christopher, *et al.*, 2015, figure reproduced with permission). 94

Figure 23: Comparative anatomy of the human and chimpanzee pelvis. Adapted from (Gruss and Schmitt, 2015, figure reproduced with permission) 99

Figure 24: Radiograph of a mouse pelvis and lower limbs. 101

Figure 25: Dissection of the pelvic arterial vasculature and medial-superficial hindlimb of a mouse specimen, with arteries dilated and fixed with red coloured resin. (1) aorta, (2) common iliac arteries, (3) internal iliac artery, (4) external iliac artery, (5) femoral artery. (Adapted from Kochi *et al.*, 2013, figure reproduced with permission)..... 103

Figure 26: Example of an injury-risk curve. (Adapted from Yoganandan *et al.*, 2016, figure reproduced with permission)..... 104

Figure 27: (a, left) shock tube with mounting platform, fenestrated steel fence restricting lower limb flail, and position of mouse (represented with model). (b, right): aerial view with restriction of lower limb flail to 45° group, demonstrating the angle as measured from the midsagittal plane. 111

Figure 28: Three repeat blast wave characterisation tests, delivering a maximum peak pressure of 4.28 bar, mean plateau pressure of 1.72 bar, and shock impulse of 24 bar milliseconds. 117

Figure 29: Vascular injury-risk curve as a function of maximum allowable angle of lower limb flail..... 121

Figure 30: (a, left): Lower limb amputated mouse with pubic symphysis disruption, pubic rami fractures and left sided sacroiliac joint disruption. (b, right): 135° lower limb flail mouse with pubic symphysis disruption, pubic rami fractures and bilateral sacroiliac joint disruption. 123

Figure 31: Experimental sand sizes used, scaled to human values, shown alongside ideally distributed particle sizes. *a* = human median value. *b* = human 85th centile. *a* = lower limit of experimental sand range. *b* = upper limit of experimental sand range. % pass (combined) describes the percentage of total volume of sand passing a specific sieve size; sieve size (mm) relates to the diameter of each hole within the sieve. 134

Figure 32: Gas gun with under-body sand blast mounting platform, fenestrated steel fences and mouse. Mouse represented with model. 137

Figure 33 (a, top) Aerial view of schematic illustrating initial sand stream passing through offset fenestrated steel fences, causing dispersion of the sand prior to impact with the specimen. (b, bottom) Oblique view of schematic illustrating initial sand stream passing through offset fenestrated steel fences, causing dispersion of the sand prior to impact with the specimen 138

Figure 34: Photographs showing (a, top) the initial sand stream exiting the gas gun (1.), passing through the dispersion fence to be converted into multiple streams (2.), followed by (b, bottom) dispersion into a widely distributed spread of high velocity sand (3.). Arrow annotation represents the direction of travel of the sand after exiting the gas gun. 139

Figure 35: Left: pre-test, uninjured mouse. Right: mouse injured with sand blast at 252 m/s sustaining pelvic fractures with (A) sacroiliac joint disruption and (B) pubic rami fractures, (C) abdominal injury with free air in the abdomen, perineal injury, and (D) an open tibial fracture with surrounding extensive soft tissue loss. The increased density on mouse on the right represents sand debris. 142

Figure 36: Injury-risk curves for (a) perineum injury, (b) lower limb degloving, (c) abdominal injury, (d) traumatic amputation, and (e) pelvic fracture as a function of average sand velocity; 95% CI is represented with dashed lines. 145

Figure 37: Bar chart displaying the v_{25} , v_{50} and v_{75} for each type of injury; 95% CI is represented with variability whiskers. 146

Figure 38: The mechanism of injury of dismounted pelvic blast. (a) Casualty stands on an IED which detonates, causing the initial blast wave to compress the surrounding soil. (b) Sand is ejected at high velocity towards the casualty, causing soft tissue degloving and skeletal disruption. (c) The casualty is impacted by the blast wind, resulting in lower limb

flail with separation of the pubic symphysis. (d) The blast wind completes the amputation at the level of the initial disruption, whilst continued leg flail results in opening of the sacroiliac joint and vascular injury..... 151

Figure 39: (a, top) upright mice with pelvic protection worn at the level of the greater trochanters (left), anterior superior iliac spines (middle), or no protection (right). (b, bottom) supine mice with pelvic protection worn at the level of the greater trochanters (left), or no protection (right). Mouse represented with model..... 158

Figure 40: (a, left) shock tube with front-on blast mounting platform and mouse. (b, right) shock tube with under-body blast mounting platform and mouse. Mouse represented with model..... 161

Figure 41: (a) dissection of a mouse with uninjured arterial tree: (A.) aorta, (B.) common iliac artery, (C.) external iliac artery, (D.) internal iliac artery. (b) dissection of a mouse with common iliac vascular injury: (A.) aorta, (B.) transected common iliac artery, (C.) external iliac artery, (D.) internal iliac artery. (c) dissection of a mouse with internal iliac vascular injury: (A.) aorta, (B.) common iliac artery, (C.) external iliac artery, (D.) transected internal iliac artery. (d) Dissection of a mouse with external iliac vascular injury: (A.) aorta, (B.) common iliac artery, (C.) transected external iliac artery, (D.) internal iliac artery..... 166

Figure 42: Histology at 40x magnification showing arterial tissue (sample excised from external iliac artery). 167

Figure 43: (Left) pre-blast radiograph of unprotected mouse. (Right) post-blast radiograph of unprotected mouse, showing (A.) displaced sacroiliac joint disruption with (B.) displaced pubic rami fractures. 169

Figure 44: (Left) pre-blast radiograph of a mouse with pelvic protection worn at the level of the ASIS. (Right) post-blast radiograph of a mouse with pelvic protection worn at the level of

the ASIS, showing (A.) minimally displaced sacroiliac joint disruption with (B.) displaced pubic rami fractures. 170

Figure 45: (Left) pre-blast radiograph of a mouse with pelvic protection worn at the level of the greater trochanters. (Right) post-blast radiograph of a mouse with pelvic protection worn at the level of the greater trochanters, showing (A.) an uninjured pelvis with (B.) bilateral lower limb traumatic amputations 171

Figure 46: A buried explosive is detonated, with the resultant shockwave compressing the surrounding sandy gravel soil. Immediately following this, gas from the explosion is released at high velocity and acts to eject this compressed soil at supersonic speeds. The soil is carried upwards from the ground by the gas flow to project, dependent upon the soil's characteristics, at an angle of between 45 and 120 degrees, in a cone shape. Image adapted from Ramasamy *et al.*, 2009..... 181

Figure 47: Experimental sandy gravel sizes used, scaled to human values, shown alongside ideally distributed particle sizes. A. = human median value. B. = human 85th centile. A = lower limit of experimental sandy gravel range. B = upper limit of experimental sandy gravel range. % pass (combined) describes the percentage of total volume of sandy gravel passing a specific sieve size; sieve size (mm) relates to the diameter of each hole within the sieve. ... 184

Figure 48: (a, top) schematic illustrating the experimental setup showing the gas-gun outlet with mounting platform and mouse. (b, bottom) aerial view of schematic illustrating initial sandy gravel stream passing through distal outlet to impact with offset lower limb of mouse. Mouse represented with model. 186

Figure 49: Mouse injured with high velocity sand blast, sustaining a right sided lower limb traumatic amputation 189

Figure 50: Images illustrating the stages of traumatic amputation secondary to high velocity sand blast. (a) Immediately pre-impact. (b) Point of initial impact. The sandy gravel has

begun to move through and around the tissues of the lower limb at high velocity. Due to the experimental setup the foot has evaded the trajectory of the sandy gravel, whilst the limb above has begun to fragment and displace relative to the foot below. (c) The foot has been pulled upward into the trajectory of the sandy gravel, whilst the skeletal and soft tissues above are now significantly fragmented and displaced. (d) The lower limb has now been entirely displaced, with soft tissue stripping on the periphery of the blast now evident as the muscle is seen moving outwards. (e) As the sand blast dissipates, the remaining surrounding soft tissues can be seen more clearly to be stripped and displaced. (f) Completed traumatic amputation..... 190

Figure 51: Four separate injuries of worsening severity sustained following impact with high velocity sand blast. (a) burst lacerations and skin tears seen at I. (b) involvement of the underlying subcutaneous and muscular layers, with muscle tears and stripping seen at II. (c) associated open segmental femoral fracture seen at III, with extensive surrounding soft tissue damage and loss. (d) Complete limb avulsion with traumatic amputation seen at IV. 191

Figure 52: Traumatic amputation risk curves as a function of average sandy gravel velocity. (a) 0.1 – 0.3 mm dry sandy gravel. (b) 0.1 – 0.3 mm wet sandy gravel. (c) 0.5 – 1.0 mm dry sandy gravel. (d) 0.5 – 0.1 mm wet sandy gravel. (e) combined (ideally distributed) dry sandy gravel. (f) combined (ideally distributed) wet sandy gravel. 95% CI represented with dashed lines..... 193

Figure 53: Tier 1 pelvic personal protective equipment. (Lewis et al., 2013, figure reproduced with permission).....202

Figure 54: Experimental setup showing cadaveric thigh with issue combat trousers (represented by model) positioned within target chamber. Top, oblique view. Bottom, aerial view. A: proximal thigh, B: medial thigh, C: lateral thigh, D: distal thigh, E: dispersion fence.205

Figure 55: Experimental setup showing cadaveric thigh with issue combat trousers prior to (top) and during (bottom) impact with high velocity sand. A: proximal thigh, B: medial thigh, C: lateral thigh, D: distal thigh, E: dispersion fence, F: high-velocity sand blast207

Figure 56: Tier 1 pelvic personal protective equipment worn on cadaveric thigh; post-impact delivered to region of two-layer high-performance knitted silk protection.....208

Figure 57: Exemplar damage sustained by issue combat trousers (left) and PPE (right) following impact with high-velocity sand211

Figure 58: Exemplar wounds sustained by control group following impact with high-velocity sand212

Figure 59: Exemplar wounds sustained by PPE group following impact with high-velocity sand212

Figure 60: A soldier wearing Tier 2 pelvic protective equipment modified to include the suggested position of the pelvic protective binder, as worn at the level of the greater trochanters. (Adapted from Lewis *et al.*, 2013, figure reproduced with permission).....222

List of Tables

Table 1: Collected UK JTTR data. For continuous variables, median value with range given in parenthesis.	58
Table 2: Logistic regression for documented injury patterns to mortality (top) and pelvic vascular injury (bottom). Significant P values (significance set at $p < 0.05$) and the associated odds ratios are highlighted in bold. B: the coefficient for the constant. S.E.: the standard error around the coefficient for the constant. Wald: the Wald chi-square test, that tests the null hypothesis that the constant equals 0. Df: the degrees of freedom for the Wald chi-square test.	60
Table 3: Type of pelvic fractures according to Tile criteria across all mice groups.	119
Table 4: Incidence and location of vascular injury across main cohort. Results presented as numerical value (%). ^a Bilateral injuries.	120
Table 5: Types of injuries sustained across all mice. ^a Excluding control specimen.	143
Table 6: Pelvic fracture patterns sustained.....	143
Table 7: The 25%, 50% and 75% risks of injury (v_{25} , v_{50} and v_{75} respectively) for each type of injury (95% CI in parenthesis).....	146
Table 8: Incidence and relative risk of pelvic fracture and vascular injury across all groups. RR, relative risk. CI, confidence intervals. GT, greater trochanters. ASIS, anterior superior iliac spines. UB, under-body. * $p < 0.05$. **injury not present ($p < 0.001$). ^a Redundant term.	164
Table 9: Classification of pelvic fractures according to Tile criteria and location of most proximal vascular injury across all groups. GT, greater trochanters. ASIS, anterior superior iliac spines. UB, under-body. ^a bilateral injuries. * $p < 0.05$	165
Table 10: Two sample Kolmogorov-Smirnov test to assess for significant differences between the distribution of injury-risk curves. P values shown.....	192

Table 11: The velocities (m/s) at 25%, 50% and 75% risk of injury (v_{25} , v_{50} and v_{75} respectively) for traumatic amputation across all group. 95% confidence intervals (CI) in parenthesis.....	194
Table 12: Number, surface area and depth of injuries sustained. *Deep to subcutaneous tissues involving underlying fascial and muscular layers.....	210

Chapter 1

Introduction

1.1 Scope of the chapter

This chapter provides context to the research that follows in this thesis. After introducing the global burden of blast injury, the clinical problem investigated within this thesis is highlighted and the research aims defined. The chapter finishes by providing the thesis structure and chapter synopses.

1.2 Introduction

The recent military conflicts in Iraq and Afghanistan have seen blast injury as the leading mechanism of wounding and death, with the Improvised Explosive Device (IED) as the weapon of choice (Russell *et al.*, 2014). An IED is capable of causing multiple severely injured casualties with a single blast event, and these weapons have posed a substantial threat to Coalition troops. In the civilian setting, the use of IEDs by terrorist organisations has increased steadily over the last 40 years, whilst landmines, cluster munitions, and other explosive remnants of war remain an ongoing threat (Edwards *et al.*, 2016).

The Coalition troop on foot patrol was noted with increased frequency over recent conflicts to sustain a pattern of blast injury consisting of traumatic amputation of at least one lower extremity (typically proximal transfemoral amputation), a severe injury to another extremity, and pelvic, abdominal or urogenital wounding (Ficke *et al.*, 2012a). This injury pattern was termed the dismounted (on foot) complex blast injury (DCBI) and has been described as one of the most challenging patterns of injury to emerge from the wars in Iraq and Afghanistan (Cannon *et al.*, 2016). One of the leading risk factors for increased mortality in this pattern of injury is that of pelvic injury (Figure 1); the mortality of casualties that sustained a blast related traumatic amputation was seen to rise from 22.9% to 60.8% when an associated pelvic fracture was present (Webster *et al.*, 2018).

Advances in prehospital intervention, rapid evacuation protocols, and medical and surgical management have improved the survivability of battlefield injuries from 69.7% in World War II to 88.6% in Iraq (Mazurek and Ficke, 2006). Following a review of the recent deaths of UK military service personnel from 2002 - 2013, the Mortality Peer Review Panel considered 91% non-survivable (Russell *et al.*, 2014). As such, future research strategies should focus on mitigation as opposed to treatment of injury to improve outcomes.

The mechanism of injury, cause of death, and contribution of associated injuries to the mortality of the dismounted pelvic blast injury casualty are not known. The research presented within this thesis aims to address these gaps in knowledge, to provide information of use to the clinician and researcher, and fundamentally to drive innovation towards the development of protective and mitigative strategies for the dismounted pelvic blast injury casualty.

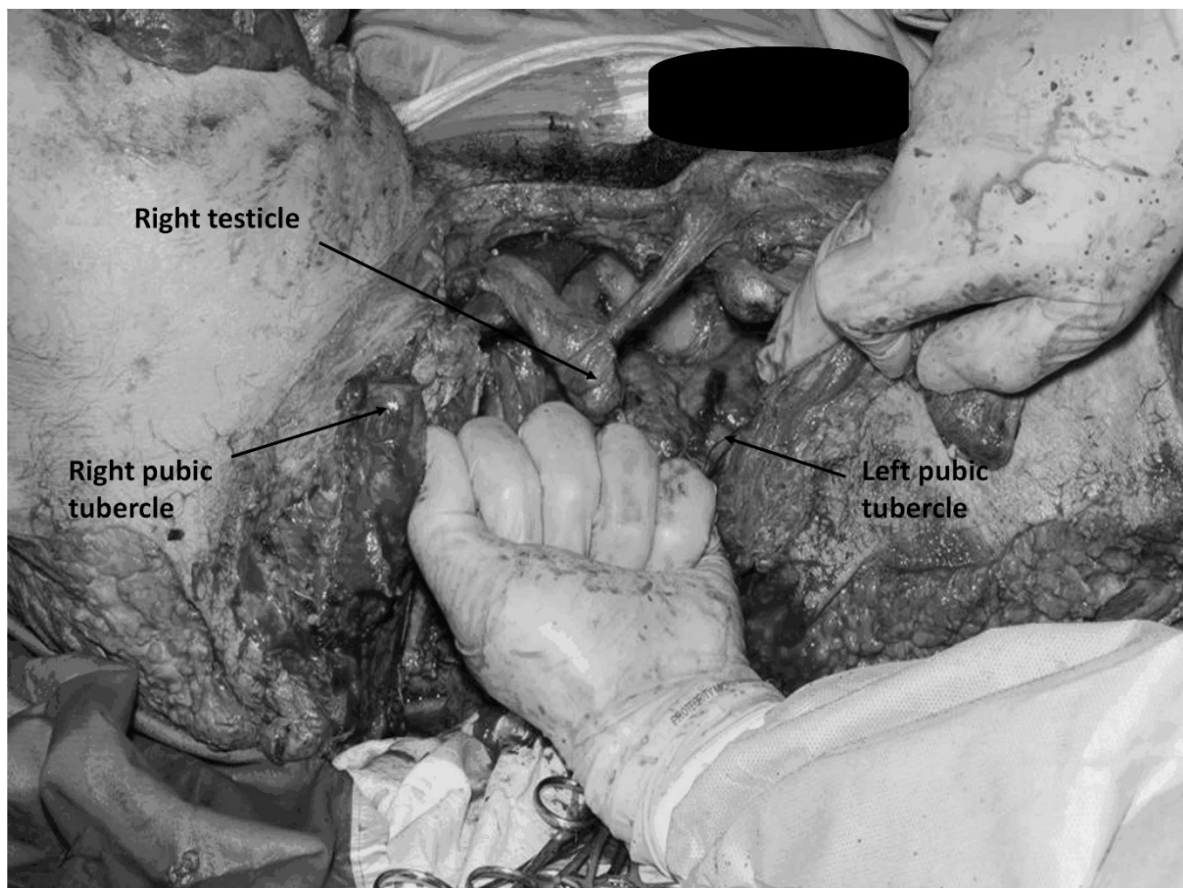


Figure 1: Intra-operative photograph showing a pelvic blast injury. The soldier sustained bilateral traumatic proximal femoral amputations in addition to his pelvic injuries. (Ramasamy *et al.*, 2012, figure reproduced with permission)

1.3 Aims

The aims of the research presented in this thesis are:

- 1) Identify the causes of death of the dismounted pelvic blast injury casualty
- 2) Assess the contribution of associated injuries to this injury pattern and overall mortality
- 3) Review current management and mitigation strategies of dismounted pelvic blast injury
- 4) Understand and describe the mechanism of injury of dismounted pelvic blast
- 5) Propose mitigation strategies based on the findings of this research

1.4 Thesis structure

Chapter 1 has provided a brief introduction and context to the research, highlighted the clinical problem, and defined the research aims.

Chapter 2 reviews blast injury and the pelvis, first discussing explosive devices in modern warfare, the mechanisms of blast injury in general, and normal pelvic anatomy. The chapter subsequently discusses the different patterns of pelvic injuries sustained by a civilian population, and reviews military classification systems of pelvic injury. The chapter finishes by reviewing UK military experience of pelvic blast injury in Iraq and Afghanistan. In particular, this focuses on the differences in injury patterns sustained by casualties who have developed pelvic fractures following blast from a mounted (in vehicle) environment and how these differ to the dismounted (on foot) casualty.

Chapter 3 discusses the morbidity and mortality of dismounted pelvic blast injury. This starts with an analysis of battlefield data, investigating the injury patterns, cause of death and risk factors for the pelvic blast injury casualty. The chapter discusses and identifies where future management and mitigation strategies should focus.

Chapter 4 reviews the literature and discusses current management and mitigation strategies for the dismounted pelvic blast injury casualty. This begins by reviewing current treatment options, before going on to review the literature regarding current mitigation strategies and the role they have played in limiting the injury pattern identified in the previous chapter. Hypothesised mechanisms of injury and the subsequent research direction of the thesis in dismounted pelvic blast are described.

Chapter 5 reviews and assesses the suitability of different experimental platforms and models for investigating blast injury, and the statistical methodology used in injury-risk analysis. The chapter describes the most suitable experimental platforms, model, and statistical analysis methods to investigate the hypothesised mechanisms of injury in subsequent experiments.

Chapter 6 investigates the lower limb flail hypothesis as a mechanism of injury in the dismounted pelvic blast casualty. A novel experimental setup utilising a mouse model of dismounted pelvic blast injury with a shock-tube mediated blast wave is described. Blast-mediated lower limb flail is reproduced and subsequently limited to assess its association with unstable pelvic fracture patterns and vascular injury. The findings are discussed and the association of lower limb flail to dismounted pelvic blast injury described.

Chapter 7 investigates the high velocity sand blast hypothesis as a mechanism of injury in the dismounted pelvic blast casualty. A novel experimental setup utilising a mouse model within a gas gun system delivering high velocity sand is described. High velocity sand blast is reproduced, the velocity of which is subsequently controlled to assess its association to injury. The findings are discussed and the association of high velocity sand blast to dismounted pelvic blast injury described. The chapter finishes by highlighting the key factors for which to target mitigative strategies and determines the subsequent research direction of the thesis.

Chapter 8 investigates novel pelvic personal protective equipment as a mitigation strategy in a mouse model of dismounted pelvic blast injury. The experimental setup of chapter 6 is utilised to assess this protection strategy. The findings are discussed, and proof of concept of pelvic protective equipment limiting lower limb flail is described.

Chapter 9 investigates the injury mechanism of traumatic amputation, with a view to optimise protective equipment to mitigate against this associated injury. A modified gas-gun experimental setup of that used in Chapter 7 is utilised to investigate high velocity sand blast as a mechanism of injury causing traumatic amputation. The findings are reviewed in conjunction with published literature and a novel injury mechanism of traumatic amputation is proposed.

Chapter 10 follows on from the findings of the previous chapter to investigate mitigation strategies against this proposed mechanism. The capacity of current military personal protective equipment for mitigating injury caused by high-velocity sand blast is investigated. A human cadaveric model of gas-gun mediated high-velocity sand blast is used to simulate the effect of energised environmental debris on injury to a cadaveric thigh, equipped with standard combat trousers, and quantify the reduction in wound severity by an additional under-layer of Tier 1 personal protective equipment. The findings and suitability of Tier 1 personal protective equipment to mitigate high-velocity sand blast are discussed and recommendations for future mitigation strategies are made.

Chapter 11 summarises the findings of the research performed as discussed in this thesis. This describes the critical injury patterns and cause of death of the dismounted pelvic blast injury casualty, the mechanisms of injury resulting in these injuries, and the novel protective equipment proposed to mitigate against these. Future research proposals are suggested, and this thesis on dismounted pelvic blast injury is concluded.

Chapter 2

Blast Injury and the Pelvis

2.1 Scope of the chapter

Chapter 2 reviews blast injury and the pelvis. It discusses explosive devices in modern warfare, the mechanisms of blast injury in general, and normal pelvic anatomy. The chapter subsequently moves on to discuss the different patterns of pelvic injury sustained by a civilian population, and reviews military classification systems of pelvic injury. The chapter finishes by reviewing UK military experience of pelvic blast injury in Iraq and Afghanistan; in particular, this focuses on the differences in injury patterns sustained by casualties who have developed pelvic fractures following blast from a mounted (in vehicle) environment and how these differ to the dismounted (on foot) casualty.

2.2 Explosive devices in modern warfare

The most recent military conflicts have seen blast injury as the leading mechanism of wounding and death, with the Improvised Explosive Device (IED) rising as the signature weapon of choice (Mcfate and Moreno, 2005). This has changed the nature of injuries from penetrating gunshot wounds in prior conflicts, to the extensive, heavily contaminated tissue loss associated with blast injury (Owens *et al.*, 2008). Injuries sustained from explosives are dependent upon a number of factors, including the nature of the explosive device, the environment in which the explosion occurred, the distance of the casualty from the device and any personal protective equipment (PPE) worn by the casualty.

Improvised explosive devices represent the most common threat to soldiers worldwide. They have become the weapon of choice where enemy forces do not have access to traditional weapons and so create devices from accessible materials. It is thought that their use will continue to rise, given the relative ease and low cost to manufacture and activate (Kluger *et al.*, 2004). The NATO Allied Joint Publication (AJP)-3.15(B) definition of an IED is:

“A device placed or fabricated in an improvised manner incorporating destructive, lethal, noxious, pyrotechnic or incendiary chemicals and designed to destroy, incapacitate, harass or distract. It may incorporate military stores, but is normally devised from non-military components.” (Allied Joint Doctrine, 2012)

Non-standardised and non-regulated, their use can have unpredictable effects. An IED consists of an explosive with fusing mechanism, surrounded by casing with or without added material to create a fragmentation effect (Thurman, 2017). Fragments impacting casualties may originate from a preformed source (e.g., notched casing), added material (e.g., ball bearings) or the surrounding environment (e.g., soil from a buried IED).

They are frequently termed ‘victim operated IEDs’ due to the casualty inadvertently triggering the explosive. IEDs can also be delivered by suicide bombers or initiated remotely by enemy forces. In Afghanistan, low-technology victim operated pressure-plated IEDs, command-wire IEDs, radio-controlled IEDs and suicide IEDs collectively posed a significant threat (MOD, 2016).

2.2.1 Blast physics

Explosive devices inflict injury through the formation of an explosion - the phenomenon of a rapid increase in volume and pressure that results from a sudden release of energy (Cullis, 2001). They are substances which have within themselves energy stored in the form of molecular bonds. When these bonds are broken, as initiated by a detonator, an immense quantity of energy is released. The detonator is in itself a smaller explosive with highly sensitive initiator material activated by mechanical, electrical or magnetic switch. When activated, the detonator releases a supersonic exothermic blast to the surrounding less sensitive but high energy main charge. This travels through and compresses the surrounding material, resulting in a chemical reaction in which the solid or liquid explosive is subsequently transformed into a gas with the liberation of a large amount of energy, at a near exponential rate (Stuhmiller *et al.*, 1991). This rapid chemical reaction occurs with chemical decomposition at speeds greater than the speed of sound – a process known as propagation. This reaction and release of energy is almost instantaneous. The result is a region of highly compressed and heated gas which expands to occupy a volume far greater than the original explosive: pressure at the point of the detonation is 20-30 GPa (200,000 – 300,000 atmospheric pressure) with temperatures reaching 7,000°C (Cullis, 2001). The rapid expansion of gas compresses the surrounding air which propagates supersonically away from the point of detonation. This is known as a blast wave. The blast wave consists of two parts: a shock wave of high pressure (the peak / static overpressure) and compressed gas, which travels at supersonic speed,

followed closely by a blast wind – an increase in pressure (the dynamic overpressure) and a mass movement of air, travelling at subsonic speeds.

The blast wave is defined by its pressure and direction of travel. Within an ideal free-field space, where the blast wave does not come into contact with any interference, this would propagate perpendicular to the surface of the explosive as a sphere. The pressure changes and wave characteristics of an explosion within a free-field blast are classically described by Friedlander (Friedlander, 1946) (Figure 2).

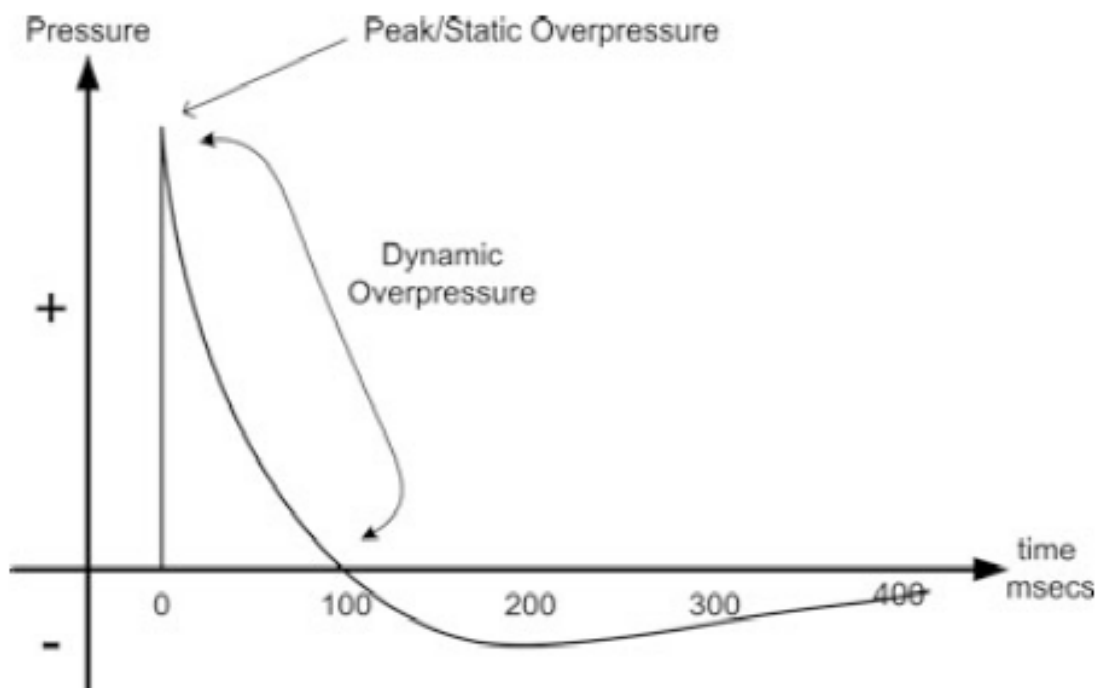


Figure 2: Friedlander wave form in a simple free field explosion (Edwards and Clasper, 2016, figure reproduced with permission)

A simple free-field explosion as described above rarely occurs in conflict. The blast wave comes under the influence of sand, water and solid objects resulting in complex wave forms

with further reflection and refraction, and varying modalities of energy transfer. Semi-confined (and enclosed) spaces generate an environment where, due to repeated reflection and refraction, large pressures are created for extended periods of time. An example of the pressure changes and wave characteristics of an explosion within a semi-confined space can be seen below (Figure 3):

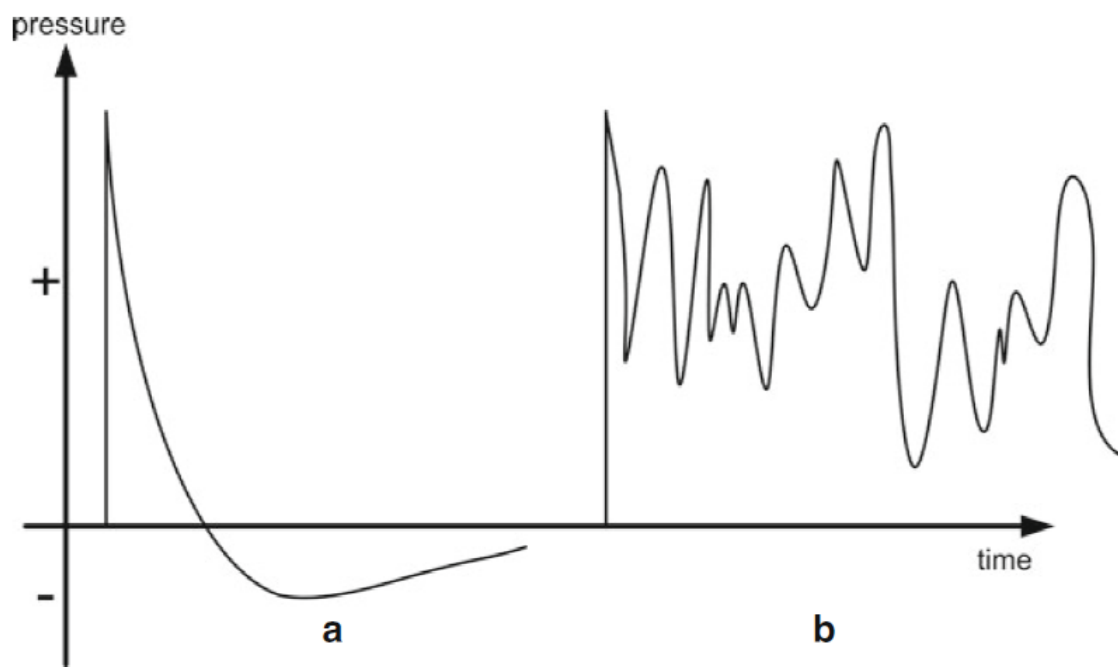


Figure 3: Pressure wave form of (a) a simple free field explosion and (b) a semi-confined blast (Edwards and Clasper, 2016, figure reproduced with permission)

The energy a blast wave carries is a function of the area under the curve and as such the sustained pressure of a blast wave within a semi-confined space results in further energy transfer to a casualty, increasing the lethality of an explosion (Dearden, 2001).

2.2.2 Mechanisms of blast injury

The mechanisms by which an explosion injures a casualty have traditionally been divided into four categories: primary, secondary, tertiary, and quaternary blast injury. This classification was first described by Zuckerman during the Second World War (Zuckerman, 1941). Since this time, the US Department of Defence added a fifth category: quinary (Department of Defense, 2008).

Primary effects of blast injury are caused directly from the shock-wave overpressure. Injury can result from direct transmission of the wave through susceptible tissues, as well as compression and acceleration. Changes in stress propagation between materials of different densities and impedance results in differential acceleration with spallation (throwing off of materials), implosion (compression of less dense compartments) and shearing forces (inertial effects due to relative movement of tissues to one another) (Stuhmiller *et al.*, 1991). This is most pronounced in the tissue / air interfaces of the lung, gastrointestinal tract, and auditory system. The shock-wave overpressure also affects solid abdominal organs, the musculoskeletal system and the brain (Cooper and Taylor, 1989; Hull and Cooper, 1996; Courtney and Courtney, 2015). Most survivors of blast injury have sustained secondary or tertiary injuries, with few surviving significant primary blast injuries. This is due to casualties with the necessary blast loading being killed immediately from a combination of all effects, or dying subsequently from respiratory failure secondary to traumatic blast-lung injury (TBLI) caused by primary blast (Leibovici *et al.*, 1996).

Secondary effects are due to penetrating injury caused by energised fragments accelerated by the blast wind such as casing, shrapnel, or the surrounding environment (sand, soil, or gravel). This fragmentation effect is the most lethal mechanism following explosions, due to its increased area of effect compared to that of the primary shock wave. This is due to the energy of these fragments being subjected to the inverse square rule of dissipation, whilst the energy

of the shock wave diminishes more quickly as it is subject to the inverse cube rule of dissipation (Edwards and Clasper, 2016). Fragments are likely to therefore injure more casualties and contribute a more significant portion of the burden of injury as the distance from the explosion increases (Figure 4).

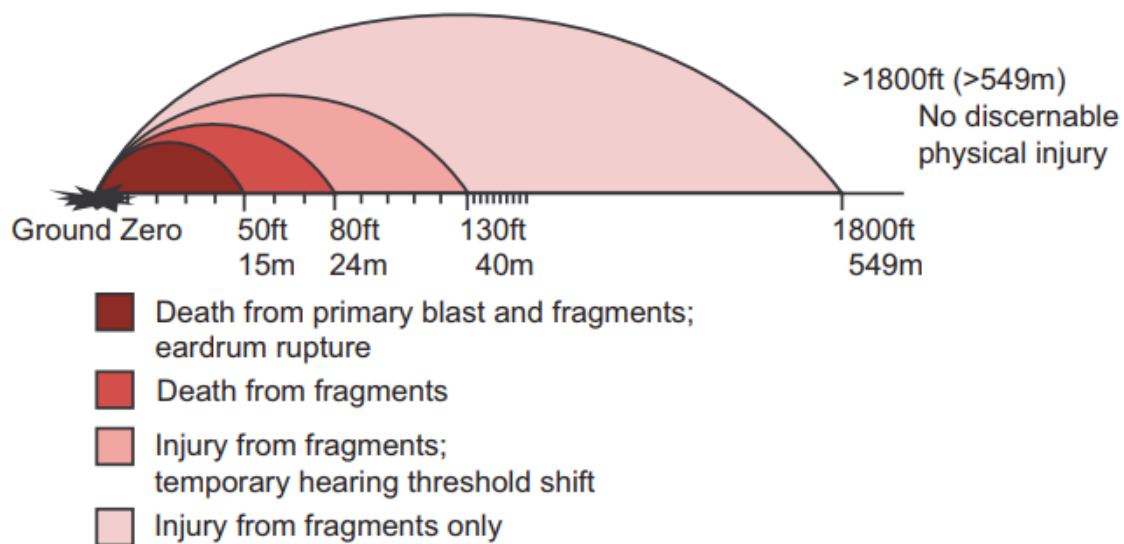


Figure 4: Morbidity and mortality as a function of distance from explosive (Champion *et al.*, 2009, figure reproduced with permission)

Tertiary effects relate to the displacement of the body (or solid objects into the body) due to the blast wind. Head injuries, fractures and crush injuries are common. Injury may occur due to impact of the body into solid objects, or through relative restraint of one part of the body compared to another (e.g., flailing of a limb). Solid-blast injury relates to transmission of force through a solid structure, such as a vehicle floor or a casualty's own body armour (behind armour blunt trauma). Solid-blast from a vehicle floor may result from under-vehicle explosions, with the floor of the vehicle rapidly accelerating and impacting with the casualty

(Ramasamy, A. M. Hill, *et al.*, 2011). Behind armour blunt trauma is non-penetrating injury caused by deformation of a casualty's armour, with transfer of energy to the casualty (Cannon, 2001).

Quaternary effects consist of a miscellaneous group of blast injuries not attributable to other groups. These include burns, inhalation injuries and toxic effects associated with the blast (Turégano-Fuentes *et al.*, 2008).

Quinary effects consist of specific non-explosion related effects resulting in a hyper-inflammatory state, which is out of proportion to the blast injuries sustained. This can occur with the deliberate addition of biological, chemical, or nuclear products to an explosive device. The casualty may sustain a resultant radiation injury, bacterial, fungal or viral infection (Kluger *et al.*, 2007).

These different mechanisms of blast injury can have altering injury patterns depending upon the region of the body affected. To fully understand the injuries sustained to the pelvis following blast, it is important to first appreciate the normal anatomy of the pelvis and its surrounding structures.

2.3 Pelvic anatomy

The pelvis consists of paired iliac, ischial, and pubic bones in a ring-like structure. These meet anteriorly at the pubic symphysis and join posteriorly to the sacrum at the paired sacroiliac joints (Figure 5).

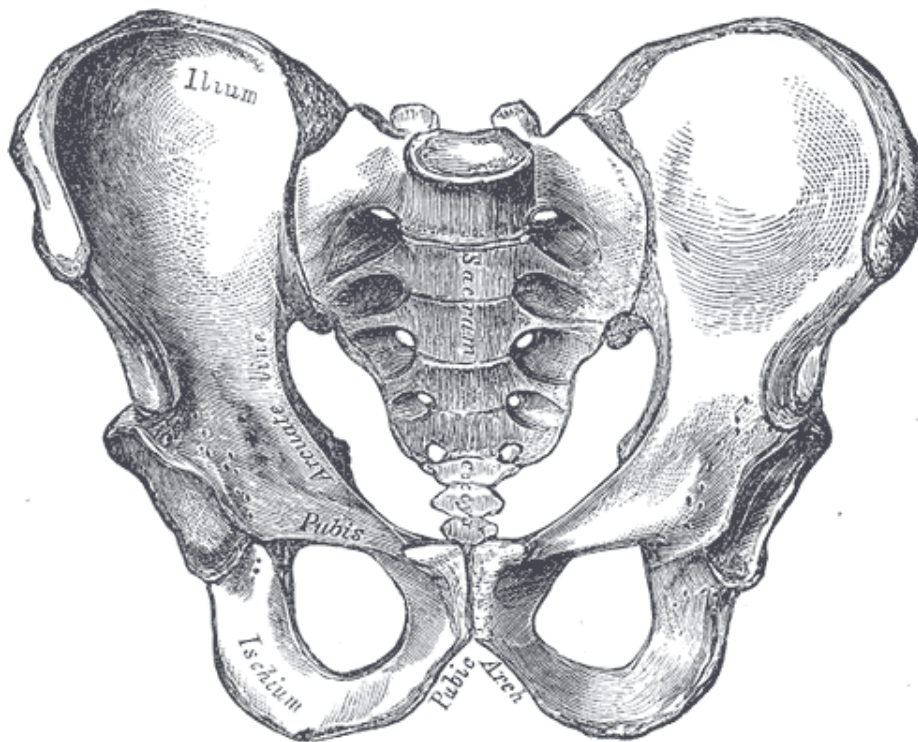


Figure 5: The bony pelvis (Gray, 1918)

The pubic symphysis is a unique joint consisting of a fibrocartilaginous disc compressed between the hyaline cartilage articular surfaces of the pubic bones. It resists tensile, shearing, and compressive forces. Four ligaments reinforce the pubic symphysis anteriorly, posteriorly, superiorly and inferiorly (Becker *et al.*, 2010) (Figure 6).

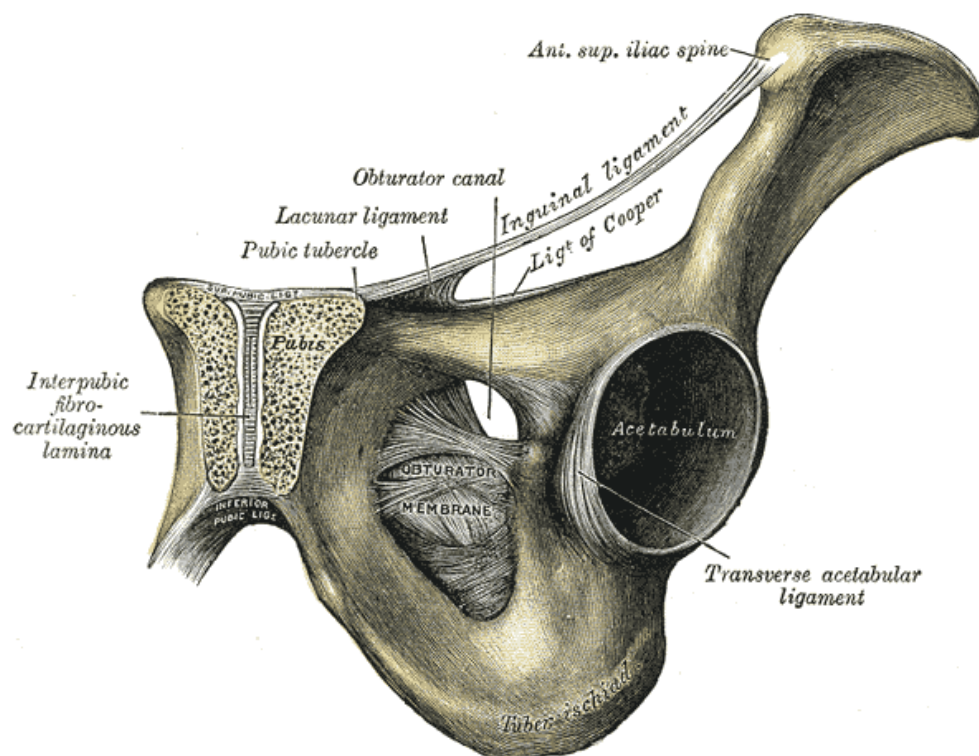


Figure 6: The pubic symphysis (Gray, 1918)

The sacroiliac joints are synovial joints, reinforced by a strong network of ligamentous structures. These include the sacroiliac ligaments (anterior, posterior, dorsal and interosseous), sacrospinous ligaments, sacrotuberous ligaments and iliolumbar ligaments (Egund and Jurik, 2014) (Figure 7).

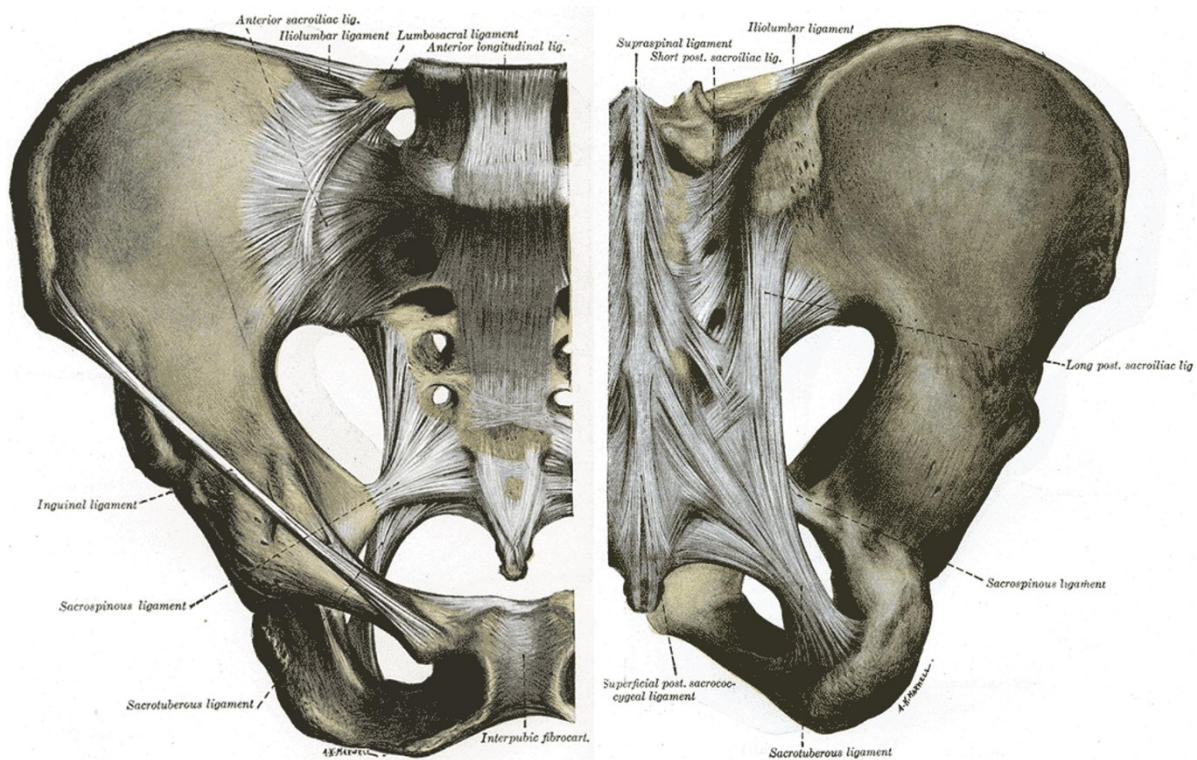


Figure 7: Pelvic ligamentous structures (Gray, 1918)

Organs and significant structures contained within the pelvis that are at risk of injury include the bladder, ureters and urethra, small and large bowel, reproductive organs, lumbar and sacral nerve plexuses, and the pelvic vasculature. The pelvis contains within it a rich network of vasculature, connecting the abdominal aorta to the pelvic organs and musculature, and the lower limbs. The great vessels originate from the aorta and consist of paired common iliac arteries, which branch to become the external and internal iliac arteries. Both the internal and external arteries have further smaller branches which subsequently navigate within the pelvis. The venous drainage follows that of its arterial counterparts (Standing, 2016) (Figure 8).

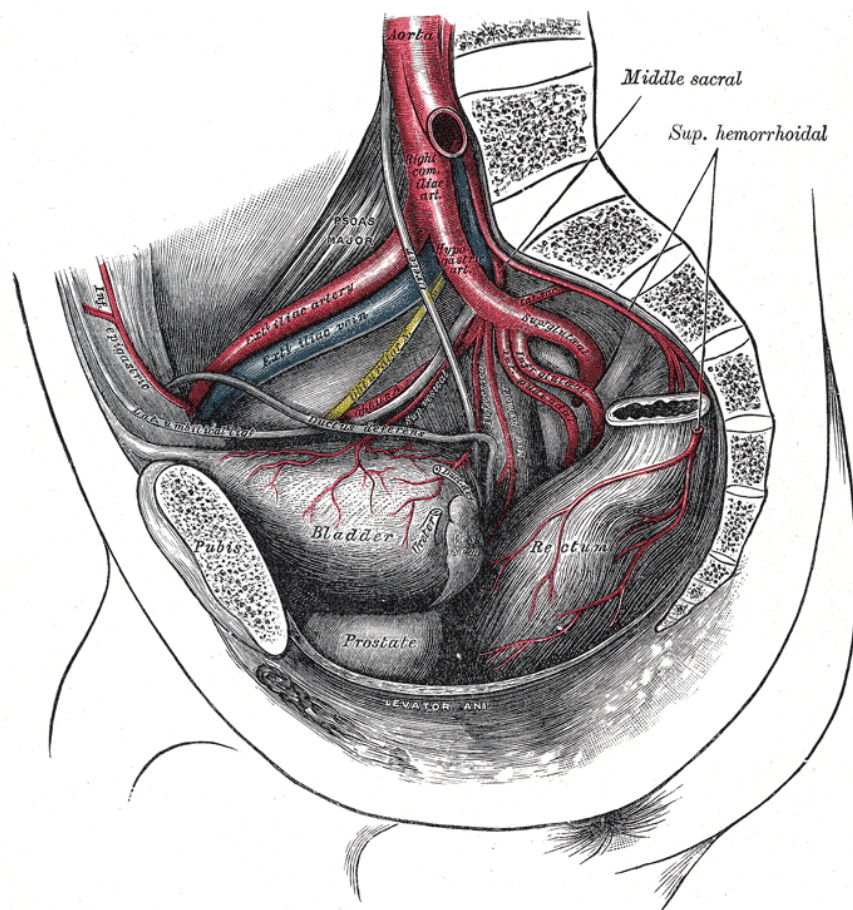


Figure 8: Pelvic arterial vasculature (Gray, 1918)

2.4 Pelvic injury classifications

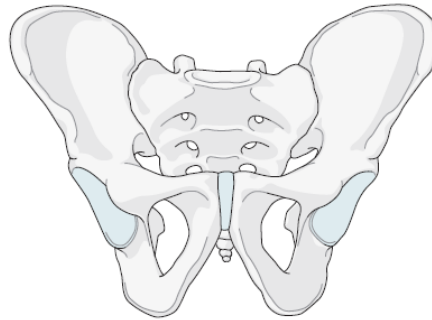
An injury to the pelvis places all these structures at risk. The sequelae can include organ failure, permanent neurological compromise, and major haemorrhage. Major haemorrhage from a pelvic vascular injury can be challenging to treat, particularly in the immediate setting, as it is a type of non-compressible haemorrhage (defined as vascular disruption which cannot be controlled by compression) (Stannard *et al.*, 2013). This compares to compressible haemorrhage, such as a major vascular injury in the thigh, which is amenable to immediate haemorrhage control via compressive techniques (such as tourniquet application). Pelvic injuries vary greatly in type and severity due to the injury mechanism and as such, several classification systems have been described for these complex injuries.

2.4.1 Civilian pelvic injury classification systems

Most pelvic ring disruptions in the civilian population occur in motor vehicle accidents (~ 60%), falls from height (~ 30%) or crush injuries (~ 10%) (Schmal *et al.*, 2005). Failure of the pelvic ring occurs either through direct compression, shearing forces, or through a traction mechanism such as forced abduction of the hip. Several commonly used classification systems exist for civilian pelvic fractures, which can be based on location, stability or injury mechanism (Burgess *et al.*, 1990; Tile, 1996; AO Foundation, 2018) .

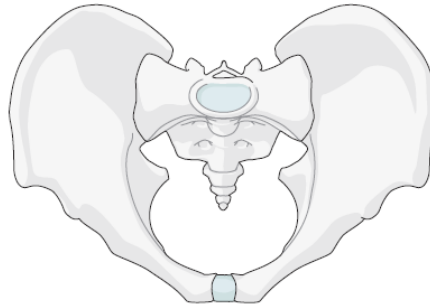
Pelvic ring

Bone: Pelvis 6



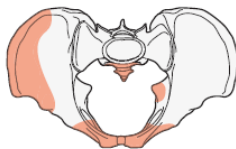
61

Location: Pelvis, pelvic ring 61

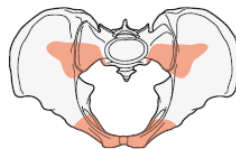


Types:

Pelvis, pelvic ring, **intact posterior arch**
61A



Pelvis, pelvic ring, **incomplete disruption of posterior arch**
61B



Pelvis, pelvic ring, **complete disruption of posterior arch**
61C

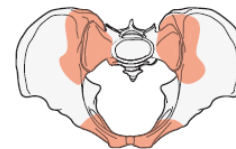


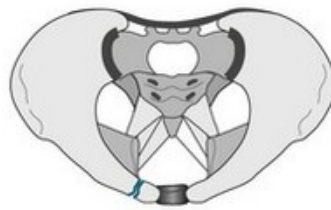
Figure 9: AO/OTA Classification (AO Foundaton, 2018, figure reproduced with open access)

The AO/OTA Fracture and Dislocation Compendium is a detailed classification system which describes all fractures according to their location and morphology (AO Foundaton, 2018). It does not provide any information regarding stability, injury mechanism, associated injuries or prognosis. The system is coded with a combination of letters which describe the bone fractured, the location of the fracture within the bone, and its morphology (simple, wedge or multi-fragmentary). With regards pelvic ring fractures, the classification focuses on whether there is an intact, partially disrupted or completely disrupted posterior arch (Figure 9). Further subclassification subsequently describes the fracture based on its location and the Young-Burgess Classification injury type, as will be discussed.

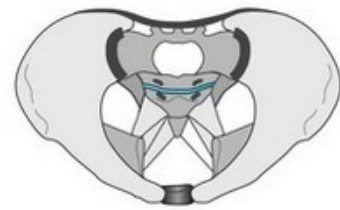
Tile A



A1
Avulsion injury
Not involving the ring



A2
Stable
Minimal displacement

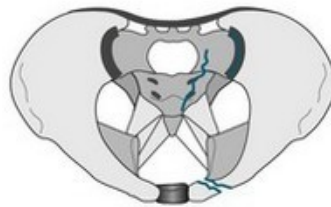


A3
Transverse fractures of
sacrum or coccyx

Tile B



B1
Unilateral



B2
Lateral compression injury
Internal rotation instability



B3
Bilaterally rotational instability

Tile C



C1
Unilateral



C2
Bilateral
One side rotationally unstable
One side vertically unstable



C3
Bilaterally vertically unstable

Figure 10: Tile classification. (Milenković and Mitković, 2020, figure reproduced with open access)

Tile classification describes pelvic fractures based on overall pelvic ring stability, and provides a general guide to treatment (Tile, 1996). The classification system divides injuries into type A (stable pelvic ring), type B (partially stable) and type C (unstable) (Figure 10). The partially stable type B injuries include “open book” and “bucket handle fractures”, which are caused by

external and internal rotation forces, respectively. Type C injuries have complete disruption of the posterior sacroiliac complex. These injuries are inherently unstable and most often caused by high energy trauma. Increased severity of fracture type on this classification system has been shown to correlate with increased mortality (Gänsslen *et al.*, 1996).

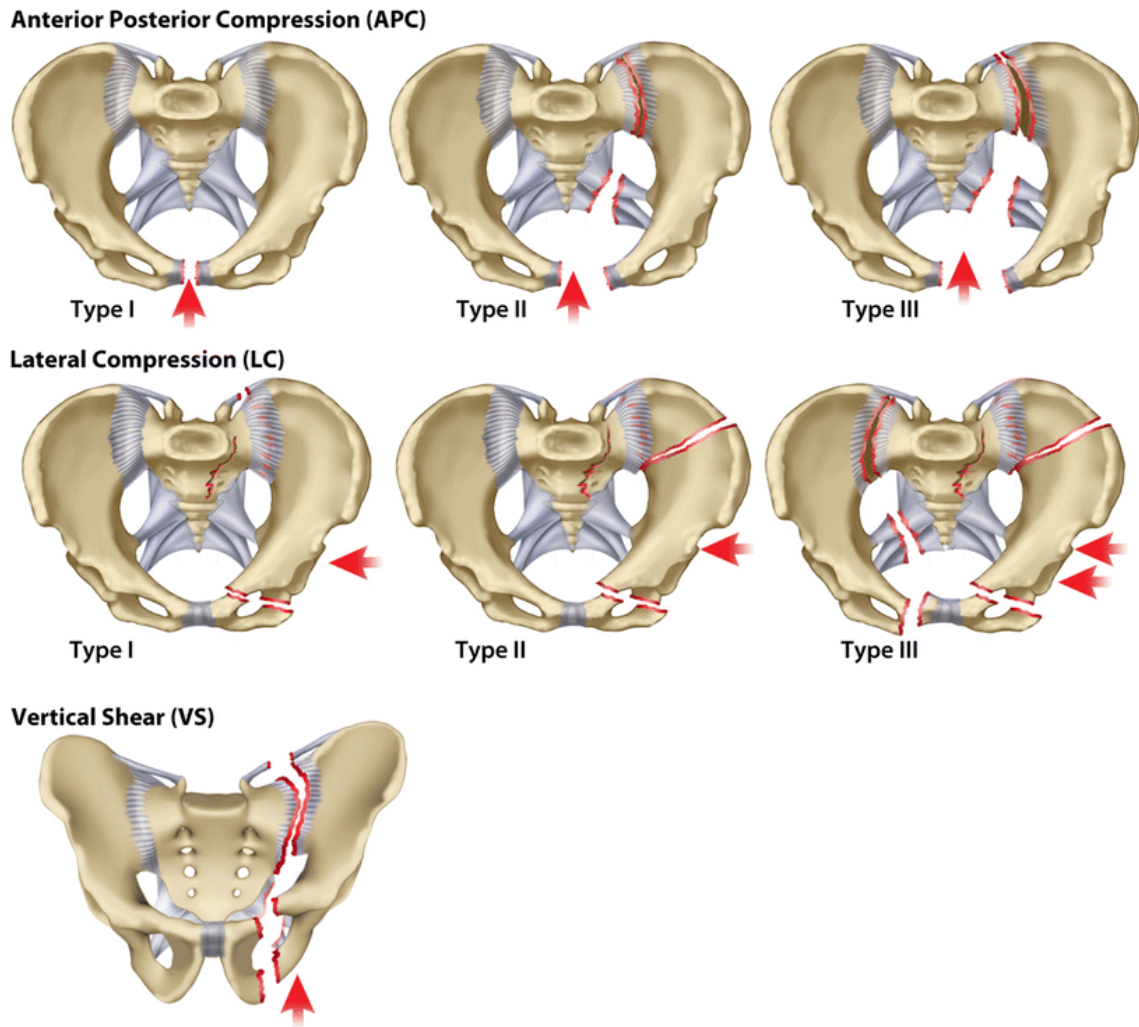


Figure 11: Young-Burgess Classification (Alton and Gee, 2014, figure reproduced with permission)

The Young-Burgess classifications describes pelvic fractures due to their injury mechanism, and has important implications for management and prognosis (Burgess *et al.*, 1990). Injury patterns consist of lateral compression, anterior-posterior compression (APC), or vertical shear. Within each category is a grade of severity (Type I, II or III) (Figure 11).

Vertical shear injuries occur with falls from height, with force transmitted through the pelvis resulting in superior displacement of the ileum. Lateral compression injuries most often occur through lateral impacts sustained in motor vehicle collisions (Dalal *et al.*, 1989). APC injuries most often occur from high energy crush injuries, such as motorcyclists impacting with the fuel tank during a collision. Pelvic failure in this mechanism occurs through external rotation of an iliac blade, with a resultant disruption and displacement of the pubic symphysis and sacroiliac joint(s) in the most severe cases (type III). This is an inherently unstable fracture pattern (Pennal *et al.*, 1980) and associated with significant intra-pelvic vascular injury – typically from branches of the great iliac vessels that cross the sacroiliac joints. Of these groups, APC injuries have the highest associated mortality, with Young’s original paper citing 20% mortality in civilian casualties (Burgess *et al.*, 1990). Converse to the other fracture patterns, mortality in this group occurs predominately directly due to these vascular injuries as opposed to other associated non-pelvic injuries (Dalal *et al.*, 1989).

2.4.2 Military pelvic fracture classification systems

The mechanisms of injury resulting in pelvic blast fractures are fundamentally different from those seen in civilian injuries and as such, civilian classification systems are of limited utility. However, no military classification systems focusing specifically on pelvic fracture are in use. Global injury scoring systems are used to provide a predictor of overall mortality. The Military Injury Severity Score (mISS), a modification of the Injury Severity Score, provides a predictor of mortality based upon incorporating the sum of the three most severely injured anatomical

areas. It provides a better predictor of combat mortality for military casualties than the Injury Severity Score, but does not accurately predict severity in IED related pelvi-perineal trauma patients (Mossadegh *et al.*, 2013; Le *et al.*, 2016). A focused cumulative anatomic scoring system for military perineal and pelvic blast injury, based on the abbreviated injury score, has been developed to provide a mortality predictor more tailored to pelvic blast injuries (Mossadegh *et al.*, 2013). The scoring system incorporates urogenital injury, anorectal injury, and pelvic fracture. Its utility in describing pelvic fracture patterns however is limited. Pelvic fractures are scored from 0 – 6 based upon increased severity of fracture patterns, as determined by the Young-Burgess classification (Mossadegh *et al.*, 2013). Whilst providing predictors of mortality, these scoring systems do not provide detailed information regarding military pelvic fracture patterns of injury.

2.5 Military pelvic fracture patterns of injury

Pelvic trauma has emerged as one of the most severe injuries to be sustained by the casualty of a blast and is not uncommon: a review of military fatalities during Operation Enduring Freedom and Operation Iraqi Freedom identified 26% had sustained pelvic fractures (Bailey *et al.*, 2011). A differentiation in injury pattern has been made between the mounted (in vehicle) and dismounted (on foot) casualty of a blast event. Singleton *et al.*, 2013 demonstrated an important difference between these two environments; casualties mounted at the time of injury were found most likely to die from a CNS injury, followed by intra-cavity haemorrhage. Converse to this, the dismounted casualty was seen to be more likely to die from extremity and junctional haemorrhage (Singleton *et al.*, 2013) (Figure 12).

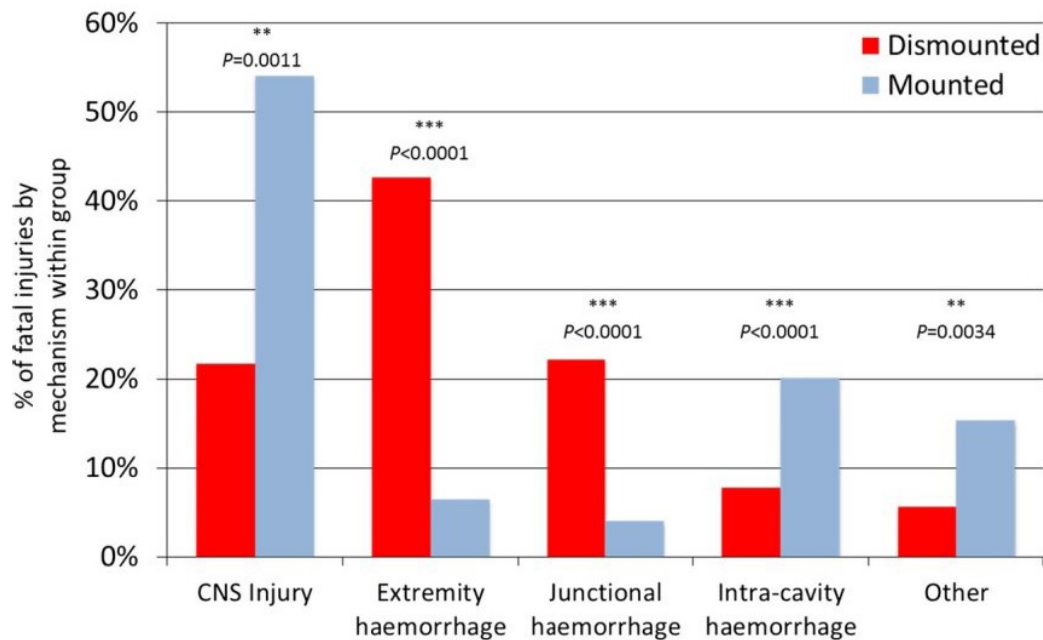


Figure 12: Differences in incidence of injury patterns in the mounted and dismounted casualty (Singleton *et al.*, 2013, figure reproduced with permission)

Similarly, pelvic fracture patterns differ relating to the environment (mounted or dismounted) at time of injury. Dismounted casualties were seen to have predominantly unstable pelvic ring fractures, with the majority sustaining disruption to the pubic symphysis (69% dismounted vs 33% mounted) and sacroiliac joint(s) (72% dismounted vs 33% mounted). In contrast to this, mounted patients most commonly had fractures to the pubic rami (52% vs 36% dismounted) and spinal column (46% vs 20% dismounted). The associated mortality rates of the two groups were found to be the same (50.7% dismounted vs 50% mounted) (Webster *et al.*, 2018).

Several authors have described the pelvic fracture patterns of blast injury casualties. The injury patterns of a cohort of dismounted blast military casualties that had survived the initial blast injury to attend a level 3 Military Hospital in Afghanistan has been described; of the thirty-four casualties with pelvic fracture, 88% had sustained unstable Tile type B or C patterns of injury.

Of fatalities with pelvic fractures, 100% were Tile Type B or C (Oh *et al.*, 2016). A separate cohort categorised sixty-three military pelvic fractures over an eight-year period in accordance with Young and Burgess criteria and described the associated mortality; the most common injury and also the one with the highest mortality was APC-type fractures, where mortality was noted to rise with fracture severity (grade I, 67%; grade II, 74%; and grade III, 93% mortality) (Mossadegh *et al.*, 2012).

The difference in pelvic fracture patterns between mounted and dismounted casualties highlights the likelihood of different mechanisms of injury. The hypothesised mechanism of pelvic fracture to the mounted casualty is under-vehicle tertiary blast injury, leading to a direct crush effect of the pelvic bones closest to the vehicle seat at the time of injury (the pubic rami), with relative sparing of the pubic symphysis due to the posterior tilt of the pelvis in the seated position (moving the symphysis away from the site of energy transfer). The energy load subsequently transfers proximally up through the casualty via their stable pelvic ring, resulting in spinal fractures, before the casualty is thrown upwards resulting in thoraco-abdominal and CNS injuries (Singleton *et al.*, 2013; C. E. Webster *et al.*, 2018). The mechanism of injury of the dismounted blast casualty, however, has not been described. Several hypotheses have been proposed; these will be discussed in detail in the following chapters.

2.6 Conclusion

Chapter 2 has highlighted that the cause of death and pelvic fracture patterns differ between mounted and dismounted blast-injury casualties. Whilst the overall mortality is the same, there are likely to be differing mechanisms of injury causing this. The dismounted casualty has been shown to have unstable pelvic ring fractures and the cause of death thought to be secondary to junctional and extremity haemorrhage, whilst the mounted casualty has been shown to have predominately stable pelvic ring fractures and the cause of death thought to be secondary to

associated injuries. As such, the mounted casualty is unlikely to benefit from management or mitigative strategies to reduce mortality by limiting injury to the pelvis, and so this was not explored further within this thesis for this group. In order to develop management and mitigative strategies for the dismounted casualty, further information regarding the cause of death, associated injuries and how they contribute to mortality, and the mechanism of injury are required. The first study of this thesis therefore is to review the battlefield data to assess these factors, which will be explored in the next chapter.

Chapter 3

Dismounted Pelvic Blast Injury: Battlefield Data

This chapter is published in part:

Rankin, I. A., Webster, C. E., Gibb, I., Clasper, J. C. and Masouros, S. D. (2020) 'Pelvic injury patterns in blast', *Journal of Trauma and Acute Care Surgery*. 88(6), pp. 832–838.

3.1 Scope of the chapter

Chapter 3 discusses the morbidity and mortality of dismounted pelvic blast injury. This starts with an analysis of battlefield data, investigating the cause of death and risk factors for the pelvic blast injury casualty. Dr Claire Webster first collected the data used within this chapter during her preceding PhD at Imperial College London (Webster, 2017); data collection and any analyses are accredited throughout as appropriate. The data were subsequently re-analysed as part of this thesis to identify patient management, the risk of associated injuries of the dismounted blast casualty to pelvic vascular injury and death, and the association of sacroiliac joint displacement on CT to death. The chapter finishes by concluding these findings and identifying where future management and mitigation strategies should focus.

3.2 Dismounted blast injury

An association of dismounted blast injury with unstable pelvic fracture patterns, traumatic amputation and substantial perineal injury has been reported (Andersen *et al.*, 2012; Cannon *et al.*, 2016). This pattern of injuries was noted with increasing frequency in recent military conflicts and termed dismounted (on foot) complex blast injury (Ficke *et al.*, 2012a). Dismounted complex blast injury (DCBI) was one of the most challenging patterns of injury to emerge from the wars in Iraq and Afghanistan. This pattern of injury involves traumatic amputation of at least one lower extremity (typically proximal transfemoral amputation), a severe injury to another extremity, and pelvic, abdominal, or urogenital wounding. Its incidence rose throughout the conflicts, with a higher percentage of patients sustaining traumatic amputations, genitourinary injuries and open pelvic fractures as the conflicts progressed; in 2010, the number of casualties sustaining triple limb amputations was double that of the preceding eight years combined (Report of the Army Dismounted Complex Blast Injury Task Force, 2011). Of key significance, a leading risk factor for increased mortality in this pattern of injury is that of pelvic fracture. Of casualties sustaining a traumatic amputation, the mortality rate rises from 22.9% to 60.8% when there was an associated pelvic fracture (Webster *et al.*, 2018). Similarly an increase in mortality has been reported amongst patients with substantial perineal injury with the addition of pelvic fractures; this has been described in one cohort as high as 71% (Mossadegh *et al.*, 2012). The combination of these injuries and the relative risk each poses to pelvic vascular injury or mortality has not been explored previously.

No data on civilian incidents exist examining the effects of pelvic trauma secondary to blast injury. The mortality of civilian casualties with high energy pelvic fractures from non-blast mechanisms has been reported at 8-14% (Sathy *et al.*, 2009). The cause of death arises either from associated injuries, or haemorrhage directly from the pelvic injury (Demetriades *et al.*,

2002; Smith *et al.*, 2007). The incidence of pelvic fracture patients that subsequently went on to require angioembolisation for pelvic vascular injury in the civilian setting has been reported at 5.5%, with an associated mortality of 45% (Hamill *et al.*, 2000). The incidence and mortality rate due directly to blast-related pelvic vascular injury, as opposed to associated injuries, is not known.

The literature is inconsistent regarding pelvic fracture pattern in civilian patients as predictive of mortality. Whilst some studies have found association, others have been unable to demonstrate this (Burgess *et al.*, 1990; Demetriades *et al.*, 2002; O'Sullivan *et al.*, 2005). Military data have shown a high incidence of unstable pelvic fracture patterns following blast injury, but no data exist regarding fracture pattern as predictive of mortality (Oh *et al.*, 2016).

With IEDs and blast trauma no longer limited to military environments, both military and civilian surgeons and emergency doctors may be required to manage the blast injury casualty. Assessing the burden of non-compressible pelvic vascular injury following blast, whilst predicting pelvic vascular injury and its relative risk of mortality from clinical or radiological signs, would be advantageous for patient management and mitigation strategies. As such, a retrospective study was performed as part of this thesis (1) to identify the incidence and mortality rate of blast-related pelvic trauma from a military cohort of patients, (2) to assess the odds ratio of unstable pelvic fracture patterns, traumatic amputation, substantial perineal injury, and vascular injury to mortality, and (3) to assess specific pelvic fracture patterns association to vascular injury and mortality.

3.3 Dismounted Pelvic Blast injury: morbidity and mortality

The UK Joint Theatre Trauma Registry (JTTR) was interrogated to identify those sustaining pelvic fractures due to an explosive injury during the conflicts in Iraq and Afghanistan, from 2003 to the end of the conflict in 2014. The UK Joint Theatre Trauma Registry (JTTR) is a

prospectively collected trauma database of every casualty admitted to a deployed UK medical facility or killed on deployed operations. Data on all injured casualties treated by the UK DMS (including UK military, coalition forces, detainees, and the civilian population) is collected. These data are subsequently returned to the Royal Centre for Defence Medicine (RCDM) in Birmingham (UK) where it is added to the JTTR. The JTTR is held and maintained by the Academic Department of Military Emergency Medicine (ADMEM) (Smith *et al.*, 2007). The JTTR hold continuous data on this battle injured cohort from 2003. Data are held electronically with hard copies accompanying patients to definitive care. The initial entry criterion for the JTTR was a casualty injured severely enough to trigger a deployed trauma team activation although this was expanded in 2007 to include any casualty returning to RCDM for definitive treatment (Smith *et al.*, 2007). UK service deaths from trauma undergo a full post-mortem examination following repatriation to the UK. This is carried out by a Home Office Pathologist. A military research nurse or other member of ADMEM attends each of these formal examinations. The findings are noted and compared to the formal report produced by the pathologist before entry on to the JTTR (Smith *et al.*, 2007). In all cases, individual injuries (as detailed in clinical notes, imaging reports and post-mortem examinations) are added using the AIS (Military) dictionary with additional free text detail (Smith *et al.*, 2007). The UK JTTR data is, as such, a complete cohort database with no missed cases.

Inclusion criteria were all pelvic trauma with AIS >1 sustained via a blast mechanism to UK or allied military personnel and coalition civilians. Collected UK JTTR data included patient age, gender, incident year, new injury severity score (NISS), worst affected body region (as per highest AIS score), mortality (including wounded in action and survived, killed in action prior to medical intervention, died of wounds following initial medical intervention), time from injury to medical facility, and specific lower extremity injuries (including lower extremity traumatic amputation, substantial perineal injury of AIS >1 (defined as soft tissue injury to the

lower torso, including external genitalia and / or rectum), pelvic fracture stability (defined as stable with posterior arch intact, or unstable including incomplete and complete disruption of the posterior arch) and pelvic vascular injury (defined as named iliac vessel injury, or documented 'pelvis substantial deformation and displacement with associated vascular disruption; with major retroperitoneal haematoma'). It was not possible for me to include mounted or dismounted status in this data collection, due to their classified nature.

Computed Tomography (CT) image analysis

A CT data analysis was performed by Dr Webster to correlate displacement of the sacroiliac joints on CT to vascular injury (Webster, 2017). This CT data included analysing the CT scans of both alive and deceased casualties of pelvic blast. The mounted status was included in this data collection by Dr Webster, for which all reported scans in this thesis are of dismounted casualties. These collected data were available for repeat statistical analysis, for correlating displacement distance to mortality. It was not possible to correlate the recorded CT displacement distance measurements with the relevant casualties from the UK JTTR, and so these data could only be analysed in isolation.

The ilium was measured in relation to the sacrum for displacement in anterior-posterior (AP), superior-inferior (SI) and lateral directions. Where displacement was not present, a value of 0 mm was recorded. The superior-inferior displacement was measured using the most inferior aspect of the iliac portion of the sacroiliac joints, against the most inferior portion of the sacrum in coronal views (Figure 13a). Anterior-posterior displacement was measured in axial views, using the distance between the most anterior aspect of the iliac portion of the sacroiliac joints and the most anterior aspect of the corresponding sacrum (Figure 13b). Lateral displacement was measured in axial views; the distance between the joint line varies due to the concavity of

the sacroiliac joints and as such, the widest separation of the joint lines between the sacrum and ilium was taken (Figure 13c). The CT data was reported as accurate to 1 mm.

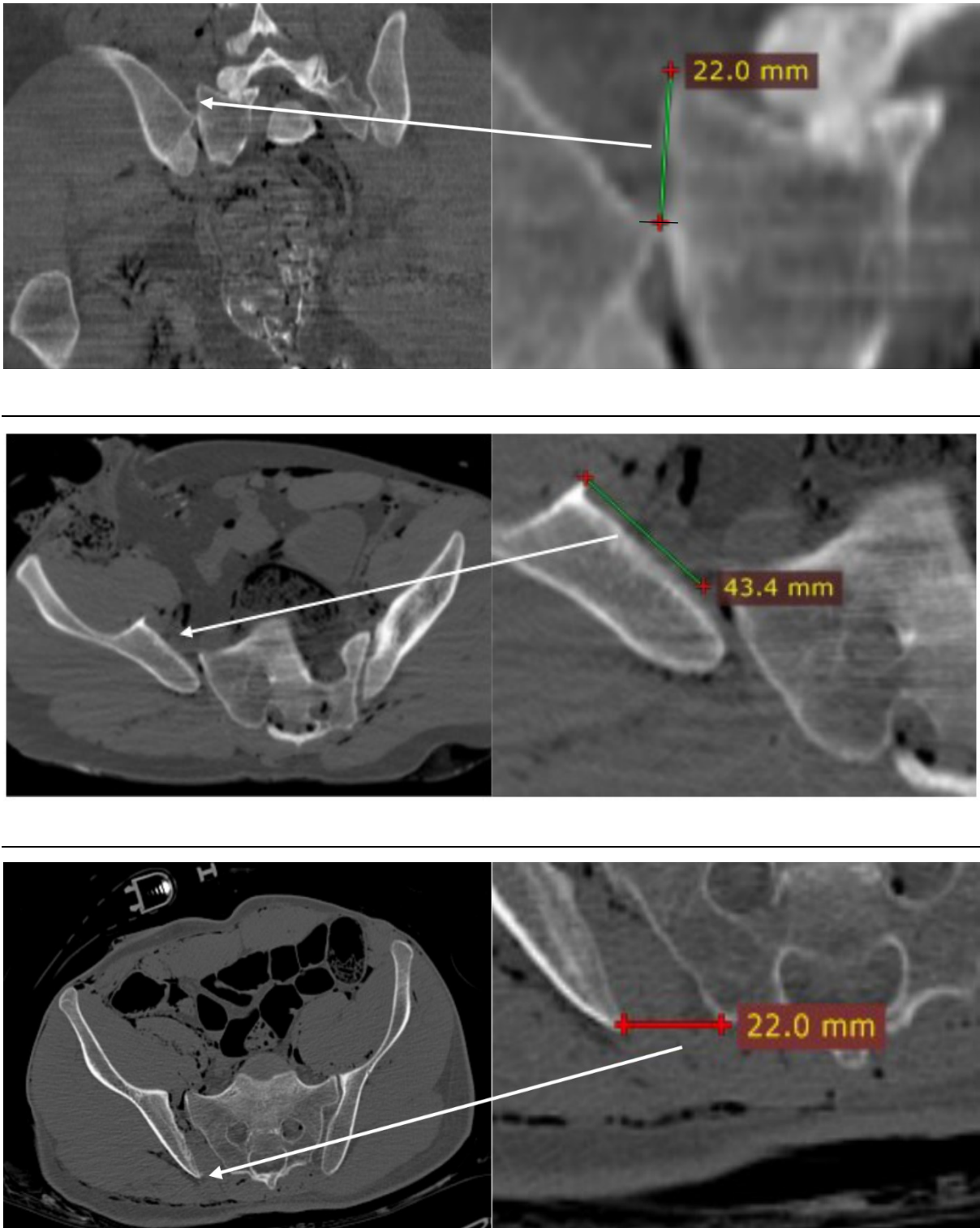


Figure 13: Quantifying pelvic disruption on CT. (a, top) superior-inferior, (b, middle) anterior-posterior, and (c, bottom) lateral.

Statistical analysis

Data analyses were performed using IBM SPSS statistics version 23. Crosstabulation with Pearson's Chi-square test was used to assess significant differences in categorical variables within the data collection. Logistic regression to assess for specific lower extremity injuries association to mortality was performed, with significance set at $p < 0.05$. A separate logistic regression was performed to assess for the association of specific lower extremity injuries to pelvic vascular injury.

On Dr Webster's CT data, the Mann-Whitney test was used to assess whether there were significant differences between AP, SI and lateral displacement of the sacroiliac joints and the presence of vascular injury. Receiver operating characteristic (ROC) curves were used to assess the association between displacement distance of the sacroiliac joints and vascular injury, and again repeated for association for mortality. ROC curves are used as a statistical test to set thresholds for diagnostic criteria of a test. In this study, including the displacement distance of the sacroiliac joints as part of a logistic regression would have been the most suitable test to use. As it was not possible to correlate this CT data with the UK JTTR data, ROC curve analysis was used as a suboptimal test for hypothesis generating only, and not for diagnostic accuracy. ROC curve analysis was used as a hypothesis generating tool, to look for association between distances, vascular injury, and death. The area under the ROC curve (AUROC) was subsequently calculated with 0.9 – 1 indicating excellent association, 0.8 – 0.9 good, 0.7 – 0.8 fair, and < 0.7 fail. The limitations of this test and the CT data collected will be discussed later in this chapter.

Permissions and Data Management

Permission to perform this study was granted by the Royal College of Defence Medicine (reference number: 48/2014). Data were anonymised, with all identifiable features removed, and stored in a secure location.

3.3.1 Results

Between 2003 and 2014, 365 patients who had sustained pelvic fractures secondary to a blast mechanism were identified. 184 casualties did not survive their injuries (50.4% mortality rate), of which 130 (71%) were killed in action prior to medical intervention, and 54 (29%) died of wounds following initial medical intervention. The collected data for all casualties, survivors and fatalities is shown in Table 1. Pelvic fracture stability was not documented for 27 casualties. Time to medical facility was not documented for 118 casualties.

	All casualties	Survivors	Fatalities
Total	365	181	184
Age	24 (range 4 – 51)	26 (4 – 24)	24 (13 – 51)
Gender	358 males (98%)	176 males (95%)	182 males (99%)
Incident year	2010 (2003 – 2014)	2011 (2006 – 2014)	2010 (2003 – 2014)
New injury severity score	57 (4 – 75)	34 (4 – 75)	75 (12 – 75)
Worst affected body region (highest AIS)	178 (49%) lower extremity 73 (20%) head 48 (13%) abdomen 29 (8%) thorax 15 (4%) spine 23 (6%) other	110 (61%) lower extremity 24 (13%) abdomen 17 (9%) thorax 15 (8%) head 8 spine (4%) 7 (4%) other	68 (37%) lower extremity 58 (32%) head 24 (13%) abdomen 12 (6.5%) thorax 7 (3.5%) spine 15 (8%) other
Time from incident to medical facility	66 minutes (8 – 1600)	60 (10 – 1600)	74 (8 – 1381)
Traumatic amputation	200 (53%)	181 (44%)	120 (65%)
Perineal injury	181 (50%)	63 (35%)	118 (64%)
Unstable pelvic fractures	192 (53%)	54 (35%)	128 (70%)
Pelvic vascular injury	159 (44%)	44 (24%)	115 (63%)

Table 1: Collected UK JTTR data. For continuous variables, median value with range given in parenthesis.

Pelvic vascular injury, unstable pelvic fracture patterns, traumatic amputation rates, and perineal injury (AIS >1) rates were higher in the mortality group, compared to survivors, when assessed individually using a 2x2 table chi square analysis ($p < 0.05$). A logistic regression model with odds ratios ($n = 338$; uncoded pelvic stabilities not included in analysis) including traumatic amputation, perineal injury, unstable pelvic fracture patterns and pelvic vascular injury showed significant association for all variables, excluding traumatic amputation, to mortality.

Unstable pelvic fracture patterns, traumatic amputation rates, and perineal injury (AIS >1) rates were higher in the pelvic vascular injury group, compared to those that did not sustain vascular injury, when assessed individually using a 2x2 table chi square analysis ($p < 0.05$). A second logistic regression model with odds ratios ($n = 338$; uncoded pelvic stabilities not included in analysis) including traumatic amputation, perineal injury, and unstable pelvic fracture patterns showed significant association for perineal injury and unstable pelvic fracture patterns, but not traumatic amputation, to pelvic vascular injury. The results of these models are shown in Table 2.

Association to mortality								
Variables in the Equation	B	S.E.	Wald	df	Significance (p value)	Odds ratio	95% C.I. for Odds ratio	
							Lower	Upper
Traumatic Amputation	0.174	0.295	0.347	1	0.557	1.19	0.667	2.122
Unstable pelvic fracture patterns	0.74	0.31	5.685	1	0.017	2.096	1.141	3.852
Perineal injury	0.817	0.29	7.948	1	0.005	2.265	1.283	3.998
Pelvic vascular injury	1.075	0.299	12.892	1	< 0.001	2.93	1.629	5.268
<i>Constant</i>	-1.379	0.217	40.441	1	0	0.252		
Association to pelvic vascular injury								
Variables in the Equation	B	S.E.	Wald	df	Significance (p value)	Odds ratio	95% C.I. for Odds ratio	
							Lower	Upper
Traumatic Amputation	-0.575	0.352	2.672	1	0.102	0.563	0.283	1.121
Perineal injury	1.353	0.327	17.136	1	< 0.001	3.871	2.039	7.347
Unstable pelvic fracture patterns	2.997	0.345	75.323	1	< 0.001	20.022	10.176	39.394
<i>Constant</i>	-1.273	0.209	37.062	1	0	0.28		

Table 2: Logistic regression for documented injury patterns to mortality (top) and pelvic vascular injury (bottom). Significant P values (significance set at $p < 0.05$) and the associated odds ratios are highlighted in bold. B: the coefficient for the constant. S.E.: the standard error around the coefficient for the constant. Wald: the Wald chi-square test, that tests the null hypothesis that the constant equals 0. Df: the degrees of freedom for the Wald chi-square test.

Pelvic vascular injuries (n = 159) were documented as major retroperitoneal haematoma in 125 cases, a named iliac artery in 14 cases, iliac vein in 3 cases, unilateral iliac artery and vein in 5 cases, bilateral iliac artery in 4 cases, and bilateral iliac artery and vein in 8 cases.

CT imaging data was available for analysis in 103 dismantled casualties. Analysis of individual fracture patterns identified opening of the pubic symphysis (> 2.5 cm) and opening of ≥ 1 sacroiliac joint to be significantly associated with pelvic vascular injury ($p < 0.001$). Pubic rami, sacral, iliac, and acetabular fractures were not associated with vascular injury. Lateral displacement of the sacroiliac joints was most significantly associated with pelvic vascular injury (median 5.5 mm (range 0 – 30) vs. median 3.0 mm (range 0 – 19) $p < 0.001$). The amount of lateral displacement of the sacroiliac joints was found to be a fair predictor of both pelvic vascular injury and mortality, for use in hypothesis testing, with AUROCs of 0.73 (95% CI 0.63 – 0.83, $p < 0.001$) (Figure 14) and 0.70 (95% CI 0.59 – 0.80, $p < 0.01$) (Figure 15) respectively.

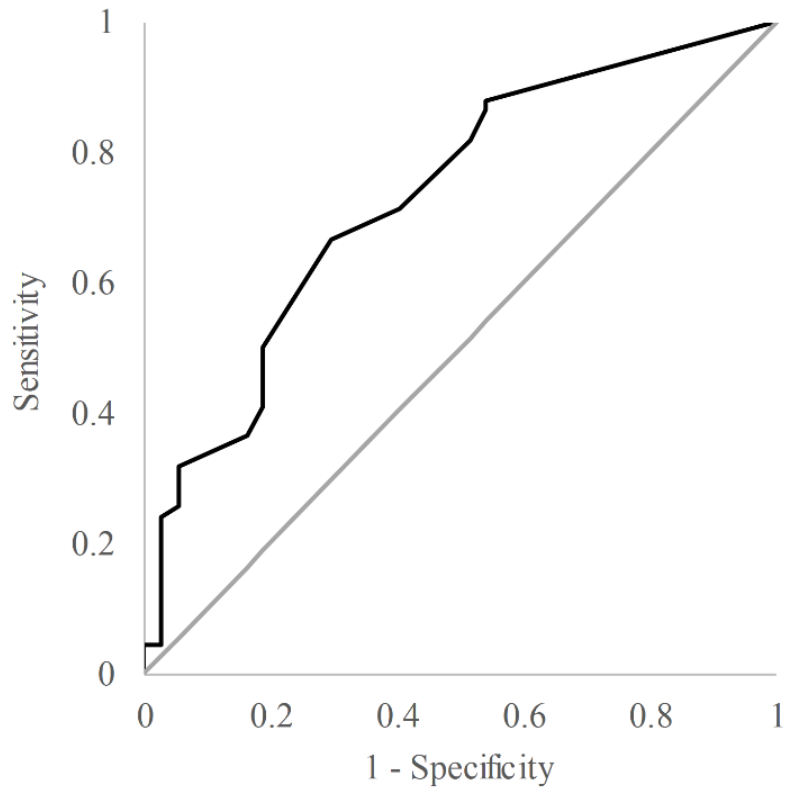


Figure 14: ROC curve analysis for lateral displacement distance of the sacroiliac joints as predictive of pelvic vascular injury (AUROC 0.73, 95% CI 0.63 – 0.83, $p < 0.001$).

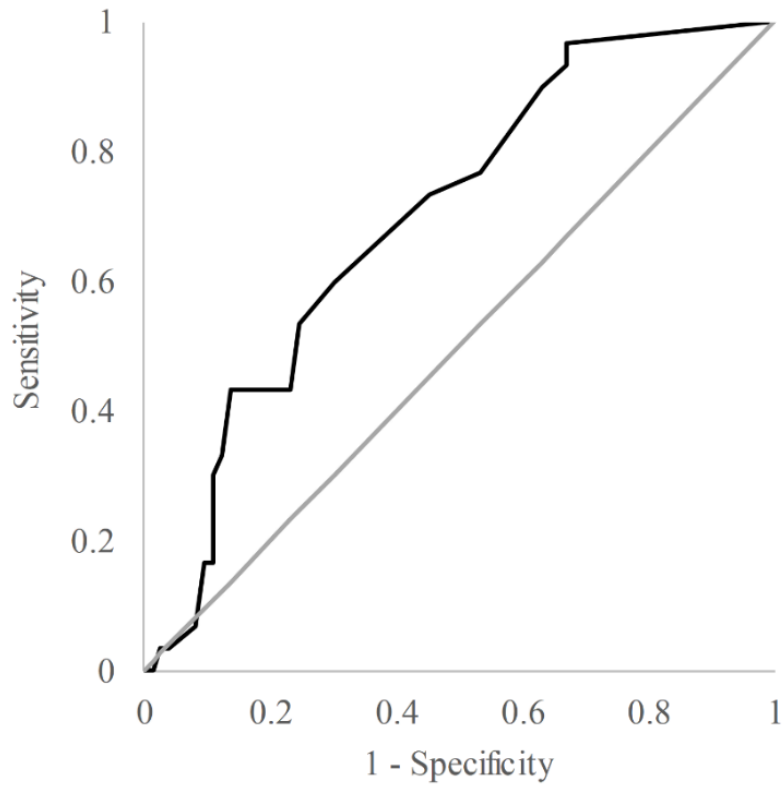


Figure 15: ROC curve analysis for lateral displacement distance of the sacroiliac joints as predictive of mortality (AUROC 0.70 (95% CI 0.59 – 0.80, $p < 0.01$).

AP and SI displacements of the sacroiliac joints were found to be significantly associated with vascular injury (AP median 0 mm, range 0 – 40, interquartile range (IQR) 3.25 *vs.* median 0 mm, range 0 – 4, IQR 0, $p = 0.006$; SI median 0, range 0 – 33, IQR 0.5 *vs.* median 0, range 0 – 10, IQR 0, $p = 0.03$) but had poor and failed ability for predicting vascular injury, with AUROCs of 0.63 (95% CI 0.52 – 0.74, $p = 0.031$) and 0.59 (95% CI 0.47 – 0.70, $p = 0.159$) respectively. AP and SI displacements of the sacroiliac joints similarly had failed and poor ability for predicting mortality, with AUROCs of 0.59 (95% CI 0.46 – 0.71, $p = 0.167$) and 0.63 (95% CI 0.50 – 0.76, $p = 0.039$) respectively.

3.3.2 Discussion

This study analysed the injury patterns of military pelvic blast trauma using the largest cohort to date published in the open literature from the recent conflicts in Iraq and Afghanistan. Pelvic vascular injury, unstable pelvic fracture patterns and perineal injury were found to have increased odds of mortality. Traumatic amputation was found to not be significantly associated with mortality, in the context of these other injuries. The greatest increased risk of mortality arose from pelvic vascular injury, with an odds ratio of 2.93. Substantial perineal injury and unstable pelvic fracture patterns were found to have increased odds of pelvic vascular injury; particularly, unstable pelvic fracture patterns showed an odds ratio of 20.02. Traumatic amputation was found to not be significantly associated with pelvic vascular injury, in the context of these other injuries. Analysis of CT data showed disruption of the pubic symphysis and sacroiliac joints, and lateral displacement of the sacroiliac joints, to be significantly associated with pelvic vascular injury.

Pelvic fractures in the civilian population are frequently associated with injuries to other body regions. These concurrent injuries were often the cause of death instead of the pelvic trauma

itself (Demetriades *et al.*, 2002). Similar findings were seen in this study. In this study the specific cause of death is not documented in the UK JTTR, however, the highest scoring AIS body region has been used by previous authors as a surrogate of this (Singleton *et al.*, 2013). The lower extremity was documented as the most severely affected body region in 37% of fatalities, meaning 63% of fatalities are believed to have died secondary to causes other than their lower extremity (including pelvic injuries).

As such, these mortality findings were in one regard similar to civilian pelvic fracture patients, where the mortality was principally due to associated injuries. These findings were different, however, in that the cause of death of a far greater proportion of patients was secondary to pelvic vascular injury. The incidence of pelvic vascular injury associated with pelvic fractures in the civilian setting has been reported at 5.5% (Hamill *et al.*, 2000). This, however, does not include patients who died before any medical treatment could be started and, as such, is likely an under reported value. The incidence of pelvic vascular injury in this study was substantially higher at 44% (159 of the total 365 pelvic fracture cohort) with an associated mortality of 72% when present (115 fatalities of a total 159 vascular injuries). Excluding those who died prior to medical treatment, the incidence remains high at 34% (74 of 235 casualties that did not die prior to medical intervention) with an associated mortality of 41% (30 of 74 casualties). This puts the burden of non-compressible pelvic haemorrhage likely to be significantly higher within blast-injury related pelvic fractures than those sustained from a non-blast mechanism.

It was not possible to assess mounted status in the present study for use alongside the JTTR data, due to inability to acquire this classified information. However, as discussed in chapter 2, previous research where mounted status has been available has shown the cause of death in the mounted casualty to be predominantly head or thoracic trauma, hypothesised to be due to the casualty being thrown upwards within the vehicle, whilst the cause of death in the dismounted

blast casualty has been shown to arise predominately from extremity and junctional haemorrhage (Singleton *et al.*, 2013).

A limitation of the CT AUROC analyses of the data provided by Dr Webster is that the observed values do not represent the full extent of dynamic displacement of the pelvis that occurred *in situ*. Furthermore, the CT imaging (and therefore displacement measurements) were taken in some cases following application of a pelvic binder. As such, these findings may not be truly reflective of – and may underestimate the degree of – tissue displacement that occurred at the time of the explosive event. In addition, the CT data was taken for the point at maximum displacement, on separate and individual slices, without reconstruction of the images such that they might not have been aligned. As such, these results should be interpreted with caution, as due to the possibility of systematic error from incorrect measurements. The analysis of the CT data is considered here only to aid in hypothesis testing, namely that lateral displacement of the SI joints is associated with vascular injury and mortality and so warrants further investigation; the analysis of the CT data, however, cannot be used as a diagnostic tool.

71% of fatalities died prior to medical intervention, suggesting the need to consider mitigation as opposed to management strategies to reduce mortality rates. Personal protective equipment to limit lateral displacement of the pelvis may present a possible mitigation strategy upon which future research could focus.

Unstable pelvic fractures and perineal injury were found to have increased odds ratio for pelvic vascular injury. Whilst found not to be significant following logistic regression, traumatic amputation occurred far more frequently in association with pelvic vascular injury (occurring in 68%, with 108 of the 159 pelvic vascular injury casualties having sustained a concurrent traumatic amputation).

In casualties of blast where this triad of injuries – traumatic amputation, perineal injury and unstable pelvic fractures – is present consideration of immediate progression to cessation of non-compressible pelvic haemorrhage should be considered, in particular where unstable pelvic fracture patterns are seen as these were found to have 20 times greater odds of pelvic vascular injury when compared to stable pelvic fracture patterns. In the first instance damage limitation surgery for haemorrhagic control should be considered. For example, cross-clamping of the aorta followed by pelvic packing and direct pelvic vessel ligation via laparotomy (Oh *et al.*, 2016). Management options will be discussed in more detail in the following chapter.

Inherent limitations are associated with a retrospective study. Risk of bias of this study was assessed as low to medium across most domains: patient exposure of pelvic fractures secondary to blast injury was documented in previously created records, for which those documenting the data at the time were unaware of this study's hypothesis. Cases (pelvic fracture with vascular injury, mortality) and controls (pelvic fracture without vascular injury, mortality) underwent valid and reliable diagnostic procedures including clinical injury documentation, CT scan findings and a post-mortem pathologist report. It is possible that information is missed at this stage, resulting in a reporting bias or inadequate data: for example, pelvic fracture in several cases was documented, whilst the type and stability of fractures was not reported. The UK JTTR is thought to have collected all suitable cases: due to the poly-trauma nature of casualties with pelvic fractures resulting in vascular injury, casualties will have presented to medical facilities for further treatment or died on scene and underwent post-mortem CT and pathologist examination. This is a particular strength of the UK JTTR database, as no reporting bias results from missed injuries of the deceased casualty. Similarly, all controls are thought to have been properly selected, with all casualties sustaining a blast injury resulting in pelvic fracture thought to have received further treatment or post-mortem examination. Appropriate statistical

analysis was performed for all documented injury patterns, to account for any prognostic injury patterns to mortality. There is, however, insufficient data within this study to assess the impact of changing evacuation paradigms throughout the conflict.

3.3.3 Conclusion

Casualties of pelvic blast injury are at significant risk of a non-compressible pelvic vascular injury. The overall mortality for casualties with pelvic fractures secondary to blast was 50%, rising to 72% in those with a pelvic vascular injury. Unstable pelvic fracture patterns, substantial perineal injury, and pelvic vascular injury all had significantly increased odds ratios of mortality (2.01, 2.27 and 2.93 respectively). Initial management of these patients should focus upon controlling non-compressible pelvic bleeding, in addition to managing any concurrent injuries. Lateral displacement of the sacroiliac joints was suggested from ROC curve analysis, as a hypothesis generating tool, to be associated with pelvic vascular injury. Mitigation strategies aiming to prevent lateral displacement of the pelvis following blast may result in fewer fatalities and a reduced injury burden.

3.4 Chapter conclusion

Having identified the areas upon which future research and interventions should focus in order to reduce mortality, the next step in this thesis was to review and discuss the current management and mitigation strategies of the dismounted pelvic blast injury casualty. This will be explored in the following chapter.

Chapter 4

Dismounted Pelvic Blast Injury: Management and Mitigation

This chapter is published in part:

Rankin, Iain A., Ramasamy, A. and Cooper, J. (2019) 'Blast injuries to the pelvis: essential lessons learned', *Journal of Trauma and Orthopaedics*, 07(04), pp. 52–54.

4.1 Scope of the chapter

Chapter 4 reviews the literature and discusses current management and mitigation strategies for the dismounted pelvic blast-injury casualty. This starts by reviewing current treatment options, including immediate haemorrhage control, management of orthopaedic injuries, and management of associated injuries. The chapter then goes on to review the literature regarding current mitigation strategies and the role they have played in limiting the injury patterns previously identified. The chapter finishes by discussing the hypothesised mechanisms of injury in dismounted pelvic blast, identifies which mechanisms warrant further evaluation, and sets the subsequent research direction of this thesis.

4.2 Management of the pelvic blast injury casualty

The global experience with severe, multisystem blast injuries, as seen with dismounted pelvic blast and its associated injuries, was limited until recent conflicts. Following recent conflicts, several management strategies have been developed aiming to improve outcomes. Specific treatment developments to improve survivability have included pre-hospital tourniquet application, rapid evacuation to surgical care with advanced resuscitation techniques, and subsequent multidisciplinary surgical interventions with perioperative critical care (Kragh *et al.*, 2009; Chovanes *et al.*, 2012; Kotwal *et al.*, 2016). The management of dismounted pelvic blast injury can be broadly separated into initial resuscitation and haemorrhagic control, orthopaedic injuries, and associated injuries.

4.2.1 Initial resuscitation and haemorrhage control

The top priority in the management of dismounted pelvic blast injury is haemorrhage control, beginning on-field prior to hospital intervention. Dismounted pelvic blast-injury patients frequently require massive blood transfusions (≥ 10 units of packed red blood cells over 24 hours) and the receiving facility's massive transfusion protocol should be initiated early (Oh *et al.*, 2016). A ratio of 1:1:1 of packed red blood cells, fresh-frozen plasma and platelets has been shown to be the most successful protocol for replenishing blood loss whilst correcting acidosis and coagulopathy (Johansson and Stensballe, 2010). Use of rotational thromboelastometry in the later stages of resuscitation can identify individual coagulation profile defects which may modify component administration (Jiang *et al.*, 2016). Both hypocalcaemia and hyperkalaemia are complications of major haemorrhage and massive blood transfusion and are associated with increased mortality (Hästbacka and Pettilä, 2003; Aboudara *et al.*, 2008). Continued point of care monitoring is therefore required and their presence proactively managed. Both pelvic vascular injury and associated traumatic amputation (TA) present sources of major

haemorrhage from which exsanguination can occur. On field haemorrhage control can be achieved in cases of TA with the use of the Combat Application Tourniquet (CAT Resources, SC, USA). Lakstein *et al.* showed a 78% success rate of haemorrhage control in a group of 91 patients where a tourniquet was utilised, however, this included all forms of traumatic haemorrhage and was not specific to TA (Lakstein *et al.*, 2003). Where shock is absent, their pre-hospital use is strongly associated with reduced mortality (Kragh *et al.*, 2009). For a more proximal TA where tourniquet application is not practical (such as the groin), advanced haemostatic products can be used to achieve haemostasis. These products include Chitosan, a polysaccharide polymer which strongly adheres to tissues to seal the site of wounds. Wedmore *et al.* 2006 found a 97% success rate in the cessation of bleeding, or in improvement of haemostasis, in 64 cases where Chitosan was used in the combat environment (Wedmore *et al.*, 2006).

Due to its non-compressible nature, pelvic bleeding is not amenable to these measures (Morrison *et al.*, 2013). On field application of a pelvic binder over the greater trochanters aims to restore normal anatomy, compress bone bleeding, and stabilise early clot formation (Bonner *et al.*, 2011). Whilst amenable to controlling low-volume venous bleeding, it is not suitable to control large venous vascular injury nor arterial injury (Bakhshayesh *et al.*, 2016). Other methods to manage pelvic haemodynamic instability include junctional tourniquets, and invasive measures such as resuscitative endovascular balloon occlusion of the aorta (REBOA). Junctional tourniquets such as the Combat Ready Clamp (CRoC) and the Abdominal Aortic and Junctional Tourniquet (AAJT) have demonstrated the ability to achieve vascular occlusion in healthy volunteers (Smith *et al.*, 2018). However, outcomes of their use in the field have not yet been reported and animal studies have shown a high rate of ischaemia-reperfusion with compressive abdominal organ injury associated with their use (Do *et al.*,

2019). REBOA has shown a positive effect on mortality among non-compressible torso haemorrhage patients and has been used as a pre-hospital resuscitation treatment in the civilian setting for patients with exsanguinating pelvic haemorrhage (Manzano Nunez *et al.*, 2017; Lendrum *et al.*, 2019). Its use in the austere environment is limited due to the technical skill required to safely perform (Manley *et al.*, 2017). As a result, haemorrhage from pelvic vascular injury is frequently not controlled until damage control surgery is performed, with pelvic packing and direct pelvic vessel ligation via laparotomy (Oh *et al.*, 2016). Vascular control should be achieved at the most distal level possible. Initial control may be achieved through laparotomy with infra-renal control of the aorta, subsequent to which control may be moved distal to the internal and external iliac arteries (Dubose *et al.*, 2010). Although not currently in use, future treatment may include inflatable intra-abdominal foam. Different foam sealants are currently undergoing evaluation in animal models (Rappold and Bochicchio, 2016).

4.2.2 Orthopaedic injuries

Damage control orthopaedics, with external fixation techniques, form the standard treatment in the acute setting. The anteroposterior pelvic radiograph is the investigation of choice in identifying pelvic ring disruption in the critical casualty. Management includes provisional fracture stabilisation (with delayed definitive fixation), debridement of contaminated and devitalised tissue, and limb preservation surgery (where possible). Preservation of bone length may require fracture stabilisation proximal to the point of amputation, in order to salvage maximal skeletal length and salvage intervening joint levels (Major *et al.*, 2010). As dismounted pelvic blast injury results in fracture patterns of a mechanically unstable nature, emergent operative management consists of fracture stabilisation in combination with haemorrhagic control. Provisional operative stabilisation is performed using anterior superior iliac spine / iliac crest or anterior inferior iliac spine external fixation, with subsequent

definitive pelvic stabilisation carried out in a delayed fashion (Mossadegh *et al.*, 2012). In severely unstable pelvic fractures, further stabilisation may be provided with the addition of a compact external fixator at the pubic tubercles, aiding stability across the pubic symphysis (Penn-Barwell *et al.*, 2014). Definitive fixation of complex open pelvic fractures can include iliosacral screws, with anterior disruption managed with internal fixation, external fixation, or a combination of techniques. Open pelvic fractures are common, as dismantled blast casualties sustain massive soft tissue destruction (Ramasamy *et al.*, 2012). The principles of blast wound management emphasise extensive debridement, wound irrigation, and negative pressure dressings. Subsequent soft tissue coverage and reconstruction is performed in a delayed fashion (Valerio *et al.*, 2014). In contrast to non-blast open pelvic fractures, as a result of the high degree of soft-tissue disruption and environmental contamination, deep infection rates in dismantled pelvic blast injury patients can reach 80%; one series reported a 57% removal of metalwork rate due to infection with prolonged bed rest subsequently required to achieve union (Ramasamy *et al.*, 2012). Owing to this severe contamination, subsequent wound reconstructive problems and risk of metalwork infection, external fixation should be considered as a definitive treatment in preference to internal fixation (Ramasamy *et al.*, 2012).

Blast-related traumatic amputations are provisionally managed with debridement and completion of the amputation utilising a length-preserving technique. Widespread soft tissue destruction is common and extensive debridement is required to reduce subsequent infection rate. Systemic debridement of nonviable skin, subcutaneous tissue, fascia, muscle, periosteum and bone from the primary zone of injury to healthy tissue is essential to reduce the later risk of sepsis (Bumbasirevia *et al.*, 2006). Repeat debridement operations over the initial days after injury are required, as blast effects on tissue viability are not always apparent at the initial debridement. Tissues in close proximity to the primary blast region may initially appear viable

but become non-viable over time; frequently the zone of injury is deceptively large (Bumbasirevia *et al.*, 2006). Debridement of devitalised tissue in high femoral traumatic amputations may require early hip disarticulation or rarely, hemi-pelvectomy (Andersen *et al.*, 2012). Where possible residual limb length should be salvaged, as this is a critical determinant of amputee function. Guillotine amputations, which sacrifice limb length and soft tissue, are not performed for this reason (Herard and Boillot, 2012). The primary consideration for management of traumatic amputations is working and closing within the zone of injury, which often encompasses the entire extremity. As such, preserving a functional limb is prioritised at the expense of increased risk of infection and heterotopic ossification (Potter *et al.*, 2007). In a patient with an intact but mangled extremity, the decision to attempt limb salvage against performing a primary amputation can be challenging. In cases of severe upper limb trauma, limb salvage should be attempted to optimize the patient's subsequent function. As in lower limb trauma, this consists of haemorrhage control, provisional fracture stabilization with external fixation, extensive debridement, fasciotomies as indicated, subsequent definitive fixation and soft tissue coverage.

Bacterial and invasive fungal infections (IFIs) are common and present a cause of late mortality. Bacterial infections occur in up to 40% of combat casualties with severe open fractures (Brown *et al.*, 2010). Intravenous prophylactic antibiotics should be administered as soon as possible, ideally within three hours of blast injury. At the initial debridement stages, antibiotic-impregnated beads may be implanted in proximity to fracture sites. Prophylactic antibiotics should be continued for 24 – 72 hours. Their use beyond this is determined by the presence of an established infection or delayed wound closure (Hospenthal *et al.*, 2011). Invasive fungal infections when present are challenging to treat, and outcomes remain poor. From a cohort of 1133 US military personnel injured by all mechanisms on duty between 2009

and 2011, 77 cases (6.8%) of trauma-related invasive fungal infections were identified. Specific risk factors for the development of IFI included blast injuries (OR: 5.7; CI: 1.1-29.6), dismounted at the time of injury (OR: 8.5; CI: 1.2-59.8); and above the knee amputations (OR: 4.1; CI: 1.3-12.7) (C. J. Rodriguez *et al.*, 2014). Intravenous antifungals should be administered in addition to debridement of necrotic tissue. Antifungals may not concentrate sufficiently at the site of infection due to thrombosis and distal necrosis. Due to this, and recurrent necrosis, extensive debridement can be required (C. Rodriguez *et al.*, 2014). One series described six casualties diagnosed with IFI, of which 50% went on to require amputation (Tully *et al.*, 2009). In a further cohort of thirty casualties diagnosed with IFI, despite aggressive early treatment, 7 (23%) patients required high-level amputation and 2 (6.7%) died.

4.2.3 Associated injuries

As highlighted in the previous chapter, dismounted pelvic blast injury is frequently accompanied by significant perineal injuries. It is important to recognise the significance of associated injuries and their management options. In addition to lower extremity amputation, pelvic injury is frequently accompanied by urogenital and colorectal injuries as part of the dismounted pelvic blast-injury pattern. Risk of urogenital trauma is increased 3-fold with an associated pelvic ring fracture (Fleming *et al.*, 2012). A traumatic partial or complete loss of genitalia has been observed in up to 25% of patients with a pelvic blast injury (Mossadegh *et al.*, 2012). In patients with pelvic fracture, bladder or urethral injuries should be suspected with the presence of blood at the urethral meatus, scrotal bruising, or a high rising prostate on digital rectal exam. Investigations including a retrograde urethrogram can be performed to evaluate for urethral injury whilst a CT cystourethrogram can subsequently be performed to assess for bladder injury. In the presence of a urethral injury, a suprapubic catheter is sited. Clinical suspicions of testicular rupture or scrotal penetration warrant further surgical exploration as do

any penetrating intra or extraperitoneal bladder injuries. The principal aim of treatment is directed at preservation of viable reproductive tissue. Initial management of perineal and urogenital injury involves copious, low-pressure wound irrigation, debridement, and closure. Where closure is not possible, negative pressure dressings are applied. (Williams and Jezior, 2013) Bladder injuries can be closed primarily or in circumstances where the bladder is destroyed, it can be packed open with bilateral ureteral stents externalized. Severely contused ureters should be stented, and any discrete lacerations repaired. Any further reconstruction should be performed in a delayed fashion and not attempted during the initial damage control surgery (Williams and Jezior, 2013).

Colorectal injuries in combat casualties are associated with a mortality of 33% (Glasgow *et al.*, 2012). One study reviewing anal trauma identified 37% of casualties having a concurrent pelvic fracture – this cohort was not however limited to blast casualties, but all combat casualties (Glasgow *et al.*, 2014). The presence of colorectal injury should therefore be sought to be identified and managed early in dismounted pelvic blast-injury patients. Inspection of the perineum, buttock and perianal tissues is required. Digital rectal exam is performed to assess for sphincter function, luminal compromise, haematochezia, or foreign bodies. Clinical concerns of rectal injury warrant further investigation with rigid proctoscopy or flexible proctosigmoidoscopy, if available. Blast injury to the anus, rectum or sigmoid colon are strong indications for a diverting colostomy. Abdominal perineal resection may be required in cases of massive pelvi-perineal wounds with rectal destruction and pelvic necrosis (Glasgow *et al.*, 2014).

With multiple life threatening injuries in the polytrauma pelvic blast-injury patient, index operative procedures should be prioritized with the surgical team leader (Wisner *et al.*, 1993). Haemorrhage control of pelvic vascular injury and traumatic amputations is priority. The most

critical operative procedures are proximal haemorrhage control, contamination control, completion of amputations, bladder repair and colonic diversion (Gordon *et al.*, 2018).

The published literature and battlefield data from the recent conflicts have highlighted both the high level of care that dismounted pelvic blast injury casualties received and, despite this, the high mortality associated with it. The injuries sustained from a high-energy explosive in the dismounted casualty are often non-survivable. Upon reviewing the deaths of UK military service personnel from 2002 - 2013, the Mortality Peer Review Panel judged 91% to be unavoidable – despite the advanced casualty evacuation protocols and the treatment methods described (Russell *et al.*, 2014). As such, future research strategies should focus on prevention or mitigation of injury in order to best improve outcomes of dismounted pelvic blast injury.

4.3 Mitigation strategies

As discussed in the previous chapter, the percentage of casualties with dismounted complex blast injury rose dramatically in 2010, as conflict moved to the Afghanistan theatre of operation (Report of the Army Dismounted Complex Blast Injury Task Force (2011)). Converse to the expansive desert within the Iraq theatre of operation, the varied, largely mountainous terrain within Afghanistan brought a shift in operational tactics. Patrolling was predominantly conducted on foot, outside of the relative protection of armoured vehicles (Andersen *et al.*, 2012). Heavy armour incorporated into military vehicles, such as that of the Mine-Resistant Ambush-Protected (MRAP) vehicle, offered excellent protection (Feisckert, 2009). Dismounted soldiers were, as such, more vulnerable to the signature weapon of recent conflicts as encountered in roadside bombs and anti-personnel mines.

In order to mitigate the increasing rate of pelvic injuries, an Urgent Operational Requirement was raised in order to field pelvic personal protective equipment (PPE) as of September 2010 (Lewis *et al.*, 2013). This exists in three hierarchical tiers, designed to be worn in conjunction

with one another in response to the perceived threat. Tier 1 was fielded in September 2010, consisting of a silk under layer to be worn under combat trousers covering from waist to knees. It aims to mitigate the effects of secondary blast injury cause by soil, fragmentation, or shrapnel to the soft tissues of the pelvis, perineum, and upper thigh. Tier 2 was fielded in February 2011, consisting of an armoured genital protection piece, worn over both combat trousers and Tier 1, aiming to provide additional protection to the groin, buttocks, perineum, and inner thigh. On routine patrol, soldiers are equipped wearing Tiers 1 and 2 (Figure 16).



Figure 16: Tier 1 pelvic protection (left) (Lewis *et al.*, 2013) and Tier 2 (right) (Saunders and Carr 2018) (Figures reproduced with permission)

Tier 3 was fielded in September 2011, designed to be worn by Counter-IED operators during high risk and short duration tasks. It consists of armoured over-trousers, covering the upper leg, femoral artery, and a wider area of the abdomen (Figure 17).



Figure 17: Tier 3 pelvic protection being worn over combat trousers (Lewis *et al.*, 2013, figure reproduced with permission)

The efficacy of this pelvic PPE has been explored in a study by Saunders and Carr, 2018. The authors utilised ballistic protective fabric, representative of the properties of Tier 2 PPE, placed over a steel frame in an experimental setup aimed to replicate a blast injury in the field. The protective fabric was centred on the steel frame 80 cm above a sand substrate, below which was a spherical charge of undefined mass (not disclosed due to military classification) buried at depths ranging from 50 to 150 mm. Twelve specimens were tested, with the charge at varying depths and utilising different sand substrates. In all circumstances, the Tier 2 PPE was penetrated, but not perforated, by secondary blast projectiles. The authors concluded the Tier 2 protection was adequate to protect against the effects of secondary blast injury.

Evidence of injury reduction from fragmentation wounds has been demonstrated by a difference in the pattern of injuries suffered by personnel wearing pelvic PPE and those not. On reviewing injury data of 174 casualties attending a role 3 hospital in Afghanistan, those wearing Tier 1 pelvic PPE were 9.5 times – and those wearing both Tiers 1 and 2 10.1 times – less likely to sustain a fragmentation wound to the pelvis than those unprotected (Breeze, L S Allanson-Bailey, *et al.*, 2015). A reduction in urogenital injury has also been observed. A cohort of 58 casualties wearing pelvic PPE was compared to a historical matched control group of 61 casualties not wearing pelvic PPE. Patients with any level of lower extremity amputation from dismounted blast injury were included. The use of pelvic PPE was associated with an absolute reduction of genitourinary injury of 31% (Oh *et al.*, 2015).

No reduction in the burden of fatal pelvic injury has been noted since the fielding of pelvic PPE in 2010 (Oh *et al.*, 2016; Gordon *et al.*, 2018). In order to improve upon current mitigation strategies, the mechanism of injury which results in fatal dismounted pelvic blast injury must be explored. Currently, this mechanism of injury is not known.

4.4 Hypothesised mechanisms of injury

Three hypothesised mechanisms of injury to cause pelvic fracture following blast have been proposed: axial load via the femoral head, flail of the lower limbs, and blast wind and fragmentation (C. E. Webster *et al.*, 2018).

4.4.1 Axial load hypothesis

Dr Claire Webster investigated the axial load hypothesis as part of her preceding PhD at Imperial College London (Webster, 2017). The mechanistic theory was of load propagation via the lower extremity to the pelvis, via interaction of the femoral head acting upon the acetabulum, to transfer an axial load from the blast to the pelvis. Instead of acetabular fracture, the resultant forces were hypothesised to cause superolateral separation of the hemi-pelvis with disruption occurring through the pubic symphysis and sacroiliac joint(s).

In order for the correct transmission of forces, this mechanism would require a casualty to be standing directly on top of an IED. This was explored through a physical model with human cadavers, utilising a drop rig to apply force through the femur to the pelvis. In this experimental model, it was found that the resultant load preferentially resulted in fracture of the femur, with minimal load transfer to the pelvis. Only following preceding iatrogenic removal of the pubic symphysis and injury to the anterior sacroiliac ligaments was the load transfer sufficient to cause dislocation of the sacroiliac joint on the ipsilateral side of the pelvis. The results of the physical model experiments led to the conclusion that axial load was an unlikely mechanism of injury in pelvic blast.

The research went on to explore this further by means of a Finite Element (FE) model of the pelvis, to recreate and expand upon the physical model experiments. Based upon this FE model, it was concluded that axial load alone was unlikely to cause significant disruption of the pubic symphysis and sacroiliac joints. FE simulations to investigate forces other than axial load

acting upon the pelvis were subsequently performed; the combination of anterior-posterior compression (APC) and a laterally displacing force created deformation patterns that were thought to cause the pubic symphysis and sacroiliac joint disruption seen in pelvic blast injury.

4.4.2 Flail Mechanism hypothesis

As described in Dr Webster's FE model, for the deformation pattern of dismounted pelvic blast injury to occur, both APC and laterally displacing forces are required. One hypothesis of the mechanism of injury resulting in these forces is through a combination of the blast wind acting on the pelvis to generate APC, with outward flail of the lower limb (generated by the same blast wind) causing a laterally displacing force. The combination of these two actions would cause the hemipelvis to displace laterally with disruption at the pubic symphysis and sacroiliac joints.

Lower limb flail has similarly been explored as the mechanism of injury resulting in TA. As discussed in the previous chapter, a significant correlation exists between TA and dismounted pelvic blast injury. This suggests that they may share the same mechanism of injury. The first widely accepted hypothesis for the mechanism of injury of traumatic amputation was described as a combination of primary blast injury resulting in diaphyseal fracture to the long bones of the femur or tibia, with the subsequent blast wind (tertiary blast injury) resulting in separation and amputation of the limb as the legs flailed outwards (Hull and Cooper, 1996). Purely primary blast injury had been seen to result in diaphyseal bone fracture (Hull, 1992), whilst blast wind in isolation (as replicated by ejecting fast jet pilots subjected to windblast,) had been seen to cause peri-articular injuries – fractures or dislocations – due to lower limb flail (Ring *et al.*, 1975). Data historical to the conflicts in Iraq and Afghanistan had shown < 2% of patients to have peri-articular TA. As such, purely lower limb flail was felt unlikely to cause TA and the theory of primary blast injury mechanism resulting in diaphyseal fracture, with subsequent

lower limb flail (tertiary blast injury) caused by the blast wind resulting in TA, was proposed (Hull, 1992; Hull *et al.*, 1994; Hull and Cooper, 1996).

More recently, the flail mechanism in isolation as a cause of TA was re-explored. Singleton 2013 reviewed the UK JTTR to identify and review the post-mortem CTs of casualties that had sustained TA (Singleton *et al.*, 2014). 146 cases sustaining 271 TAs were identified. There were 71 fatalities sustaining 141 TAs which subsequently went on to have post-mortem CTs. Singleton 2013 found that almost 1 in 4 of the post-mortem group sustained through-joint TA and that of these, 3 in 4 had either no associated fracture or a fracture remote from the level of amputation – an injury pattern not explained by the shock-wave mechanism of injury and inferring the lower limb flail mechanism in isolation (Singleton *et al.*, 2014). Furthermore, no link (as previously described) between traumatic amputation and traumatic blast-lung injury (as occurs in casualties of primary blast injury) was seen. The authors did note that although modern blast-injury data do not support a link between significant primary blast injury and TA, there is insufficient evidence to discount previous TA mechanism theories; however, their findings contrasted with the previously accepted theory of TA.

To explain both injury patterns of TA associated with diaphyseal shaft fracture and of TA associated with through-joint injury, the authors proposed the hypothesis that the position of the casualty in relation to the explosive is the causative factor as to whether diaphyseal fracture with TA or through-joint TA occurs. In both scenarios, however, lower limb flail secondary to tertiary blast was a required injury mechanism. With the strong correlation of TA to dismounted pelvic blast injury, lower limb flail is again implicated as a possible mechanism of injury and necessitates further investigation within this thesis.

4.4.3 Sand Blast Hypothesis

Secondary blast injury is responsible for extensive soft tissue injury in victims of a dismounted blast, including fragmentation wounds and degloving injuries (Ramasamy, A. Hill, *et al.*, 2011). Whilst secondary blast injury from energised fragments has been clearly identified as a significant contributor to mortality, the contribution of energised environmental debris (soil, sand, and gravel) to injury patterns of the dismounted blast injury casualty is not known. With displacement of large volumes of soil or sand, blast wind and fragmentation may be severe enough to damage or displace the pelvis via a ‘sand blast’ effect. The process by which a blast casualty is injured by high velocity soil or sand has not been investigated previously. Although less implicated from current research than the flail mechanism, the sand blast hypothesis is supported as a possible contributing factor to the injury pattern of dismounted pelvic blast, for which further investigation within this thesis will be performed.

4.5 Conclusion

The hypotheses of both lower limb flail and sand blast mechanisms of injury warrant further review. The first step towards understanding the mechanism of injury in dismounted pelvic blast is to reproduce it within a physical model. Multiple platforms and physical models upon which to investigate blast injury have been described; these will be explored in the following chapter.

Chapter 5

Dismounted Pelvic Blast Injury: Experimental Platforms and Models

5.1 Scope of the chapter

Chapter 3 showed that dismounted pelvic blast injury casualties are at a significant risk of non-compressible pelvic vascular injury, unstable pelvic fractures, perineal injury, and traumatic amputation. Chapter 4 highlighted that the mechanism of injury is not known and discussed several hypotheses, including lower limb flail and sand blast. The next step in this thesis was therefore to investigate these potential mechanisms of injury. Chapter 5 reviews and assesses the suitability of different experimental platforms and human surrogate models for investigating blast injury, as well as their applicability to exploring these hypothesised mechanisms of injury. The chapter starts by discussing the advantages and disadvantages of each platform, before focusing on suitable experimental human surrogate models for use within these platforms. The chapter goes on to discuss the statistical methodology used in injury-risk analysis and its application in subsequent experiments. The chapter finishes by listing the most suitable experimental platforms, human surrogate model, and statistical analysis methods to investigate the hypothesised mechanisms of injury in dismounted pelvic blast.

5.2 Platforms to investigate blast injury

Multiple different research platforms have been developed to investigate blast injury. This is in part due to the complex and destructive nature of blast. Whilst field studies utilising explosives are useful for investigating certain aspects of blast injury, as will be discussed, they pose distinct challenges and limitations that restrict their use. To overcome these limitations, blast-injury mechanisms (primary to quaternary) must be de-coupled to be reproduced in a controlled laboratory environment. Several platforms that allow this will now be discussed, including their individual advantages and disadvantages. These include:

- Shock tube system
- Gas gun system
- Free-field blast testing
- Drop towers
- Under-body blast simulators
- Miscellaneous platforms
- Computational modelling

Following review, the platforms most suitable to investigate each hypothesised mechanism of injury of dismantled pelvic blast are discussed.

5.2.1 Shock Tube

The shock tube is the most widely used research platform for generating the pressure profile of a blast wave (T.-T. Nguyen *et al.*, 2018). The specification of each shock tube varies across research centres. The Imperial College London shock tube consists of a 3.8m long, stainless steel, air-driven system with a 60mm internal bore (Figure 18 a). To generate a wave, the driver section of the shock tube is first charged to a predetermined pressure. This pressure is

maintained within the driver section by mylar diaphragms in the diaphragm assembly. On the opposite side of the diaphragm assembly is the driven tube, which is maintained at ambient pressure. Upon rupture of the diaphragms, these high- and low- pressure regions are connected. This generates a blast wave which travels rapidly along the driven section of the shock tube to exit and impact with the specimen mounted in the adaptor platform at the end of the tube. As discussed in chapter 2, a blast wave consists of an initial area of over pressure (the peak pressure, also referred to as ‘the shock front’) followed by a sustained period of pressure (a period of varying duration and impulse, also referred to as ‘the blast wind’). The shock tube is capable of altering these three variables to tailor a blast wave of the user’s choosing (for example, replicating an open, partially confined or fully confined blast), in a well-controlled and reproducible fashion (Figure 18 b). The Imperial College London shock tube is capable of delivering blast waves with peak blast overpressure ranging from 0.5 to 10 bar. With size limitations, shock tubes are suitable for use to study the effects of blast on small animal models, excised organs or tissues, and cell cultures (Eftaxiopoulou *et al.*, 2016; Logan *et al.*, 2018; Vogel *et al.*, 2019). In this manner, the shock tube is able to reproduce primary (the blast wave) and tertiary (displacement of the body in relation to itself or its surroundings) blast injury. Researchers have attempted to reproduce secondary blast injury with a shock tube system but have been unable to create the projectile velocities encountered during blast, due to poor coupling between the pressure wave and projectiles: a large-scale shock tube coupled with glass generated fragments with impact velocities only ranging from between 8 – 35 m/s (Hayda *et al.*, 2004).

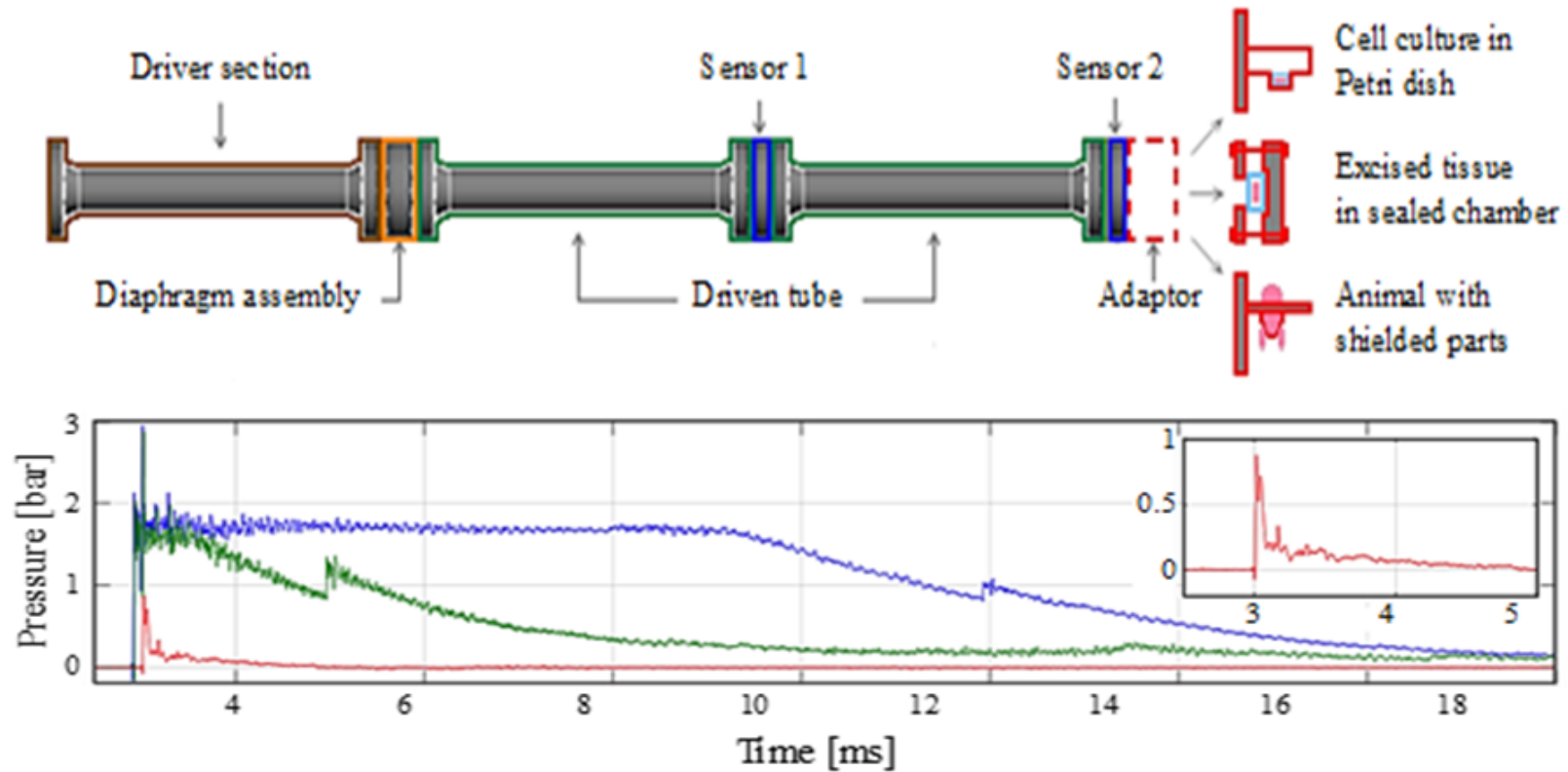


Figure 18: (a, top) Schematic of the Imperial College London shock tube, with adaptors for use with cell, tissue, or small animal research. (b, bottom) Examples of different blast wave pressure profiles with varying peak pressure, duration and impulse (Nguyen *et al.*, 2018, figure reproduced with permission).

5.2.2 Gas Gun

The gas gun system is capable of delivering projectiles at high velocity, replicating the effects of secondary blast injury. Gas gun systems have been used to test the mechanical behaviours of materials and to study penetrating injuries by blast fragments (Randjbaran, 2013; Nguyen *et al.*, 2020). The Imperial College London gas gun consists of a 32 mm internal bore single-stage system with a breech capable of charging up to 200 bar-litre with compressed air or helium (Figure 19). To accelerate the chosen projectile, the reservoir section of the gas gun is charged to a predetermined firing pressure. Similar to the shock tube, the pressure is maintained within the reservoir section by mylar diaphragms. This utilises a priming section which is charged to a low pressure, which lowers the pressure gradient across the mylar diaphragm (containing the reservoir system) and prevents it from rupturing early. At the point of initiating firing of the gas gun, the pressure in the prime section is vented. This increases the pressure gradient across the mylar diaphragm and results in rupture, with release of the pressurised gas. This pressurised gas then accelerates a projectile-carrying sabot through a 3-metre-long barrel to achieve the desired velocity as it enters the target chamber, the velocity of which is proportional to the reservoir pressure chosen. The system needs to accommodate projectiles of different sizes and dimensions (e.g., a fragment simulating projectile, or a mass of sand), which can be achieved through modifying the sabot delivery system. Modifications to the sabot including varying vessel size or customised front plates. The sabot is separated from the projectile as it enters the target chamber by means of impact with the sabot stripper - a customised block of stainless steel with a central passage for the projectile. This device stops the sabot, whilst allowing passage of the projectile of choice through the central passage. The Imperial College London gas gun is capable of accelerating projectiles to speeds of up to 600 m/s. Size limitations of the sabot and delivery barrel ultimately limit the size of the desired projectile. As such, the gas gun

system is suitable to study the effects of high velocity projectiles on small animal models, or excised organs and tissues (Nguyen and Masouros, 2019; Nguyen *et al.*, 2020).

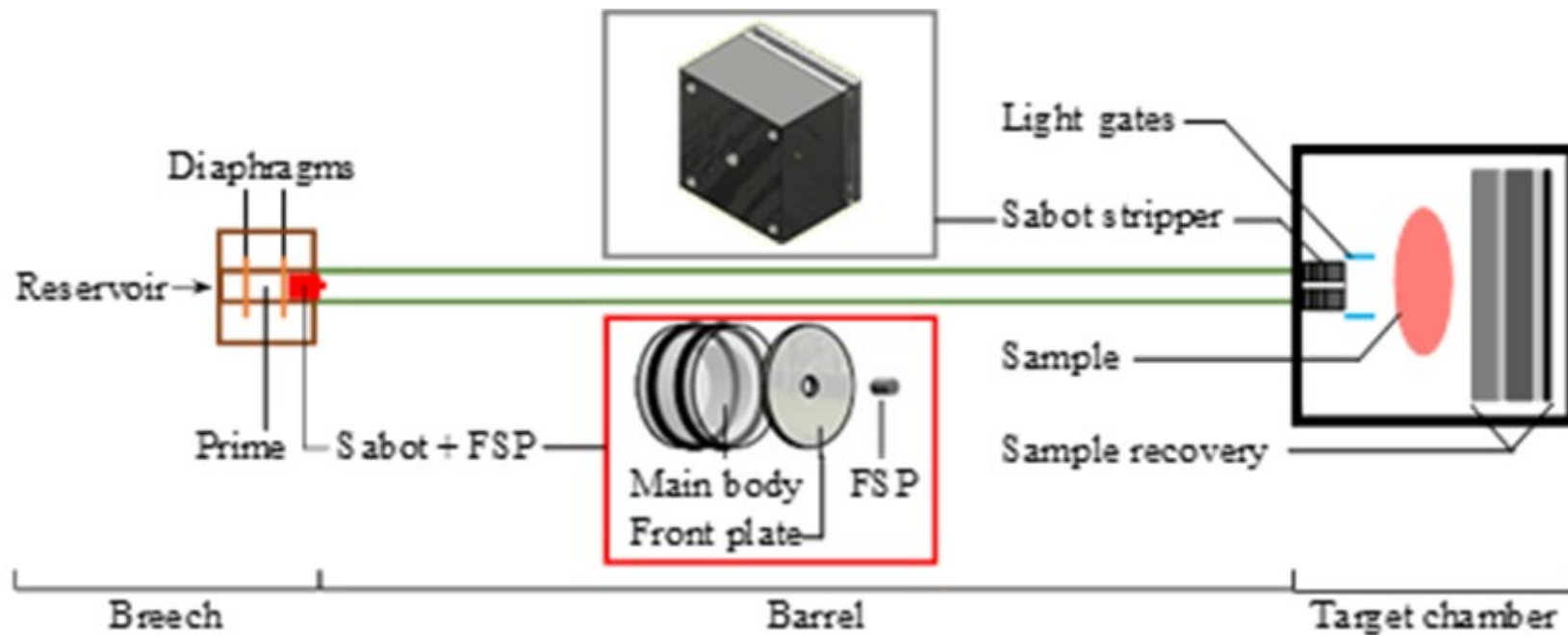


Figure 19: Schematic of the Imperial College London gas gun, with sabot adapted for delivery of a small, metallic fragment simulating projectile (FSP) (Nguyen *et al.*, 2018, figure reproduced with permission).

5.2.3 Free-field blast testing

Free field blast tests utilise explosives detonated in an open space, generating a blast wave to then assess its characteristics (Figure 20). They are principally used in the assessment of large-scale targets, such as vehicles or infrastructure, or to assess mortality thresholds. They have been used to provide a substantial database of information regarding mortality thresholds of small to medium sized animal species and how these relate to the human (D. R. Richmond *et al.*, 1962; Bowen *et al.*, 1968). The destructive nature of these tests makes them unsuitable for assessing injury specifics, due to the associated difficulties with accurate instrumentation, reliability and reproducibility (Risling *et al.*, 2012). Blast tests utilising small charges within partially confined chambers have been used to assess the effects on smaller targets, however, these present the same difficulties described (Bauman *et al.*, 2009).



Figure 20: Aerial photograph of 5000 kg trinitrotoluene (TNT) detonated to investigate blast effects (TNO Defence Security and Safety, 2020, figure reproduced with permission).

5.2.4 Solid-blast injury platforms

Several platforms have been developed to study the effect of solid-blast injuries. These injuries include crush injuries obtained through tertiary blast effects, and those obtained from a mounted under-body blast (a further contributor to the tertiary blast injury category).

5.2.4.1 Drop tower

The drop tower system can be used to study injuries caused by blunt impact, evaluate the impact strength of different materials, and characterise tissue at high strain rates. The system consists of a mass dropped in a vertical channel from a pre-determined height to strike a specimen mounted on a base plate (Figure 21a). The energy delivered at impact is related to the weight of the mass and the height from which it is dropped (Figure 21b).

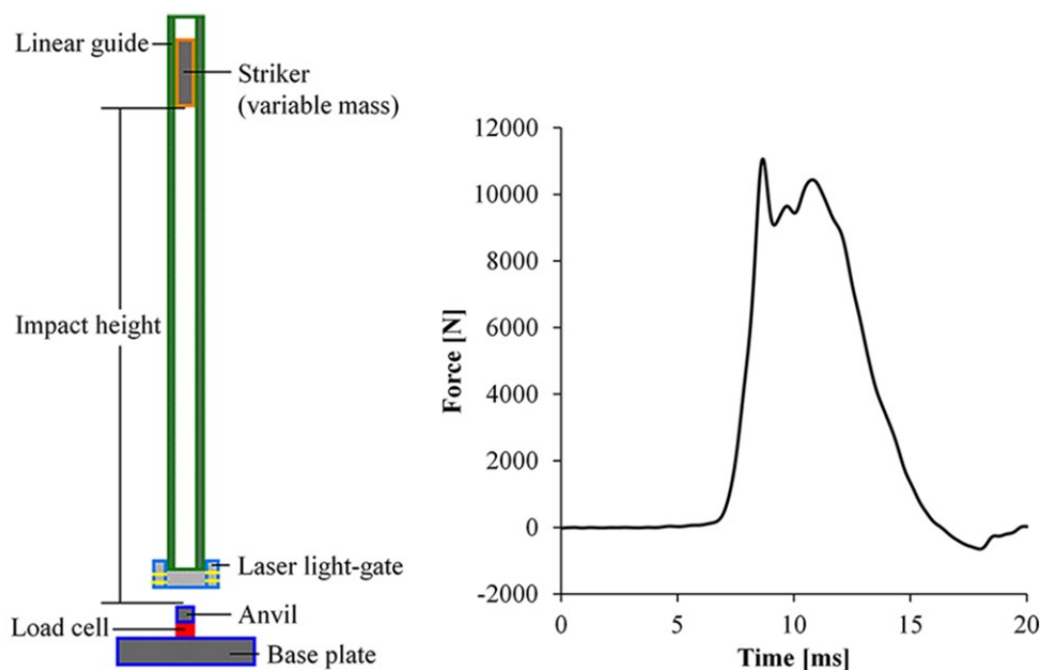


Figure 21: (a, left) Schematic of Imperial College London drop tower. (b, right) Typical force-time response curve (Nguyen *et al.*, 2018, figure reproduced with permission).

The drop tower is suitable to study the effects of solid-blast crush injuries on specific anatomical regions through quantifying both loading and compressive tolerances (Stemper *et al.*, 2015; Carpanen *et al.*, 2019). It is not suitable for assessing the dynamic mechanism of injury hypothesised with lower limb flail nor for recreating sand blast.

5.2.4.2 Under body blast simulators

Under body blast simulators are bespoke pieces of equipment designed with the aim of delivering the acceleration pulses seen in under body blast to individual anatomical regions or whole post-mortem human surrogates (Figure 22). The biomechanical responses of the relevant body region can then be extracted through sensors attached at specific locations on the specimen, including accelerometers, strain gauges and load cells.

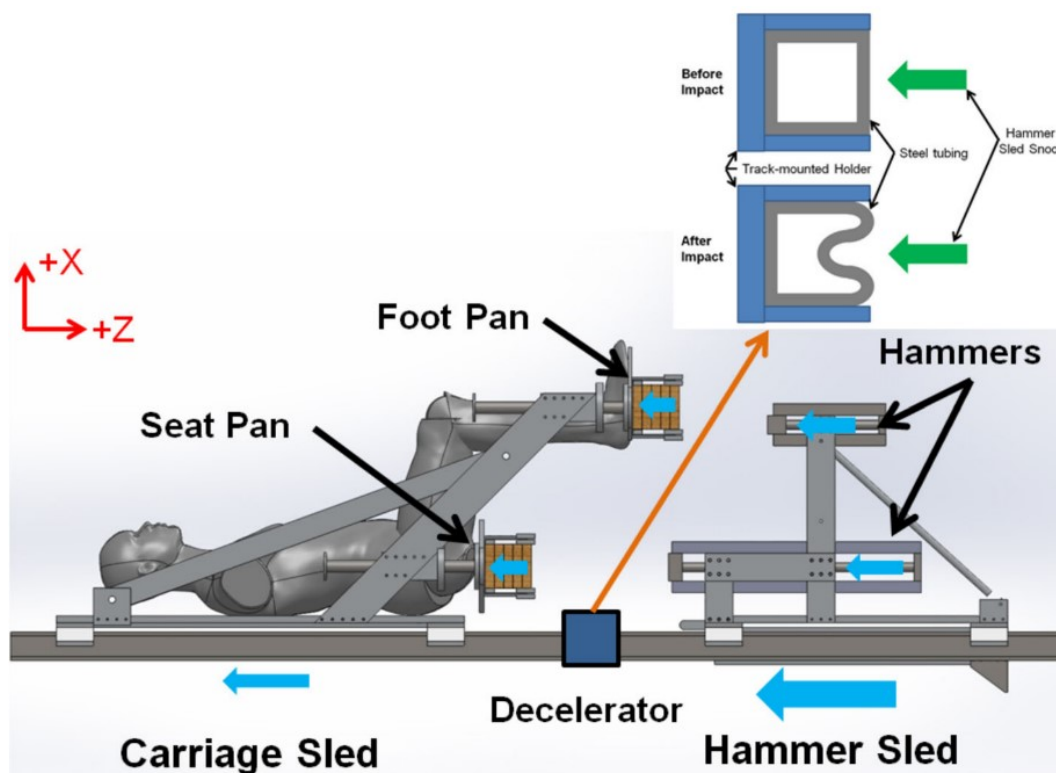


Figure 22: Schematic of an under-body blast simulator. (Bailey, Christopher, *et al.*, 2015, figure reproduced with permission).

Numerous under body blast simulators are in use; however, their suitability is limited to the mounted casualty and as such they are not explored further within this thesis (Yoganandan *et al.*, 1996, 2015; Dosquet, 2004; McKay and Bir, 2009; Quenneville *et al.*, 2011; Masouros *et al.*, 2013; Bailey, McMurry, *et al.*, 2015; Danelson *et al.*, 2015).

5.2.5 Miscellaneous

The Split-Hopkins Pressure Bar is used to generate a longitudinal stress wave in order to study the effects of blast loading on biological tissues and cells (Chen *et al.*, 2019). Whilst used widely in this regard, it is not suitable to investigate the mechanisms of injury of dismounted pelvic blast. Other platforms including laser induced stress waves and high-pressure jet streams have been described to study specific aspects of blast-induced organ damage; their use is similarly limited and as such they also are not explored further within this thesis (Fung *et al.*, 1985; Satoh *et al.*, 2010).

5.2.6 Computational modelling

Several computational models are available to investigate injury biomechanics. Of these, finite element analysis (FEA) is the most widely used for the analysis of solid mechanics. FEA was developed for stress analysis of large objects with complex geometry. The analysis involves obtaining the geometry of the chosen part (for example, the human pelvis) from imaging such as computed tomography or magnetic resonance imaging. From this, a computer-aided design model can be made. This model is meshed, a process by which it is split into multiple small regions – the finite elements. Material properties of known values are assigned across these elements and the initial boundary conditions (including loading) are assigned. From this, a simulation can be run, and the results interpreted. In essence, FEA enables computerised mechanical testing on structures of known material properties under a variety of specified loading conditions. In this manner, FEA is a useful platform for obtaining further information

once the correct hypothesis is known, however, it does not provide a platform for testing and drawing conclusions on novel hypotheses for which the loading conditions are not known. FEA models require validation against experimental data. No such data exists for the dismantled pelvis. The development of an FEA model would be to expand on knowledge gained experimentally. As no experimental data exists, the focus of this thesis was to generate experimental data both to aid understanding and to serve as data against which future FEA models can be compared.

5.2.7 Experimental platforms conclusion

This thesis aims to investigate two hypothesised mechanisms of injury of dismantled pelvic blast: lower limb flail and high velocity sand blast. The lower limb flail mechanism of injury hypothesises that a blast wave causes rapid limb displacement, resulting in pelvic injury. As such, the experimental platform required must reproduce a blast wave to interact with an experimental specimen with pelvis and lower limbs intact. Whilst free field blast testing may allow this mechanism to be carried out on human cadaveric tissue, as discussed, its inherent destructive nature makes it unsuitable to assess the injury specifics of this mechanism. As such, the shock tube was determined the most suitable platform for this investigation. Due to the inherent size limitations of shock tube systems, a human cadaveric pelvis with lower limbs cannot be used. As such, a suitable small animal model, with blast waves and injury thresholds scaled to the human, is required.

The high velocity sand blast mechanism of injury hypothesises that sand, soil, or other environmental debris, when propelled towards the casualty at high velocity, may be sufficient to cause injury. In particular, when large volumes of soil or sand impact with the casualty this may be severe enough to damage or displace the pelvis via a 'sand blast' effect. The gas gun system is suitable to delivery projectiles of choice at speeds of up to 600 m/s and as such is

suitable to investigate the effects of high velocity sand. Limitations of this system are similar to the shock tube, namely the equipment size allows only a small volume of sand to be propelled. As such, in order to examine the effects of high velocity sand impacting with a casualty in volumes similar to those hypothesised to occur during dismounted blast, similarly, a suitable small animal model is required.

5.3 Animal models

With the requirement for a small animal model for use in the described experimental platforms, the next step in this thesis was to review suitable animal models. Animal models have been used extensively in trauma and orthopaedic research (Martini *et al.*, 2001). Similarly, animal models have been used extensively in blast research, particularly small animal models utilising a shock tube system (Richmond *et al.*, 1959; D. R. Richmond *et al.*, 1962; Bowen *et al.*, 1968; Sundaramurthy *et al.*, 2012; Jean *et al.*, 2014; Eftaxiopoulou *et al.*, 2016). Whilst small animal models utilising a shock tube have been used to investigate blast injury, animal models have not previously been used to investigate blast injury to the pelvis. As such, a literature review was performed to identify the most suitable animal model for use, due to their similarity to the human pelvis.

Humans are the only strictly bipedal mammals (Patnaik *et al.*, 2016). Because of this, there have been significant evolutionary differences in the morphology of the human pelvis, when compared to that of non-human primates and quadrupeds. The bipedal mode of locomotion evolved in the human lineage approximately 5 – 7 million years ago (Lovejoy, 2005). This evolution brought a significant change to human anatomy – with particular reference to the pelvis. The main shift in anatomy of the bipedal pelvis from that of non-human primates and quadrupeds arises from a reduction in the distance between the hip joint and the sacroiliac joint in the bipedal pelvis. The ilium is shorter, wider, and expanded in the sagittal plane. This gives

a comparatively compressed pelvis, where the top of the sacrum comes to lie directly opposite the pubic symphysis (Schultz, 1949). The sacrum is shorter, wider, more ventrally concave and rotated anteriorly compared with non-human primates (Gruss and Schmitt, 2015). Consequently, there is a reduction in the anteroposterior (AP) diameter and a widening in the transverse diameter of the pelvic inlet, whilst the pelvic outlet is greatest in the AP diameter (Rosenberg, 1992; Patnaik *et al.*, 2016). This gives the bipedal birth canal a ‘twisted’ channel, through which a neonate must rotate to facilitate exit (Trevathan, 2015). This expansion is partly accomplished by lengthening and upward rotation of the pubic rami (Häusler and Schmid, 1995; Simpson *et al.*, 2008). These changes are associated with shortening and flaring of the ischia, with a consequent wider subpubic angle (Gruss and Schmitt, 2015). This feature is not present in quadrupeds or non-human primates. Similar to the quadruped, non-human primates have pelvic inlets and outlets longer in AP diameter than in transverse, and a comparatively elongated pelvis. The ilium lies lateral and parallel to the vertebral column, with the lower lumbar vertebrae adjoined to the ilium. In the bipedal pelvis, the shorter iliac blades serve to lower the centre of mass and avoid entrapment of the lumbar vertebrae, allowing a lumbar lordosis posture to aid in upright walking. Further to this, the iliac blades are rotated in orientation from the coronal to sagittal plane. This allows the gluteal muscles – primarily gluteus medius – to cross laterally over the hip, making them abductors rather than extensors and allowing them to play a significant role in pelvic balance and bipedal walking (Gruss and Schmitt, 2015). Non-human primates are not strict bipedal mammals, spending a significant period of their time in a quadrupedal posture. As such, their pelvis shares more in common with that of the quadrupedal pelvis (Figure 23).

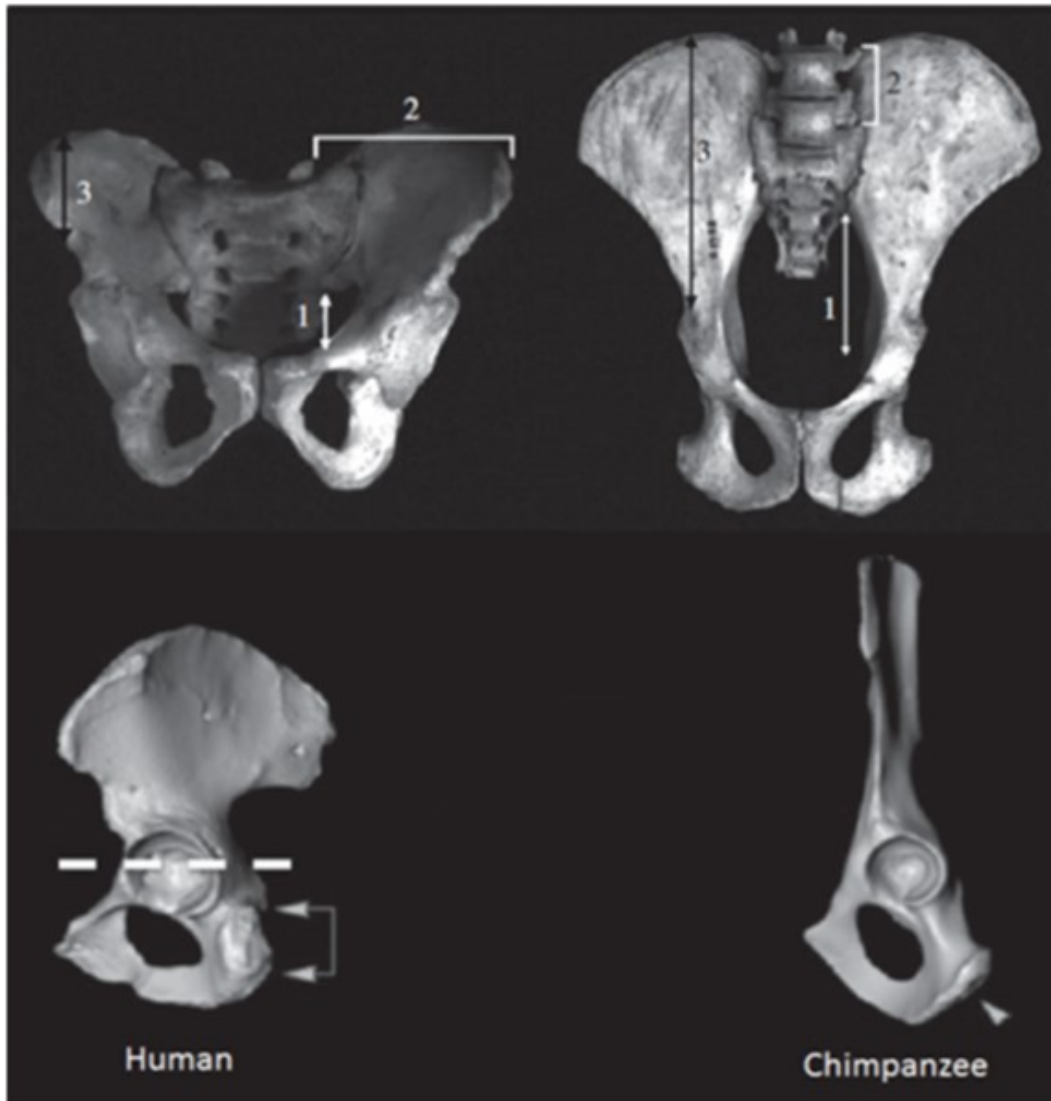


Figure 23: Comparative anatomy of the human and chimpanzee pelvis. Adapted from (Gruss and Schmitt, 2015, figure reproduced with permission)

As discussed earlier in this chapter, human cadavers are too large for further investigation utilising the shock tube or gas-gun systems. Similarly, non-human primates (such as chimpanzees) are too large to be used in either system. Furthermore, availability of both human cadaveric material and non-human primate specimens is limited. Due to the size restrictions and availability limitations of both human cadavers and non-human primates, further consideration was given the most suitable small animal quadruped pelvis.

5.3.1 The small animal quadruped pelvis

As previously discussed, in the mechanically unstable pelvic injury patterns of the dismantled blast injury casualty, there is most commonly disruption of the pubic symphysis and sacroiliac joints. To identify the most suitable pelvic small animal model, attention was subsequently focused upon these joints for similarities to the human pelvis.

When reviewing the mammalian pubic symphysis, it can broadly be broken down into three categories. These three categories are based on whether the innominate bones are (1) fused, (2) connected by a ligamentous band, or (3) separated by cartilage at the symphysis (Ruth, 1932). As described in chapter 2, the human pubic symphysis consists of a fibrocartilaginous disc compressed between the articular surfaces of the pubic bones. This is a relatively unique joint amongst animal species, however, a primarily fibrocartilaginous joint has also been observed in, mice, female guinea pigs and female bats (Gamble *et al.*, 1983; Steinetz *et al.*, 1983; Ortega *et al.*, 2003). This is thought to be an adaptation to pregnancy, with this joint transforming into a flexible and elastic interpubic ligament in response to the hormone relaxin (Knobil and Neill, 2006). Of note, mice and humans are the only animal species for which a fibrocartilaginous joint is seen in both females and males (Ortega *et al.*, 2003). Other quadruped pubic symphyses consist primarily of hyaline cartilage (Dyce *et al.*, 2010).

There is little information published on the sacroiliac joints of the female bat and guinea pig, whilst the sacroiliac joints of the mouse are a recognised animal model in the investigation of sacroiliac joint disease (Shi *et al.*, 2003; Redlich *et al.*, 2004; Hayer *et al.*, 2010; Uderhardt *et al.*, 2010; Treuting *et al.*, 2018; Grunstra *et al.*, 2019). The sacroiliac joints of the mouse are atypical synovial joints, similar to that of humans, for which the tissues are similar between species (Zhang, 2003; Treuting *et al.*, 2018). The similarity of the pubic symphysis and

sacroiliac joints, in addition to the increased availability of mice compared to female bats or guinea pigs, made the mouse the small animal model of choice for further review.

The main morphological differences of the mouse to the human pelvis are that the mouse ilia are larger in the axial plane, whilst shorter in the sagittal and coronal planes. In addition, the pubic rami are shorter compared to those of humans. As such, the human pelvis is comparatively compressed in the axial plane respective to the mouse (Figure 24).



Figure 24: Radiograph of a mouse pelvis and lower limbs.

When focusing on lower limb flail as the mechanism of injury, these morphological differences are minimised in the upright posture for which the angle of rotation at the hip is similar between the species. Further consideration must also be given to the respective forces of the mouse femur relative to the human femur, acting upon the pelvis. The mouse femur accounts for 15.1% of total skeletal length, whilst the human femur is comparatively heavier and accounts for

26.7% of total skeletal length (Feldesman *et al.*, 1990; Di Masso *et al.*, 2004). As such, a proportionally greater moment could be expected to act upon the human pelvis during blast-induced lower limb flail compared to the mouse. These factors will be considered in any subsequent experiments and the potential impact on outcomes examined.

The pelvic vasculature of the mouse follows that of the human; the common iliac artery arises from the aorta before branching to give the internal and external iliac arteries (Figure 25). This contrasts with several other animal species whereby the external and internal iliac arteries arise directly from the aorta (Kochi *et al.*, 2013). The murine arterial and venous system is histologically similar to that of humans. The only difference arises in the presence of vasa vasorum, which can be found in the elastic artery wall of humans but not mice; they are required to supply the inner portion of the arterial wall (which exceeds the diffusion limit), and are not found in smaller, murine arteries (Treuting *et al.*, 2018).

The mouse was therefore chosen as the appropriate animal model for this research as:

- It has a fibrocartilaginous pubic symphysis, as in the human
- The sacroiliac joints of the mouse are similar, and a recognised animal model in investigation of sacroiliac joint disease
- The pelvic vasculature system is similar, for which it follows the same course as that of the human
- In the upright posture, the angle of rotation of the hip is similar between species
- The bony anatomy on radiographs is similar, excluding the mouse pelvis being comparatively elongated compressed in the axial plane

Due consideration will be given and discussed when inferring the results and conclusions of any findings for subsequent interpretation to human injury risk.

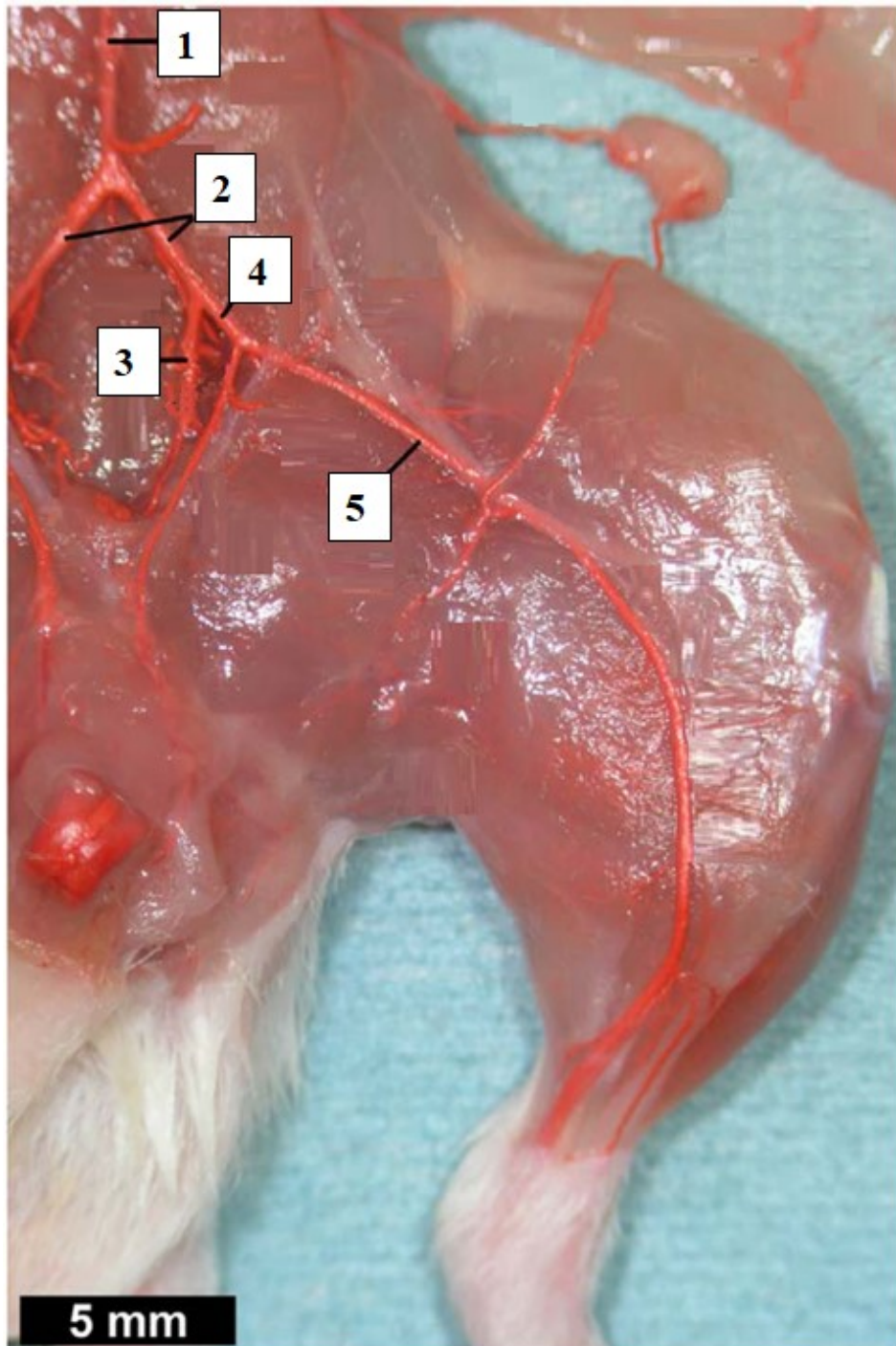


Figure 25: Dissection of the pelvic arterial vasculature and medial-superficial hindlimb of a mouse specimen, with arteries dilated and fixed with red coloured resin. (1) aorta, (2) common iliac arteries, (3) internal iliac artery, (4) external iliac artery, (5) femoral artery. (Adapted from Kochi *et al.*, 2013, figure reproduced with permission).

5.4 Injury risk evaluation

Following recreation of the mechanism of injury of dismounted pelvic blast, an evaluation of injury risk to modifiable variables is required in order to develop mitigation strategies. Injury-risk curves provide a statistical method to analyse these and are used frequently to evaluate outcome measures in injury biomechanics. They define the probability of any given injury as a function of an injury criterion (Figure 26). An injury criterion is defined as a parameter which correlates with the injury of the body area under consideration, for a specific loading condition. Parameters that can be measured when testing could include, for example, linear acceleration experienced by a body part, the global forces or moments acting on the body, or the velocity of an injuring projectile.

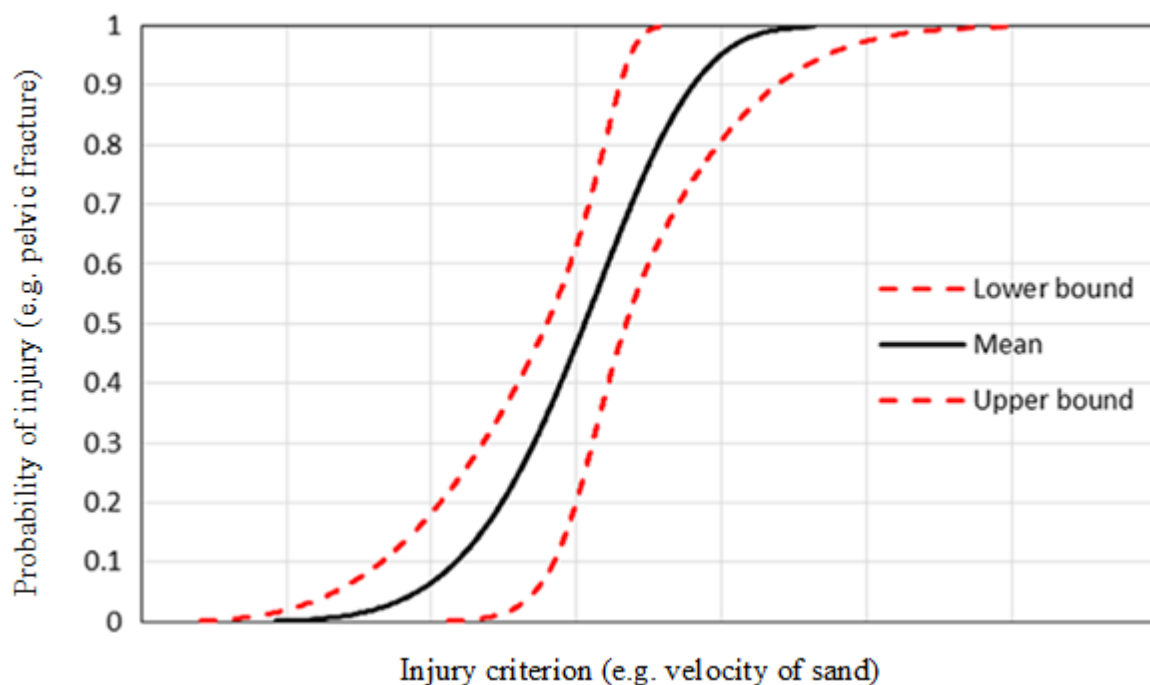


Figure 26: Example of an injury-risk curve. (Adapted from Yoganandan *et al.*, 2016, figure reproduced with permission)

The experimental outcome data of a series of experiments is used to generate these curves as part of a survival analysis. Survival analysis is a statistical technique commonly used in clinical studies to determine survival time after onset of disease. Survival analysis considers the censoring status of time as a variable (the exact time of an event may not be known, but that it falls within a known range). For the purposes of injury biomechanics, the time variable is replaced by the injury criterion of interest. This method is recommended due to its ability to accommodate this differing censor status which incorporates biomechanical rationale better than simple sensor data. (Yoganandan *et al.*, 2016).

The probability of risk generated by this method is shown in the equation:

$$probability\ of\ risk = 1 - \exp\left(-\int_0^x h(u)du\right)$$

The probability of risk is expressed in terms of the hazard function h , where h is the instantaneous risk of injury and $h(u)du$ is the probability of a subject being injured between u and $u + \Delta u$, given that the subject is not injured until u (the injury criterion value) (Petitjean *et al.*, 2015). For each analysis, the distribution of the risk probability is assumed. Examples of distribution are log-normal, log-logistic, and Weibull. For a Weibull distribution, the hazard function is continuously increasing with the loading severity according to the shape and parameter coefficients (k and λ) generated by the data such that:

$$probability\ of\ risk = 1 - \exp\left(-\left(\frac{x}{\lambda}\right)^k\right)$$

As such, the injury curve can be reported by stating the distribution type and coefficients.

The injury-risk curve represents the best estimate of the probability of risk. Depending upon samples size, censoring status, and distribution of the test data relative to the curve, confidence intervals to the curve may vary. Confidence intervals are calculated using the

same methodology as the curve with the normal approximation of error (Petitjean *et al.*, 2015).

In addition to providing confidence in the data levels, the confidence intervals may be used to provide a quality index of the injury curve for a given metric. A normalised confidence interval size (NCIS) may be generated by dividing the difference between the upper (95%) and lower (5%) confidence intervals by the size of the estimated probability at that level. The NCIS provides a simple index of the validity of that injury curve at each level of risk. Categories of quality index based on the NCIS include good (NCIS 0 to 0.5), fair (NCIS 0.5 to 1), marginal (1 to 1.5) and unacceptable (over 1.5) (Petitjean *et al.*, 2015).

5.4.1 Scaling of animal models

For appropriate interpretation of injury risk evaluation in animal research, scaling is required. Scaling is the process by which the dose (input) and response (output) of an animal model is adjusted, such that the clinical outcomes of an animal model can be translated to the human equivalent. Input variables may be modified based on physical parameters, such as animal size, whilst output variables may be modified based upon differing pathology, or pathophysiology, of the species. Scaling methods are based upon the assumption that successfully scaling the dose between species will result in a similar response between species (Panzer *et al.*, 2014). Blast tolerance in small and large animal models, and how they scale to the human, have been described extensively in relation to pulmonary blast literature, where a strong correlation between animal size and blast injury tolerance (with regards traumatic blast lung injury) has been established (Bowen *et al.*, 1968). Scaling laws for other traumatic variables in small animal models in blast may consider factors such as force, mass and velocity (Panzer *et al.*, 2014).

5.5 Chapter Conclusion

On the basis of this chapter, it can be concluded that 1) the shock tube and gas gun systems are appropriate platforms to investigate dismounted pelvic blast injury (investigating the hypothesised mechanisms of injury of lower limb flail and high velocity sand blast respectively), 2) the mouse is an appropriate animal model for use in these investigations, and 3) injury curves can be used to quantify the risk based on specific parameters. The first mechanism of injury to be investigated in this thesis is lower limb flail; this will be explored in the following chapter.

Chapter 6

Mechanisms of Injury: Lower Limb Flail in the Mouse Model

This chapter is published in part:

Rankin, Iain A., Nguyen, T. T., Carpanen, D., Clasper, J. C. and Masouros, S. D. (2019)

‘Restricting Lower Limb Flail is Key to Preventing Fatal Pelvic Blast Injury’, *Annals of*

Biomedical Engineering, 47(11), pp. 2232–2240.

6.1 Scope of the chapter

Chapter 4 discussed the hypothesised mechanisms of injury which may contribute to the dismantled pelvic blast-injury patterns described in Chapter 3. These mechanisms included lower limb flail and high-velocity sand blast. Chapter 5 showed that the shock-tube system was an appropriate platform, and the mouse an appropriate model, to investigate the hypothesised lower limb flail mechanism of injury. In this chapter, lower limb flail as a mechanism of injury in the dismantled pelvic blast casualty is investigated. A novel experimental setup utilising a mouse model of dismantled pelvic blast injury with a shock-tube mediated blast wave is described. Blast-mediated lower limb flail is reproduced and subsequently limited to assess its association with unstable pelvic fracture patterns and vascular injury. An injury-risk curve is

developed to associate restriction of lower limb flail to the probability of vascular injury. Associated traumatic amputation is noted and the relationship between traumatic amputation and pelvic injury following blast is discussed. To decouple the effect of the wave itself from that of the resultant lower limb flail on pelvic injury, pre-blast surgical amputation at the hip or knee was performed. The chapter describes these findings before concluding on the association of lower limb flail to dismantled pelvic blast injury and advising the subsequent research direction of this thesis.

6.2 Introduction

Chapter 3 highlighted pelvic vascular injury as the leading cause of mortality in the dismantled pelvic blast injury casualty. The mechanism by which blast in the dismantled casualty leads to pelvic vascular injury is not known. As discussed in Chapter 4, for the deformation pattern of dismantled pelvic blast injury to occur, both anteroposterior compression (APC) and laterally displacing forces acting upon the pelvis are required. One mechanism of injury hypothesised to cause these forces is a combination of the blast wind acting on the pelvis to generate APC, in addition to outward flail of the lower limb (generated by the same blast wind) causing a laterally displacing force. The combination of these two actions would cause the hemipelvis to fracture and displace laterally, with disruption at the pubic symphysis and sacroiliac joints. This mechanism of injury – blast-mediated lower limb flail – has not previously been investigated in a physical experimental model. In addition to being implicated in pelvic blast injury, lower limb flail has also been suggested as a mechanism of injury in traumatic amputation. Traumatic amputation strongly correlates with blast-mediated pelvic fracture and suggests their mechanisms of injury may be linked.

As discussed in Chapter 5, the shock-tube apparatus utilising a mouse model is a suitable experimental setup to study this mechanism of injury. If this can be reproduced, injury-risk

analysis can be performed to evaluate the risk of pelvic vascular injury to any modifiable variables identified, such as the degree of lower limb flail.

As such, the aims of the study described in Chapter 6 were (1) to replicate dismantled pelvic blast injury in the mouse model utilising a shock tube mediated blast wave, (2) to investigate a link between pelvic injury and traumatic amputation in the context of blast-mediated lower limb flail, and (3) to evaluate the effects of restricting lower limb flail on mitigating the severity of pelvic bony and vascular injury. The hypothesis was that unstable, displaced pelvic fracture patterns and pelvic vascular injury are associated with blast-wave mediated lower limb flail and are linked to traumatic amputation.

6.3 Methods

Animal experimental design and procedures were carried out in compliance with the UK Animal (Scientific Procedures) Act 1986. Shock tube testing was conducted on fresh-frozen cadaveric male MF-1 (outbred, ex-breeder, wild type) mouse specimens (8 – 9 weeks of age, Charles River Ltd, UK). Mice were chosen at 8 – 9 weeks of age due to the availability of ex-breeder sexually mature male mice at this age range. Specimens were stored at -20°C and subsequently thawed at room temperature ($21\pm 2^{\circ}\text{C}$) for 3 – 4 hours prior to testing. Mice were secured on a stainless-steel platform, distal to the outlet flange of the Imperial College London double diaphragm shock tube (Nguyen *et al.*, 2014). Three cable ties were applied to secure specimens in position – across the abdomen, thorax, and neck – whilst allowing free range of motion of the lower limbs. A fenestrated steel fence was attached to the platform's central restraint, positioned at varying angles from the midline, to restrict outward flail of the lower limb (Figure 27 a). The main cohort of 103 mice had tests conducted with the steel fence at 45° , 60° , 90° , 105° , 135° , and unrestricted (180°), as measured of each side from the midsagittal plane (Figure 27 b).

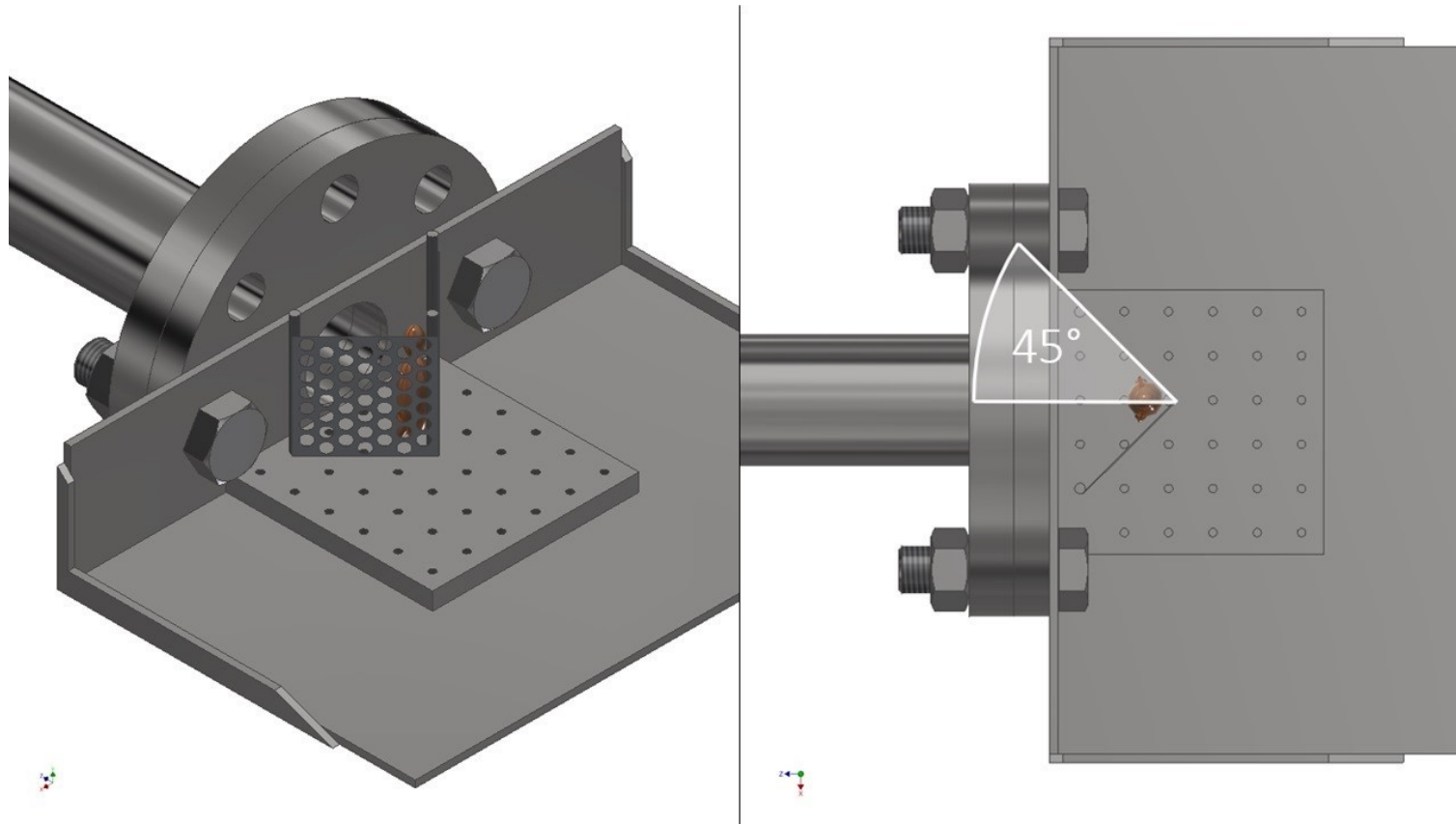


Figure 27: (a, left) shock tube with mounting platform, fenestrated steel fence restricting lower limb flail, and position of mouse (represented with model). (b, right): aerial view with restriction of lower limb flail to 45° group, demonstrating the angle as measured from the midsagittal plane.

Scaling of the blast wave

The lethal median dose (LD₅₀), causing fatal TBLI in the mouse is reached at shock-tube plateau pressures of 29.0 – 30.7 psi with durations of 3 – 6000 ms (Richmond *et al.*, 1959, 1961; D. R. Richmond *et al.*, 1962; D. Richmond *et al.*, 1962). These values were taken to be the upper limit of the blast wave for use within this study. As will subsequently be discussed, the chosen shock wave was representative of a blast wave falling below the LD₅₀ observed in previous studies to cause fatal TBLI, but a sufficient insult to cause pelvic vascular transection due to lower limb flail.

Traumatic amputation

In order to investigate both the influence of limb flail and traumatic amputation on pelvic injury, 40 mice were assigned to one of three further groups: bilateral amputation at the hip, bilateral amputation at the knee, and bilateral traumatic above knee amputation. The hypothesis was that lower limb flail was essential to cause pelvic injury, and that the injury caused to the pelvis from lower limb flail would occur prior to traumatic amputation (with loss of the lower limb). As such, it was hypothesised that 1) bilateral amputation at the hip would result in no vascular injury (due to complete loss of the lower limb flail mechanism, with interaction of the mouse pelvis to the blast wave only), 2) bilateral amputation at the knee, as may occur if a below knee traumatic amputation occurred prior to flail of the lower limb, may or may not result in vascular injury (dependent on if flail of the entire lower limb, or the thigh alone, is required to cause pelvic injury), and 3) bilateral traumatic above knee amputation would result in vascular injury, as the force delivered from the lower limb to the pelvis would cause pelvic injury to occur prior to loss of the lower limb (and therefore flail mechanism) during the process of traumatic amputation.

Bilateral amputation at the hip

Mice underwent bilateral lower limb amputation at the hip prior to testing, to examine the injury pattern when the effects of lower limb flail on the pelvis (and any effect on subsequent pelvic injury) are eliminated. Amputation was performed with a posterior approach to the hip joint, disarticulation of the hip, removal of the lower limb and subsequent closure with 4.0 nylon sutures (Ethilon Nylon Suture, Ethicon, New Jersey, USA).

These mice represent a negative control group: the procedures and boundary conditions of the experiment are maintained as closely as possible, except that the hypothesised effects of lower limb flail are removed entirely. The possibility of removal of the limbs altering the blast conditions was considered – a reflected wave off the lower limbs, following interaction of the lower limbs with the initial blast wave, may have been removed. A further option considered for a negative control included disarticulation of the limbs, followed by reassembling the disarticulated mouse with the legs placed beside it. This negative control would maintain the same boundary conditions – including any reflected blast wave from the lower limbs. The most suitable negative control was chosen to be complete removal of the limbs: any lost reflected blast wave – in the otherwise open environment of the blast platform – was considered negligible, whilst re-assembling the position of the limbs beside the mouse could introduce further variables such as impact of the limbs with the pelvis causing trauma.

Bilateral amputation at the knee

Amputation at the knee was performed to examine the injury pattern as may occur if a below knee traumatic amputation occurred, prior to flail of the lower limb. Amputation was performed with a through knee incision made at the patellar tendon, removal of the leg and foot, and subsequent closure with 4.0 nylon sutures. These mice were subsequently tested upon with unrestricted lower limb flail.

Bilateral traumatic above knee amputation

The third group of mice sustained a prior crushing injury to both mid-femurs to ensure that bilateral traumatic above knee amputations occurred during the blast wave experiments. A small drop tower was utilised to deliver a standardised impact (250 g striker, released from 50 cm height) to a triangular-prism-shaped anvil, placed at the mid-point of the femur (T.-T. Nguyen *et al.*, 2018). The anvil was used to produce a crush injury to the soft tissues of the thigh and a transverse femoral shaft fracture, with no disruption in skin continuity. Radiographs were taken post procedure to ensure correct positioning (mid-shaft) of the injury. These mice were subsequently tested upon with unrestricted lower limb flail.

Mobile platform

In addition, in order to investigate the effects of modifying the boundary conditions of the platform to the injuries sustained by the mouse, a third experimental group was studied utilising a mobile platform. The hypothesis was the modifying the platform from static to mobile would not alter the injury patterns seen. A total of thirty mice were included within this group. The above-described mounting platform was positioned within a sliding track, to allow a potential backwards movement from the blast wave of 5 cm.

Data acquisition

In order to allow shock wave characterisation, pulse evolution along the shock tube was monitored with piezoelectric pressure sensors (Dytran Instruments 2300V1, California, USA) positioned both within and at the outlet flange of the shock tube. Preliminary testing was performed with a piezoelectric pressure sensor at the point of impact of the mouse specimen (in place of the mouse), for shock wave characterisation.

To record and confirm the degrees of movement of the lower limbs in response to the shock wave generated, a high-speed digital video camera (Vision Research Phantom v210, Ametek; New Jersey, USA) utilising a vertical view point was used. Images were recorded at 72,000 frames-per-second at a resolution of 128 x 152 pixels.

Injury scoring

Following the tests, specimens underwent radiographic imaging (Fluoroscans InSight™-FD, Hologic Inc., USA) and subsequent dissection to identify pelvic bony and vascular injury. Fractures were classified in accordance with the Tile criteria (Tile, 1996). Vascular injuries were confirmed macroscopically during dissection. Vascular injury was defined as complete transection of a vessel, with the most proximal large vessel injury noted. 10% of macroscopically identified vascular injuries were taken for histological processing and reviewed to confirm that they were correctly identified as vascular tissue. Associated traumatic amputation and its level was also noted.

Statistical analysis and development of the risk function

NCSS statistical software was used for statistical analysis (Utah, USA). A one-way ANOVA with a Tukey HSD post hoc comparison to determine if there were differences in injury type (Tile Type B vs. Type C) between all groups of mice was performed. A Bonferroni corrected p-value of 0.0083 was used to compensate for multiple comparisons ($0.0083 = 0.05/6$). Weibull survival analysis was used to examine the association between range (angle from the midline) of lower limb flail and vascular injury. The amputation and mobile platform subgroups were excluded from this survival analysis. The Weibull regression model is $P(x) = 1 - e^{-(x/\lambda)^\kappa}$, where P is the probability of injury, x is the predictor variable, and λ and κ are the corresponding coefficients associated with the predictor variable. To derive the survivability curves, data were classified as left censored where vascular injury was present. The normalized confidence

interval size (NCIS) of the survivability curves was determined upon the ratio of the width of the CI to the magnitude of the predictor variable, at a specific risk level.

6.4 Results

Shock wave characterisation

Preliminary testing and subsequent shock wave characterisation identified a suitable shock wave to allow for pelvic injury, whilst minimising injuries deemed to be non-survivable thoraco-abdominal trauma (Figure 28).

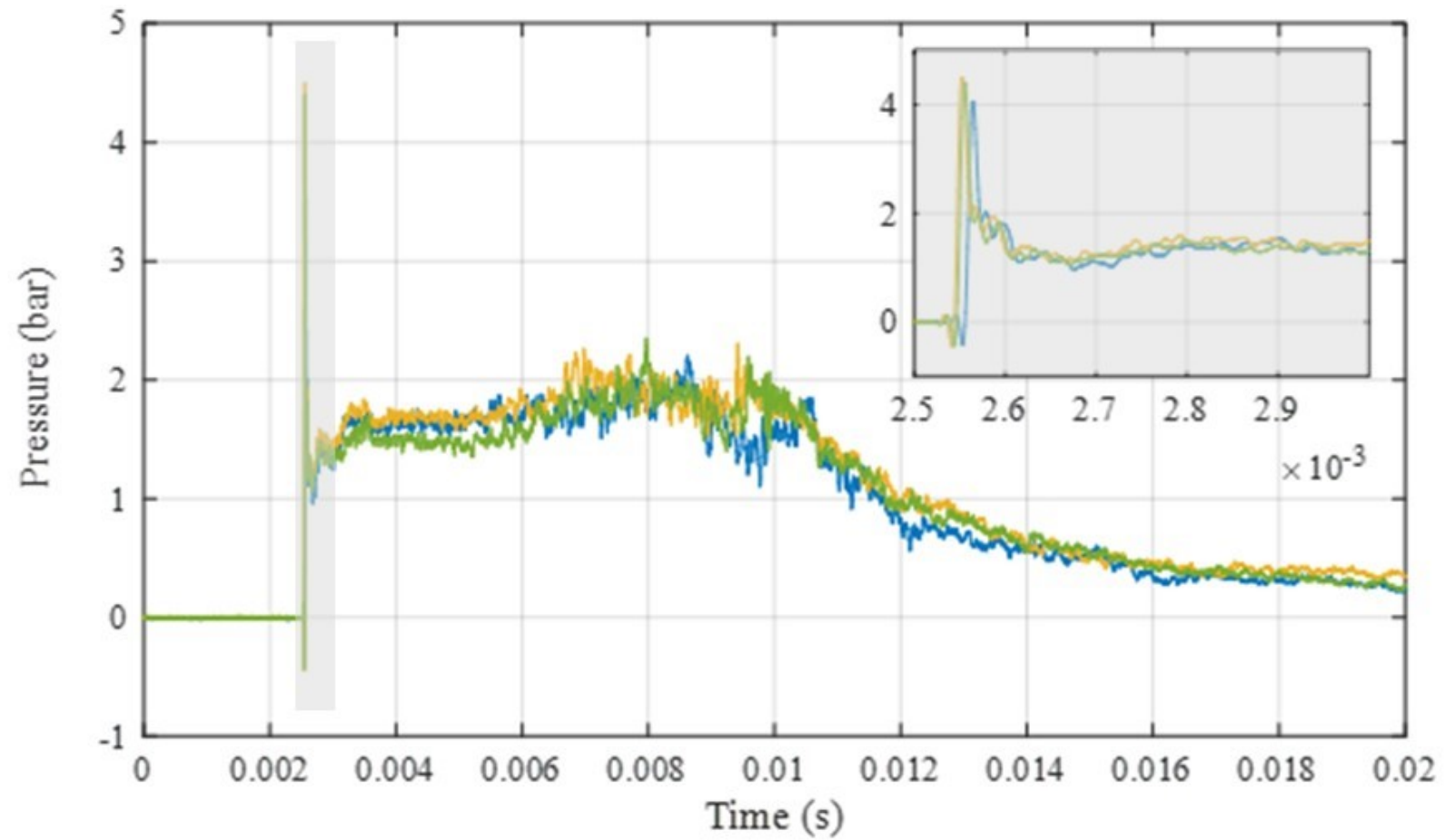


Figure 28: Three repeat blast wave characterisation tests, delivering a maximum peak pressure of 4.28 bar, mean plateau pressure of 1.72 bar, and shock impulse of 24 bar milliseconds.

Pelvic fractures

The incidence of pelvic fractures across all groups was 100%. Pubic symphysis and sacroiliac joint disruption predominated, with an incidence of 82% and 100% respectively. Table 3 details the type of pelvic fractures according to Tile criteria across all mice groups tested and the number of mice allocated to each group.

Mouse group	Number of mice	B1	B2.1	B2.2	B3	C1.1	C1.2	C1.3	C2	C3
<u>Main Cohort</u>	103	27	0	0	7	0	43	4	14	8
45° Flail	20	16	0	0	4	0	0	0	0	0
60° Flail	20	3	0	0	1	0	13	0	2	1
90° Flail	20	7	0	0	2	0	7	0	3	1
105° Flail	20	1	0	0	0	0	15	1	2	1
135° Flail	20	0	0	0	0	0	6	3	7	4
180° Flail	3	0	0	0	0	0	2	0	0	1
<u>Subgroups</u>										
Amputated at hip	20	14	0	0	6	0	0	0	0	0
Amputated at knee	10	0	0	0	0	0	2	0	7	1
Above knee TA group	10	0	0	0	0	0	3	0	6	1
Moving platform 45°	10	9	0	0	1	0	0	0	0	0
Moving platform 90°	10	0	0	0	0	0	7	0	3	0
Moving platform 135°	10	0	0	0	0	0	1	0	8	1

Table 3: Type of pelvic fractures according to Tile criteria across all mice groups.

A one-way ANOVA showed statistically significant differences between the main cohort groups with regards to fracture types (F-value = 29.16, DF = 5, $p < 0.0001$). A Tukey HSD post hoc comparison test revealed significant differences between the 45° group, who sustained entirely Type B injuries, and all other groups. Significant differences also existed between the 90° group and the 105° and 135° groups, due to a higher proportion of Type B injuries within the 90° group.

Vascular injury

Vascular injury was present in 73 (71%) of the 103 mice within the main cohort. Table 4 details the incidence of vascular injury across the different degrees of restriction of lower limb flail in the main cohort.

Mouse group	Number of mice	Vascular Injury	Aorta	Common iliac	External iliac	Internal iliac
45° Flail	20	0 (0)	0 (0)	0 (0)	0 (0)	0 (0)
60° Flail	20	14 (70)	0 (0)	7 (50)	5 (37)	2 (13)
90° Flail	20	14 (70)	0 (0)	0 (0)	^a 10 (71)	^a 5 (36)
105° Flail	20	20 (100)	6 (30)	9 (45)	5 (25)	0 (0)
135° Flail	20	20 (100)	12 (60)	8 (40)	0 (0)	0 (0)
180° Flail	3	3 (100)	0 (0)	^a 3 (100)	1 (33)	0 (0)
Total	103	73 (71)	18 (24)	^a 28 (38)	^a 22 (30)	^a 8 (11)

Table 4: Incidence and location of vascular injury across main cohort. Results presented as numerical value (%). ^aBilateral injuries.

Histology confirmed arterial and venous vascular tissue in all samples obtained.

Vascular injury increased with increasing lower limb flail; the 50% risk of vascular injury associated with lower limb flail was 66° (95% CI 59° to 75°) with a low NCIS of 0.24. The full injury-risk curve with associated 95% CI is shown below in Figure 28.

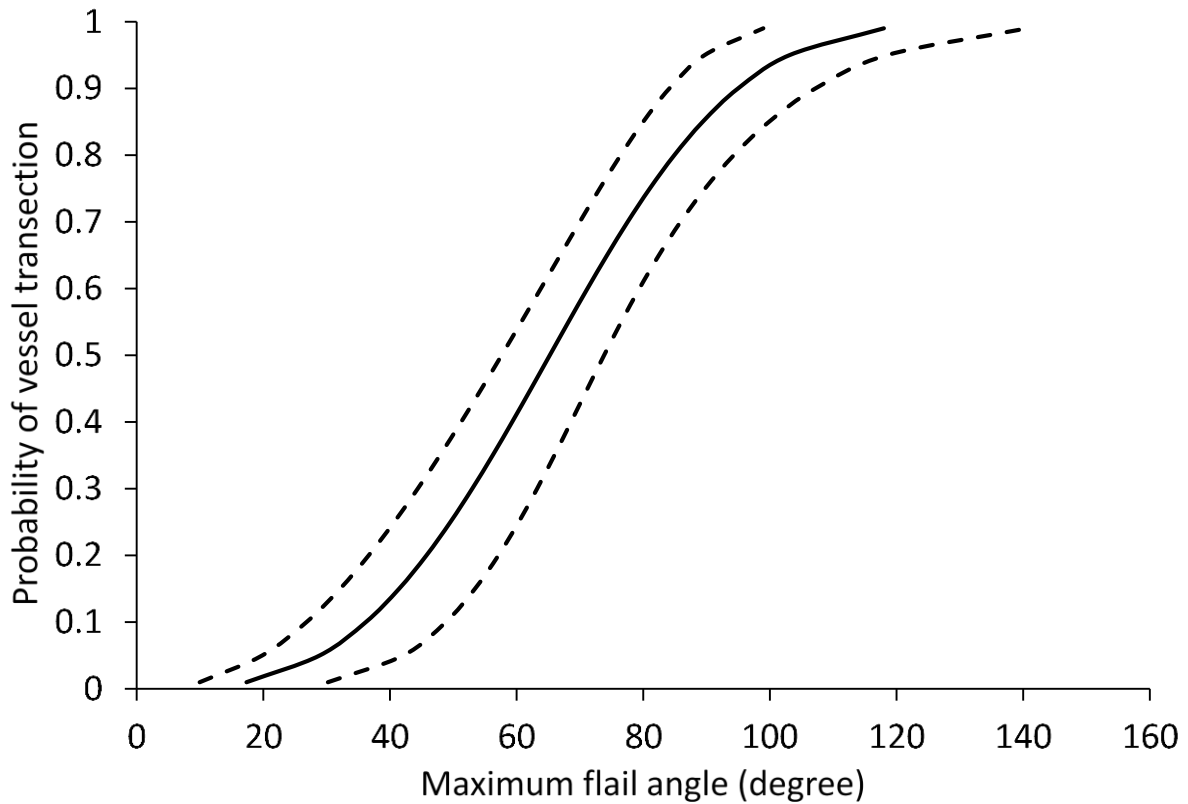


Figure 29: Vascular injury-risk curve as a function of maximum allowable angle of lower limb flail

Traumatic amputation

Nine mice (8%) across the main cohort sustained a traumatic amputation. This was at the level of the hip in three (3%), femur in two (2%), and tibia in four (4%).

All mice which received a pre-test crush injury to the femoral midshaft went on to sustain bilateral traumatic amputations at the level of the femur. There was a 100% incidence of vascular injury in this traumatic above knee amputation group

No mice with amputation at the hip sustained a vascular injury. There was a 100% incidence of vascular injury within the amputation at the knee group.

Mobile platform

No significant differences were seen in the incidence of vascular injury when comparing the mobile platform groups (45°, 90°, 135°) with the non-mobile equivalent groups.

6.5 Discussion

This study replicated dismounted pelvic blast injury in the mouse model, via a shock-tube mediated blast wave. It is the first study to investigate a physical model of dismounted pelvic blast injury. The mice with iatrogenic lower limb amputation at the hip presented a cohort for which the effects of lower limb flail were removed. These mice developed exclusively Tile type B fractures, which were minimally displaced (Figure 30 a). They were subsequently found to have no vascular injury. This was similar to the mice restricted to 45° of lower limb flail and in contrast to the mice seen at higher degrees of lower limb flail. The latter groups sustained vascular injury with Tile type C fractures, which were significantly displaced (Figure 30 b).



Figure 30: (a, left): Lower limb amputated mouse with pubic symphysis disruption, pubic rami fractures and left sided sacroiliac joint disruption. (b, right): 135° lower limb flail mouse with pubic symphysis disruption, pubic rami fractures and bilateral sacroiliac joint disruption.

The findings suggest that lower limb flail transfers load which result in external rotation and lateral displacement of the hemipelvis. This, in combination with the blast wave impacting directly upon the pelvis, generates unstable, displaced pelvic ring fractures. Pelvic bony displacement, and subsequent displacement of the intra-pelvic soft tissues, is hypothesised to be responsible for tension on the vasculature and subsequent rupture. An association of vascular injury to increasing lower limb flail was seen in this study. The injury curve presented (Figure 29) displays a 50% probability of vascular injury at 66° of lower limb flail, with a low

NCIS. It shows a clear link between increasing angle of lower limb flail and major vascular injury.

Battlefield data has shown unstable pelvic fracture patterns consisting of PS and SI joint disruption, with posterior pelvic bleeding, as characteristic of the most severe pattern of dismounted blast injury (Chapter 3). This model has reproduced this pattern of injury with PS and SI disruption, unstable fracture patterns and vascular injury occurring posteriorly at the bifurcation of the external and internal iliacs.

These findings, corroborated by battlefield data, suggest that lower limb flail is likely a cause for an unstable pelvic fracture with posterior pelvic bleeding to occur in dismounted victims of an explosive insult.

Vascular injury was defined as complete transection of a major vessel. In several specimens, no vascular injury was found. All mice identified as having no vascular injury were explored to confirm uninjured arterial and venous vasculature. Small vascular injury may have been missed due to the use of cadaveric mice, where active bleeding was not observed. As such the conclusions drawn from this paper focus on major vascular injury, such as that of the common, external, or internal iliacs. In cases of severe disruption of the arterial tree, proximal to the pelvic vasculature, the aorta was noted as the most proximal vascular injury. In the remainder of cases, vessel transection and complete discontinuity was noted to have occurred in the immediate vicinity of the bifurcation of the common iliac artery. 10% of samples were taken to confirm vascular type. In all histological samples the presence of both arterial and venous tissue was noted, suggesting that disruption of both the arterial and venous vasculature had occurred.

In this study a shock tube replicated the effects of a primary blast wave but has not replicated the effects of secondary (such as soil or sand projectile) blast injury. This is seen as a strength but also a limitation of this study. Isolating the effects of the blast wave on injury has allowed

it to be decoupled from secondary blast. This is viewed as a strength and has allowed for clear identification of the injury mechanism in this study. A limitation, however, is that it is thought likely that the effects of secondary blast injury would compound the injuries seen. It is hypothesised that the lower-than-expected traumatic amputation rates seen in this study (than would be expected from the battlefield data described in Chapter 3) are due to this absence. The effects of secondary blast injury on the injury patterns of dismounted pelvic blast will be investigated further in the next chapter of this thesis.

As discussed in Chapter 4, traumatic amputation has previously been hypothesised to occur due to the blast wave coupling with long bones with a resultant diaphyseal fracture, before limb flail completes the amputation (Hull and Cooper, 1996). This was not observed in this study, at rates which match the degree of traumatic amputation seen in association with pelvic fracture as noted from battlefield data (Chapter 3). In agreement with other authors, limb flail is felt necessary for traumatic amputation to occur (Hull and Cooper, 1996; Singleton *et al.*, 2014). The lower rates of traumatic amputation seen in this study may be hypothesised to be due to a blast wave of inadequate pressure to generate diaphyseal fracture, or due to the absence of secondary blast injury causing an initial disruption to the soft tissues of the thigh. At higher loading conditions the threat was felt to be non-survivable, due to thoraco-abdominal injury, and so this was thought unlikely to be the cause. All mice which had sustained a pre-test crush impact to the thigh went on to sustain above knee traumatic amputations, suggesting an element of injury in addition to the flail mechanism is required. These mice also sustained displaced pelvic fractures with vascular injury. This contrasts with the mice amputated at the hip, who sustained no pelvic displacement or vascular injury. These findings suggest that the process of pelvic displacement and vascular injury occur during flail, prior to above knee traumatic amputation, whilst the femur is still able to transfer loads resulting in lateral displacement and external rotation of the pelvic girdle. Mice which received pre-test through knee amputations

similarly went on to display displaced pelvic fractures with vascular injury, suggesting that the thigh – but not the leg – is the essential component in lower limb flail causing injury. This may account for the high rate of above knee traumatic amputations, but not below knee amputations, seen in association with pelvic blast injury (Mossadegh *et al.*, 2012; Webster *et al.*, 2018). These findings suggest that above knee amputation may happen in conjunction with dismounted pelvic blast injury, but that below knee amputation may occur through an unrelated injury mechanism.

Preliminary testing indicated injury to occur at lower flail angles than unrestricted (180°) flail. As such the unrestricted flail group within the main cohort was not continued beyond the preliminary three mice. Experiments with a mobile platform were performed to ascertain if changing the boundary conditions would alter injuries seen. No differences were seen in the rates of vascular injury across the mobile and stationary platform groups.

As highlighted in Chapter 5, the mouse was chosen as a suitable animal model due to its similarities to the human pelvis at the areas of key interest from battlefield data: the pubic symphysis, sacroiliac joints, and pelvic vasculature. Several factors must be taken into consideration when inferring the results and conclusions of these findings in the mouse model, for subsequent interpretation to human injury risk. The main morphological differences of the mouse to the human pelvis are that the human pelvis is comparatively compressed in the axial plane, whilst elongated in the sagittal and coronal planes (Lovejoy, 2005). Despite these morphological differences, the conclusions of this study focus solely on outward flail of the lower limb as the mechanism of injury. In the upright posture, as in this study, the angle of rotation is similar between the species. As explored in the amputated mice, it is the outward motion of the femur causing a lateral displacing force upon the pelvis, which results in displaced fractures and vascular injury. As such, the morphological differences of the pelvis between species are minimised when focusing upon this mechanism of injury and conclusion.

Further consideration must also be given to the respective forces of the mouse femur, and that of the human femur, acting upon the pelvis. The human femur is comparatively heavier and accounts for more of total skeletal length (Feldesman *et al.*, 1990; Di Masso *et al.*, 2004). As such, a proportionally greater moment is expected to act upon the human pelvis during blast compared to the mouse. It is unclear how this would alter the injury curve, however, as the human pelvis may have proportionally greater strength to resist this greater moment. It is uncertain therefore how these data scale to the human. Irrespective of scaling, this study has shown that limitation of lower limb flail mitigates the severity of pelvic injury and likelihood of vascular injury in the mouse model, and so a similar effect would be expected in the human.

Scaling laws for small animal models in blast consider factors including force, mass and velocity, but no scaling laws exist for translating angle of flail, as in this study (Panzer *et al.*, 2014). Blast tolerance in small and large animal models, and how it scales to the human, has been described previously in relation to traumatic blast lung injury (TBLI) (Bowen *et al.*, 1968). The lethal median dose (LD₅₀), causing fatal TBLI in the mouse is reached at shock-tube plateau pressures of 29.0 – 30.7 psi with durations of 3 – 6000 ms (Richmond *et al.*, 1959, 1961; D. R. Richmond *et al.*, 1962; D. Richmond *et al.*, 1962). The shock wave in this study delivered a mean plateau pressure of 1.72 bar (24.9 psi) sustained over 7.6 ms. The maximum peak pressure in this study was 4.28 bar (62 psi) and sustained for less than 0.008 ms. Due to the short duration, this falls below any possible LD₅₀ estimations from injury curves derived from the above studies (D. Richmond *et al.*, 1962). As such, the chosen shock wave was thought to be representative of a blast wave falling below the LD₅₀ observed in previous studies to cause fatal TBLI (the upper threshold of blast resulting in mortality), but a sufficient insult to cause pelvic vascular transection due to lower limb flail. Preliminary work performed in the current study tested lower blast thresholds for mice with unrestricted flail. A single mouse was

tested utilising a lower blast threshold with a blast wave of maximum peak pressure 1.55 bar (36% of that used within this study). This mouse sustained no injuries. Three mice were tested utilising a blast wave of maximum peak pressure 2.71 bar (63% of that used within this study). Of these, two mice sustained injury whilst one did not. There is insufficient data from this preliminary work to generate an injury risk curve to assess a dose-response for injury in the unrestricted mouse, however, the preliminary work suggests that the threshold required to achieve pelvic injury is close to that required to achieve TBLI.

As highlighted in Chapter 5, reproducing blast mediated lower limb flail in the human is challenging due to the limitations of free field blast tests and the suitability of shock tubes only for small animal models (Nguyen *et al.*, 2014; T.-T. Nguyen *et al.*, 2018). Future research strategies are required to overcome the obstacles of free field blast tests, or progress dismantled blast-injury research through the development of larger shock tubes to simulate the dismantled blast environment with human cadavers. Any future research could adopt a scaling of 1:1 as a starting point, until further data corroborates or indicates otherwise. Although it is unclear how these data scales to the human, one factor is clear: limitation of lower limb flail mitigates the effect of pelvic injury in this mouse model. Any restriction of flail in the human, through military personal protective equipment, would be beneficial to mitigate the effects of dismantled pelvic blast injury.

6.6 Conclusion

This chapter set out to quantify the effects of a blast wave on dismantled pelvic blast injury using a small animal model. The results suggest that lower limb flail is necessary for an unstable, fatal pelvic fracture to occur. Restriction of lower limb flail was shown to reduce the probability of vascular injury, and therefore of mortality. An injury-risk curve was developed which associates restriction of lower limb flail to the probability of vascular injury; restriction

to 66° flail results in a 50% probability of vascular injury. Scaling these angles of restriction to the human is unclear, however, any degree of restriction would be beneficial in mitigating the effects of injury. These findings determine a key mechanism of injury to the lower body in dismounted blast and suggest a mitigation strategy not previously considered. Limitation of lower limb flail in the next generation of personal protective equipment may reduce the high mortality rates associated with dismounted pelvic blast injury.

Lower limb flail has been shown in this study to result in unstable pelvic fractures and vascular injury, however, aspects of dismounted pelvic blast injury patterns are missing. As noted from the battlefield data discussed in Chapter 3, traumatic amputation is seen to occur in combination with these injuries in the dismounted blast injury casualty. Furthermore, significant perineal injury is seen in combination with pelvic fracture in the dismounted complex blast injury casualty, which was not observed within this current study. The lack of traumatic amputation and significant perineal injury in this current study is hypothesised to be due to the absence of secondary blast injury (such as high velocity sand). The next step in this thesis was therefore to investigate the hypothesised mechanism of injury of high velocity sand blast in order to ascertain its contribution to the injury pattern seen in dismounted pelvic blast injury. This will be investigated in the following chapter.

Chapter 7

Mechanisms of Injury: High Velocity Sand Blast

This chapter is published in part:

Rankin, Iain A., Nguyen, T.-T., Carpanen, D., Clasper, J. C., & Masouros, S. D. (2020). A New Understanding of the Mechanism of Injury to the Pelvis and Lower Limbs in Blast. *Frontiers in Bioengineering and Biotechnology*, 8, 960.
<https://doi.org/10.3389/fbioe.2020.00960>

7.1 Scope of the chapter

As discussed in Chapter 3, dismantled pelvic blast injury casualties are at a significant risk of non-compressible pelvic vascular injury, unstable pelvic fracture patterns, perineal injury, and traumatic amputation. Chapter 4 highlighted both lower limb flail and high velocity sand blast as potential mechanisms to cause these injury patterns in the dismantled pelvic blast casualty. Chapter 6 reproduced displaced pelvic fractures with vascular injury in a mouse model, caused by a shock-tube mediated blast wave. It linked these injuries to outward flail of the lower limbs. A lack of traumatic amputation and perineal injury with this model was noted, however, and suggested a further mechanism of injury was required to produce the full pattern of injury seen

in dismantled pelvic blast injury. This missing mechanism of injury is hypothesised to be high velocity sand blast. Chapter 7 investigates high velocity sand blast as a mechanism of injury in the dismantled blast casualty. A novel experimental setup utilising a mouse model within a gas gun system delivering high velocity sand is described. High velocity sand blast is reproduced, the velocity of which is subsequently controlled to assess its association to injury. Injury-risk curves are developed to correlate velocity of sand to each of the individual types of injury described. The chapter discusses these findings, proposes a novel mechanism of injury for traumatic amputation, and describes a detailed proposal for the mechanism of injury of dismantled pelvic blast injury. The chapter finishes by highlighting the key factors for which to target mitigative strategies and determines the subsequent research direction of this thesis.

7.2 Introduction

Across all blast injury mechanisms, secondary blast injury caused by propelled energised fragments are the most common wounding modality seen in recent conflicts (Covey and Ficke, 2016; Edwards and Clasper, 2016). These energised fragments may be from the explosive device itself or objects from the surrounding environment. Whilst secondary blast injury from energised fragments has been clearly identified as a significant contributor to mortality, the contribution of energised environmental debris (soil, sand and gravel) to injury patterns of the dismantled blast casualty is not known (Covey and Ficke, 2016). Chapter 6 hypothesised that the lower-than-expected rates of traumatic amputation and perineal injury were due to the absence of secondary blast injury. The mechanism of injury resulting in traumatic amputation and perineal injury is not clearly understood. Traumatic amputation in the dismantled blast casualty has been hypothesised to occur due to a combination of primary and tertiary blast mechanisms; fracture of the long bone from the blast wave followed by the blast wind completing the amputation (Hull and Cooper, 1996). Other authors have indicated tertiary blast

alone to be implicated, as lower limb flail propagated by the blast wind results in amputation. No consensus has been reached on the mechanism of injury for traumatic amputation and no model has reproduced the perineal injuries seen in dismounted pelvic blast injury, nor the abdominal injuries that can be seen in dismounted complex blast injury (as discussed in Chapter 3).

The method by which soil propagates following blast is known. Upon detonation, buried explosive devices generate a shockwave which compresses the surrounding soil. Gas from the explosion is released at high velocity and acts to eject this soil, propelling it at supersonic speeds of up to 900 m/s (depending upon soil characteristics and explosive mass) (Tremblay *et al.*, 1998). The energised fragments subsequently rapidly decelerate to 600 m/s or less before impacting casualties (Bowyer, 1996). The direction of expansion of the soil ejecta is heavily dependent on the soil's properties; the result, however is typically an inverse cone with a projection angle of between 45 and 120 degrees (Grujicic *et al.*, 2008). Upon impact, the physical momentum transfer from the soil ejecta is likely to cause displacement and produce significant injury to the dismounted casualty. The process by which the casualty gets injured has not been investigated in a physical model. As discussed in Chapter 5, the gas gun system is a suitable platform for measuring the effects of a projectile delivered with high velocity at a small animal model.

Accordingly, the aims of this study were (1) to replicate impact from propelled high velocity soil as occurs following blast in a small animal mouse model, utilising a gas-gun system, and (2) to investigate the effect of increasing velocity on the resulting injury pattern. The hypothesis of this study was that high velocity soil ejecta would contribute to the injury pattern seen in dismounted pelvic blast injury and play an essential role in the severity of both soft tissue and skeletal injury alike.

7.3 Methods

The experimental design and procedures were carried out in compliance with the UK Animal (Scientific Procedures) Act 1986. Testing was conducted using the same animal model of fresh-frozen cadaveric male mouse specimens described in the previous chapter (male MF-1, out-bred, ex-breeder, wild type, 8 - 9 weeks of age). Specimens were stored at -20°C and thawed at room temperature ($21 \pm 2^{\circ}\text{C}$) prior to testing.

Sand size and properties were chosen based upon NATO unclassified AEP-55 recommendations for typical sandy gravel soil granulometry (NATO/PfP Unclassified, 2006). The sand size distribution was subsequently scaled to the murine model based upon recommended animal scaling parameters in blast, where the scale is equal to the length of a parameter of the human species divided by that of the animal species used ($\lambda_L = L_1/L_2$) (Panzer *et al.*, 2014). The thigh circumference of each species was taken as the representative parameter for scaling, in view of traumatic amputation of the lower limb being a primary outcome. Median mouse thigh circumference was calculated as 2.7 cm (range 2.6 – 3.1 cm) from specimens ($n = 22$), whilst human thigh circumference was taken from literature as 55 cm (White and Churchill, 1971). From this, an upscaling of 20x for sand size was utilized ($\lambda_L = 55 / 2.7 = 20$). A minimum sand size cut-off of 0.1 mm was taken to avoid sublimation of sand particles smaller than this at high velocity. A sandy gravel aggregate size range as closely representative to human scaled values was subsequently chosen, ranging from the human ideal particle size median value to the 85th centile value, consisting of 60% sandy gravel sized 0.1 to 0.3 mm, 20% sized 0.3 to 0.5 mm, and 20% sized 0.5 – 1 mm. The sand was saturated with water prior to testing, as per NATO AEP-55 recommendations. The experimental sand sizes and distribution used (scaled to human values) are shown alongside those recommended in NATO AEP-55, ideally distributed particle sizes in Figure 31 (NATO/PfP Unclassified, 2006).

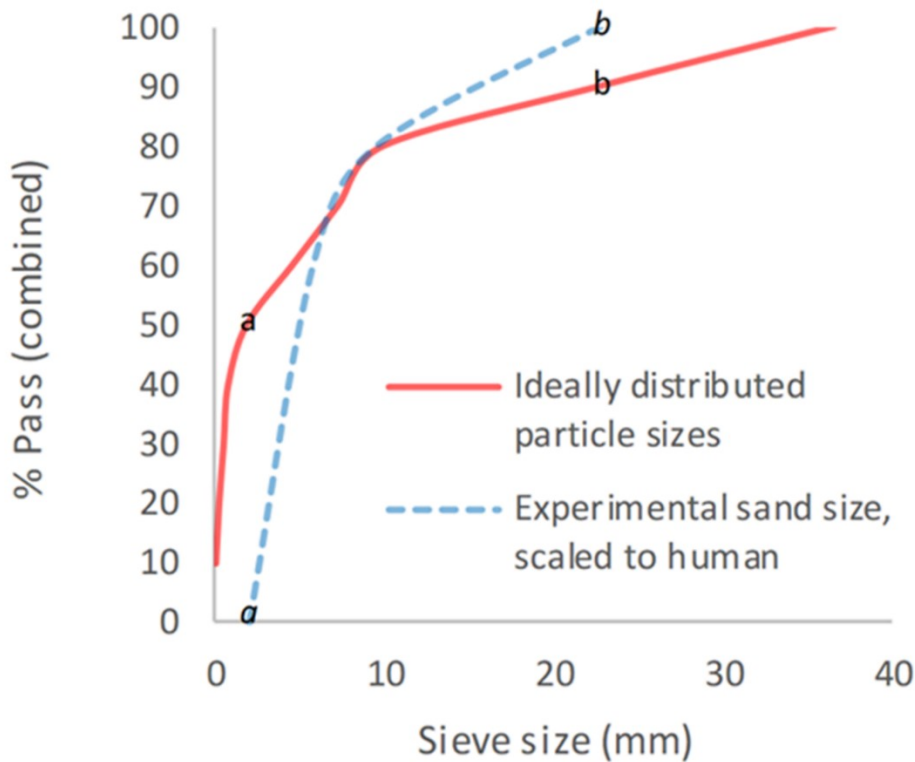


Figure 31: Experimental sand sizes used, scaled to human values, shown alongside ideally distributed particle sizes. a = human median value. b = human 85th centile. a = lower limit of experimental sand range. b = upper limit of experimental sand range. % pass (combined) describes the percentage of total volume of sand passing a specific sieve size; sieve size (mm) relates to the diameter of each hole within the sieve.

NATO unclassified AEP-55 provides recommendations for non-buried anti-personnel explosives and buried anti-tank explosives. A minimum depth of 1.5 m is recommended for the test conditions of a buried anti-tank explosive. There are no recommendations for minimum or maximum depth of buried anti-personnel explosives (NATO/PfP Unclassified, 2006). No guidance for buried anti-personnel explosives in the published literature could be identified. Given the increased charge of an anti-tank explosive compared to anti-personnel explosives,

and for the purposes of this study investigating high-velocity sand blast, the expected blast conditions of an anti-personnel IED buried at 30 cm was utilised. The sand mass was subsequently determined based upon the volume of sand that would be expected to be carried by the blast of an IED buried to a depth of 30 cm. As discussed in the introduction of this chapter, the direction of expansion of sand ejecta is heavily dependent on the sand's properties; the result, however is typically an inverse cone with a projection angle of between 45 and 120 degrees (Grujicic *et al.*, 2008). As such, the volume of an inverse cone with a height (IED buried depth) of 30 cm and blast venting angle (cone opening angle) ranging from 45 to 120 degrees, was used to calculate the total volume of sand that would be expected within the cone's trajectory. This equates to a total volume of sand contained within the blast path as ranging from 4900 cm³ (45 degrees) to 18,300 cm³ (120 degrees). The density of sand saturated with water has been shown to be 2078 kg /m³ (Lajeunesse *et al.*, 2017). Based on this density, these volumes of sand equate to sand masses ranging from 10.2 to 38 kg. The sand mass distribution was scaled to the murine model based upon recommended animal scaling parameters in blast, where the scale is equal to the mass of the human species divided by that of the animal species used ($\lambda_m = m_1/m_2$) (Panzer *et al.*, 2014). Median mouse mass was calculated as 36.0 g (range 29.3 – 41.0 g) from specimens (n = 22), whilst human mass was taken from literature as 72.6 kg (White and Churchill, 1971). From this, an upscaling of 2000x for sand mass was utilized ($\lambda_L = 72600 / 36 = 2000$). Given these scaling parameters, this equates a sand mass ranging from 5.1 g (10,200 g / 2000) to 19 g (38,000 g / 2000). A sabot was designed to accommodate sand with a water saturated sand weight ranging from 8 to 11 g. When scaled, this equates to 16 to 22 kg; this range of sand mass could be expected in an IED buried to 30 cm, with a blast projection angle ranging from 55 to 105 degrees.

The sand was housed within a hollow polycarbonate sabot which was loaded into the firing chamber of a double-reservoir gas-gun system (T. T. N. Nguyen *et al.*, 2018). Within this system, a 2-litre reservoir charged with air and a Mylar[®] diaphragm firing mechanism was used to accelerate the sabot-sand unit down a 3-m-long, 32-mm-bore barrel. The output velocity, which can range between 20 m/s and 600 m/s, was controlled by the thickness of the Mylar[®] diaphragm. To accelerate the sabot-sand unit to the desired velocity, the reservoir section of the gas gun was charged to a predetermined firing pressure. The pressure was maintained within the reservoir section by a Mylar[®] diaphragm of appropriate thickness (ranging from 50 to 150 μm). The system utilises a priming section, which is charged to a pressure below the rupture pressure of the diaphragm. This reduces the pressure gradient across the mylar diaphragm (containing the reservoir system) and prevents it from rupturing early, as the reservoir is filled. At the point of initiating firing of the gas gun, the pressure in the prime section is vented, resulting in rupture of the diaphragm, with release of the pressurised gas. This accelerates the sabot-sand unit down the barrel to exit into the target chamber, where the sabot is separated from the sand by a sabot-stripper constructed from aluminium and polycarbonate slabs and a heavy stainless-steel block. The sabot is halted at this point, while the sand continues to travel towards the murine specimen at the intended terminal velocity.

Mice were secured in a supine posture on a polyurethane foam mount within the target chamber. A single cable tie across the thorax was applied to secure the specimens in position on the mount, whilst leaving the pelvis and lower limbs exposed. A single control test was performed utilising the maximum gas-gun pressure to be used in experiments, with the absence of any sand ejecta. This was performed in order to ascertain whether any injurious effects are caused by the pressurised air alone. This control test was performed on a single control mouse specimen. In order to simulate the sand-ejecta-spread, two interconnecting fenestrated steel

fences, separated by 5 mm and offset to one another by 50% of the diameter of each fenestration, were placed distal to the gas-gun outlet and 50 mm proximal to the mount (Figure 32). Offsetting of the fenestrated steel fences changed the initial stream of sand delivered by the gas gun into multiple individual streams of differing trajectories, which subsequently dispersed into a widely distributed spread of high velocity sand. Figures 33 a and 33 b illustrate this setup in the aerial and oblique views, respectively. Figure 34 a shows a photograph of the initial sand stream being converted into multiple streams, followed by Figure 34 b which shows the sand dispersing into a widely distributed spread of high velocity sand.

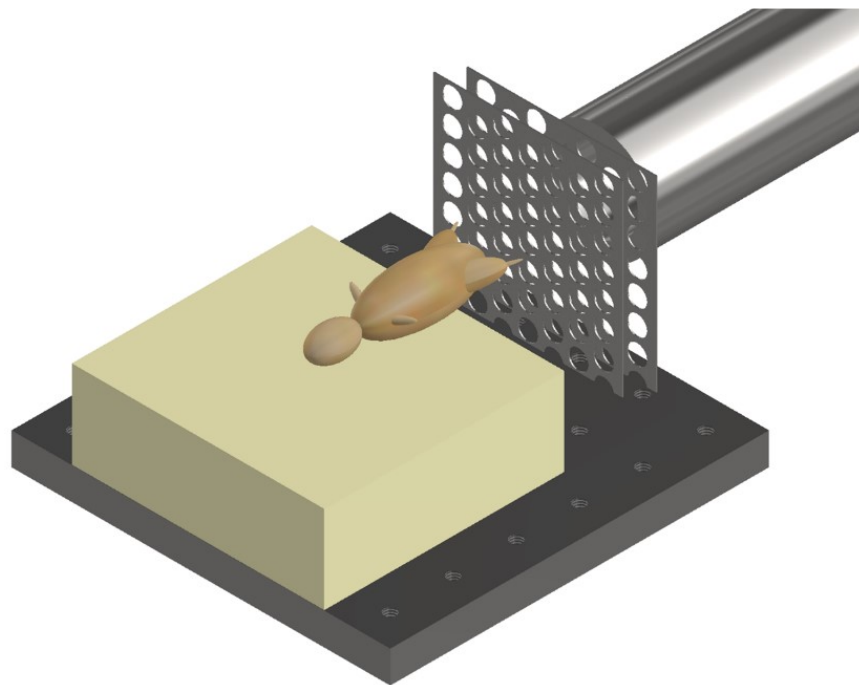


Figure 32: Gas gun with under-body sand blast mounting platform, fenestrated steel fences and mouse. Mouse represented with model.

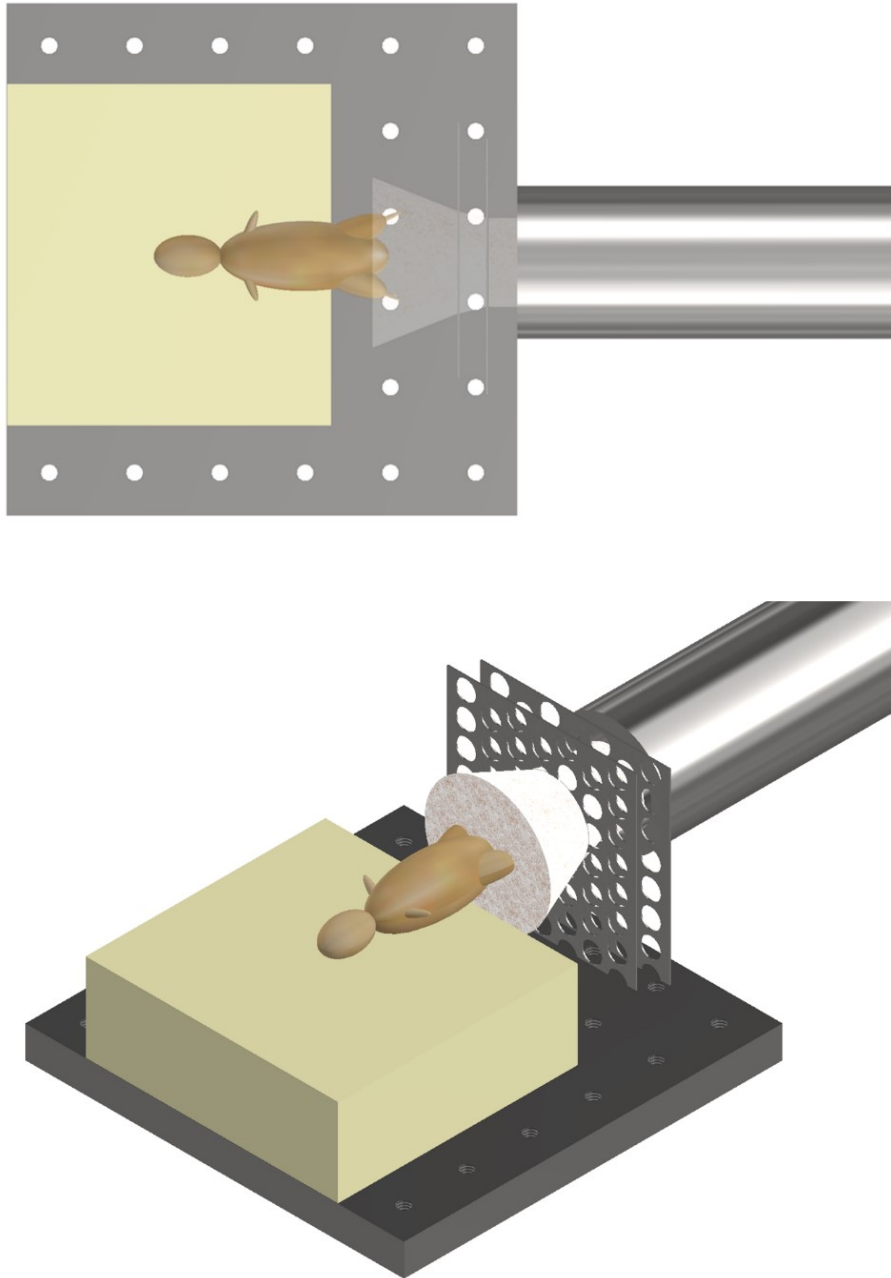


Figure 33 (a, top) Aerial view of schematic illustrating initial sand stream passing through offset fenestrated steel fences, causing dispersion of the sand prior to impact with the specimen. (b, bottom) Oblique view of schematic illustrating initial sand stream passing

through offset fenestrated steel fences, causing dispersion of the sand prior to impact with the specimen

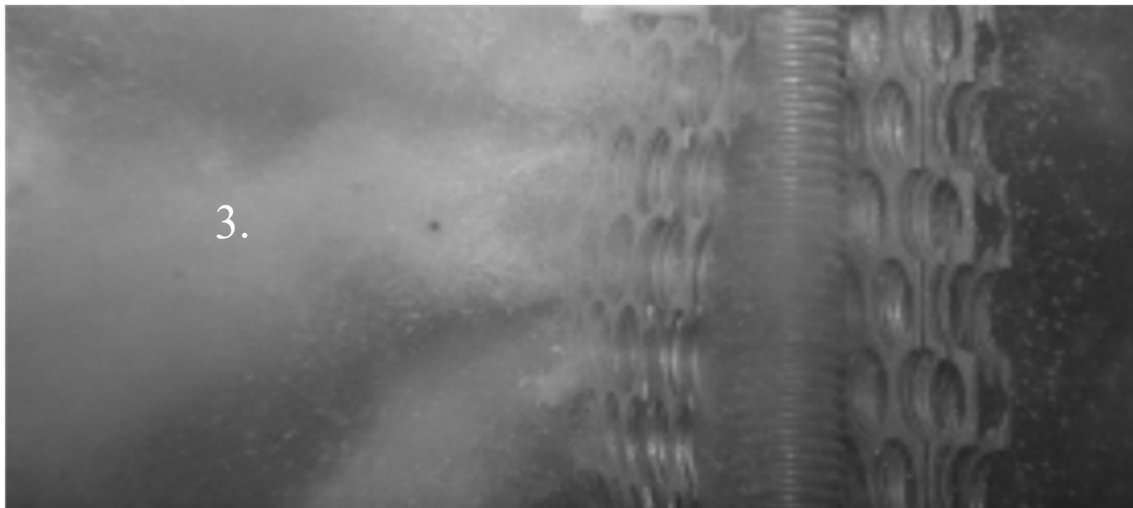
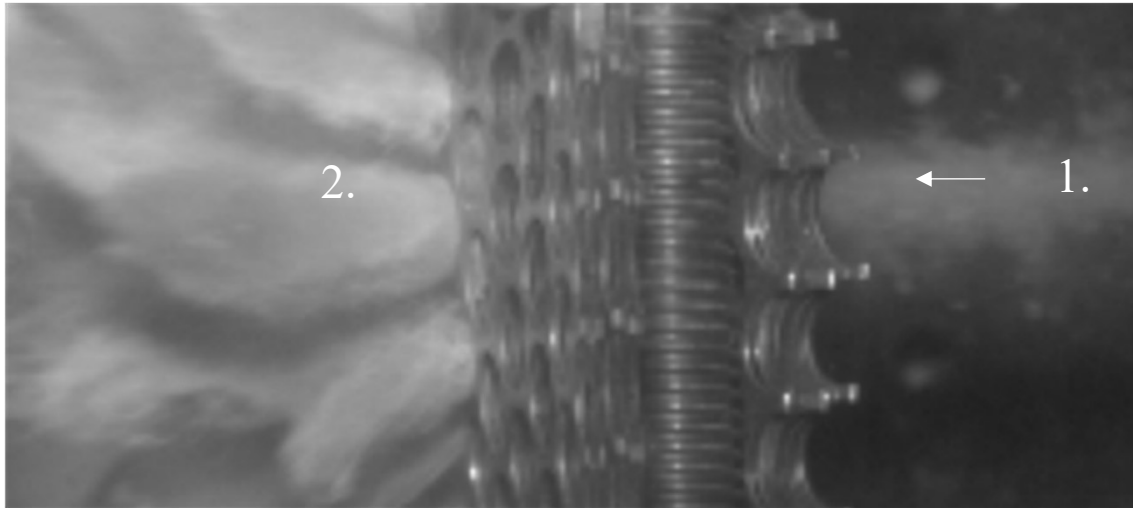


Figure 34: Photographs showing (a, top) the initial sand stream exiting the gas gun (1.), passing through the dispersion fence to be converted into multiple streams (2.), followed by (b, bottom) dispersion into a widely distributed spread of high velocity sand (3.). Arrow annotation represents the direction of travel of the sand after exiting the gas gun.

The speed of the sand particles at the point of impact with the sample was estimated using high-speed photography (Phantom VEO710L, AMETEK, USA) at 68000 fps. An average velocity for the sand cloud as a whole was determined based upon identifying and tracking four unique points spread across the distributed sand. These points varied in velocity and were chosen from the front, front-centre, centre, and centre-back of the peripheries of the sand spread. From this, the mean with standard deviation of the velocity of the sand spread as a whole was calculated.

Injury scoring

Prior to and following each test, mouse specimens underwent radiographic imaging using a mini-C-arm (Fluoroscanner® InSight™ FD system, USA) to identify any fractures in the specimen and assist with injury classification. Subsequent to this, specimens underwent dissection to identify injury patterns. Recorded injury patterns included; (1) lower limb degloving; (2) soft tissue pelvic and perineal injury (the Faringer system was used to classify the location of the soft-tissue injury anatomically (Faringer *et al.*, 1994): zone I (perineum, anterior pubis, medial buttock, posterior sacrum), zone II (medial thigh, groin crease), or zone III (posterolateral buttock, iliac crest)); (3) lower limb traumatic amputation; (4) open abdominal injury; and (5) pelvic fracture. Pelvic fractures were classified in accordance with the Tile criteria (Tile, 1996): Type A (pelvic ring stable), Type B (pelvic ring rotationally unstable, vertically stable), and Type C (pelvic ring rotationally and vertically unstable). Where a lower limb open fracture was present with extensive soft tissue loss, the injury was classified as a traumatic amputation.

Statistical analysis and Development of the Risk Function

The NCSS statistical software was used for statistical analysis (version 12, Utah, USA). A likelihood-criteria best-fit analysis, with the aid of probability plots, was performed to choose the distribution that best fit the data for each injury type. The Weibull distribution was shown

to be the best fit in the majority of cases; hence, it was chosen as the probability distribution to represent the risk for all injury types observed in this study. Weibull survival analysis was used to examine the association between sand velocity and each category of injury. The Weibull regression model is $P(v) = 1 - e^{-(v/\lambda)^\kappa}$, where P is the probability of injury, v (the average velocity of sand) is the predictor variable, and λ and κ are the corresponding coefficients associated with the predictor variable. To derive the survivability curves, data were classified as left censored where injury was present and right censored where there was no injury. The normalized confidence interval size (NCIS) of the survivability curves was determined as the ratio of the width of the 95% confidence interval (CI) to the magnitude of the predictor variable at a specific risk level.

7.4 Results

Replication of impact with high velocity soil ejecta

Twenty-two cadaveric mice were used, including the control specimen. No injuries were seen in the control. Average sand velocity ranged from 166 ± 12 m/s to 271 ± 24 m/s. Median sand mass was 10g (range) (range 2.6 – 3.1 cm). Radiographs showing an uninjured mouse next to a mouse injured by sand blast are shown in Figure 35. Table 5 details the types of injuries seen across all mice. Table 6 details the pelvic fracture patterns sustained.

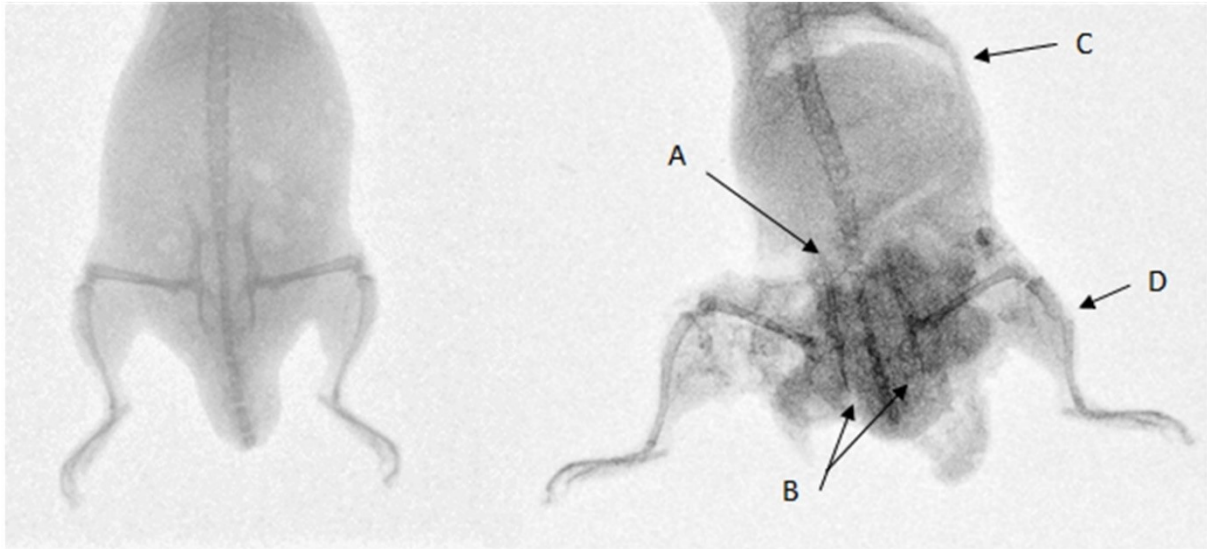


Figure 35: Left: pre-test, uninjured mouse. Right: mouse injured with sand blast at 252 m/s sustaining pelvic fractures with (A) sacroiliac joint disruption and (B) pubic rami fractures, (C) abdominal injury with free air in the abdomen, perineal injury, and (D) an open tibial fracture with surrounding extensive soft tissue loss. The increased density on mouse on the right represents sand debris.

Total number of mice ^a	Injured mice	Lower limb degloving injuries	Soft tissue pelvic and perineal injuries	Including Faringer zones			Open abdominal injuries	Traumatic amputations	Pelvic fractures
				1	2	3			
21	16 (76%)	14 (67%)	14 (67%)	11	12	5	8 (38%)	7 (33%)	5 (24%)

Table 5: Types of injuries sustained across all mice. ^aExcluding control specimen.

Pelvic fractures	Tile classification	Pubic rami	Pubic symphysis disruption	Acetabulum	Iliac wing	Sacrum	Sacroiliac joint disruption
5	5 (100%) Type C	5 (100%)	0 (0%)	1 (20%)	3 (60%)	1 (20%)	4 (80%)

Table 6: Pelvic fracture patterns sustained

Effects of increasing velocity on injury patterns

Increasing velocity produced injury patterns of worsening severity. Figures 36 a – e shows the full injury-risk curves with 95% CIs for perineal injury (36 a), lower limb degloving (36 b), open abdominal injury (36 c), traumatic amputation (36 d), and pelvic fracture (36 e). The NCIS of all injury curves for the velocity at 50% risk of injury (v_{50}) were found to be low, at less than 0.25. The 25%, 50% and 75% risks of injury (v_{25} , v_{50} and v_{75} respectively) for each type of injury are displayed as bar graphs in Figure 37 and detailed in Table 7.

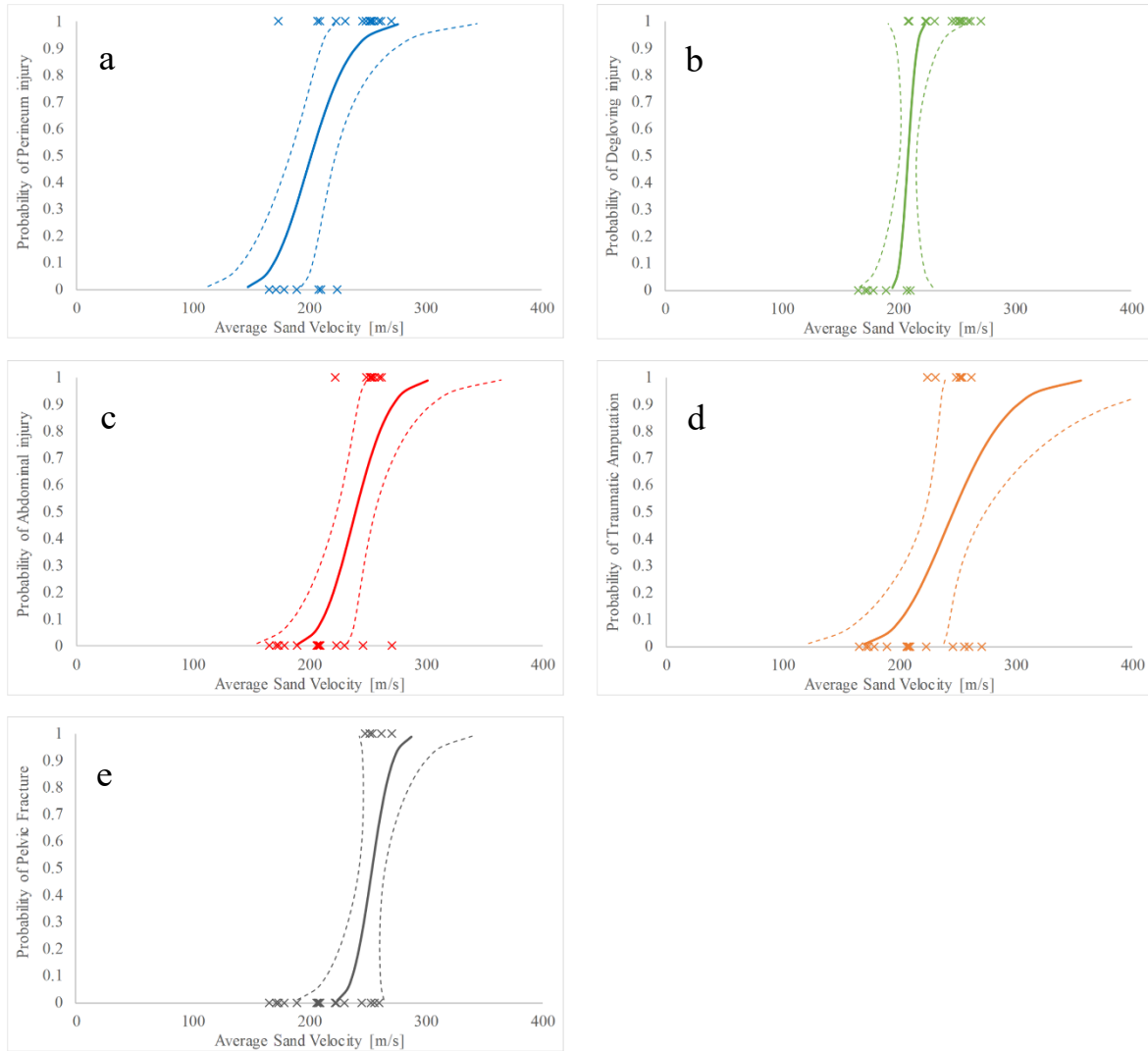


Figure 36: Injury-risk curves for (a) perineum injury, (b) lower limb degloving, (c) abdominal injury, (d) traumatic amputation, and (e) pelvic fracture as a function of average sand velocity; 95% CI is represented with dashed lines.

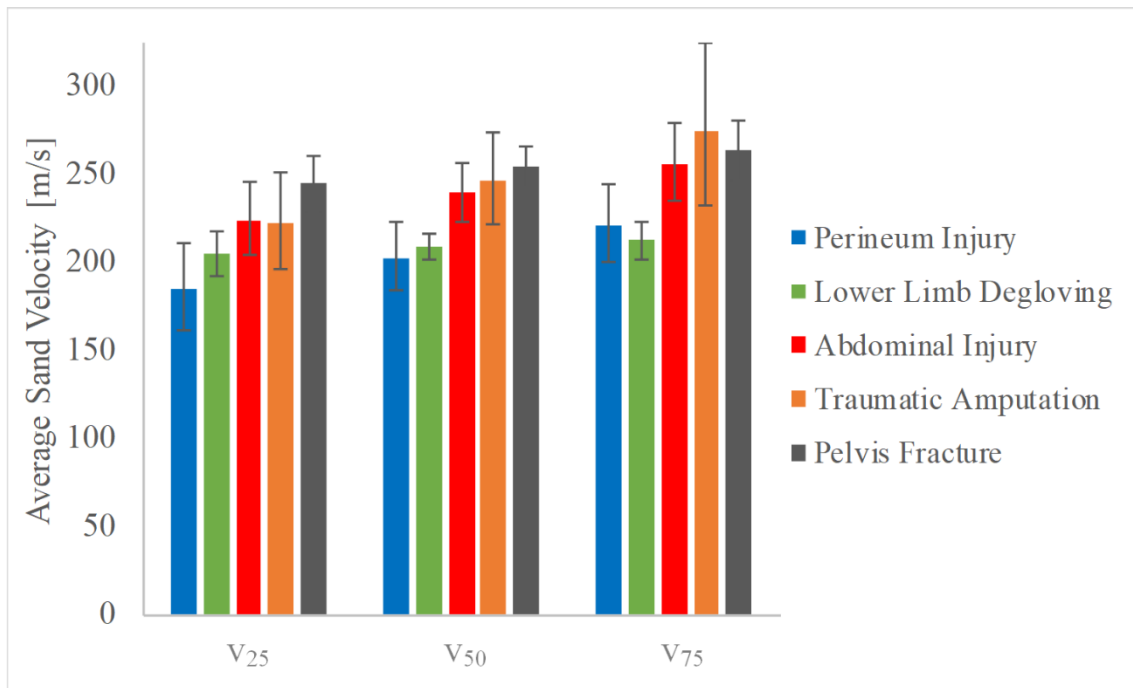


Figure 37: Bar chart displaying the v_{25} , v_{50} and v_{75} for each type of injury; 95% CI is represented with variability whiskers.

	v_{25} (m/s)	v_{50} (m/s)	v_{75} (m/s)
Lower limb degloving	205 (193 – 217)	208 (202 – 216)	212 (202 – 223)
Perineum Injury	185 (162 – 211)	202 (183 – 223)	221 (200 – 245)
Traumatic Amputation	222 (197 – 250)	247 (222 – 274)	274 (232 – 324)
Abdominal Injury	224 (205 – 246)	239 (223 – 257)	256 (235 – 278)
Pelvic Fracture	245 (230 – 261)	254 (243 – 265)	263 (246 – 281)

Table 7: The 25%, 50% and 75% risks of injury (v_{25} , v_{50} and v_{75} respectively) for each type of injury (95% CI in parenthesis)

7.5 Discussion

The first aim of this study was to replicate secondary blast injury caused by high velocity sand blast in a mouse model using a gas-gun system. The hypothesis was that high velocity sand blast causes extensive soft tissue and skeletal disruption and plays an essential role in the injury pattern seen in dismounted pelvic blast injury. The pattern of injury in dismounted blast was reproduced in this study's model as predicted (Figure 35) (Ficke *et al.*, 2012b).

Additionally, progressively worsening severity of injuries was seen with increasing sand velocity. Lower speeds were associated with soft tissue disruption to the perineum and lower extremities whilst higher speeds resulted in open abdominal injury, traumatic amputation, and pelvic fracture. The injury curves presented (Figures 36 a – e) show a link between increasing sand velocity and likelihood of injury, with each curve demonstrating low NCIS at the 50% probability of injury.

Pelvic fractures secondary to blast in the dismounted casualty are inherently unstable in nature, consisting of predominately pubic symphysis and sacroiliac joint disruption followed by pubic rami, sacral and acetabular fractures (Chapter 3). The experimental setup in Chapter 6 demonstrated a link between shock-tube mediated outward flail of the lower limbs and displaced pelvic fractures with vascular injury. These fractures consisted predominately of pubic symphysis and sacroiliac joint disruption, with minimal rami, sacral or acetabular fractures. A limitation of this study was the lack of secondary blast injury, which was hypothesised would worsen the injuries seen. In the current study, high velocity sand has recreated secondary blast injury in the mouse model, which has resulted in pelvic fractures predominately at the pubic rami, with posterior disruption at the sacroiliac joints or iliac wing, and sacral or acetabular fractures. Notably, no pubic symphysis disruption was seen. The combination of the findings in these two studies consequently explains more fully the mechanism of pelvic injury of the dismounted casualty: lower limb flail (tertiary blast injury)

results principally in pubic symphysis and sacroiliac joint disruption with vascular injury, whilst high velocity sand blast (secondary blast injury) results principally in pubic rami fractures (with associated posterior pelvic disruption), sacral and acetabular fractures. This mechanism of injury explains the observation from battlefield data and suggests that pelvic fractures seen following dismounted blast are due to both secondary (sand blast) and tertiary (lower limb flail) blast-injury modalities.

Lower limb flail (tertiary blast injury) has been hypothesised to cause pelvic bony displacement following the initial fracture with subsequent displacement of the intrapelvic soft tissues causing pelvic vascular injury (Chapter 6). Military clinical data have shown that pelvic vascular injury occurs predominately at the posterior pelvis, with significant retroperitoneal bleeding (Chapter 3). It was identified as the injury with the single greatest risk of mortality in the dismounted pelvic blast injury casualty, followed by traumatic amputation. Whilst not explored further in this study, traumatic amputation presents with vascular injury both at the zone closest to the blast (where widespread damage and anatomical destruction is present) and at a zone more proximal to this, with lacerations of small and large blood vessels. These vascular injuries proximal to the zone of destruction result in surgical amputation being subsequently required at a level higher to the zone of traumatic amputation (Clasper and Ramasamy, 2013). Furthermore, surgical amputations may be required in cases where a tensile stretching injury to the major vasculature of the extremity has been applied during limb flail, or where a soft tissue injury (without traumatic amputation) following sand blast has resulted in vascular injury. As such, the injury risk threshold for traumatic (and subsequently required surgical) amputation may be under-represented in the present study.

Several mechanisms of injury for blast-related traumatic amputation have been described. This was first hypothesised to be due to a combination of the initial blast wave (primary blast injury) resulting in diaphyseal fracture to the long bones of the femur or tibia, with the subsequent

blast wind (tertiary blast injury) resulting in separation and amputation of the limb (Hull and Cooper, 1996). More recent data have contested this mechanism: review of post-mortem CT data from recent conflicts showed no link (as previously described) between traumatic amputation and primary blast lung injury and a higher rate of through-joint traumatic amputation than previously seen, which is an injury pattern not explained by the shock-wave mechanism of injury (Singleton *et al.*, 2014). The authors suggested lower limb flail (tertiary blast injury) in isolation as an independent mechanism for blast-mediated traumatic amputation. The traumatic amputation rates seen in the animal study in Chapter 6 were far lower than what is seen in battlefield data. In the Chapter 6 study, when a pre-test crush was applied to the thigh causing tissue disruption, all mice subsequently sustained traumatic amputations following lower limb flail in simulated blast-wave conditions. The working hypothesis following this was that the lower-than-expected traumatic amputation rates were due to the absence of secondary blast injury causing an initial disruption to the tissues of the thigh. In the current study, traumatic amputation was seen to occur at high velocities (v_{50} traumatic amputation: 247 m/s, 95% CI: 222 – 274 m/s), whilst soft tissue disruption alone (lower limb degloving) was present at lower velocities (208 m/s, 95% CI: 202 – 216 m/s). The research shown in Chapter 6 linked an initial injury to the tissues of the thigh to subsequent traumatic amputation following lower limb flail; based on this research, it may be inferred that the combination of sand blast with limb flail would likely result in traumatic amputation at lower velocities. Whilst sand blast in isolation is sufficient to cause traumatic amputation, it is unlikely to be experienced in isolation in an explosion. As such, the following novel mechanism of injury causing traumatic amputation in the dismounted casualty is proposed: an initial secondary blast injury (high velocity sand blast) causes disruption to the soft tissues of the limb, with or without skeletal disruption, following which the blast wind and resultant limb flail (tertiary blast injury) complete the traumatic amputation at the level of the disruption.

Whilst environmental debris following blast is linked to infection and delayed amputation, high velocity sand blast has not been implicated previously as a causative component of traumatic amputation in the dismounted casualty (Khatod *et al.*, 2003; Covey and Ficke, 2016). These mechanisms of injury of dismounted pelvic blast trauma, resulting in pelvic fracture and traumatic amputation, are illustrated in figure 38 a – d.

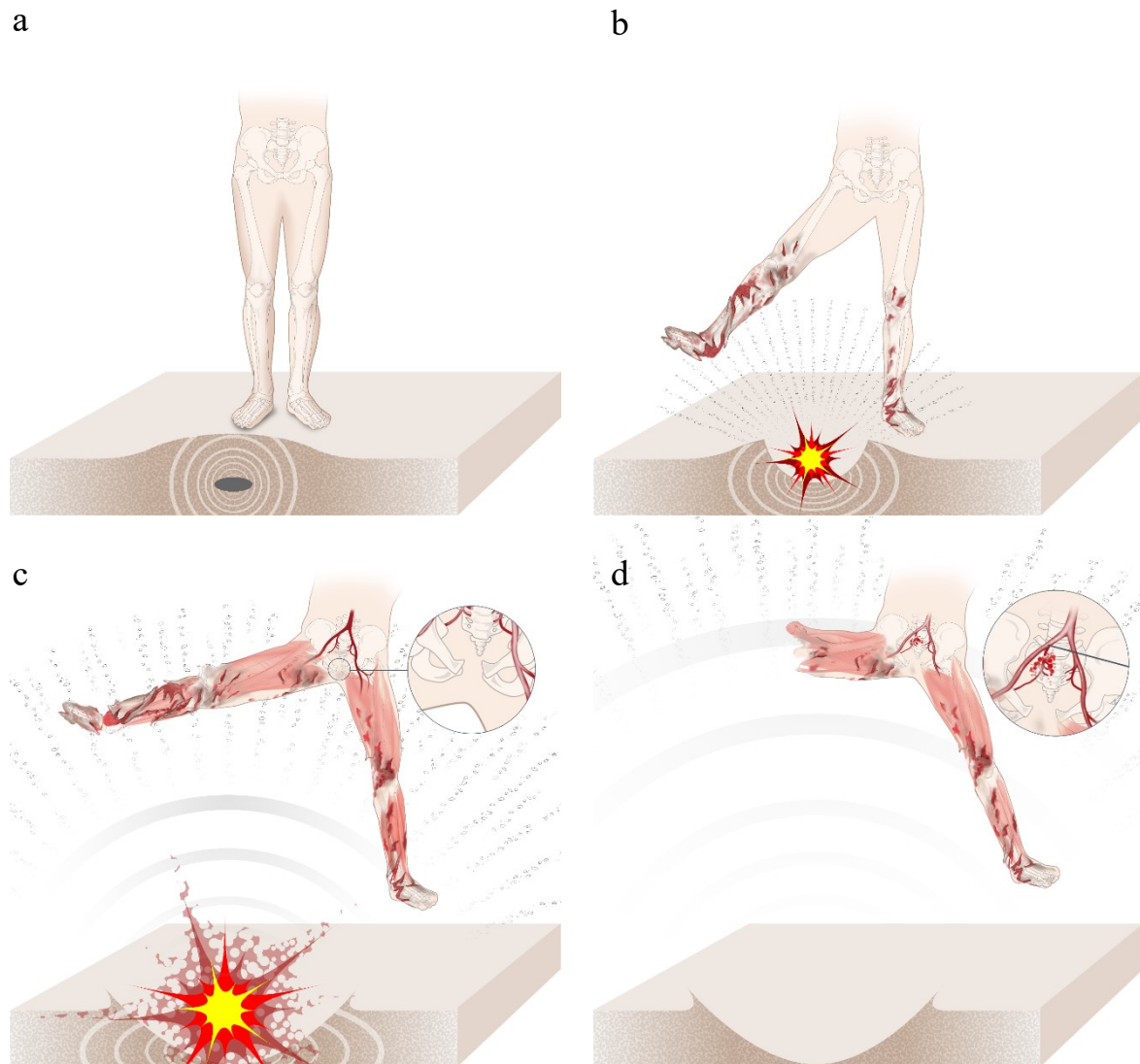


Figure 38: The mechanism of injury of dismounted pelvic blast. (a) Casualty stands on an IED which detonates, causing the initial blast wave to compress the surrounding soil. (b) Sand is ejected at high velocity towards the casualty, causing soft tissue degloving and skeletal disruption. (c) The casualty is impacted by the blast wind, resulting in lower limb flail with separation of the pubic symphysis. (d) The blast wind completes the amputation at the level of the initial disruption, whilst continued leg flail results in opening of the sacroiliac joint and vascular injury.

*With thanks to Visualmedics for creating the illustrations used in figures 38 a – d
(Medical Illustration Studio - Visualmedics, 2020)*

The initial velocity of sand blast reaches up to 900 m/s following the initial energy from the explosion, but rapidly decelerates to 600 m/s or less before impacting casualties (Bowyer, 1996; Tremblay *et al.*, 1998). In the current study, the v_{50} for sand blast to cause traumatic amputation in the mouse model was 247 m/s (95% CI: 222 – 274 m/s), with a sand size when scaled to the human ranging from 2.0 – 20 mm. No comparable human research has been performed previously with which to evaluate these findings. Research investigating the risk of fracture to human cadaveric tibiae when impacted by a gas-gun delivered 4.5mm fragment simulating projectile, however, has shown that similar velocities resulted in fracture: the v_{50} for fracture was shown to be 271 m/s (95% CI: 241 – 301 m/s) (Nguyen *et al.*, 2020). No previous research has quantified the risk of soft tissue injury (degloving, perineal or open abdominal injury) or pelvic fracture caused by energised sand or fragments.

Whilst the current study's findings have shown sand to be an injury mechanism at velocities encountered during blast, scaled animal models cannot be expected to be exact replicates of what occurs in humans (Bowen *et al.*, 1968; Bowyer, 1996; Panzer *et al.*, 2014). In this study, the resting position of the mouse prior to injury in the experimental setup is with hips abducted. This abducted starting position of the lower limbs of the mouse pre-test differs from the starting position of the dismounted soldier's lower limb when pre-blast. The difference in these starting positions may have implications for injury thresholds, due to differences in the subsequent displacement distance of the femurs and resultant transfer of force. It is unclear how this would affect the injury curves. One possibility is that the injury curves for traumatic amputation and pelvic fracture in the human may lie further to the right, with decreased risk of injury, due to the smaller relative surface area initially exposed to the sand blast compared to the mouse model in this study. In contrast, the lever arm and therefore moment generated about the point of injury and traumatic amputation of the femur may be relatively greater in the human compared to the mouse; this would push the injury curve to the left, with increased risk of

injury. A further limitation of the mouse model that must be taken into consideration is the differences of geometry of the femoral head and acetabulum between the two species. In the mouse, the ilia are larger in the axial plane, whilst shorter in the sagittal and coronal planes. As such, the amount of bony structure in line with the loading direction superior to the acetabulum is relatively smaller than the human pelvis, which may result in a reduced amount of structural support when loading in a caudal to cranial direction. This difference may allow for a greater amount of limb flail than would be witnessed in the human and therefore increase the probability of injury. In contrast to this and as discussed in previous chapters, the mouse femur is comparatively smaller than the human femur, accounting for only 15% of total skeletal length compared to the human femur accounting for 27% of total skeletal length (Feldesman *et al.*, 1990; Di Masso *et al.*, 2004). As such, in the human, a proportionally greater moment could be expected to act upon the point of initial disruption caused by high velocity sand when compared to the mouse, increasing the probability of injury. It is uncertain therefore how these data scale to the human. Irrespective of scaling, however, this study has shown that sand causes significant injury at high velocity, resulting in extensive soft tissue and skeletal disruption in the mouse model and a similar effect would therefore be expected in the human.

The experimental setup of this study, in succession with the previous work utilising a shock-tube mediated blast wave in Chapter 6, has allowed for the injurious mechanisms of dismounted blast (primary to tertiary) to be decoupled in the mouse model. Reproducing high velocity sand blast in the human is challenging due to the limitations of gas-gun systems to deliver sufficient quantities of sand; preliminary human cadaveric work may involve assessing the impact of sand blast on individual body regions or tissue types. Computational modelling could be used in combination with the results from this study to assess the effects of modified boundary conditions or mitigative strategies on injury patterns. Future research may involve investigating mitigation strategies for sand blast to the lower limbs. Military pelvic protective equipment

introduced during the recent conflict in Afghanistan resulted in a reduction in the number of perineal soft tissue injuries, so similar strategies to mitigate lower limb soft tissue and skeletal injury (and, by extension, traumatic amputation) should be considered (Breeze, L S Allanson-Bailey, *et al.*, 2015; Oh *et al.*, 2015)

7.6 Conclusion

This study is the first to replicate the mechanism of injury of high velocity sand blast. The results suggest that sand ejecta following an explosive event can cause both soft tissue and skeletal injury alike at high velocities. Injury-risk curves developed in this study showed progressively worsening severity of injuries with increasing ejecta velocity. A novel mechanism of injury causing traumatic amputation in the dismounted casualty was described, which may occur independently or exacerbate those previously described by other authors. These findings implicate high velocity sand blast, in addition to limb flail, as a critical mechanism of injury in the dismounted blast casualty and these injury mechanisms should be key focuses of future research and mitigation strategies.

From this study and that described in Chapter 6, two critical mechanisms of injury in dismounted pelvic blast injury have been described. It was demonstrated that limitation of lower limb flail resulted in a reduction in pelvic vascular injury, whilst reducing velocities of energised sand resulted in reduced traumatic amputation and perineal injury rates. As the most lethal of these injury patterns is pelvic vascular injury, the research direction of this thesis is subsequently focused on developing mitigative strategies to limit this. The first step in this process is to provide a proof of concept of personal protective equipment that would limit lower limb flail and therefore pelvic vascular injury. This concept will be explored in the following chapter.

Chapter 8

Mitigation Strategies: Pelvic Personal Protective Equipment

This chapter is published in part:

Rankin, Iain A., Nguyen, T.-T., Carpanen, D., Darwood, A., Clasper, J. C., & Masouros, S. D. (2020). Pelvic Protection Limiting Lower Limb Flail Reduces Mortality. *Journal of Biomechanical Engineering*, 20(1156). <https://doi.org/10.1115/1.4048078>

8.1 Scope of the chapter

In this thesis, the mechanism of injury in dismounted pelvic blast has been shown in a mouse model to be secondary to blast-wave mediated outward flail of the lower limbs and high velocity sand blast (Chapters 6 and 7). Of the injuries sustained by the dismounted pelvic blast casualty, pelvic vascular injury was shown to have the highest relative risk of fatality (Chapter 3). With increasing lower limb flail in the mouse model, increasingly displaced pelvic fractures, and an increase in the incidence of pelvic vascular injury were seen (Chapter 6). The development of a mitigative strategy to reduce the risk of flail-mediated pelvic vascular injury, through examining concepts for pelvic personal protective equipment (PPE), is now the

research focus of this thesis. Chapter 8 investigates a proof-of-concept PPE as a mitigation strategy in dismounted pelvic blast injury. The established experimental setup utilising a mouse model of dismounted pelvic blast injury with a shock-tube mediated blast wave of Chapter 6 is used to examine this. Pelvic protection worn at the level of the anterior superior iliac spines is compared to protection worn at the level of the greater trochanters and the relative risk of each to pelvic fracture and pelvic vascular injury is described. The findings are discussed, and proof of concept of pelvic protective equipment limiting lower limb flail to reduce the incidence of pelvic vascular injury in a small animal model is described.

8.2 Introduction

To protect the pelvis, principally the perineum and external genitalia, pelvic PPE was introduced to UK military personnel in 2011. For soldiers on routine patrol, this PPE consisted of a silk under layer and an armoured genital protection piece (Lewis *et al.*, 2013). The introduction of this PPE resulted in a decrease in both fragmentation wounds to the pelvis and an absolute reduction of genitourinary injury (Breeze, L S Allanson-Bailey, *et al.*, 2015; Oh *et al.*, 2015). However, no reduction in the rate of fatal pelvic vascular injury has been noted since its introduction (Oh *et al.*, 2016; Gordon *et al.*, 2018).

In this thesis, the first step in the development of pelvic PPE is to provide proof of concept of pelvic protection. Based on the findings from the experimental work presented in Chapter 6, a hypothesis was formed: limitation of lower limb flail, through wearing a restrictive reinforced pelvic binder over the greater trochanters as pelvic PPE, would result in a reduction in pelvic vascular injury. This may result in reduced functional mobility, however, and so alternative PPE positioning was also considered. In order to examine the ability of pelvic PPE to limit pelvic bony displacement, but not limit lower limb mobility, a restrictive reinforced binder

worn proximal to the hip joints at the level of the anterior superior iliac spine (ASIS) on the pelvis was also considered.

As such, the aims of this study were (1) to replicate dismantled pelvic blast injury in a small animal model utilising a shock-tube mediated blast wave and (2) to provide proof of concept of the pre-application of a reinforced pelvic protective binder, worn at either the level of the anterior superior iliac spine (ASIS) or the greater trochanters, in providing a reduction in the incidence of pelvic vascular injury following blast. The hypothesis of this study was that pre-application of a reinforced pelvic protective binder worn at the level of the greater trochanters, through limiting lower limb flail and preventing bony pelvic displacement, would reduce the rate of pelvic vascular injury; pelvic protection worn at the level of the ASIS was hypothesised to have a lesser effect.

8.3 Methods

The experimental design and procedures were carried out in compliance with the UK Animal (Scientific Procedures) Act 1986. Shock tube testing was conducted using the previously established model on fresh-frozen male cadaveric mouse specimens. Specimens were stored at -20°C and thawed at room temperature ($21 \pm 2^{\circ}\text{C}$) prior to testing. A total of fifty mice were included. These were divided into standing and supine cohorts. Within the standing cohort, thirty mice were assigned to one of three groups: ten mice with pelvic protection worn at the level of the lower pelvis and including the greater trochanters of the thigh (GT group), ten mice with pelvic protection worn at the level of the upper pelvis around the anterior superior iliac spines (ASIS group), and ten mice with no pelvic protection (control group) (Figure 39 a). Within the supine cohort, twenty mice were assigned to one of two groups: ten mice with pelvic protection worn at the level of the greater trochanters (under-body GT group) and ten mice with no pelvic

protection (under-body control group) (Figure 39 b). As will be discussed below, no ASIS protection group was included in the supine cohort.

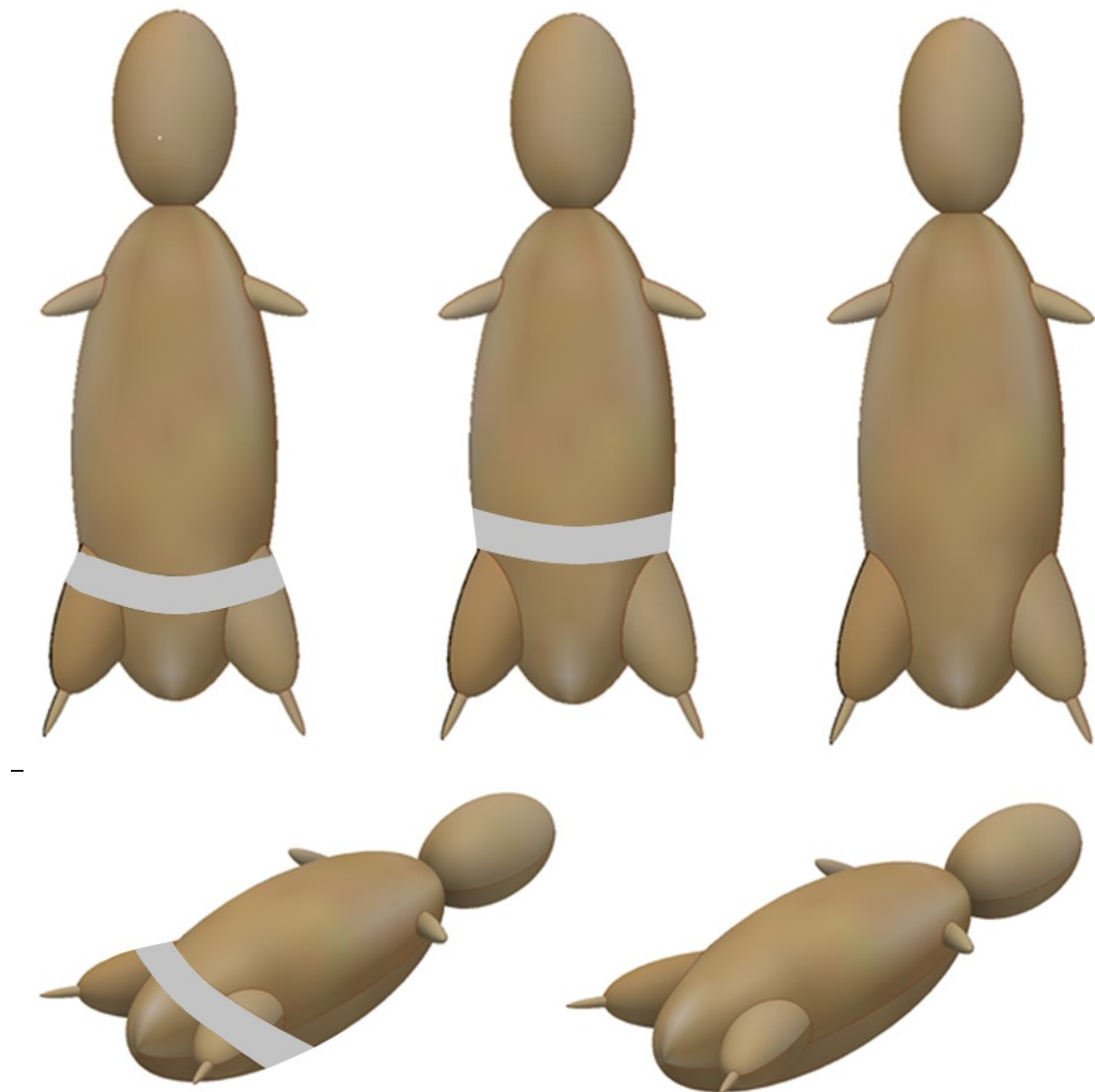


Figure 39: (a, top) upright mice with pelvic protection worn at the level of the greater trochanters (left), anterior superior iliac spines (middle), or no protection (right). (b, bottom) supine mice with pelvic protection worn at the level of the greater trochanters (left), or no protection (right). Mouse represented with model.

Pelvic protection consisted of a 4.8 mm wide by 1.2 mm thick nylon belt with a tensile strength of 215.6 N. A belt width of 4.8 mm was chosen to allow coverage of the intertrochanteric region of the mouse femur, whilst minimizing further pelvic coverage. Once applied, in order to standardise the application of the protective equipment across specimens, belts were pre-tensioned to a set compressive force using a tension-limiting applicator. The protective belt was tightened around the mouse to a compressive force of 20 N, at which point the belt was locked in position. This was the minimum force that the tension-limiting applicator was able to apply to the pelvic protection and was chosen to minimise soft tissue deformation during application. However, as will be discussed, the degree of soft tissue deformation was likely higher than what would be possible for a combatant. Initial positioning was confirmed prior to testing with radiographic imaging (Fluoroscan InSight™-FD, Hologic Inc., USA).

Mice within the standing cohort were positioned to replicate a blast wave received front-on, secured upright on a stainless-steel platform distal to the outlet flange of the Imperial College London double diaphragm shock tube. Three restraints were applied to secure specimens in position whilst not limiting lower limb mobility: across the abdomen, thorax, and neck (Figure 40 a). These restraints created boundary conditions which allowed for the initial positioning of the mouse on the platform to be maintained throughout the blast, whilst allowing for free movement of the pelvis and lower limbs.

Mice within the supine cohort were positioned to replicate an under-body blast wave. Mice were placed supine on 0.3 mm diameter polyester suspension threads, distal to and with lower limbs facing towards the outlet flange of the double diaphragm shock tube (Figure 40 b). The boundary conditions within this cohort allowed for uninhibited movement of the mouse following blast, with no restriction to any part of the body. Suspension threads were sufficiently supportive to hold the mouse in place but broke easily to allow normal blast displacement

during experiments. The mouse subsequently received by a decelerating safety net immediately distal to mounting platform.

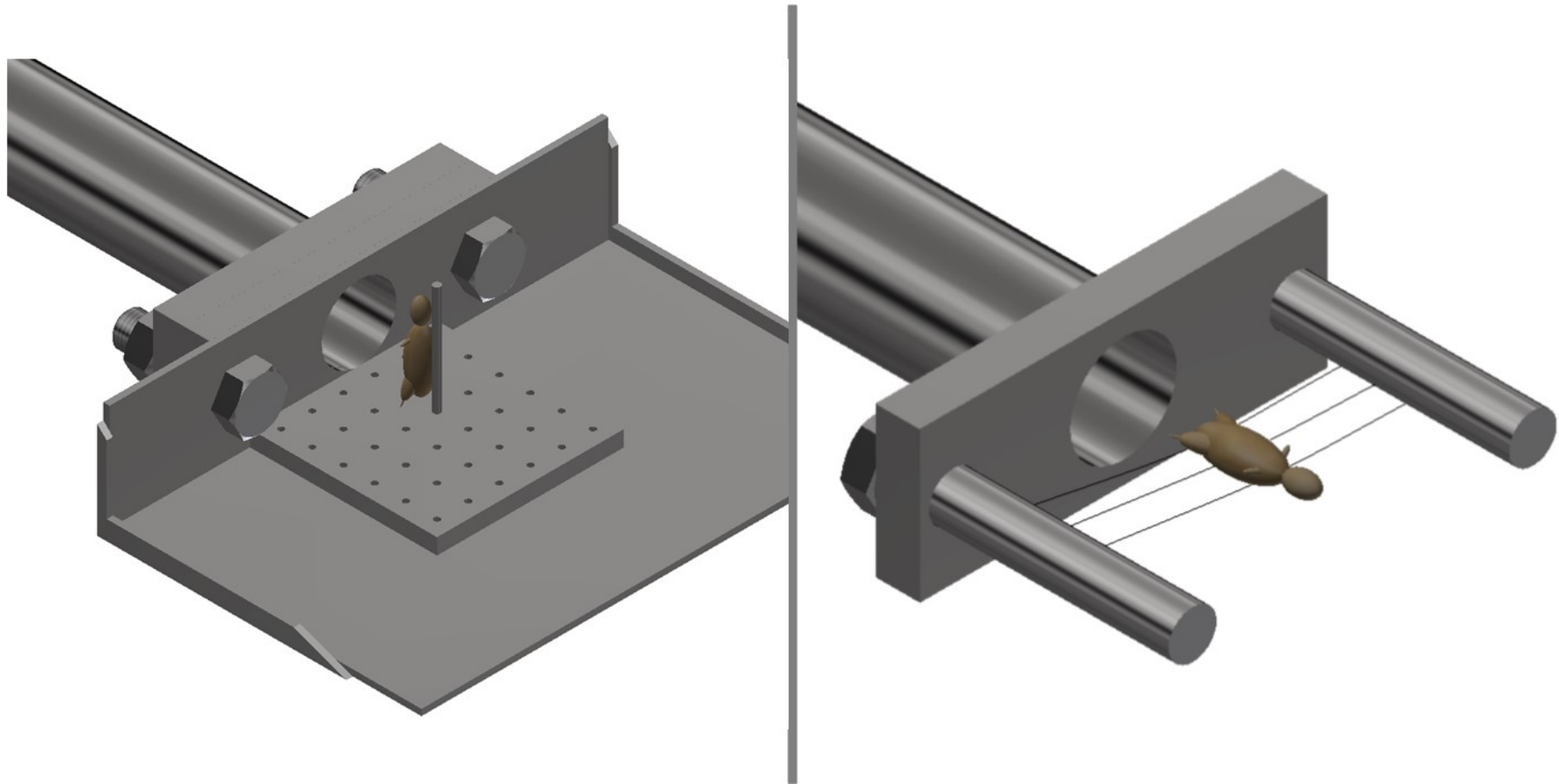


Figure 40: (a, left) shock tube with front-on blast mounting platform and mouse. (b, right) shock tube with under-body blast mounting platform and mouse. Mouse represented with model.

Shock wave pressures were chosen and replicated based upon previous work, which correlated lower limb flail to pelvic blast injury in the same small animal model (Chapter 6, Figure 27). This setup utilises a scaled shock wave sufficient to cause pelvic injury in the mouse model (mean peak pressure of 4.28 bar, plateau pressure of 2.23 bar, and shock impulse of 24 bar ms), whilst below the anticipated threshold to result in fatal traumatic blast-lung injury.

A high-speed digital video camera (Vision Research Phantom v210, Ametek; New Jersey, USA) utilising a vertical view point perpendicular to the shock tube was used to record the event of the shock wave impacting the mouse specimen, to confirm positioning throughout. Images were recorded at a resolution of 128×152 pixels at 72,000 frames-per-second.

Following the tests, specimens underwent radiographic imaging (Fluoroscanner InSight™-FD, Hologic Inc., USA) and dissection to identify pelvic fracture and vascular injury. These were confirmed macroscopically, with 10% of vascular injury samples taken for histological verification. Histological samples were fixed in 10% buffered neutral formalin and stored at room temperature ($21 \pm 2^\circ\text{C}$) overnight. Samples were then fixed, dehydrated, and embedded in paraffin wax. These were sliced with a microtome, affixed to microscope slides, rehydrated, and stained with haematoxylin and eosin. Slices were then viewed using standard light microscopy. Vascular injury was defined as complete transection, with the most proximal injury noted. Fractures were classified in accordance with the Tile criteria: type A (pelvic ring stable), type B (pelvic ring rotationally unstable, vertically stable), and type C (pelvic ring rotationally and vertically unstable) (Tile, 1996). Associated lower extremity fracture with or without traumatic amputation was also noted.

Data analysis was performed using IBM SPSS statistics version 25 (IBM, New York, USA). Crosstabulation with Pearson's Chi-square test was used to assess for significant differences in incidence of pelvic fracture, vascular injury, and Tile classification type of protected vs.

unprotected groups. Relative risk (RR) analysis was performed for incidence of pelvic fracture and performed for incidence of vascular injury, comparing protection groups to the respective control groups.

8.4 Results

The incidence and relative risk of pelvic fractures and vascular injuries across all groups is shown in Table 8. Table 9 displays the classification of pelvic fractures according to the Tile criteria, and the location of the most proximal vascular injury across all groups. Pelvic vasculature injury findings on dissection are shown in Figures 41 a – d. In all samples obtained, histology confirmed the presence of vascular tissue (Figure 42).

Significant differences were noted for a reduction in fracture incidence of GT groups compared to controls ($p < 0.01$) and elimination of vascular injury ($p < 0.001$). The ASIS group showed no reduction in fracture incidence but a reduction in vascular injury incidence (RR 0.6, 95% CI 0.4 – 1.0, $p = 0.025$). A significant difference was noted across all protection groups when comparing their Tile classification, with fewer type C fracture patterns and more Type B fracture patterns within the protection groups ($p < 0.01$).

Associated lower extremity fracture with or without amputation was not significantly different across all groups but showed a trend to increase amongst the protected groups (control: 7, ASIS: 9, GT: 10; supine control: 7, supine GT: 10). Separate risk analysis performed for all GT protection groups (both standing and supine combined) vs. all unprotected groups (standing and supine combined) showed a significant difference, due to more lower extremity fractures with or without amputation in the GT protection groups (20 vs. 14, $p < 0.01$).

Mouse group	Number of mice	Pelvic fracture (%)	RR of pelvic fracture (95% CI)	Vascular injury (%)	RR of vascular injury (95% CI)
Pelvic protection GT	10	5 (50)	0.5 (0.3 - 0.9)*	0 (0)	0**
Pelvic protection ASIS	10	10 (100)	1 ^a	6 (60)	0.6 (0.4 – 1.0)*
No protection	10	10 (100)	1 ^a	10 (100)	1 ^a
UB, pelvic protection GT	10	3 (30)	0.3 (0.1 - 0.8)*	0 (0)	0**
UB, no protection	10	10 (100)	1 ^a	10 (100)	1 ^a

Table 8: Incidence and relative risk of pelvic fracture and vascular injury across all groups. RR, relative risk. CI, confidence intervals. GT, greater trochanters. ASIS, anterior superior iliac spines. UB, under-body. * $p < 0.05$. **injury not present ($p < 0.001$). ^a Redundant term.

Mouse group	Number of mice	Pelvic fracture (%)	Tile Classification			Most proximal vascular injury				
			A	B	C	Vascular injury (%)	Internal iliac vasculature	External iliac vasculature	Common iliac vasculature	Aorta
Pelvic protection GT	10	5 (50)	0	5 (100)*	0	0	0	0	0	0
Pelvic protection ASIS	10	10 (100)	0	4 (40)*	6 (60)	6 (60)	1	4	1	0
No protection	10	10 (100)	0	0	10 (100)	10 (100)	0	4 ^a	6 ^a	1
UB, pelvic protection GT	10	3 (30)	0	3 (100)*	0	0	0	0	0	0
UB, no protection	10	10 (100)	0	0	10 (100)	10 (100)	5	3	2	0

Table 9: Classification of pelvic fractures according to Tile criteria and location of most proximal vascular injury across all groups. GT, greater trochanters. ASIS, anterior superior iliac spines. UB, under-body. ^abilateral injuries. *p < 0.05.

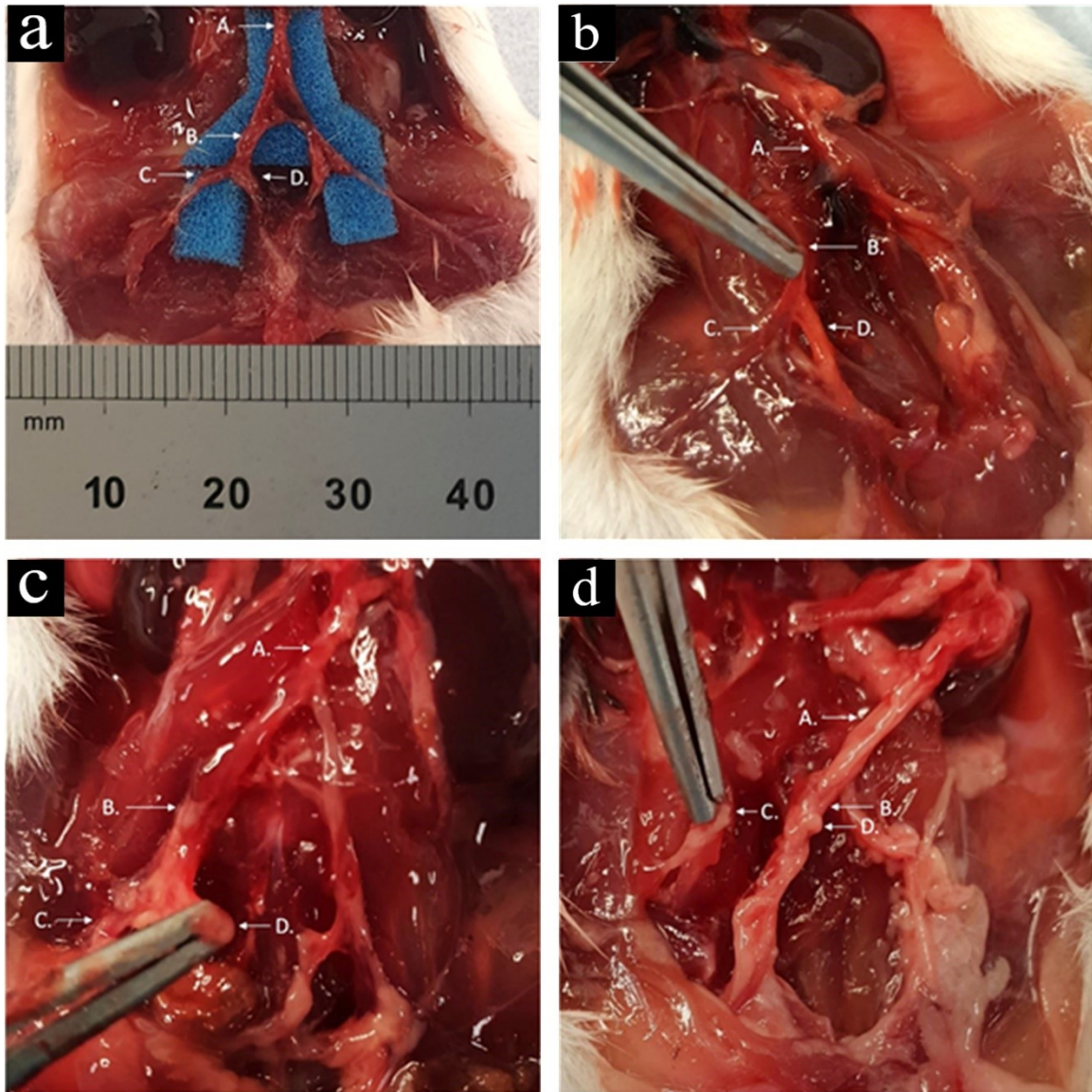


Figure 41: (a) dissection of a mouse with uninjured arterial tree: (A.) aorta, (B.) common iliac artery, (C.) external iliac artery, (D.) internal iliac artery. (b) dissection of a mouse with common iliac vascular injury: (A.) aorta, (B.) transected common iliac artery, (C.) external iliac artery, (D.) internal iliac artery. (c) dissection of a mouse with internal iliac vascular injury: (A.) aorta, (B.) common iliac artery, (C.) external iliac artery, (D.) transected internal iliac artery. (d) Dissection of a mouse with external iliac vascular injury: (A.) aorta, (B.) common iliac artery, (C.) transected external iliac artery, (D.) internal iliac artery.

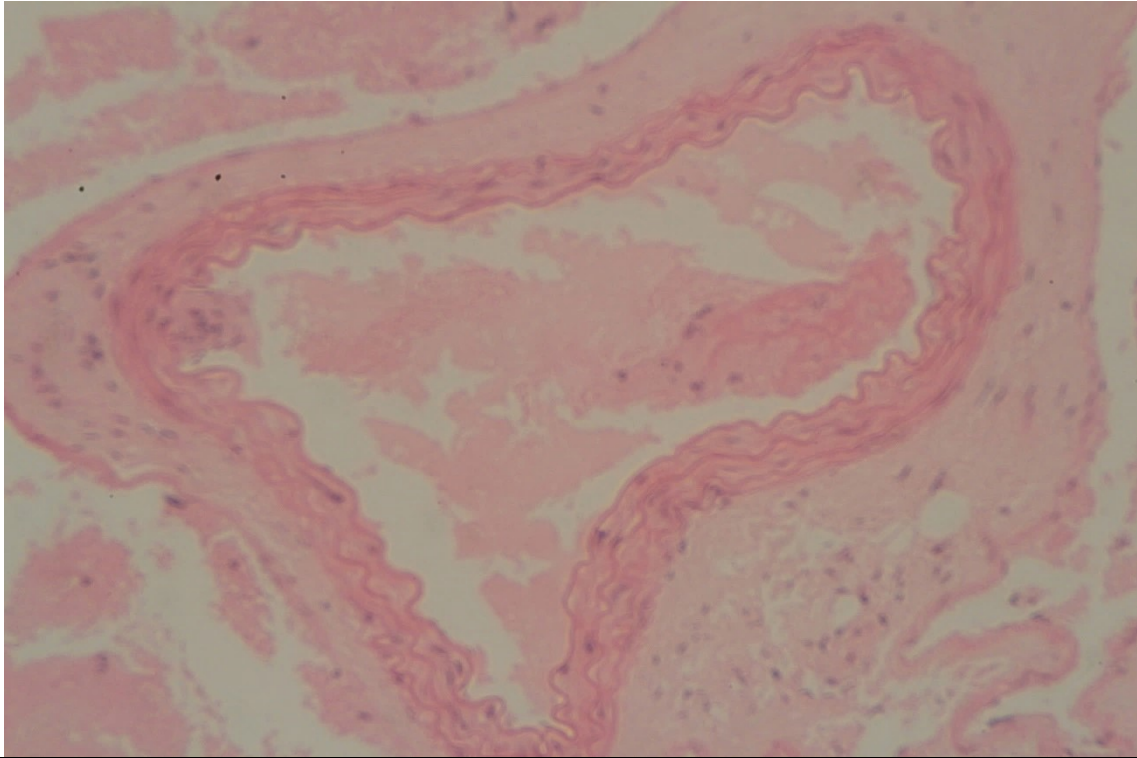


Figure 42: Histology at 40x magnification showing arterial tissue (sample excised from external iliac artery).

8.5 Discussion

This study used an established mouse model of fatal dismounted pelvic blast injury and demonstrated that the introduction of a reinforced pelvic protective binder worn at the level of the greater trochanters, through limiting lower limb flail, can reduce the injury severity. It was shown previously in Chapter 6 that lower limb flail transfers load which result in lateral displacement of the hemipelvis, displacement of intra-pelvic soft tissues, and a subsequent rupture of pelvic vasculature. In addition, where the lower limbs were removed prior to subjecting specimens to a blast wave, pelvic fractures were minimally displaced and vascular injury was absent. In this current study, pelvic protection worn at the level of the greater trochanters limited lower limb flail and prevented vascular injury following both front-on and under-body blast waves. In contrast, pelvic protection providing a degree of limitation to pelvic bony displacement but not lower limb flail (when worn at the level of the ASIS) showed a minimal reduction in vascular injury, with the confidence intervals of the relative risk ratio approaching 1 (RR 0.6, 95% CI 0.362 – 0.995, $p < 0.05$).

Mice with no protection showed pelvic injury patterns consistent with the dismantled blast injury. Pelvic fractures were rotationally and vertically unstable with significant displacement (Figure 43). Vascular injury was seen in all cases, predominately at the common or external iliac vessels.

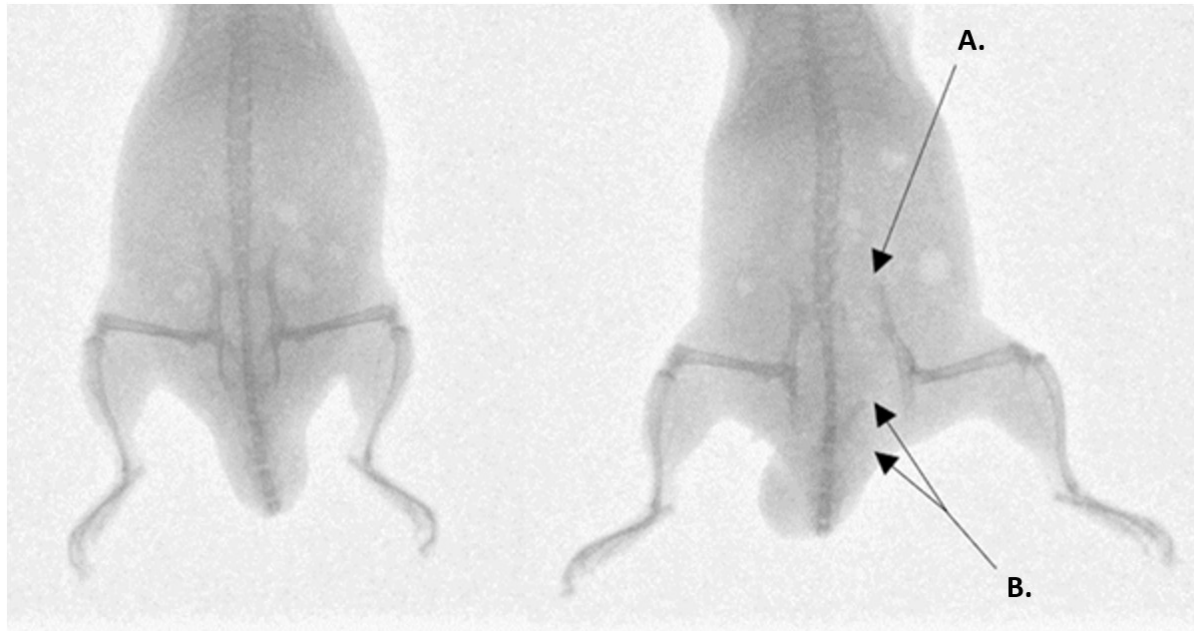


Figure 43: (Left) pre-blast radiograph of unprotected mouse. (Right) post-blast radiograph of unprotected mouse, showing (A.) displaced sacroiliac joint disruption with (B.) displaced pubic rami fractures.

Protection worn at the level of the ASIS was found to have no effect on the incidence of pelvic fracture but as noted, was associated with a minimal reduction in vascular injury. Fracture classification showed a significant decrease in the number of Tile type C fractures (with an increase in Type B) when compared to unprotected mice ($p = 0.025$). As such, protection worn at the level of the ASIS offered some degree of protection in mitigating the injurious effects of dismantled blast on the pelvis and associated vasculature (Figure 44).

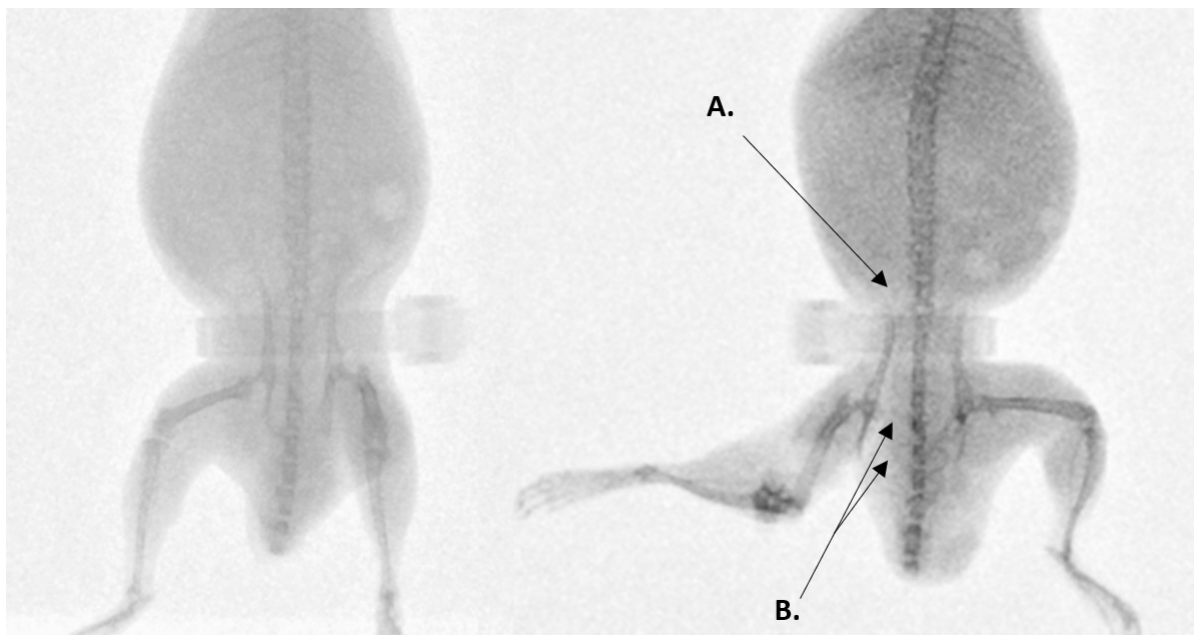


Figure 44: (Left) pre-blast radiograph of a mouse with pelvic protection worn at the level of the ASIS. (Right) post-blast radiograph of a mouse with pelvic protection worn at the level of the ASIS, showing (A.) minimally displaced sacroiliac joint disruption with (B.) displaced pubic rami fractures.

Protection worn at the level of the greater trochanters was found to have the greatest reduction in severity of injury: a reduction in pelvic fracture incidence was seen in both front-on (RR 0.5, 95% CI 0.3 – 0.9, $p < 0.01$) and under-body (RR 0.3, 95% CI 0.1 – 0.8 $p < 0.01$) blast, with elimination of vascular injury in both groups ($p < 0.001$) (Figure 45).

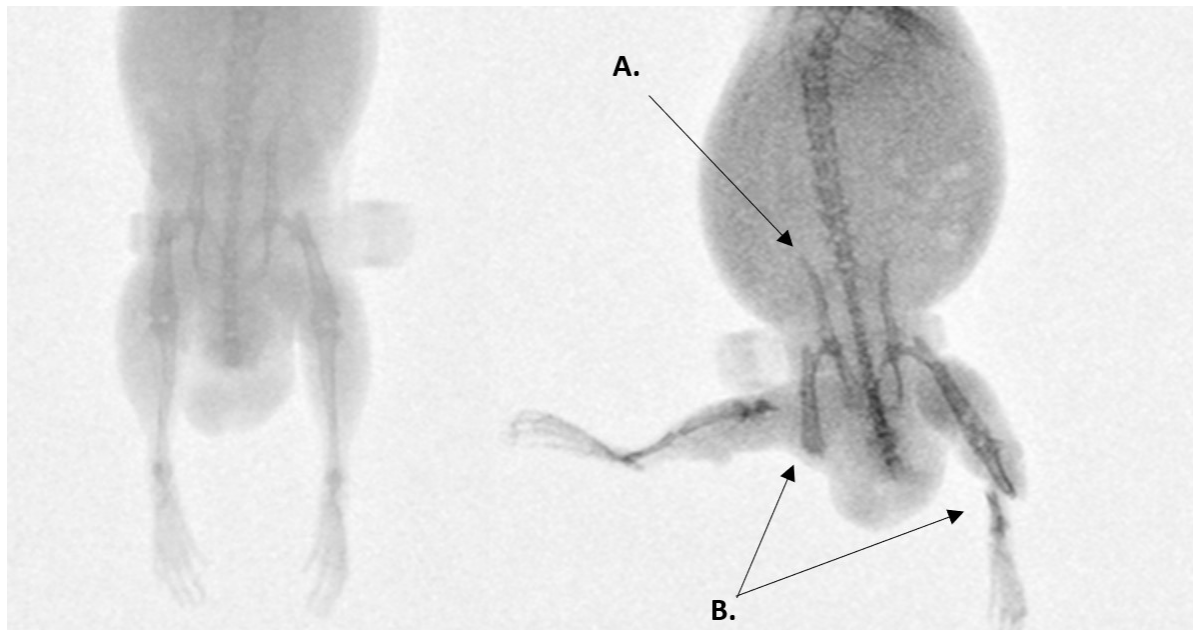


Figure 45: (Left) pre-blast radiograph of a mouse with pelvic protection worn at the level of the greater trochanters. (Right) post-blast radiograph of a mouse with pelvic protection worn at the level of the greater trochanters, showing (A.) an uninjured pelvis with (B.) bilateral lower limb traumatic amputations

An increase in associated lower extremity fractures with or without traumatic amputation was noted within the pelvic protection GT groups. This is thought to be due to the increase in stress distal to the pelvic protection within the lower limb. Thigh movement was restricted as the pelvic protection was worn, whilst leg movement was not. As such, the distal lower limb was mobile during loading from the blast wave whilst the thigh was restricted (and subsequently

unable to transfer load to the pelvis), leading to fracture or amputation of the lower extremity at a point distal to the GT of the femur. In this setting, the femur is sacrificed as a crumple zone where energy is dissipated, instead of it being transferred to the pelvis. In contrast to this, lower than expected rates of traumatic amputation were seen in the control group. As discussed in previous chapters, the hypothesis for this is that in this study, a shock tube was used to replicate the effects of a primary blast injury mechanism (consisting of a high-pressure shock wave followed by a high-speed blast wind of decaying pressure) but not the effects of a secondary blast injury mechanism (injury due to fragments accelerated by the blast wind, such as soil projectile or blast fragmentation). In Chapter 6, secondary blast injury was hypothesised to contribute to the occurrence of traumatic amputation and the lower-than-expected rates of traumatic amputation seen in this study are thought to be due to the lack of secondary blast injury in this same model. Traumatic amputation has been shown to be associated with pelvic fracture and pelvic vascular injury: 68% of all casualties with a pelvic vascular injury secondary to blast had an associated traumatic amputation (Chapter 3). As such, the increased fracture rate seen in the protection groups is thought unlikely to translate to an increase in traumatic amputation incidence amongst dismounted pelvic blast injury casualties. Where pelvic vascular injury was to be spared in preference of lower limb vascular injury (following traumatic amputation), it is hypothesised this would result in lower mortality rates. Military data have shown compressible vascular injury to the lower limb to have a substantially lower mortality rate than non-compressible pelvic vascular injury (Patel *et al.*, 2018; Chapter 3). In the case of a lower limb vascular injury due to traumatic amputation, pre-hospital haemorrhage control can be achieved with the use of tourniquets. For more proximal traumatic amputation where tourniquet application is not practical, advanced haemostatic products can help achieve haemostasis. This is in contrast to non-compressible pelvic vascular injury, where it is challenging to achieve haemostasis prior to surgical intervention

(Chapter 4). As 62% of fatalities of dismounted pelvic blast injury died at the scene (Chapter 3), and 91% of military deaths during recent conflicts were deemed to be unavoidable despite best treatment (Russell, Hunt and Delaney, 2014), this mitigation strategy is viewed as a potentially life – although not limb – saving intervention.

Future mitigation strategies would need to assess the associated risk of lower limb fracture, the blast threat level at which this occurs, and if this protection would therefore be applicable to all military personnel or, for example, counter-IED operators only. The effect of future mitigation strategies should be investigated in less severe blast conditions, to identify if traumatic amputation occurs with pelvic protection at milder blast loading environments which would otherwise be insufficient to cause pelvic injury. Due to the lower-than-expected traumatic amputation observed in the control group within the present study – due to the lack of secondary blast effects in the experimental model – it is not suitable to assess this within this experimental setup. This should be performed where blast conditions accurately reproduce secondary blast and replicate the expected traumatic amputation rates in control groups, for example, in an open free-field blast test.

Vascular injury was defined as complete transection of a major vessel. In several specimens no vascular injury was found. These mice were surgically explored to confirm uninjured arterial and venous vasculature, however, due to the absence of active bleeding in cadaveric mice small vessel injury may have been missed. As such, the conclusions drawn from this research focus on large vascular injury. In one case, severe disruption of the arterial tree proximal to the pelvic vasculature was seen; the aorta was noted as the most proximal vascular injury in this case. Across other mice to have sustained vascular injury, vessel transection was noted to have occurred in the immediate vicinity of the bifurcation of the common iliac artery. Histological samples showed both arterial and venous tissue. In combination with complete vessel transection observed macroscopically on dissection, this was thought to represent injury to both

vascular types. However, a possible limitation of these findings is that collateral vessels have been obtained during histological preparation. As such, the conclusions of this study focus upon major vascular injury but do not specify vascular type.

The shock-tube mediated blast wave chosen for this study was based on that used in Chapter 6. These blast-wave pressures fall below the lethal median dose observed in earlier mouse studies investigating fatal traumatic blast-lung injury, but have been demonstrated to cause pelvic vascular injury (Richmond *et al.*, 1962; Bowen, Fletcher and Richmond, 1968; Chapter 6). The waveforms produced by shock tubes have been argued by some authors to not be representative of blast in the field, due to excessive air flow, which raises the possibility that the loading in the current experiments is confounded by non-blast phenomena (Chandra *et al.*, 2012). However, other authors have highlighted with free field testing that the high air flow ‘blast wind’ that follows the initial shock front is an essential component of the blast wave and subsequent injury patterns (Cullis, 2001). This blast wind is known to cause blast injuries in particular to the limbs, including traumatic amputation (de Candole, 1967; Mellor and Cooper, 1989). As such, this should be viewed as an essential component of blast injury in the context of lower limb trauma.

Testing was first performed on the standing cohort, which showed minimal mitigative benefit in the ASIS protection group compared to the control group, whilst the GT protection group showed complete elimination of vascular injury. As such, the ASIS protection group was not continued within the subsequent supine cohort group, which were tested investigating the GT protection vs. control only.

In order to standardise the application of the protective equipment both within and across groups, a tension-limiting applicator was utilised; the protective belt was tightened around the mouse to a compressive force of 20 N, at which point it was locked in position. This was the minimum force that the tension-limiting applicator was able to apply to the pelvic protection.

A high degree of soft tissue deformation was noted on the radiographs following application of the pelvic protection at this tension. The most notable soft tissue deformation is seen in the ASIS group, where the lower abdominal soft tissue has been displaced and compressed (Figure 44). A smaller but appreciable deformation can also be seen within the GT group (Figure 45). Protective equipment causing significant levels of soft tissue displacement are unlikely to be suitable for continuous use in the soldier population and this factor needs to be accounted for in the design of future protective equipment. As shown in Chapter 6, limitation of lower limb flail is key to preventing fatal pelvic blast injury, irrespective of any compressive effect upon the pelvis. This previous work showed that the pelvis could be spared, and vascular injury prevented, through surgical removal of the lower limbs (and therefore flail) prior to blast - without any additional compression added to the pelvis. The current study has provided proof of concept and shown that a wearable piece of equipment can be used to prevent pelvic vascular rupture by limiting outward flail of the lower limbs. As such, this soft tissue deformation is hypothesised not to be required in the design of future protective equipment, where the wearable armour is required only to limit lower limb flail. Future research development could include incorporating this protective band into the armoured genital protection piece of soldiers on routine patrol. As the groin piece sits at the level of the greater trochanters, a restrictive band could be implemented at this position to create a protective ring to limit outward flail of the lower limbs; when incorporated into the genital protection piece in this manner, high levels of soft tissue deformation at baseline would not be expected. Where future experiments aim to replicate the current study in human cadaveric specimens utilising a tensioned belt, it is unclear how a 20 N compressive force applied to the mouse belt would scale to the human. A human cadaveric study has shown the minimum applied tension required to achieve complete reduction of symphysis diastasis with a pelvic belt was 177 ± 44 N and 180 ± 50 N in the partially stable and unstable pelvis respectively, whilst one brand of pelvic binder has a tension

limiting application of 150 N (Bottlang *et al.*, 2002; Knops *et al.*, 2010). As tensioning of the belt in this study is to aid in retaining position of the belt, and not reducing the pelvis, an upper starting point of a belt application limited to 150 N could be considered in the first instance, before pilot work indicates adjusting the tension accordingly. With regards the size of the belt, adopting the same scaling parameters used for size in this experiment of 20 x, a 96 mm (4.8 mm x 20) wide belt is suggested for use in the first instance.

Several factors must be taken into consideration when incorporating the findings of this study for development of future protective equipment. Protective equipment worn on the pelvis at the level of the greater trochanters eliminated vascular injury through restricting movement of the femurs and load through the pelvis. As a static restraint, this provides marked restriction of lower limb mobility. Whilst such protection may not be practical for soldiers on routine foot patrol (although this would require Human Factors research to assess), enhanced protection has been used on soldiers in certain roles, who were at higher risk, such as specialised explosive search teams. In this select military cohort, the benefits of a static restraint may outweigh the limitations. This study has provided proof of concept of novel pelvic protection; future product development should consider designs which balance compromising mobility against survivability. Future development of protection for the soldier on routine foot patrol should consider allowing movement under low loading rates but prevent it at higher rates, such as those incurred with rapid movement of the limbs during a blast event. Improvements upon the physical model should consider replicating the effects of secondary blast injury from soil ejecta or shrapnel, as these may impact upon the protective equipment's suitability and mitigating efficacy.

8.6 Conclusion

This study is the first to provide proof of concept of pelvic protective equipment limiting lower limb flail to reduce the incidence of pelvic vascular injury in a small animal model. The results suggest that protective equipment worn at the level of the greater trochanters can prevent limb flail and pelvic fracture displacement. Protection worn higher on the pelvis was shown to not limit flail or eliminate vascular injury but resulted in a marginal reduction of injury severity. These findings propose a novel mitigation strategy which aims to reduce the high mortality rates associated with dismounted pelvic blast injury.

Chapter 9

The Mechanism of Injury of Traumatic Amputation

9.1 Scope of the chapter

Proof of concept pelvic protective equipment, which limits lower limb flail, has now been shown in a cadaveric mouse model to reduce the rate of pelvic vascular injury following a shock-tube mediated blast wave (Chapter 8). Future considerations for mitigation strategies will now focus on protecting against the associated injuries of dismounted pelvic blast. Traumatic amputation (TA) was shown to have the subsequent highest relative risk of fatality of any individual injury following pelvic vascular injury (Chapter 3). The current proof of concept pelvic protective equipment does not mitigate traumatic amputation and may result in an increase in the risk of this injury. In this chapter the injury mechanism of traumatic amputation is investigated, with a view to optimising blast protection to mitigate the risk of this injury. High-velocity sand blast was implicated as a mechanism of injury causing traumatic amputation in Chapter 7. In this current chapter, a modified gas-gun experimental setup of that developed in Chapter 7 is utilised to further examine this mechanism of injury. High-speed cameras capturing the moment of sand blast impact and subsequent stages of traumatic

amputation, when viewed in conjunction with post-impact injury analysis, allow for further characterisation of the pattern and development of this injury. Several variables in sandy gravel are assessed, for which injury-risk curves generated showed a positive correlation with sandy gravel velocity but not size or moisture content. Previous experiments within this thesis and literature are examined and an updated injury mechanism of traumatic amputation is described, producing a shift in the understanding of traumatic amputation due to blast.

9.2 Introduction

Blast-mediated traumatic amputation is one of the most common and defining injuries of any IED attack (Ramasamy, Hill and Clasper, 2009). This injury represents a significant cause of morbidity and mortality. It is associated with fatality either directly through haemorrhage, or indirectly as a marker of other severe blast trauma (Mellor and Cooper, 1989). With regards to morbidity, a US-Army study showed only a 2.3% return-to-duty rate for soldiers who had sustained a traumatic amputation (of whom most had suffered only partial hand or foot loss) (Kishbaugh *et al.*, 1995). From a civilian perspective, the 2013 Boston Marathon bombing caused 17 lower limb traumatic amputations and a further 10 severe soft tissue extremity injuries (King *et al.*, 2015); the morbidity in these civilian injuries is likewise extensive with reduced mobility, phantom limb pain, and an overall reduced quality of life reported (Sinha *et al.*, 2011; Azocar *et al.*, 2020). To limit the overall mortality of dismounted pelvic blast injury, and to reduce the morbidity associated with traumatic amputation, an accurate understanding of the mechanism of injury is required.

As discussed in Chapter 7, the mechanism of injury by which blast results in traumatic amputation is not clearly understood. Whilst high velocity environmental debris was shown to cause a cohort of injuries, including traumatic amputation, the exact mechanism by which the traumatic amputation had occurred was not examined specifically. Furthermore, variables in

the environmental debris to injury risk were not examined. With regards to the type of environmental debris, North Atlantic Treaty Organization (NATO) standards for testing protection against a buried explosive device defines the testing conditions as utilising a soil type which is of a sandy gravel composition (NATO/PfP Unclassified, 2006). It is not clear how modifiable variables of the sandy gravel soil may affect injury risk outcomes.

As discussed in Chapter 7, when a buried explosive is detonated, the resultant shockwave compresses this surrounding sandy gravel soil. Immediately following this, gas from the explosion is released at high velocity and acts to eject this compressed soil at supersonic speeds, which rapidly decelerate to below 600 m/s before impacting with casualties (Bowyer, 1996; Tremblay *et al.*, 1998). The soil is carried upwards from the ground by the gas flow to project, dependent upon the soil's characteristics, at an angle of between 45 and 120 degrees, in a cone shape (Figure 46). With dry soil, easier venting of gaseous detonation products results in a wider spread. In contrast, water saturated soil resists gaseous venting to a greater degree; this results in a tunnelling effect and concentration of the soil in a vertical direction, which may result in increased injury at the point of impact (Grujicic *et al.*, 2008; Ramasamy, Hill, Hepper, *et al.*, 2009). The effect that variations in sandy gravel soil moisture content may have on the injury risk of traumatic amputation is not known.

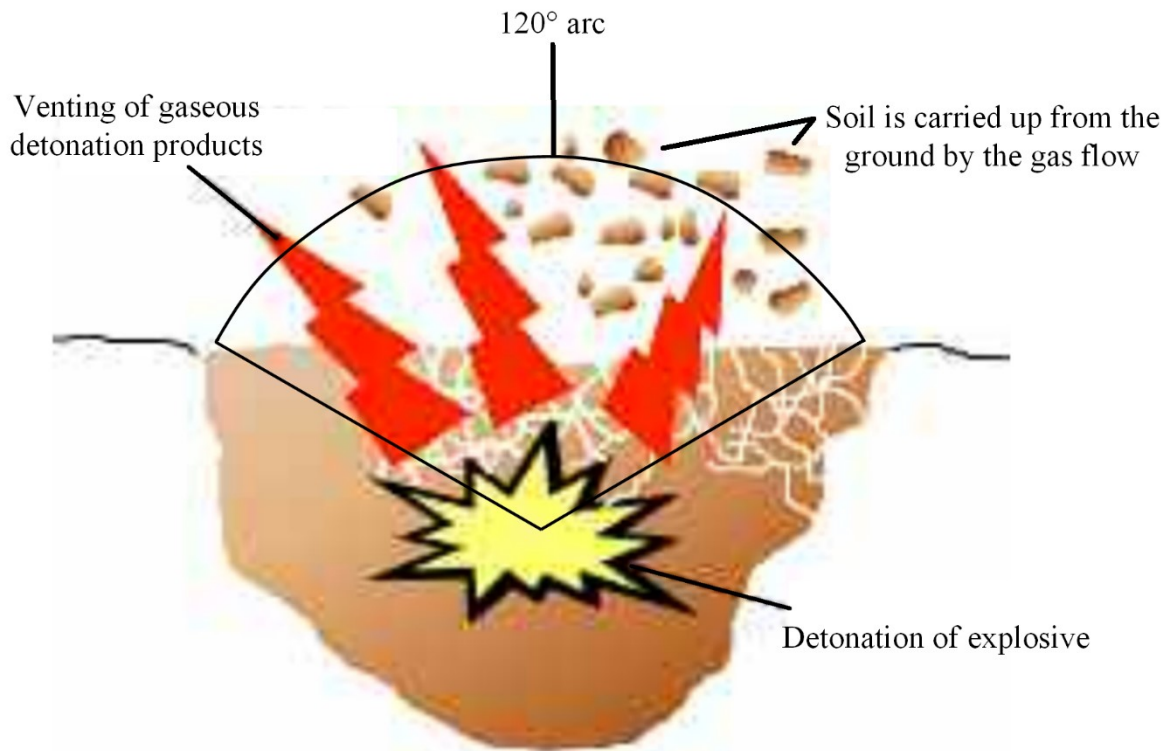


Figure 46: A buried explosive is detonated, with the resultant shockwave compressing the surrounding sandy gravel soil. Immediately following this, gas from the explosion is released at high velocity and acts to eject this compressed soil at supersonic speeds. The soil is carried upwards from the ground by the gas flow to project, dependent upon the soil's characteristics, at an angle of between 45 and 120 degrees, in a cone shape. Image adapted from Ramasamy *et al.*, 2009

A further variable which may affect injury risk is the size of the propagated soil. Typical sandy gravel soil granulometry has been described, with ideally distributed particle sizes ranging from 0.1 to 40 mm.(NATO/PfP Unclassified, 2006) Similar to moisture content, the effect that variations in sandy gravel soil size may have on the injury risk of traumatic amputation is not known.

As such, the aims of this study were (1) to replicate isolated traumatic amputation in a cadaveric small animal mouse model, caused by propagated high velocity sandy gravel, (2) to investigate and describe the mechanism of injury of sand blast mediated traumatic amputation in detail, through high-speed video recording and injury documentation, and (3) to investigate the effect of changes in sandy gravel soil size and moisture content on the risk for sustaining traumatic amputation.

9.3 Methods

The experimental design and procedures were carried out in compliance with the UK Animal (Scientific Procedures) Act 1986. Testing was conducted using the previously established model on fresh-frozen cadaveric male MF-1 (out-bred, ex-breeder, wild type) mouse specimens (8 - 9 weeks of age, Charles River Ltd, UK). Specimens were stored at -20°C and thawed at room temperature ($21 \pm 2^{\circ}\text{C}$) for 3 – 4 hours prior to testing.

Sandy gravel soil sizes were chosen based upon NATO unclassified AEP-55 recommendations for typical sandy gravel soil granulometry (NATO/PfP Unclassified, 2006). This was subsequently scaled to the murine model based upon recommended animal scaling parameters in blast, where the scale is equal to the length of a parameter of the human species divided by that of the animal species used ($\lambda_L = L_1/L_2$) (Panzer *et al.*, 2014). The thigh circumference of each species was taken as the representative parameter for scaling, in view of traumatic amputation of the lower limb as the primary outcome. Median mouse thigh circumference was calculated as 2.7 cm (range 2.4 – 3.2 cm) from specimens ($n = 59$), whilst human thigh circumference was taken from literature as 55 cm (White and Churchill, 1971). From this, an upscaling of 20x for sandy gravel size was utilized ($\lambda_L = 55 / 2.7 = 20$). A minimum sandy gravel size cut-off of 0.1 mm was taken to avoid sublimation of sandy gravel particles smaller than this at high velocity.

Testing with different sandy gravel soil size and moisture content was performed to ascertain for any difference seen in injury risk. Three sandy gravel soil size ranges were tested, consisting of (1) ideally distributed, (2) minimum, and (3) maximum sandy gravel soil size range. These groups were further subdivided into dry or saturated with water prior to testing. This gave a total of six different sandy gravel soil test groups. The ideally distributed sandy gravel soil size range chosen consisted of sandy gravel as closely representative to human scaled values, ranging from the human ideal particle size median value to the 85th centile value, consisting of 60% sandy gravel sized 0.1 to 0.3 mm, 20% sized 0.3 to 0.5 mm, and 20% sized 0.5 to 1 mm. The minimum sandy gravel soil size group consisted of 100% sandy gravel sized 0.1 to 0.3 mm. The maximum sandy gravel soil size group consisted of 100% sandy gravel sized 0.5 to 1 mm. The experimental sand sizes and distribution used (scaled to human values) are shown alongside those recommended in NATO AEP-55, ideally distributed particle sizes in Figure 47 (NATO/PfP Unclassified, 2006).

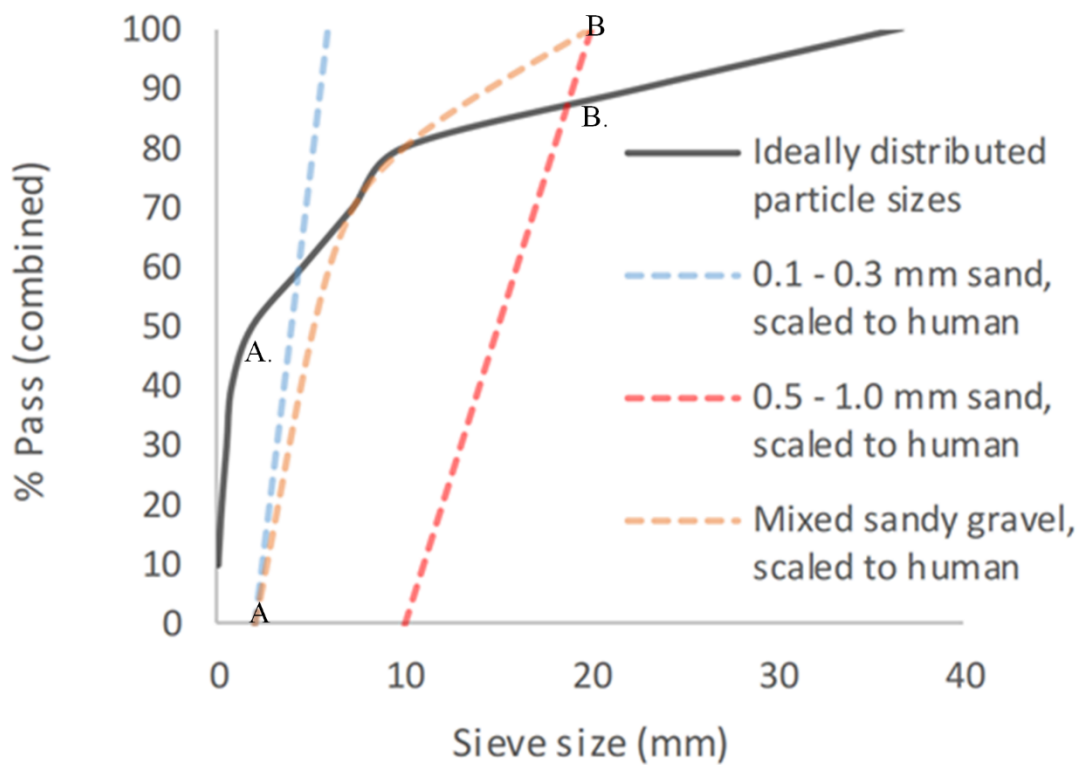


Figure 47: Experimental sandy gravel sizes used, scaled to human values, shown alongside ideally distributed particle sizes. A. = human median value. B. = human 85th centile. A = lower limit of experimental sandy gravel range. B = upper limit of experimental sandy gravel range. % pass (combined) describes the percentage of total volume of sandy gravel passing a specific sieve size; sieve size (mm) relates to the diameter of each hole within the sieve.

The sandy gravel was housed within a hollow polycarbonate sabot which was loaded into the firing chamber of a double-reservoir gas-gun system. The full experimental protocol and mechanism of this system is described in detail in previous chapters (Chapters 5 and 7). The gas-gun system accelerates the sabot-sandy-gravel unit down a barrel to exit into a target chamber, where the sabot is separated from the sandy gravel by a sabot stripper. The sabot is halted at this point, while the sandy gravel continues to travel towards the mouse specimen at the intended terminal velocity.

Mice were secured in an upright posture on a steel mount of 10 mm diameter fixed within the target chamber, 50 mm distal to the gas-gun outlet. A single cable tie across the thorax was applied to secure the specimens in position on the mount, whilst leaving the lower limbs exposed and freely mobile (Figure 48). The right lower limb was centred in the midpoint of the path of the focused sand blast. Experiments were then repeated with re-positioning of the mount to target the contralateral limb.

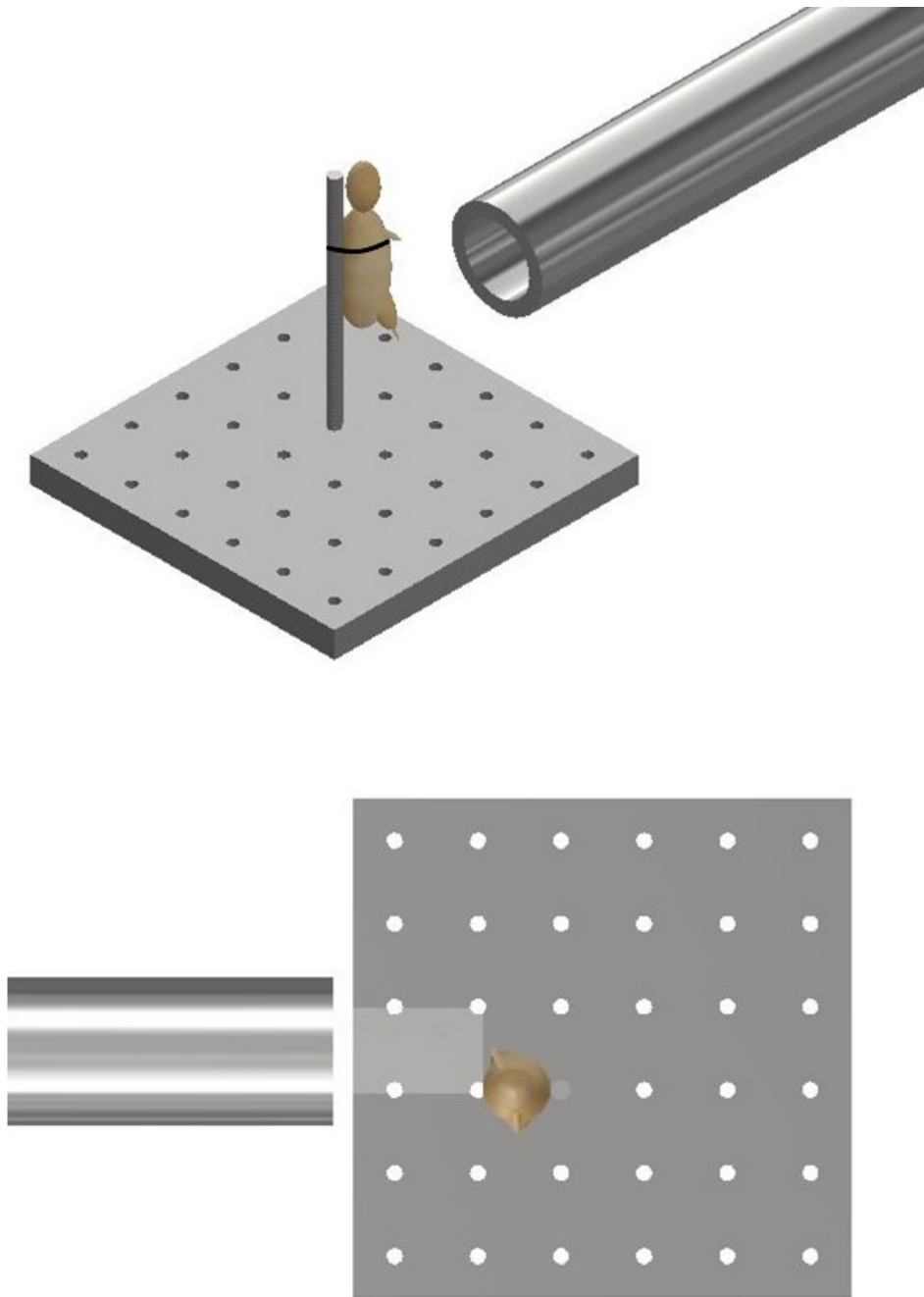


Figure 48: (a, top) schematic illustrating the experimental setup showing the gas-gun outlet with mounting platform and mouse. (b, bottom) aerial view of schematic illustrating initial sandy gravel stream passing through distal outlet to impact with offset lower limb of mouse. Mouse represented with model.

A single control test was performed utilising the maximum gas-gun pressure to be used across experiments with the absence of any sandy gravel ejecta. This was performed in order to ascertain whether any injurious effects are caused by the pressurised air alone. This control test was performed on a single mouse specimen.

The speed of the sandy gravel particles at the point of impact with the specimen was estimated using high-speed photography (Phantom VEO710L, AMETEK, USA) at 68000 fps. An average velocity for the sand blast was determined based upon identifying and tracking four unique points evenly distributed across the sandy gravel. From this, the mean with standard deviation of the velocity of the sand blast as a whole was calculated.

Prior to and following each test, mouse specimens underwent radiographic imaging using a mini-C-arm (Fluoroscanner® InSight™ FD system, USA) to identify any lower limb fractures. Following this, the specimens were reviewed to identify lower limb traumatic amputation. Where a lower limb open fracture was present with extensive soft tissue loss, the injury was classified as a traumatic amputation.

Statistical analysis and development of the risk function

The NCSS statistical software was used for statistical analysis (version 12, Utah, USA). A likelihood-criteria best-fit analysis, with the aid of probability plots, was performed to choose the distribution that best fit the data for each injury type. The Weibull distribution was shown to be the best fit in the majority of cases; hence, it was chosen as the probability distribution to represent the risk for all injury types observed in this study. Weibull survival analysis was used to examine the association between sandy gravel velocity and traumatic amputation. The Weibull regression model is $P(v) = 1 - e^{-(v/\lambda)^\kappa}$, where P is the probability of injury, v (the average velocity of the sandy gravel) is the predictor variable, and λ and κ are the corresponding coefficients associated with the predictor variable. To derive the injury-risk curves, data were

classified as left censored where injury was present and right censored where there was no injury. A *post hoc* two-sample Kolmogorov-Smirnov test was performed to assess for significant differences between the distribution of injury-risk curves across groups. A Bonferroni corrected p value of 0.0083 was used to compensate for multiple comparisons ($0.0083 = 0.05/6$).

9.4 Results

Fifty-nine cadaveric mice were used across experiments, comprising of a total of 117 lower limbs impacted by high-velocity sandy gravel soil, and one lower limb control specimen. No injuries were seen in the control specimen. The average sand blast velocity at the exit of the gun's barrel ranged from 20 ± 5 m/s to 136 ± 5 m/s. A radiograph showing a mouse which sustained a traumatic amputation due to high velocity sand blast is shown in Figure 49.



Figure 49: Mouse injured with high velocity sand blast, sustaining a right sided lower limb traumatic amputation

Images from high-speed video recording, showing the sequential stages of sand blast impact, are shown in Figure 50.

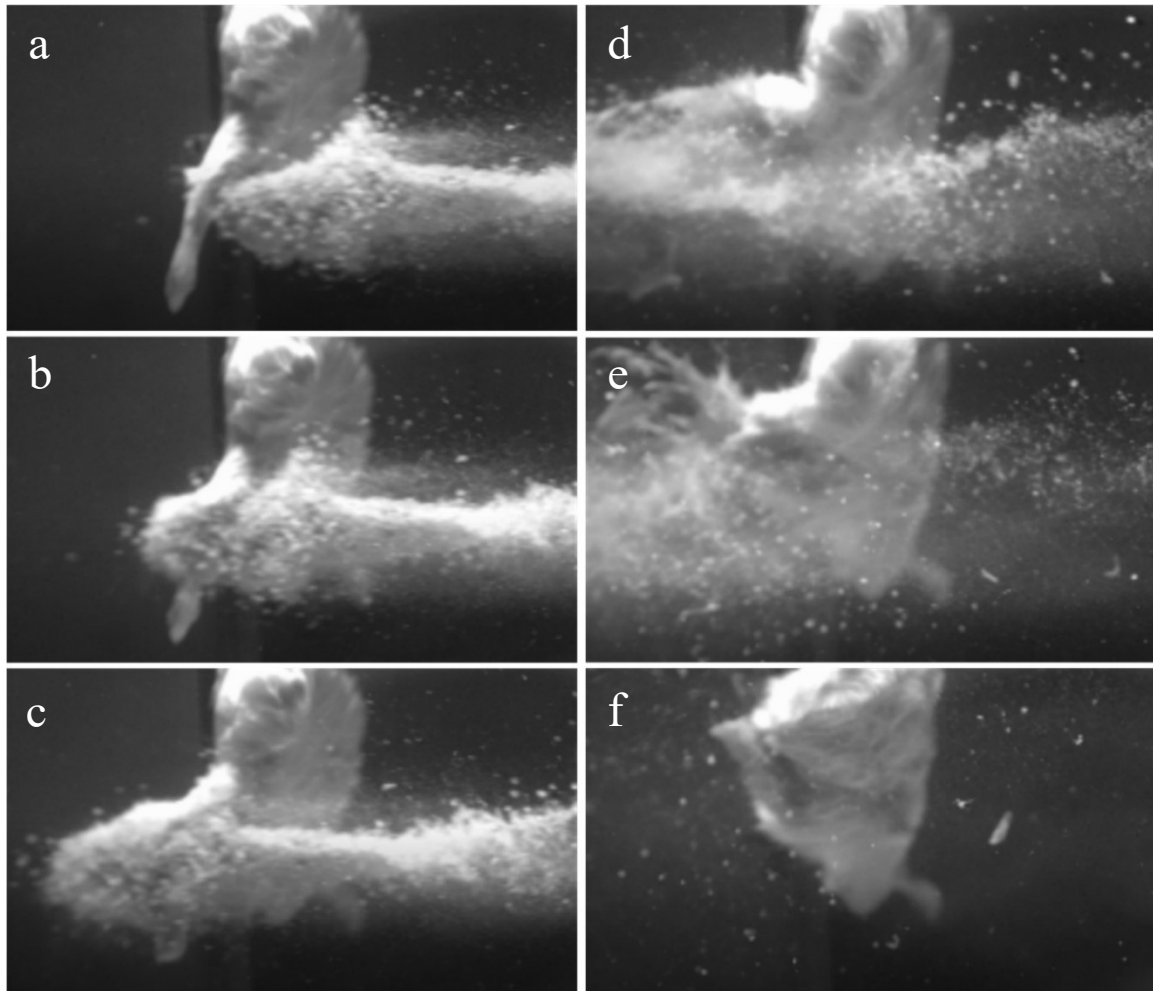


Figure 50: Images illustrating the stages of traumatic amputation secondary to high velocity sand blast. (a) Immediately pre-impact. (b) Point of initial impact. The sandy gravel has begun to move through and around the tissues of the lower limb at high velocity. Due to the experimental setup the foot has evaded the trajectory of the sandy gravel, whilst the limb above has begun to fragment and displace relative to the foot below. (c) The foot has been pulled upward into the trajectory of the sandy gravel, whilst the skeletal and soft tissues above are now significantly fragmented and displaced. (d) The lower limb has now been entirely displaced, with soft tissue stripping on the periphery of the blast now evident as the muscle is seen moving outwards. (e) As the sand blast dissipates, the remaining surrounding soft tissues can be seen more clearly to be stripped and displaced. (f) Completed traumatic amputation.

Images showing exemplar injuries sustained are shown in Figure 51; these images show increasing severity of injury: (a) initial skin lacerations and superficial wounding only, (b) skin and underlying soft tissue injury, (c) associated open fracture with extensive tissue loss, and (d) complete limb avulsion.

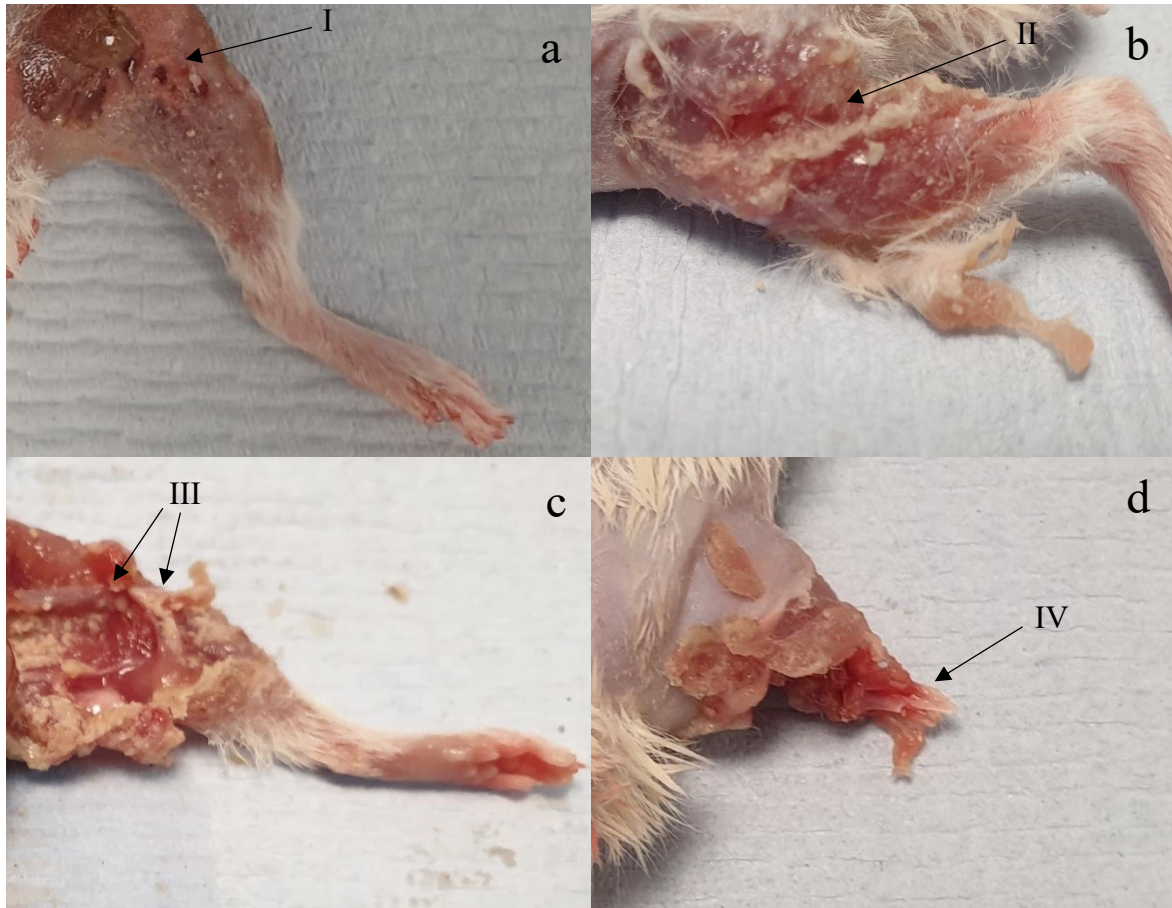


Figure 51: Four separate injuries of worsening severity sustained following impact with high velocity sand blast. (a) burst lacerations and skin tears seen at I. (b) involvement of the underlying subcutaneous and muscular layers, with muscle tears and stripping seen at II. (c) associated open segmental femoral fracture seen at III, with extensive surrounding soft tissue damage and loss. (d) Complete limb avulsion with traumatic amputation seen at IV.

Risk of traumatic amputation increased with increasing sand blast velocity across all groups. The 50% risk of traumatic amputation ranged from 70 m/s (95% confidence interval (CI) 63 – 77 m/s, normalized confidence interval size (NCIS): 0.20) in the 0.1 – 0.3 mm wet sandy gravel group to 77 m/s (95% CI 69 – 86 m/s, NCIS: 0.22) in the 0.5 – 1.0 mm dry sandy gravel group. No significant differences between the distribution of injury-risk curves for sandy gravel soil groups were seen, including across size ranges and moisture content (Table 9). Full injury-risk curves with 95% CIs are shown in Figure 55, with the 25%, 50% and 75% risks of injury presented in Table 10.

	0.1-0.3 dry	0.5-1.0 dry	Mix dry	01.-0.3 wet	0.5-1.0 wet
0.1-0.3 dry					
0.5-1.0 dry	0.591				
Mix dry	1.000	0.358			
01.-0.3 wet	0.841	0.095	0.841		
0.5-1.0 wet	0.591	0.841	0.358	0.194	
Mix wet	0.591	0.841	0.358	1.000	0.194

Table 10: Two sample Kolmogorov-Smirnov test to assess for significant differences between the distribution of injury-risk curves. P values shown

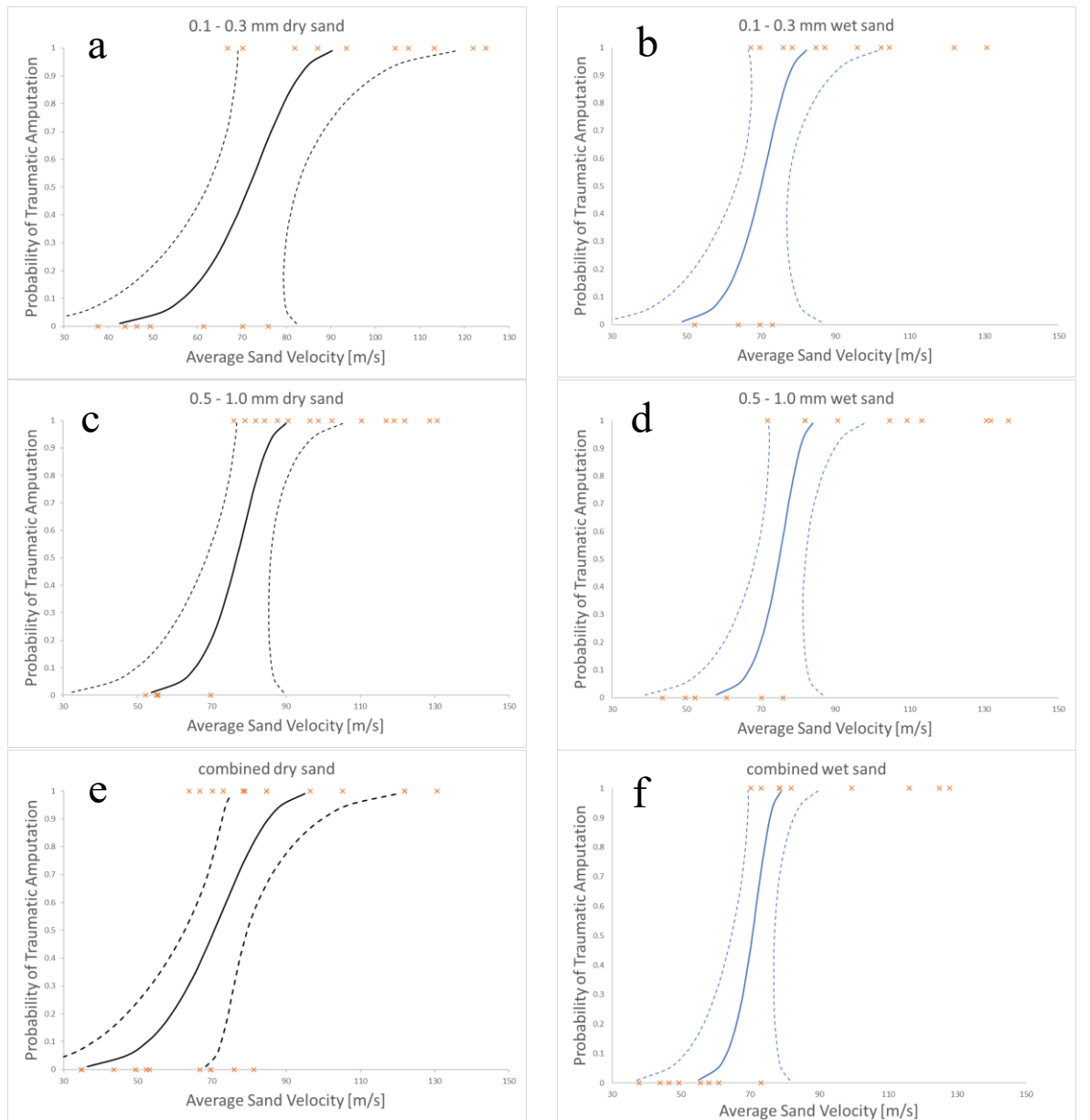


Figure 52: Traumatic amputation risk curves as a function of average sandy gravel velocity. (a) 0.1 – 0.3 mm dry sandy gravel. (b) 0.1 – 0.3 mm wet sandy gravel. (c) 0.5 – 1.0 mm dry sandy gravel. (d) 0.5 – 0.1 mm wet sandy gravel. (e) combined (ideally distributed) dry sandy gravel. (f) combined (ideally distributed) wet sandy gravel. 95% CI represented with dashed lines.

	v_{25} (95% CI) m/s	v_{50} (95% CI) m/s	v_{75} (95% CI) m/s
0.1 – 0.3 mm, dry	64 (52 – 80)	72 (63 – 83)	78 (67 – 90)
0.5 – 1.0 mm, dry	71 (60 – 85)	77 (69 – 86)	81 (74 – 89)
Ideally distributed, dry	62 (50 – 75)	71 (63 – 80)	79 (70 – 89)
0.1 – 0.3 mm, wet	65 (55 – 77)	70 (63 – 77)	74 (67 – 82)
0.5 – 1.0, wet	71 (62 – 81)	75 (68 – 82)	78 (72 – 85)
Ideally distributed, wet	67 (58 – 77)	71 (65 – 77)	74 (68 – 79)

Table 11: The velocities (m/s) at 25%, 50% and 75% risk of injury (v_{25} , v_{50} and v_{75} respectively) for traumatic amputation across all group. 95% confidence intervals (CI) in parenthesis.

9.5 Discussion

The first aim of this study was to reproduce isolated traumatic amputation due to sand blast in a cadaveric mouse model, utilising a gas-gun system. Similar to Chapter 7, this showed that high velocity sand blast is an independent mechanism of injury causing traumatic amputation, with extensive soft tissue and skeletal disruption seen at high velocities. The injury curves presented (Figure 50) show a link between increasing sandy gravel velocity and likelihood of injury. For example, ideally distributed dry sandy gravel showed a 25%, 50% and 75% risk of traumatic amputation at sand blast velocities of 62 m/s, 71 m/s, and 79 m/s, respectively.

In Chapter 7, traumatic amputation in conjunction with pelvic fractures, perineal injury, and open abdominal trauma, due to impact with a widely dispersed cloud of high velocity sandy gravel, was demonstrated. High velocity sand blast was implicated in the mechanism of injury

for traumatic amputation, however, from the injury outcome data alone a characterisation of the process was not possible. In the present study, a focused sand blast to impact the lower limb in isolation was performed. This has allowed for characterisation of the pattern, development, and underlying mechanism of injury. Based on these findings (as displayed in Figures 50 and 51), the process of traumatic amputation due to high velocity sand blast is described: an initial bolus of compressed sandy gravel soil is propagated at high velocity towards the casualty (Figure 50 a). The initial impact results in superficial burst lacerations and tears to the skin of impacted limbs (Figure 51 a). As the soil continues to propagate (Figure 50 b) it progresses to infiltrate deep to the skin spreading out both within and through tissue planes, resulting in trauma to the underlying fascia and muscular tissue, where the sand blast damages and displaces these soft tissues (Figure 51 b). With sufficient velocity, the soil progresses to fracture the underlying skeletal structures, causing segmental or multi-fragmentary fractures to the long bones of the lower limb; the ongoing impact of soil to the soft tissues of the limb has at this stage resulted in extensive soft tissue loss in association with long bone fractures (Figure 51 c). The skeletal and soft tissues are now seen to be fragmented and displaced (Figure 50 c). A critical injury point is reached, whereby the underlying integrity of both skeletal and soft tissues of the limb has been compromised (Figure 50 d). These tissues progress to be avulsed, whilst tissues in the periphery are injured and propagated outward from the point of maximal impact (Figure 50 e). At this stage, a completed traumatic amputation of the limb has occurred (Figures 50 f and 51 d).

As discussed in previous chapters, multiple mechanisms of injury for blast-related traumatic amputation have been described. The initial accepted mechanism of injury was hypothesised to be due to the initial blast shock front causing a diaphyseal fracture of the limb, with the subsequent blast wind separating and amputating the limb at the point of fracture. This theory was based on laboratory work with a goat hind limb model, which showed that a diaphyseal

fracture occurred when a long bone was impacted with a shock front but shielded from the subsequent blast wind or any associated secondary blast injury (Hull and Cooper, 1996). Of note, diaphyseal fracture occurred at distances of 0.5 m proximity to the explosive, but not at 1 m, suggesting the requirement for the casualty to be in close proximity to the explosive for this mechanism of injury to occur (Hull and Cooper, 1996). Further underpinning this mechanism was the clinical association at the time of traumatic amputation to fatal traumatic blast-lung injury, and a lack of through joint traumatic amputations (Mellor and Cooper, 1989; Hull *et al.*, 1994). More recent data have questioned this theory. Data from the conflicts in Iraq and Afghanistan showed no link between traumatic amputation and primary blast-lung injury, with a high proportion of amputees surviving their injuries; furthermore, a substantially higher incidence of through-joint traumatic amputation was seen, again questioning the shockwave mediated diaphyseal fracture mechanism of injury (Singleton *et al.*, 2014). It was hypothesised that the blast wind played a far more substantial role in the mechanism of injury for traumatic amputation and could itself be a mechanism of injury independent of other factors (Singleton *et al.*, 2014).

Chapter 6 investigated pelvic fracture and vascular injury due to a shock-tube mediated blast wave (consisting of both a shock front and subsequent blast wind) using a cadaveric mouse model. This showed traumatic amputation rates following blast far lower than what would be expected to be present in association with the pelvic fractures and vascular injury seen in the study, as compared to the battlefield data examined in Chapter 3. It was subsequently shown in Chapter 6 that when an initial injuring force to the lower limb occurred prior to impact with the blast wind, traumatic amputation occurred. The lower-than-expected traumatic amputation rates were hypothesised as likely due to the absence of any secondary blast injury from the experimental model, to cause this initial injuring force. The current study has shown that high velocity sand blast (a secondary blast-injury mechanism) can be, in and of itself, an

independent mechanism of injury causing traumatic amputation. Both shock tube and gas-gun experimental models are surrogates of the blast environment. Both platforms provide parts of the blast injury in isolation: a shock-tube system allows focused study of the shock front and blast wind (primary and tertiary blast injury) whilst the gas-gun system allows focused study of energised environmental debris (secondary blast injury). Both platforms have produced traumatic amputation, of varying incidence rates, in a cadaveric animal model. In a blast environment, all of these mechanisms (the primary shock front, the secondary energised environmental debris, and the tertiary blast wind causing bodily displacement) occur together. As such, whilst each is possible of causing traumatic amputation in isolation, the reality is likely that traumatic amputation is caused by all three of these described mechanisms synergistically, to varying degrees of each, dependent upon the blast conditions. These mechanisms acting synergistically are hypothesised to be the causative factors for both military and civilian blast-mediated traumatic amputation, where in the civilian setting the sand blast effect is replaced by explosive fragmentation and any surrounding environmental debris.

The second aim of the present study was to ascertain differences to the risk of injury from different loading conditions of the energised environmental debris, with reference to size and moisture content. No significant differences were seen across groups when comparing sandy gravel size (ideally distributed, small, large), moisture content (dry or saturated with water), or both. Whilst a type II error of non-significance is possible, the p values obtained were far from reaching significance, with values ranging from 0.194 to 1.0. As such, the data suggests accepting the null hypothesis that neither sandy gravel size nor moisture content increase the risk of traumatic amputation, as occurs following high velocity sand blast, in this model. Of note, the mass of sandy gravel was standardised across all experiments, irrespective of sandy gravel size. As such, it could be concluded that failure to reject the null hypothesis highlights

that the total mass and dissipation of energy is the determinant factor in causing injury, as opposed to the individual size of any one piece of environmental debris.

In the present study, the 50% risk of traumatic amputation ranged from 70 m/s (95% CI 63 – 77 m/s) in the 0.1 – 0.3 mm wet sandy gravel group to 77 m/s (95% CI 69 – 86 m/s) in the 0.5 – 1.0 mm dry sandy gravel group. This compares to Chapter 7 which showed the 50% risk of traumatic amputation in the mouse model to occur, following impact with a widely dispersed high velocity sand blast cloud, at 247 m/s (95% CI: 222 – 274 m/s). The same gas-gun system and standardised mass of sandy gravel was used in both experiments. In the previous work, the sandy gravel ejecta was widely dispersed to encompass a whole-body field of impact, as occurs following blast, to best recreate the boundary conditions of a blast scenario. As the present study focused on traumatic amputation in isolation, a proportionately greater mass of sandy gravel impacted with the lower limb of the specimen. As such, a greater amount of kinetic energy is expected to be imparted upon the lower limb, where kinetic energy is equal to half of an object's mass multiplied by the velocity squared. It is therefore not unexpected that traumatic amputation was seen to occur at a lower velocity than in Chapter 7, nor that any difference in injury-risk curve distribution across groups was seen, where the sandy gravel mass across these experiments was standardised.

This research has now allowed for a description in greater detail of the injury mechanism of traumatic amputation. Following the energy imparted by the initial shock wave (which itself may cause skeletal trauma, if the casualty is sufficiently close to the explosive), energised projectiles (sand blast; or fragmentation and other environmental debris in the civilian setting) are propagated at high velocity towards the casualty. This causes initial lacerations to the skin followed by continued progression through tissue planes, resulting in trauma to the underlying fascia and muscular tissue. With sufficient velocity the energised projectiles impact with the underlying skeletal structures, the cumulative effective of which causes segmental and multi-

fragmental fractures to the long bones of the limb. A critical injury point is reached, whereby the underlying integrity of both skeletal and soft tissues of the limb has been compromised. The blast wind that follows these energised projectiles completes the amputation at the level of the disruption, and traumatic amputation occurs. In cases of through-joint amputations, the energised projectiles and subsequent blast wind result in failure of the supportive soft tissues (including the ligamentous structures, but with integrity of the skeletal structures intact) to result in limb avulsion and through joint amputation.

9.6 Conclusion

A revised injury mechanism of traumatic amputation due to blast has now been described. The findings produce a shift in the understanding of traumatic amputation due to blast and inform change for mitigative strategies, in particular, through the limitation of high-velocity sand blast. The next step in developing mitigation strategies is to investigate the extent to which current personal protective equipment in use limits the effects of high-velocity sand blast. This will be explored in the following chapter.

Chapter 10

Mitigation of High-Velocity Sand Blast

10.1 Scope of the chapter

The mechanisms of injury in dismounted pelvic blast have now been shown in a mouse model to be lower limb flail resulting in pelvic vascular injury (Chapter 6), and high-velocity sand blast causing significant perineal injury (Chapter 7) and traumatic amputation (Chapters 7 and 9). A proof-of-concept mitigation strategy showed that a wearable piece of pelvic protective equipment, which limited lower limb flail, eliminated vascular injury, and reduced pelvic fracture severity (Chapter 8). To improve upon the development of any future mitigation strategies, protective equipment aiming to reduce lower limb injuries through mitigating the damaging effects of high-velocity sand blast will now be evaluated. Chapter 10 evaluates current military Tier 1 personal protective equipment (PPE) and its capacity for mitigating injury caused by high-velocity sand blast. A cadaveric model of gas-gun mediated high-velocity sand blast is used to simulate the effect of energised environmental debris on injury to a cadaveric thigh, equipped with standard combat trousers, and quantify the reduction in wound

severity by an additional under-layer of Tier 1 PPE. Post-test injury patterns are recorded, including the total surface area and depth of penetration. The findings and suitability of Tier 1 PPE to mitigate high-velocity sand blast are discussed and recommendations for future mitigation strategies are made.

10.2 Introduction

As discussed in Chapter 4, in order to mitigate the increasing rate of soft tissue injury to the pelvis and perineum, pelvic personal protective equipment (PPE) was first fielded for UK service personnel in 2010 (Lewis et al., 2013). This was provided in three hierarchical tiers, designed to be worn in conjunction with one another in response to the perceived threat. Tier 1 is an under-layer to be worn beneath issue combat trousers, covering from waist to knees (Figure 53). It is constructed from a jersey-type material with two layers of high-performance knitted silk protection stitched to the outside to protect vulnerable areas (Lewis et al., 2013). Tier 1 PPE was designed for protection against wounds caused by blast fragments. However, in view of the findings of Chapter 9, it offers the potential to mitigate severe lower limb injuries including traumatic amputation.



Figure 53: Tier 1 pelvic personal protective equipment. (Lewis et al., 2013, figure reproduced with permission)

Evidence of injury reduction from Tier 1 PPE from fragmentation wounds has been observed clinically as a difference in the pattern of injuries suffered by personnel wearing Tier 1 PPE and those not (Breeze et al., 2015). These data suggest benefit from the use of Tier 1 PPE, however, no laboratory study to date has confirmed its efficacy in mitigating the injuries sustained by energised high velocity sandy gravel soil. Similarly, no laboratory study has previously demonstrated the injurious effects of energised high velocity sandy gravel soil against human cadaveric tissue.

In addition to the threat of significant perineal injury and traumatic amputation, injuries sustained through explosive mechanisms have extensive contamination that is driven deep between tissue planes; this deep contamination subsequently requires extensive debridement. Large, complex wounds as seen in the military blast patient contain numerous pockets into which foreign contaminated material is forced (Taylor *et al.*, 2009). To manage this contamination requires a series of operations to remove the foreign material, which may worsen the level of final amputation (Clasper and Ramasamy, 2013). Foreign material found within blast wounds consist of ingrained mud, dirt and sand as well as less obvious contaminants (Taylor *et al.*, 2009). Wounds with heavy environmental contamination from mud, dirt and sand have been associated with soft tissue infection of both environmental bacterial organisms and invasive fungi (Evriviades *et al.*, 2011). The delayed morbidity and mortality of invasive bacterial and fungal infections is significant, and can result in high-level amputation or death (Brown *et al.*, 2010; C. J. Rodriguez *et al.*, 2014). As such the burden of injury from high-velocity sand blast lies not only with the initial trauma, but in mitigation of subsequent infection and sequelae.

Accordingly, the aims of this study were (1) to replicate impact and injury from propelled high velocity sandy gravel soil as occurs following blast in a human cadaveric model, utilising a gas-gun system, and (2) to investigate the effect of Tier 1 pelvic PPE on mitigating the injury patterns observed. It was hypothesised that high velocity sandy gravel soil ejecta would contribute to the soft tissue injury seen in dismounted blast and that Tier 1 pelvic PPE would mitigate the injury patterns observed.

10.3 Methods

The tests performed utilised the previously developed novel setup for investigating injury from high velocity sand, utilising a gas-gun system modified to deliver sandy gravel aggregate at

high velocities (Chapter 7). The experimental design and procedures were carried out in compliance with the Human Tissue Act 2004. Ethical approval was granted from the local regional ethics committee at the Imperial College Healthcare Tissue Bank (ethical approval number: 12-WA-0196). Experiments were carried out using twelve human cadaveric thigh samples with no prior relevant injury or pathology (median age 38 years, range 36 – 51 years). Samples were fresh frozen at -20°C and thawed at room temperature ($21 \pm 2^{\circ}\text{C}$) for 24 hours prior to testing.

As per previous research (Chapters 7 and 9), sand size and properties were chosen based upon NATO unclassified AEP-55 recommendations for typical sandy gravel soil granulometry (NATO/PfP Unclassified, 2006). As the current study utilises human cadaveric samples and not a small animal model, no subsequent scaling was performed. A sandy gravel aggregate size range was subsequently chosen to fall as closely as possible to the median value (2 mm, range 0.1 – 40 mm) of the ideally distributed particle sizes (NATO/PfP Unclassified, 2006). This consisted of sandy gravel of which 100% passed a 1 – 2 mm sieve, with any sand subsequently passing a 1 mm sieve removed (the sand size utilised in experiments therefore ranged from 1 – 2 mm). The sand was housed within a hollow polycarbonate sabot, weighed prior to, and following loading with sand.

The sabot-sand unit was subsequently loaded into the firing chamber of a double-reservoir gas-gun system, as described in detail in previous chapters (Chapters 4 and 7). In order to simulate the distribution and spread of sand ejecta as occurs following blast, two interconnecting fenestrated steel fences, separated by 10 mm and offset to one another by 50% of the diameter of each fenestration, were placed distal to the gas-gun outlet and proximal to the mount (Figure 54). Offsetting of the fenestrated steel fences changed the initial stream of sand delivered by the gas gun into multiple streams of differing trajectories which subsequently dispersed into a widely distributed spread of high velocity sand.

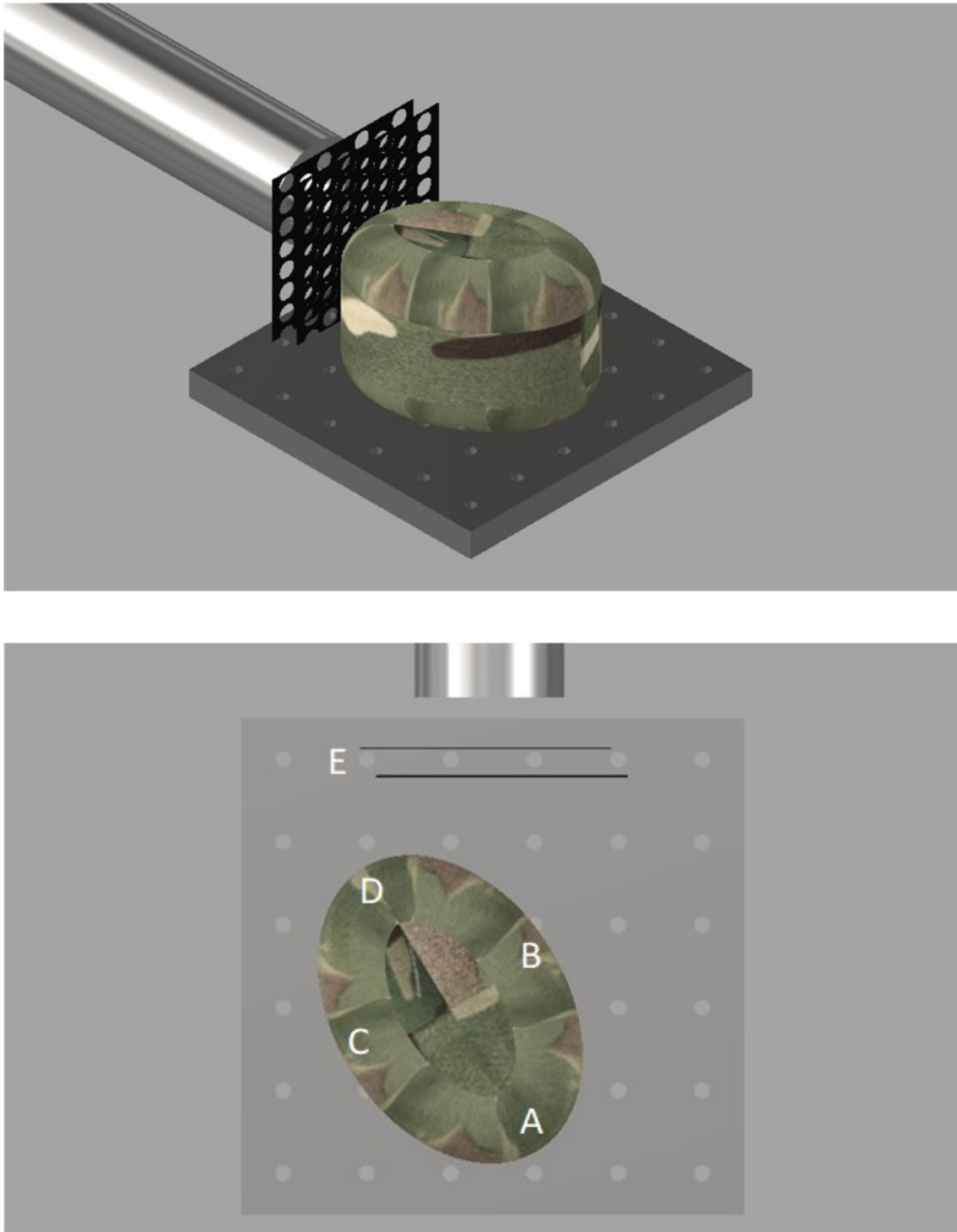


Figure 54: Experimental setup showing cadaveric thigh with issue combat trousers (represented by model) positioned within target chamber. Top, oblique view. Bottom, aerial view. A: proximal thigh, B: medial thigh, C: lateral thigh, D: distal thigh, E: dispersion fence.

The speed of the sand particles at the point of impact with the sample was estimated using high-speed photography (Phantom VEO710L, AMETEK, USA) at 68000 fps. An average velocity for the sand cloud as a whole was determined based upon identifying and tracking four unique points spread across the distributed sand. These points varied in velocity and were chosen from the front, front-centre, centre, and centre-back of the peripheries of the sand spread. Cadaveric samples were divided into one of two groups, either wearing (1) UK Military Tier 1 pelvic protection and issue combat trousers, or (2) issue combat trousers only (control group). For each individual test, a cadaveric thigh was secured in position within the target chamber. The thigh was placed in a neutral resting position with an abduction angle of 30° from the midline (Figure 55).

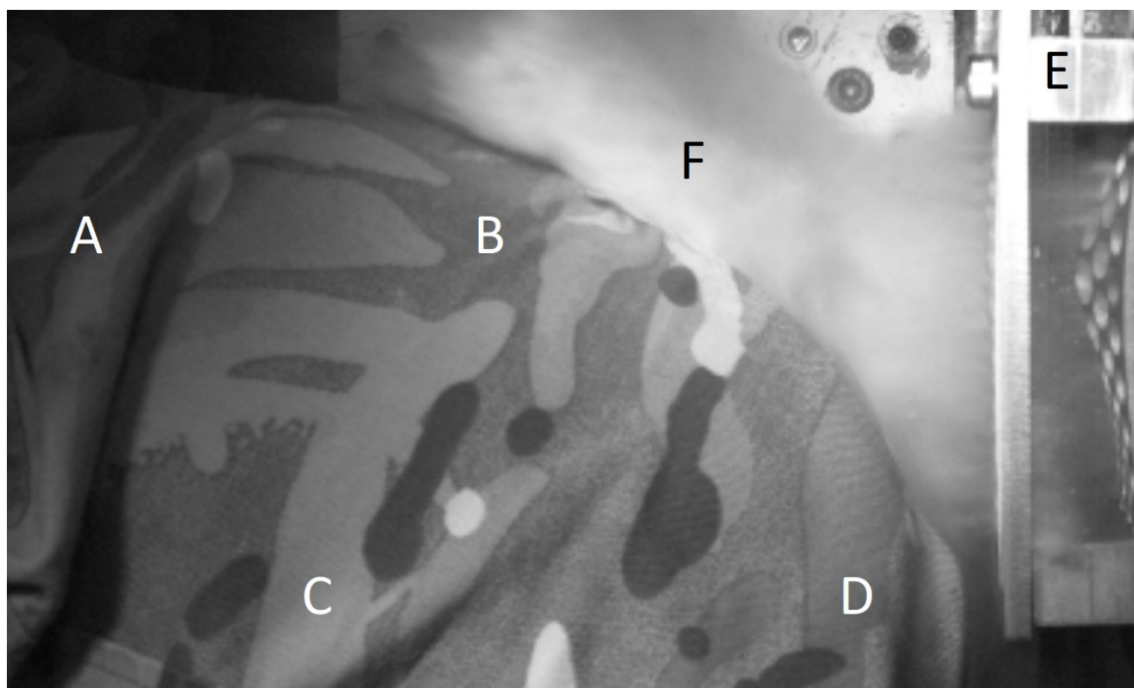
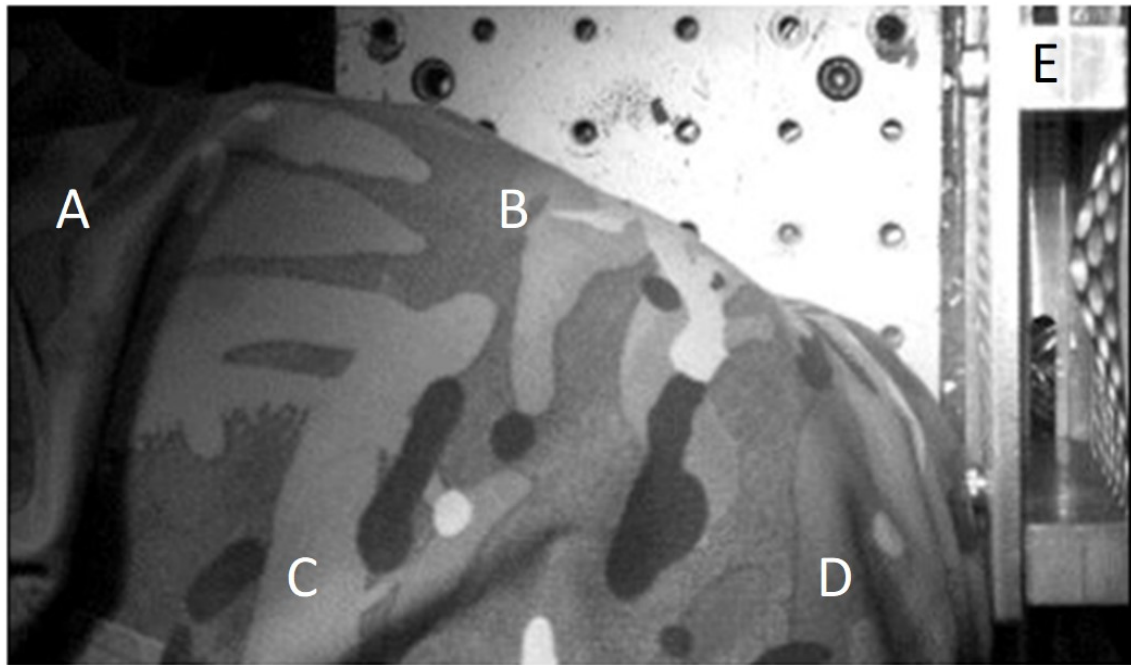


Figure 55: Experimental setup showing cadaveric thigh with issue combat trousers prior to (top) and during (bottom) impact with high velocity sand. A: proximal thigh, B: medial thigh, C: lateral thigh, D: distal thigh, E: dispersion fence, F: high-velocity sand blast

The Military Tier 1 pelvic protection was worn as a whole on the cadaveric thigh, with the sand blast directed to impact with the two layers of high-performance knitted silk protection (Figure 56).



Figure 56: Tier 1 pelvic personal protective equipment worn on cadaveric thigh; post-impact delivered to region of two-layer high-performance knitted silk protection

Following impact with the high velocity sand, samples were removed from the target chamber and taken for subsequent photography and dissection. A separate photograph was taken of each individual injury, with adjacent ruler, and the centre point of the camera parallel to the injury to avoid parallax errors. Recorded injury patterns included (1) number of injuries sustained; (2) surface area of injuries sustained (surface area per injury and total injured surface area); and (3) maximal anatomical depth of injury sustained (subcutaneous only or deep (subfascial)).

Image processing and statistical analysis

Photographed images were subsequently assessed with image processing software to calculate the surface area of injuries sustained. ImageJ was used for image processing calculations (National Institutes of Health, USA). Image scale was set, followed by tracing the outer edges of the zone of injury for each individual injury sustained to calculate the total surface area.

IBM SPSS was used for statistical analysis (version 26, IBM, USA). The Mann-Whitney test was used to assess significant differences in non-parametric data between groups, including number of injuries sustained and surface area of injuries. Cross-tabulation with Pearson χ^2 test was used to assess significant differences in categorical variables between groups, including depth of penetration (subcutaneous only vs. deep (subfascial)).

10.4 Results

Impact with high velocity sand resulted in soft tissue injuries to all samples. A total of fifty-one experimentally derived injuries were produced from 12 thigh samples. Mean sand mass delivered was $8.9 \text{ g} \pm 0.4 \text{ g}$ with a mean velocity of $519 \pm 23 \text{ ms}^{-1}$. No significant difference was seen between groups in the number of injuries sustained per sample (median 3, range 2 – 5, vs. median 5, range 3 – 6, $p = 0.051$). As detailed in Table 12, Tier 1 pelvic PPE markedly reduced the severity of injury seen vs. control: wounds deep to the subcutaneous tissues were eliminated (0 (0%) vs. 23 (77%), $p < 0.001$), a reduction in the size of the largest single wound

was seen (median 77 mm², range 43 mm² – 101 mm², vs. median 271 mm², range 150 mm² – 949 mm², p = 0.002), and a reduction in the cumulative total surface area of all wounds was seen (median 143 mm², range 115 mm² – 230 mm², vs. median 658 mm², range 529 mm² – 1319 mm², p = 0.004).

Sample	Surface area of injury sustained (mm ²)						Total surface area (mm ²)	Total deep injuries
	Injury 1	Injury 2	Injury 3	Injury 4	Injury 5	Injury 6		
Tier 1 pelvic protective equipment								
1	72	26	21	13	10	-	142	0
2	83	37	16	-	-	-	136	0
3	43	41	31	-	-	-	115	0
4	72	64	52	28	14	-	230	0
5	101	56	46	-	-	-	203	0
6	89	55	-	-	-	-	144	0
Control								
7	150*	125*	92*	74*	67*	66	574	5
8	588*	430*	193*	54	54	-	1319	3
9	325	102	71*	83	66*	-	647	3
10	177*	135	118*	52*	47*	-	529	4
11	949*	76*	42	-	-	-	1067	2
12	217*	147*	126*	110*	37*	31*	668	6

Table 12: Number, surface area and depth of injuries sustained. *Deep to subcutaneous tissues involving underlying fascial and muscular layers

Figure 57 displays the damage sustained by issue combat trousers and silk PPE following impact.

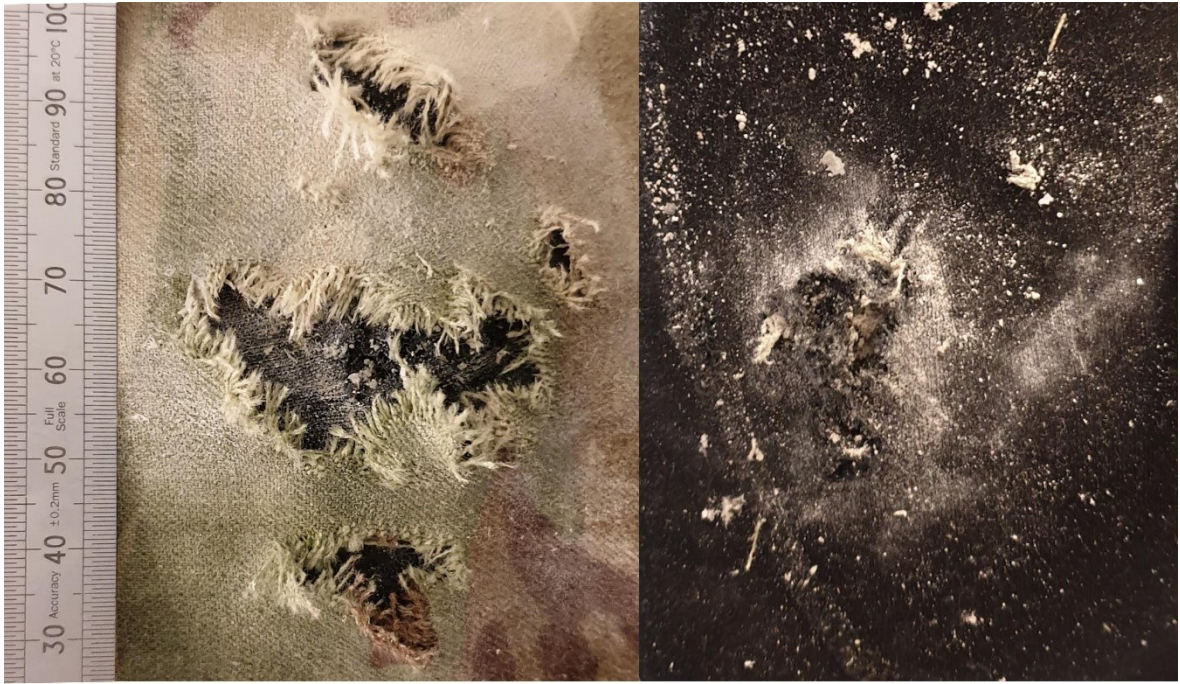


Figure 57: Exemplar damage sustained by issue combat trousers (left) and PPE (right) following impact with high-velocity sand

Figure 58 shows injuries more substantial in volume and depth as sustained in the control group, whilst Figure 59 demonstrates the substantially reduced injuries seen in the PPE group.



Figure 58: Exemplar wounds sustained by control group following impact with high-velocity sand



Figure 59: Exemplar wounds sustained by PPE group following impact with high-velocity sand

Those within the Tier 1 PPE were 77% less likely (relative risk 0.23, 95% confidence intervals 0.12 – 0.45) to sustain a penetrating injury from sand ejecta deep to the subcutaneous tissues involving the underlying fascial and muscular layers.

10.5 Discussion

This study is the first to recreate penetrating injury in a human cadaveric model from propagated high velocity sand as a simulacrum for sandy gravel soil ejecta from a blast event. Similarly, this study is the first laboratory study to confirm the efficacy of Tier 1 PPE in potentially mitigating injuries from energised high velocity environmental debris. The gas-gun system utilised is a novel mechanism of reproducing high velocity sand blast in a laboratory setting, utilising a pressurised gas-gun system, that could be used to assess the efficacy of different protective materials across a range of threats. Tier 1 pelvic PPE was shown to markedly reduce the severity of injuries in a cadaveric model by reducing the total surface area of injuries, and depth of penetration. These findings highlight the importance of Tier 1 PPE use in any environment in which blast injury to the limbs may occur.

These findings are in keeping with clinical literature examining the protective benefits of Tier 1 PPE. Breeze et al reported that from 174 casualties attending a role 3 hospital in Afghanistan, those wearing Tier 1 pelvic PPE were significantly less likely (OR = 9.5) to sustain a penetrating wound from a blast event to the pelvis than those unprotected (Breeze, L. S. Allanson-Bailey, *et al.*, 2015). This is consistent with this laboratory study, where the Tier 1 protection group were 77% less likely (relative risk 0.23, 95% confidence intervals 0.12 – 0.45) to sustain a penetrating injury from sand ejecta deep to the subcutaneous tissues involving the underlying fascial and muscular layers. In addition, the total injured superficial surface area was 4.6 times smaller (143 mm² vs. 658 mm², $p = 0.004$) in the protection group.

No previous study has described the protective benefit provided against high-velocity sand from Tier 1 PPE. A previous study has examined the mitigation effects of ballistic protective fabric, similar to the properties of Tier 2 PPE, to high velocity sand substrate following a controlled explosion (Saunders and Carr, 2018). As sand velocity or other injurious variables

were not described in this study, there is insufficient information with which to compare the methodologies or findings.

As highlighted previously, contamination following blast is extensive, as dirt and other debris are propelled along tissue planes, with infection and delayed amputation frequent (Khatod *et al.*, 2003; Covey and Ficke, 2016). Bacterial and IFI following blast can result in delayed amputation or death (Brown *et al.*, 2010; C. J. Rodriguez *et al.*, 2014). The findings of the present study show Tier 1 PPE to reduce the severity of injury sustained from energised high-velocity environmental debris and suggest the likelihood of a reduced probability of infection, through decreased soft tissue disruption and deep spreading of environmental contaminants.

Inherent limitations are associated with a cadaveric study; these include over or underestimating the effect size, and assumptions made with inferring a delayed infection risk. Fresh-frozen cadavers as utilised in this study retain the material properties of hard and, to a lesser extent, connective tissues (Crandall *et al.*, 2011). Damaging effects to soft tissues have been seen to occur when ice crystals during the freezing and thawing process disrupt the soft tissue cellular structure (Menz, 1971). With particular reference to the skin, cryopreservation maintains some viability despite the cellular trauma of freezing thawing, however, damage to the skin's architecture can be seen on histopathological analysis of cryopreserved human skin allografts (Chang *et al.*, 2014). As such, it is expected that the findings in the present study are an over-representation of the damage sustained following sand blast, with higher velocities likely required to cause the same damaging effect to a live casualty of sand-blast trauma. A non-cadaveric controlled clinical study, however, is not ethically feasible. A previous observational study has shown benefit of Tier 1 PPE vs. no protection, whilst the wearing of Tier 1 PPE has been adopted for routine use (Lewis *et al.*, 2013; Breeze, L. S. Allanson-Bailey, *et al.*, 2015). Future clinical studies should include comparing current Tier 1 PPE to full under trouser PPE leggings, to assess the rates of wound infection, delayed

amputation, and mortality. Chapters 7 and 9 highlighted the injury mechanism by which sand blast resulted in traumatic amputation in the mouse model. Adopting the use of full PPE leggings is likely to result in a reduction in the extent of soft tissue wounding in humans on the battlefield, which may in turn mitigate the risk of traumatic amputation – future prospective clinical studies are suggested.

The proof-of-concept pelvic protection introduced in Chapter 8 resulted in an increase in severe lower limb injuries as a consequence of its use. At any given blast injury threat level, injury to the pelvis and lower limbs is caused by a combination of all of the mechanisms of injury discussed within this thesis (primary to tertiary), to varying degrees of each, dependent upon the blast conditions. Whilst the proof-of-concept pelvic protective belt increased the risk of lower limb injury via tertiary blast mechanisms, the risk of lower limb injury in the present study was mitigated through decreasing the effects of secondary blast with the use of Tier 1 PPE. A combination of both protective strategies may reduce the risk of both pelvic injury and traumatic amputation. Investigation of a comparable Tier 1 PPE in any cadaveric mouse study is, however, likely to prove unprocurable; future research may involve human cadaveric or clinical, retrospective studies post PPE deployment.

10.6 Conclusion

This study is the first to recreate penetrating injury from propagated high velocity sand in a cadaveric model. It has shown Tier 1 silk pelvic protection to markedly reduce two parameters associated with severity of injury: wounds deep to the subcutaneous tissues were eliminated (0 vs. 23, $p < 0.001$) and a reduction in the total superficial surface area of injuries was seen (143 mm² vs. 658 mm², $p = 0.004$). In turn, this would be expected to reduce the probability of infection, through decreased soft tissue disruption and deep seeding of environmental contaminants. In keeping with previous animal studies (Chapters 7 and 9), these findings

implicate high velocity environmental debris such as sand ejected from blast events as a critical mechanism of injury in the blast casualty and this injury mechanism should be a key focus of future research and mitigation strategies. Future prospective clinical studies comparing current Tier 1 PPE to full under trouser PPE leggings to mitigate the effects of sand blast are suggested. Tier 1 PPE leggings may offset the increased risk of lower limb injury seen with the proof-of-concept pelvic mitigation strategy described in Chapter 8.

Chapter 11

Summary, Future Research and Conclusions

11.1 Scope of the chapter

Chapter 11 provides a summary to the research presented within this thesis. After highlighting the key points of the work, the chapter discusses future research strategies, including how to implement a protective pelvic binder into current military personal protective equipment and research assessing its suitability for use.

11.2 Thesis Summary

The aim of this work was to identify and address gaps in the knowledge of dismounted pelvic blast injury. This included identifying the cause of death, assessing the contribution of associated injuries, reviewing current management and mitigation strategies, understanding, and describing the mechanism of injury, and proposing mitigations strategies.

The UK military experience of pelvic blast injury was reviewed to identify what is already known on the differences in injury patterns of the mounted and dismounted casualty. This highlighted that mounted casualties died from causes other than their pelvic injury and so the subsequent research direction focused on the dismounted pelvic blast injury casualty. An analysis of battlefield data was performed which showed that casualties of lower extremity dismounted blast with pelvic fractures are at significant risk of a non-compressible pelvic vascular injury, with an associated mortality of 56%. Casualties that sustained unstable pelvic fracture patterns, traumatic amputation and perineal injury were at three times greater risk of sustaining a pelvic vascular injury than those without these associated injuries. Lateral displacement of the sacroiliac joints was shown to be the greatest radiological predictor of vascular injury and death, raising the hypothesis that mitigation strategies aiming to prevent lateral displacement of the pelvis following blast may result in a reduced injury burden and fewer fatalities. Current management and mitigation strategies were examined before discussing hypothesised mechanisms of injury in dismounted pelvic blast, including lower limb flail and high velocity sand blast. Different experimental models and platforms were explored and their suitability for investigating these hypotheses discussed. A novel experimental setup utilising a mouse model of dismounted pelvic blast injury with a shock-tube mediated blast wave was subsequently utilised to investigate the lower limb flail hypothesis. The results of this study suggested that lower limb flail was required for an unstable pelvic fracture with vascular injury to occur. Restriction of lower limb flail was shown to reduce the probability of

vascular injury, with an injury-risk curve developed which associated restriction of lower limb flail to the probability of vascular injury. Scaling these angles of lower limb restriction to the human is unclear, however, any degree of restriction would be beneficial in mitigating the effects of injury. The findings determined a key mechanism of injury to the lower body in dismounted blast and suggested a mitigation strategy not previously considered.

A lack of associated traumatic amputation and perineal injury in the shock tube study was hypothesised to be due to the absence of secondary blast injury (such as high velocity sand ejecta). The next step in this work was therefore to investigate the hypothesised mechanism of injury of high velocity sand blast, to ascertain its contribution to the injury pattern seen in dismounted pelvic blast injury. A novel experimental setup utilising a mouse model within a gas gun system delivering high velocity sand ejecta was developed. The results suggested that sand ejecta following an explosive event can cause both soft tissue and skeletal injury at high velocities. Injury-risk curves were developed that demonstrated a progressive worsening severity of injuries with increasing ejecta velocity. The findings implicated high velocity sand blast, in addition to limb flail, as a critical mechanism of injury in the dismounted blast casualty.

A mitigation strategy to limit lower limb flail was subsequently developed. This consisted of pelvic protective equipment which limited outward flail of the lower limbs following impact with a blast wave. This strategy was evaluated using the now established mouse model of shock-tube mediated dismounted pelvic blast injury. It demonstrated that the introduction of a reinforced pelvic protective binder worn at the level of the greater trochanters, through limiting lower limb flail, can mitigate pelvic injury severity. This was found to be effective following both front-on and under-body blast. In contrast, pelvic protection providing a degree of limitation to pelvic bony displacement but not lower limb flail (when worn at the level of the anterior superior iliac spines) showed only a minimal reduction in pelvic vascular injury. This

research provided proof of concept of pelvic protective equipment limiting lower limb flail to reduce the incidence of pelvic vascular injury in a small animal model.

The mechanism of traumatic amputation was subsequently investigated, with a view to optimising pelvic and lower limb protection to try and mitigate this injury. Having implicated high velocity sand blast as a mechanism of injury causing traumatic amputation, a modified gas-gun experimental setup of that was developed previously was utilised to further examine this. High-speed cameras capturing the moment of sand blast impact and subsequent stages of traumatic amputation, when viewed in conjunction with post-impact injury analysis, allowed for further characterisation of the pattern and development of traumatic amputation due to high velocity sand blast. Following this experiment, a novel injury mechanism of traumatic amputation was described, for which high velocity sand blast (or other secondary blast ejecta) was a critical component. This suggested that protection of the lower limb from high velocity sand blast may mitigate the risk of traumatic amputation.

The final study of this thesis expanded upon these findings by investigating potential mitigation strategies for traumatic amputation. Current military Tier 1 personal protective equipment (PPE) and its capacity for mitigating injury caused by high velocity sand blast was investigated utilising a cadaveric model of gas-gun mediated high velocity sand blast. It showed Tier 1 PPE to markedly reduce two parameters associated with severity of injury: wounds deep to the subcutaneous tissues were eliminated and a reduction in the superficial surface area of injuries was seen. Modification of Tier 1 PPE from shorts to full length leggings, to encompass the entire lower limb, is suggested to reduce the risk of severe lower limb injuries.

11.3 Future Research

Several factors must be taken into consideration when incorporating the findings of this thesis for development of future pelvic protective equipment. Protective equipment worn on the pelvis at the level of the greater trochanters eliminated vascular injury through restricting movement of the femurs and load through the pelvis. As a static restraint, this provides marked restriction of lower limb mobility. Human Factors research is required to assess the suitability of this for soldiers on routine foot patrol. Even if it proved impractical, enhanced protection has been used on soldiers in specific roles, who were at higher risk, such as specialised explosive search teams. In this select military cohort, the benefits of a static restraint may outweigh these limitations. As a starting point, this protective equipment may take the form of a binder with a level of protection which is commensurate to, and incorporated into, current military Tier 2 PPE. When incorporated at the level of the groin piece, this would cover the greater trochanters and provide the required restraint (Figure 60).



Figure 60: A soldier wearing Tier 2 pelvic protective equipment modified to include the suggested position of the pelvic protective binder, as worn at the level of the greater trochanters. (Adapted from Lewis *et al.*, 2013, figure reproduced with permission)

Prior to implementation of the protective binder in this group, future research may assess the suitability and level of protection offered by different materials which may be used to construct the binder. This may be achieved through the use of open free-field blast tests, utilising a predetermined volume of explosive at a predetermined detonation distance to represent differing threat levels. If investigating different threat levels representing less severe blast conditions, the pelvic protective binder may be investigated to identify if traumatic amputation occurs with pelvic protection at milder blast loading environments, which would otherwise be insufficient to cause dismounted pelvic blast injury. This may be achieved, where ethical considerations allow it, through post-mortem human cadaver testing, large animal cadaveric models, or alternative injury model surrogates such as anthropomorphic test devices (Crandall *et al.*, 2011).

Future research for development of protection for the soldier on routine foot patrol should consider allowing movement under low loading rates but prevent it at higher rates, such as those incurred with rapid movement of the limbs during a blast event. This may be investigated through assessing the use of a protective binder which utilises a seat belt locking mechanism, and the feasibility of this mechanism to deploy in time during blast and limb movement. Future research may also investigate the feasibility of using a strain-rate sensitive material, which is soft and flexible at baseline but hardens upon impact, and its suitability to withstand the forces transmitted during blast (Easton *et al.*, 2017).

Future research should include a clinical study comparing current Tier 1 PPE to full PPE leggings to assess the incidence of soft tissue injury, traumatic amputation, wound infection, delayed amputation, and overall mortality following blast. Adopting the use of full PPE leggings may result in a reduction in the severity of soft tissue wounding on the battlefield, which in turn could mitigate the risk of severe lower limb injury and amputation.

11.4 Conclusion

Dismounted pelvic blast injury represents a severe pattern of injury for which mortality rates remain high. The research presented within this thesis has identified pelvic vascular injury as the cause of death of the dismounted pelvic blast casualty. It showed that traumatic amputation, severe perineal injury, and lateral displacement of the sacroiliac joints are associated with pelvic vascular injury and described the mechanisms of injury by which lower limb flail and high velocity sand blast cause these destructive injuries. This thesis has proposed a novel mitigation strategy in the form of a pelvic protective binder, the implementation of which may reduce the severe injury burden and mortality rate associated with dismounted pelvic blast injury.

Bibliography

- Aboudara, M. C., Hurst, F. P., Abbott, K. C. and Perkins, R. M. (2008) 'Hyperkalemia after packed red blood cell transfusion in trauma patients.', *The Journal of Trauma: Injury, Infection, and Critical Care*, 64(Supplement), pp. S86–S91.
- Allied Joint Doctrine (2012) 'Allied Joint Doctrine for Countering – Improvised Explosive Devices', *Nato*, 15(February). Available at: <https://www.scribd.com/doc/180718058/NATO-AJP-3-15-B-Allied-Joint-Doctrine-for-Countering-Improvised-Devices-2013-uploaded-by-Richard-J-Campbell>.
- Alton, T. and Gee, A. (2014) 'Classifications in Brief Young and Burgess Classification of Pelvic Ring Injuries', *Clinical orthopaedics and related research*, pp. 2338–2342.
- Andersen, R. C., Fleming, M., Forsberg, J. A., Gordon, W. T., Nanos, G. P., Charlton, M. T. and Ficke, J. R. (2012) 'Dismounted Complex Blast Injury.', *Journal of surgical orthopaedic advances*, 21(1), pp. 2–7.
- AO Foundaton (2018) 'Fracture and Dislocation Compendium', *JOT*, 32(1).
- Azocar, A. F., Mooney, L. M., Duval, J. F., Simon, A. M., Hargrove, L. J. and Rouse, E. J. (2020) 'Design and clinical implementation of an open-source bionic leg', *Nature Biomedical Engineering*. Nature Research, 4(10), pp. 941–953.
- Bailey, A. M., Christopher, J. J., Brozoski, F. and Salzar, R. S. (2015) 'Post Mortem Human Surrogate Injury Response of the Pelvis and Lower Extremities to Simulated Underbody Blast', *Annals of Biomedical Engineering*. Springer US, 43(8), pp. 1907–1917.
- Bailey, A. M., McMurry, T. L., Poplin, G. S., Salzar, R. S. and Crandall, J. R. (2015) 'Survival Model for Foot and Leg High Rate Axial Impact Injury Data', *Traffic Injury Prevention*, 16(Suppl 2), pp. S96–S102.

- Bailey, J. R., Stinner, D. J., Blackbourne, L. H., Hsu, J. R. and Mazurek, M. T. (2011) 'Combat-related pelvis fractures in nonsurvivors', *Journal of Trauma - Injury, Infection and Critical Care*, 71(SUPPL. 1), pp. 1–4.
- Bakhshayesh, P., Boutefnouchet, T. and Tötterman, A. (2016) 'Effectiveness of non invasive external pelvic compression: A systematic review of the literature', *Scandinavian Journal of Trauma, Resuscitation and Emergency Medicine*. *Scandinavian Journal of Trauma, Resuscitation and Emergency Medicine*, 24(1), pp. 1–9.
- Bauman, R. A., Ling, G., Tong, L., Januszkiewicz, A., Agoston, D., Delanerolle, N., Kim, Y., Ritzel, D., Bell, R., Ecklund, J., Armonda, R., Bandak, F. and Parks, S. (2009) 'An Introductory Characterization of a Combat-Casualty-Care Relevant Swine Model of Closed Head Injury Resulting from Exposure to Explosive Blast', *Journal of neurotrauma*, 26, p. 841.
- Becker, I., Woodley, S. J. and Stringer, M. D. (2010) 'The adult human pubic symphysis: A systematic review', *Journal of Anatomy*, 217(5), pp. 475–487.
- Bonner, T. J., Eardley, W. G. P., Newell, N., Masouros, S., Matthews, J. J., Gibb, I. and Clasper, J. C. (2011) 'Accurate placement of a pelvic binder improves reduction of unstable fractures of the pelvic ring', *The Journal of Bone and Joint Surgery. British volume*. The British Editorial Society of Bone and Joint Surgery, 93-B(11), pp. 1524–1528.
- Bottlang, M., Simpson, T., Sigg, J., Krieg, J. C., Madey, S. M. and Long, W. B. (2002) 'Noninvasive reduction of open-book pelvic fractures by circumferential compression', *Journal of Orthopaedic Trauma*. *J Orthop Trauma*, 16(6), pp. 367–373.
- Bowen, I., Fletcher, E. and Richmond, D. (1968) 'Estimate of man's tolerance to the direct effects of air blast', *Technical Progress Report DASA-2113, Defence Atomic Support Agency, Department of Defense, U.S. Government*.
- Bowyer, G. W. (1996) 'Management of small fragment wounds: Experience from the Afghan

border', *Journal of Trauma - Injury, Infection and Critical Care*, 40((3 Suppl)), pp. S170-2.

Breeze, J., Allanson-Bailey, L. S., Hepper, A. E. and Midwinter, M. J. (2015) 'Demonstrating the effectiveness of body armour: A pilot prospective computerised surface wound mapping trial performed at the role 3 hospital in Afghanistan', *Journal of the Royal Army Medical Corps*, 161(1), pp. 36–41.

Breeze, J., Allanson-Bailey, L. S., Hepper, A. E., Midwinter, M. J. and John, M. (2015) 'Demonstrating the effectiveness of body armour: a pilot prospective computerised surface wound mapping trial performed at the Role 3 hospital in Afghanistan', *J R Army Med Corps*, 161, pp. 36–41.

Brown, K. V., Murray, C. K. and Clasper, J. C. (2010) 'Infectious complications of combat-related mangled extremity injuries in the British military', *The Journal of trauma*, 69(1), pp. S109–S115.

Bumbasirevia, M., Lesic, A., Mitkovic, M. and Bumbasirevia, V. (2006) 'Treatment of blast injuries of the extremity', *The Journal Of The American Academy Of Orthopaedic Surgeons*, 14(10 Spec No.), pp. S77-81. Available at:

<http://search.ebscohost.com/login.aspx?direct=true&db=cmedm&AN=17003215&site=ehost-live>.

Burgess, A. R., Eastridge, B. J., Young, J. W., Ellison, T. S., Ellison, P. S., Poka, A., Bathon, G. H. and Brumback, R. J. (1990) 'Pelvic ring disruptions: effective classification system and treatment protocols.', *The Journal of trauma*, 30(7), pp. 848–56.

de Candole, C. A. (1967) 'Blast injury.', *Canadian Medical Association journal*, 96(4), pp. 207–14. Available at: <http://www.ncbi.nlm.nih.gov/pubmed/6015742> (Accessed: 26 August 2019).

Cannon, J. W., Hofmann, L. J., Glasgow, S. C., Potter, B. K., Rodriguez, C. J., Cancio, L. C., Rasmussen, T. E., Fries, C. A., Davis, M. R., Jezior, J. R., Mullins, R. J. and Elster, E. A.

- (2016) 'Dismounted Complex Blast Injuries: A Comprehensive Review of the Modern Combat Experience', *Journal of the American College of Surgeons*. Elsevier, 223(4), pp. 652-664.e8.
- Cannon, L. (2001) 'Behind armour blunt trauma--an emerging problem.', *Journal of the Royal Army Medical Corps*, 147(1), pp. 87–96. Available at: <http://www.ncbi.nlm.nih.gov/pubmed/11307682> (Accessed: 27 July 2018).
- Carpanen, D., Kedgley, A. E., Shah, D. S., Edwards, D. S., Plant, D. J. and Masouros, S. D. (2019) 'Injury risk of interphalangeal and metacarpophalangeal joints under impact loading', *Journal of the Mechanical Behavior of Biomedical Materials*. Elsevier Ltd, 97, pp. 306–311.
- Champion, H. R., Holcomb, J. B. and Young, L. A. (2009) 'Injuries From Explosions: Physics, Biophysics, Pathology, and Required Research Focus Background: Explosions cause more'.
- Chandra, N., Ganpule, S., Kleinschmit, N. N., Feng, R., Holmberg, A. D., Sundaramurthy, A., Selvan, V. and Alai, A. (2012) 'Evolution of blast wave profiles in simulated air blasts: experiment and computational modeling', *Shock Waves*. Springer-Verlag, 22(5), pp. 403–415.
- Chang, S. K. Y., Lau, J. W. L. and Chui, C. K. (2014) 'Changes in mechanical, structural integrity and microbiological properties following cryopreservation of human cadaveric iliac arteries.', *Annals of the Academy of Medicine, Singapore*, 43(10), pp. 492–8. Available at: <http://www.ncbi.nlm.nih.gov/pubmed/25434619> (Accessed: 10 May 2018).
- Chen, J., Patnaik, S. S., Prabhu, R. K., Priddy, L. B., Bouvard, J.-L., Marin, E., Horstemeyer, M. F., Liao, J. and Williams, L. N. (2019) 'Mechanical Response of Porcine Liver Tissue under High Strain Rate Compression', *Bioengineering*, 6(2), p. 49.
- Chovanes, J., Cannon, J. W. and Nunez, T. C. (2012) 'The Evolution of Damage Control Surgery', *Surgical Clinics of North America*, 92(4), pp. 859–875.

Clasper, J. and Ramasamy, A. (2013) 'Traumatic amputations', *British Journal of Pain*, 7(2), pp. 67–73.

Cooper, G. J. and Taylor, D. E. (1989) 'Biophysics of impact injury to the chest and abdomen.', *Journal of the Royal Army Medical Corps*, 135(2), pp. 58–67.

Courtney, A. and Courtney, M. (2015) 'The Complexity of Biomechanics Causing Primary Blast-Induced Traumatic Brain Injury: A Review of Potential Mechanisms.', *Frontiers in neurology*. Frontiers Media SA, 6, p. 221.

Covey, D. C. and Ficke, J. (2016) 'Blast and fragment injuries of the musculoskeletal system', *Orthopedics in Disasters: Orthopedic Injuries in Natural Disasters and Mass Casualty Events*, pp. 269–280.

Crandall, J. R., Bose, D., Forman, J., Untaroiu, C. D., Arregui-Dalmases, C., Shaw, C. G. and Kerrigan, J. R. (2011) 'Human surrogates for injury biomechanics research', *Clinical Anatomy*. Clin Anat, 24(3), pp. 362–371.

Cullis, I. G. (2001) 'Blast Waves and How They Interact With Structures', *J R Army Med Corps 2001*, 147(1), pp. 16–26.

Dalal, S. A., Burgess, A. R., Siegel, J. H., Young, J. W., Brumback, R. J., Poka, A., Dunham, C. M., Gens, D. and Bathon, H. (1989) 'Pelvic fracture in multiple trauma: Classification by mechanism is key to pattern of organ injury, resuscitative requirements, and outcome', *Journal of Trauma - Injury, Infection and Critical Care*, 29(7), pp. 981–1002.

Danelson, K. A., Kemper, A. R., Mason, M. J., Tegtmeier, M., Swiatkowski, S. A., Bolte, J. H. and Hardy, W. N. (2015) 'Comparison of ATD to PMHS Response in the Under-Body Blast Environment.', *Stapp car crash journal*, 59, pp. 445–520. Available at: <http://www.ncbi.nlm.nih.gov/pubmed/26660754> (Accessed: 10 October 2018).

Dearden, P. (2001) 'New blast weapons.', *Journal of the Royal Army Medical Corps*, 147(1),

pp. 80–86.

Demetriades, D., Karauskakis, M., Toutouzas, K., Alo, K., Velmahos, G. and Chan, L. (2002) ‘Pelvic fractures: epidemiology and predictors of associated abdominal injuries and outcomes.’, *Journal of the American College of Surgeons*, 195(1), pp. 1–10.

Department of Defense (2008) ‘Efforts and Programs of the Department of Defense Relating to the Prevention, Mitigation, and Treatment of Blast Injuries’, *Annual report to Congress*. Available at: <http://www.dtic.mil/dtic/tr/fulltext/u2/a506577.pdf> (Accessed: 13 July 2018).

Do, W. S., Forte, D. M., Sheldon, R. R., Weiss, J. B., Barron, M. R., Sokol, K. K., Black, G. E., Hegge, S. R., Eckert, M. J. and Martin, M. J. (2019) *Minimally invasive preperitoneal balloon tamponade and abdominal aortic junctional tourniquet versus open packing for pelvic fracture-associated hemorrhage: Not all extrinsic compression is equal.*, *The journal of trauma and acute care surgery*.

Dosquet, F. (2004) ‘Test Methodology for Protection of Vehicle’, *Mabs 18*.

Dubose, J., Inaba, K., Barmparas, G., Teixeira, P. G., Schnu, B., Talving, P., Salim, A. and Demetriades, D. (2010) ‘Bilateral Internal Iliac Artery Ligation as a Damage Control Approach in Massive Retroperitoneal Bleeding After’, 69(6).

Dyce, K., Sack, W. and Wensing, C. (2010) *Textbook of Veterinary Anatomy*. 4th Editio.

Saunders. Available at: <https://evolve.elsevier.com/cs/product/9781416066071?role=student> (Accessed: 7 April 2018).

Easton, K., Burton, T., Ariss, S., Bradburn, M. and Hawley, M. (2017) ‘Smart Clothing for Falls Protection and Detection: User-Centred Co-Design and Feasibility Study’, in *Studies in Health Technology and Informatics*. IOS Press, pp. 152–159.

Edwards, D. S. and Clasper, J. (2016) ‘Blast Injury Mechanism’, in *Blast Injury Science and Engineering*. Cham: Springer International Publishing, pp. 87–104.

Edwards, D. S., McMenemy, L., Stapley, S. A., Patel, H. D. L. and Clasper, J. C. (2016) '40 years of terrorist bombings – A meta-analysis of the casualty and injury profile', *Injury*, 47(3), pp. 646–652.

Eftaxiopoulou, T., Barnett-Vanes, A., Arora, H., Macdonald, W., Nguyen, T.-T. N., Itadani, M., Sharrock, A. E., Britzman, D., Proud, W. G., Bull, A. M. J. and Rankin, S. M. (2016) 'Prolonged but not short-duration blast waves elicit acute inflammation in a rodent model of primary blast limb trauma', *Injury*. Elsevier, 47(3), pp. 625–632.

Egund, N. and Jurik, A. G. (2014) 'Anatomy and histology of the sacroiliac joints'.

Evriiades, D., Jeffery, S., Cubison, T., Lawton, G., Gill, M. and Mortiboy, D. (2011) 'Shaping the military wound: issues surrounding the reconstruction of injured servicemen at the Royal Centre for Defence Medicine', *Philosophical Transactions of the Royal Society B: Biological Sciences*. Royal Society, 366(1562), pp. 219–230.

Faringer, P. D., Mullins, R. J., Feliciano, P. D., Duwelius, P. J. and Trunkey, D. D. (1994) 'Selective Fecal Diversion in Complex Open Pelvic Fractures From Blunt Trauma', *Archives of Surgery*, 129(9), pp. 958–964.

Feickert, A. (2009) 'Mine-Resistant, Ambush-Protected (MRAP) Vehicles: Background and Issues for Congress'. Available at: <https://apps.dtic.mil/docs/citations/ADA502022> (Accessed: 8 February 2019).

Feldesman, M. R., Kleckner, J. G. and Lundy, J. K. (1990) 'Femur/stature ratio and estimates of stature in mid- and late-pleistocene fossil hominids', *American Journal of Physical Anthropology*, 83(3), pp. 359–372.

Ficke, J. R., Eastridge, B. J., Butler, F. K., Alvarez, J., Brown, T., Pasquina, P., Stoneman, P. and Carvalho, J. (2012a) 'Dismounted complex blast injury report of the army dismounted complex blast injury task force', *Journal of Trauma and Acute Care Surgery*, 73, pp. S520–S534.

Ficke, J. R., Eastridge, B. J., Butler, F. K., Alvarez, J., Brown, T., Pasquina, P., Stoneman, P. and Carvalho, J. (2012b) 'Dismounted complex blast injury report of the army dismounted complex blast injury task force', *Journal of Trauma and Acute Care Surgery*, 73(6), pp. S520–S534.

Fleming, M., Waterman, S., Dunne, J., D'Alleyrand, J. C. and Andersen, R. C. (2012) 'Dismounted complex blast injuries: patterns of injuries and resource utilization associated with the multiple extremity amputee', *J Surg Orthop Adv*, 21(6), pp. 32–37.

Friedlander, F. G. (1946) 'The Diffraction of Sound Pulses. I. Diffraction by a Semi-Infinite Plane', *Proceedings of the Royal Society A: Mathematical, Physical and Engineering Sciences*. The Royal Society, 186(1006), pp. 322–344.

Fung, Y. C., Yen, M. R. and Zeng, Y. J. (1985) *Characterization and modeling of thoraco-abdominal response to blast waves*.

Gamble, J., Simmons, S. and Freedman, M. (1983) 'The Symphysis Pubis', pp. 261–272.

Gänsslen, A., Pohlemann, T., Paul, C., Lobenhoffer, P. and Tscherne, H. (1996) 'Epidemiology of pelvic ring injuries', *Injury*, 27, pp. 13–20.

Glasgow, S. C., Heafner, T. A., Watson, J. D. B., Aden, M. D. J. K. and Perry, P. D. W. B. (2014) 'Initial Management and Outcome of Modern Battlefield Anal Trauma', 8, pp. 1012–1018.

Glasgow, S. C., Steele, S. R., Duncan, J. E. and Rasmussen, T. E. (2012) 'Epidemiology of modern battlefield colorectal trauma : A review of 977 coalition casualties', 73(6), pp. 503–508.

Gordon, W., Talbot, M., Fleming, M., Shero, J., Potter, B. and Stockinger, Z. T. (2018) 'High bilateral amputations and dismounted complex blast injury (DCBI)', *Military Medicine*, 183, pp. 118–122.

- Gray, H. (1918) *Anatomy of the human body*. Twentieth. Edited by W. H. Lewis.
- Bartelby.com. Available at: <https://www.bartleby.com/107/> (Accessed: 15 February 2019).
- Grujicic, M., Pandurangan, B., Qiao, R., Cheeseman, B. A., Roy, W. N., Skaggs, R. R. and Gupta, R. (2008) 'Parameterization of the porous-material model for sand with different levels of water saturation', *Soil Dynamics and Earthquake Engineering*, 28(1), pp. 20–35.
- Grunstra, N. D. S., Zachos, F. E., Herdina, A. N., Fischer, B., Pavličev, M. and Mitteroecker, P. (2019) 'Humans as inverted bats: A comparative approach to the obstetric conundrum', *American Journal of Human Biology*. Wiley-Liss Inc., 31(2), p. e23227.
- Gruss, L. T. and Schmitt, D. (2015) 'The evolution of the human pelvis: changing adaptations to bipedalism, obstetrics and thermoregulation', *Philosophical Transactions of the Royal Society B: Biological Sciences*, 370(1663), pp. 20140063–20140063.
- Hamill, J., Holden, A., Paice, R. and Civil, I. (2000) 'Pelvic fracture pattern predicts pelvic arterial haemorrhage', *Australian and New Zealand Journal of Surgery*.
- Hästbacka, J. and Pettilä, V. (2003) 'Prevalence and predictive value of ionized hypocalcemia among critically ill patients', *Acta Anaesthesiologica Scandinavica*, 47(10), pp. 1264–1269.
- Häusler, M. and Schmid, P. (1995) 'Comparison of the pelves of Sts 14 and AL288-1: implications for birth and sexual dimorphism in australopithecines', *Journal of Human Evolution*. Academic Press, 29(4), pp. 363–383.
- Hayda, R., Harris, R. M. and Bass, C. D. (2004) 'Blast Injury Research: Modeling Injury Effects of Landmines, Bullets, and Bombs', *Clinical Orthopaedics and Related Research*, 422(422), pp. 97–108.
- Hayer, S., Niederreiter, B., Nagelreiter, I., Smolen, J. and Redlich, K. (2010) 'Interleukin 6 is not a crucial regulator in an animal model of tumour necrosis factor-mediated bilateral sacroiliitis.', *Annals of the rheumatic diseases*. BMJ Publishing Group Ltd, 69(7), pp. 1403–

6.

Herard, P. and Boillot, F. (2012) 'Amputation in emergency situations : indications , techniques and Médecins Sans Frontières France ' s experience in Haiti', pp. 1979–1981.

Hospenthal, D. R. *et al.* (2011) 'Guidelines for the prevention of infections associated with combat-related injuries: 2011 update endorsed by the infectious diseases society of America and the surgical infection society', *Journal of Trauma - Injury, Infection and Critical Care*, 71(2 SUPPL. 2).

Hull, J. B. (1992) 'Traumatic amputation by explosive blast: pattern of injury in survivors.', *The British journal of surgery*, 79(12), pp. 1303–6. Available at:

<http://www.ncbi.nlm.nih.gov/pubmed/1486425> (Accessed: 27 July 2018).

Hull, J. B., Bowyer, G. W., Cooper, G. J. and Crane, J. (1994) 'Pattern of injury in those dying from traumatic amputation caused by bomb blast.', *The British journal of surgery*, 81(8), pp. 1132–5. Available at: <http://www.ncbi.nlm.nih.gov/pubmed/7953338> (Accessed: 27 July 2018).

Hull, J. B. and Cooper, G. J. (1996) 'Pattern and mechanism of traumatic amputation by explosive blast.', *The Journal of trauma*, 40(3 Suppl), pp. S198-205.

Jean, A., Nyein, M. K., Zheng, J. Q., Moore, D. F., Joannopoulos, J. D. and Radovitzky, R. (2014) 'An animal-to-human scaling law for blast-induced traumatic brain injury risk assessment', *Proceedings of the National Academy of Sciences*, 111(43), pp. 15310–15315.

Jiang, L., Jiang, S. and Zhang, M. (2016) 'The European guideline on management of major bleeding and coagulopathy following trauma: Fourth edition', *Chinese Journal of Emergency Medicine. Critical Care*, 25(5), pp. 577–579.

Johansson, P. I. and Stensballe, J. (2010) 'Hemostatic resuscitation for massive bleeding: The paradigm of plasma and platelets - A review of the current literature', *Transfusion*, 50(3), pp.

701–710.

Khatod, M., Botte, M. J., Hoyt, D. B., Meyer, R. S., Smith, J. M. and Akeson, W. H. (2003) ‘Outcomes in open tibia fractures: Relationship between delay in treatment and infection’, *Journal of Trauma*, 55(5), pp. 949–954.

King, D. R., Larentzakis, A. and Ramly, E. P. (2015) ‘Tourniquet use at the Boston Marathon bombing’, *Journal of Trauma and Acute Care Surgery*. Lippincott Williams and Wilkins, 78(3), pp. 594–599.

Kishbaugh, D., Dillingham, T. R., Howard, R. S., Sinnott, M. W. and Belandres, P. V. (1995) ‘Amputee soldiers and their return to active duty’, *Military Medicine*. Association of Military Surgeons of the US, 160(2), pp. 82–84.

Kluger, Y., Kashuk, J. and Mayo, A. (2004) ‘Terror Bombing-Mechanisms, Consequences and Implications’, *Scandinavian Journal of Surgery*, 93(1), pp. 11–14.

Kluger, Y., Nimrod, A., Biderman, P., Mayo, A. and Sorkin, P. (2007) ‘The quinary pattern of blast injury.’, *American journal of disaster medicine*, 2(1), pp. 21–5. Available at: <http://www.ncbi.nlm.nih.gov/pubmed/18268871> (Accessed: 27 July 2018).

Knobil, E. and Neill, J. D. (2006) *Knobil and Neill’s physiology of reproduction*. Elsevier.

Knops, S. P., Van Riel, M. P. J. M., Goossens, R. H. M., Van Lieshout, E. M. M., Patka, P. and Schipper, I. B. (2010) *Measurements of the Exerted Pressure by Pelvic Circumferential Compression Devices*, *The Open Orthopaedics Journal*.

Kochi, T., Imai, Y., Takeda, A., Watanabe, Y., Mori, S., Tachi, M. and Kodama, T. (2013) ‘Characterization of the Arterial Anatomy of the Murine Hindlimb: Functional Role in the Design and Understanding of Ischemia Models’, *PLoS ONE*, 8(12).

Kotwal, R. S., Howard, J. T., Orman, J. A., Tarpey, B. W., Bailey, J. A., Champion, H. R., Mabry, R. L., Holcomb, J. B. and Gross, K. R. (2016) ‘The effect of a golden hour policy on

the morbidity and mortality of combat casualties’, *JAMA Surgery*, 151(1), pp. 15–24.

Kragh, J. F., Walters, T. J., Baer, D. G., Fox, C. J., Wade, C. E., Salinas, J. and Holcomb, J. B. (2009) ‘Survival With Emergency Tourniquet Use to Stop Bleeding in Major Limb Trauma’, *Annals of Surgery*, 249(1), pp. 1–7.

Lajeunesse, J. W., Hankin, M., Kennedy, G. B., Spaulding, D. K., Schumaker, M. G., Neel, C. H., Borg, J. P., Stewart, S. T. and Thadhani, N. N. (2017) ‘Dynamic response of dry and water-saturated sand systems’, *Journal of Applied Physics*. American Institute of Physics Inc., 122(1), p. 015901.

Lakstein, D., Blumenfeld, A., Sokolov, T., Lin, G., Bssorai, R., Lynn, M. and Ben-Abraham, R. (2003) ‘Tourniquets for hemorrhage control on the battlefield: a 4-year accumulated experience.’, *The Journal of trauma*, 54(5 Suppl), pp. S221-5.

Le, T. D., Orman, J. A., Stockinger, Z. T., Spott, M. A., West, S. A., Mann-Salinas, E. A., Chung, K. K. and Gross, K. R. (2016) ‘The Military Injury Severity Score (mISS): A better predictor of combat mortality than Injury Severity Score (ISS)’, *Journal of Trauma and Acute Care Surgery*, 81(1), pp. 114–121.

Leibovici, D., Gofrit, O. N., Stein, M., Shapira, S. C., Noga, Y., Heruti, R. J. and Shemer, J. (1996) ‘Blast injuries: bus versus open-air bombings--a comparative study of injuries in survivors of open-air versus confined-space explosions.’, *The Journal of trauma*, 41(6), pp. 1030–5. Available at: <http://www.ncbi.nlm.nih.gov/pubmed/8970558> (Accessed: 27 July 2018).

Lendrum, R., Perkins, Z., Chana, M., Marsden, M., Davenport, R., Grier, G., Sadek, S. and Davies, G. (2019) ‘Pre-hospital Resuscitative Endovascular Balloon Occlusion of the Aorta (REBOA) for exsanguinating pelvic haemorrhage’, *Resuscitation*. Elsevier, 135, pp. 6–13.

Lewis, E. A., Pigott, M. A., Randall, A. and Hepper, A. E. (2013) ‘The development and introduction of ballistic protection of the external genitalia and perineum’, *Journal of the*

Royal Army Medical Corps. British Medical Journal Publishing Group, 159(suppl 1), pp. i15–i17.

Logan, N. J., Camman, M., Williams, G. and Higgins, C. A. (2018) ‘Demethylation of ITGAV accelerates osteogenic differentiation in a blast-induced heterotopic ossification in vitro cell culture model’, *Bone*. Elsevier Inc., 117, pp. 149–160.

Lovejoy, C. O. (2005) ‘The natural history of human gait and posture’, *Gait & Posture*, 21(1), pp. 95–112.

Major, B., Gordon, W. T., Strauss, C. J. E., Colonel, L., Andersen, R. C. and Potter, M. B. K. (2010) ‘Outcomes Associated with the Internal Fixation of Long-Bone Fractures Proximal to Traumatic Amputations’, pp. 2312–2318.

Manley, J. D., Mitchell, B. J., DuBose, J. J. and Rasmussen, T. E. (2017) ‘A Modern Case Series of Resuscitative Endovascular Balloon Occlusion of the Aorta (REBOA) in an Out-of-Hospital, Combat Casualty Care Setting.’, *Journal of special operations medicine : a peer reviewed journal for SOF medical professionals*, 17(1), pp. 1–8.

Manzano Nunez, R., Naranjo, M. P., Foianini, E., Ferrada, P., Rincon, E., García-Perdomo, H. A., Burbano, P., Herrera, J. P., García, A. F. and Ordoñez, C. A. (2017) ‘A meta-analysis of resuscitative endovascular balloon occlusion of the aorta (REBOA) or open aortic cross-clamping by resuscitative thoracotomy in non-compressible torso hemorrhage patients’, *World Journal of Emergency Surgery*. World Journal of Emergency Surgery, 12(1), pp. 1–9.

Martini, L., Fini, M., Giavaresi, G. and Giardino, R. (2001) ‘Sheep model in orthopedic research: a literature review’, *Comparative medicine*, 51(4), pp. 292–299.

Masouros, S. D., Newell, N., Ramasamy, A., Bonner, T. J., West, A. T. H., Hill, A. M., Clasper, J. C. and Bull, A. M. J. (2013) ‘Design of a Traumatic Injury Simulator for Assessing Lower Limb Response to High Loading Rates’, *Annals of Biomedical Engineering*. Springer US, 41(9), pp. 1957–1967.

- Di Masso, R. J., Silva, P. S. and Font, M. T. (2004) 'Muscle-bone relationships in mice selected for different body conformations', *Journal of Musculoskeletal Neuronal Interactions*, 4(1), pp. 41–47.
- Mazurek, M. T. and Ficke, J. R. (2006) 'The scope of wounds encountered in casualties from the global war on terrorism: From the battlefield to the tertiary treatment facility', *Journal of the American Academy of Orthopaedic Surgeons*. Lippincott Williams and Wilkins, 14(10).
- Mcfate, M. and Moreno, J. L. (2005) 'Iraq: the social context of IEDs', *Milit Rev.*, 25(June 2005), pp. 37–40.
- McKay, B. J. and Bir, C. A. (2009) 'Lower extremity injury criteria for evaluating military vehicle occupant injury in underbelly blast events.', *Stapp car crash journal*, 53, pp. 229–49. Available at: <http://www.ncbi.nlm.nih.gov/pubmed/20058557> (Accessed: 10 October 2018).
- Medical Illustration Studio - Visualmedics* (2020). Available at: <http://www.visualmedics.com/> (Accessed: 6 May 2020).
- Mellor, S. G. and Cooper, G. J. (1989) 'Analysis of 828 servicemen killed or injured by explosion in Northern Ireland 1970–84: The hostile action casualty system', *British Journal of Surgery*, 76(10), pp. 1006–1010.
- Menz, L. J. (1971) 'Structural changes and impairment of function associated with freezing and thawing in muscle, nerve, and leucocytes', *Cryobiology*. Academic Press, 8(1), pp. 1–13.
- Milenković, S. and Mitković, M. (2020) 'Pelvic Ring Injuries', *Acta facultatis medicae Naissensis*, 37(1), pp. 23–33.
- MOD (2016) 'Improvised Explosive Device (IED) events involving UK personnel on Op HERRICK in Helmand Province, Afghanistan', (November 2014), pp. 1–9. Available at: https://www.gov.uk/government/uploads/system/uploads/attachment_data/file/547686/20160823__IED__events_involving_UK_personnel_on_Op_HERRICK_in_Helmand_Province__

Afghanistan_O.pdf.

Morrison, J. J., Stannard, A., Rasmussen, T. E., Jansen, J. O., Tai, N. R. M. and Midwinter, M. J. (2013) 'Injury pattern and mortality of noncompressible torso hemorrhage in UK combat casualties', *Journal of Trauma and Acute Care Surgery*, 75(2 SUPPL. 2), pp. 263–268.

Mossadegh, S., Midwinter, M. and Parker, P. (2013) 'Developing a cumulative anatomic scoring system for military perineal and pelvic blast injuries', *Journal of the Royal Army Medical Corps*, 159(Supp I), pp. i40–i44.

Mossadegh, S., Tai, N., Midwinter, M. and Parker, P. (2012) 'Improvised explosive device related pelvi-perineal trauma: Anatomic injuries and surgical management', *Journal of Trauma and Acute Care Surgery*, 73(2 SUPPL. 1).

NATO/PfP Unclassified (2006) 'Procedures for evaluating the protection level of logistic and light armoured vehicles volume 2 for mine threat', *AEP-55*, 2(1), p. Annex C.

Nguyen, T.-T. and Masouros, S. (2019) 'Penetration of Blast Fragments to the Thorax', in *International Research Council on the Biomechanics of Injury Conference, IRCOBI*, pp. 687–688.

Nguyen, T.-T. N., Wilgeroth, J. M. and Proud, W. G. (2014) 'Controlling blast wave generation in a shock tube for biological applications', *Journal of Physics: Conference Series*. IOP Publishing, 500(14), p. 142025.

Nguyen, T.-T., Pearce, A. P., Carpanen, D., Sory, D., Grigoriadis, G., Newell, N., Clasper, J., Bull, A., Proud, W. G. and Masouros, S. D. (2018) 'Experimental platforms to study blast injury.', *Journal of the Royal Army Medical Corps*. British Medical Journal Publishing Group, p. jramc-2018-000966.

Nguyen, T. T. N., Carpanen, D., Stinner, D., Rankin, I. A., Ramasamy, A., Breeze, J., Proud,

- W. G., Clasper, J. C. and Masouros, S. D. (2020) 'The risk of fracture to the tibia from a fragment simulating projectile', *Journal of the Mechanical Behavior of Biomedical Materials*. Elsevier Ltd, 102, p. 103525.
- Nguyen, T. T. N., Tear, G. R., Masouros, S. D. and Proud, W. G. (2018) 'Fragment penetrating injury to long bones', *AIP Conference Proceedings*. American Institute of Physics Inc., 1979, pp. 090011-1–5.
- O'Sullivan, R. E. M., White, T. O. and Keating, J. F. (2005) 'Major pelvic fractures: identification of patients at high risk.', *The Journal of bone and joint surgery. British volume*, 87(4), pp. 530–3.
- Oh, J. S., Do, N. V., Clouser, M., Galarneau, M., Philips, J., Katschke, A., Clasper, J. and Kuncir, E. J. (2015) 'Effectiveness of the combat pelvic protection system in the prevention of genital and urinary tract injuries: An observational study', *Journal of Trauma and Acute Care Surgery*, 79(4), pp. S193–S196.
- Oh, J. S., Tubb, C. C., Poepping, T. P., Ryan, P., Clasper, J. C., Katschke, A. R., Tuman, C. and Murray, M. J. (2016) 'Dismounted Blast Injuries in Patients Treated at a Role 3 Military Hospital in Afghanistan: Patterns of Injury and Mortality', *Military Medicine*. Oxford University Press, 181(9), pp. 1069–1074.
- Ortega, H. H., Muñoz-De-Toro, M. M., Luque, E. H. and Montes, G. S. (2003) 'Morphological characteristics of the interpubic joint (Symphysis pubica) of rats, guinea pigs and mice in different physiological situations: A comparative study', *Cells Tissues Organs*, 173(2), pp. 105–114.
- Owens, B. D., Kragh, J. F., Wenke, J. C., Macaitis, J., Wade, C. E. and Holcomb, J. B. (2008) 'Combat Wounds in Operation Iraqi Freedom and Operation Enduring Freedom', *The Journal of Trauma: Injury, Infection, and Critical Care*, 64(2), pp. 295–299.
- Panzer, M. B., Wood, G. W. and Bass, C. R. (2014) 'Scaling in neurotrauma: How do we

- apply animal experiments to people?', *Experimental Neurology*, 261, pp. 120–126.
- Patel, J. A., White, J. M., White, P. W., Rich, N. M. and Rasmussen, T. E. (2018) 'A contemporary, 7-year analysis of vascular injury from the war in Afghanistan', *Journal of Vascular Surgery*. Mosby Inc., 68(6), pp. 1872–1879.
- Patnaik, S. S., Borazjani, A., Brazile, B., Weed, B., Christiansen, D., Ryan, P. L., van der Vaart, C. H., Damaser, M. and Liao, J. (2016) 'Pelvic Floor Biomechanics from Animal Models', in *Biomechanics of the Female Pelvic Floor*, pp. 131–148.
- Penn-Barwell, J. G., Bennett, P. M., Kay, A. and Sargeant, I. D. (2014) 'Acute bilateral leg amputation following combat injury in UK servicemen', *Injury*, 45(7), pp. 1105–1110.
- Pennal, G. F., Tile, M., Waddell, J. P. and Garside, H. (1980) 'Pelvic disruption: Assessment and Classification.', *Clinical orthopaedics and related research*, (151), pp. 12–21.
- Petitjean, A., Trosseille, X., Yoganandan, N. and Pintar, F. A. (2015) 'Normalization and Scaling for Human Response Corridors and Development of Injury Risk Curves', in *Accidental Injury*. New York, NY: Springer New York, pp. 769–792.
- Potter, B. K., Burns, T., Lacap, A., Granville, R. and Gajewski, D. (2007) 'Heterotopic Ossification Following Traumatic and Combat-Related Amputations: Prevalence, Risk Factors, and Preliminary Results of Excision', pp. 476–486.
- Quenneville, C. E., McLachlin, S. D., Greeley, G. S. and Dunning, C. E. (2011) 'Injury tolerance criteria for short-duration axial impulse loading of the isolated tibia', *Journal of Trauma*, 70(1), pp. E13–E18.
- Ramasamy, A., Evans, S., Kendrew, J. M. and Cooper, J. (2012) 'The open blast pelvis: The significant burden of management', *The Bone & Joint Journal*, 94-B(6), pp. 829–835.
- Ramasamy, A., Hill, A. M. and Clasper, J. C. (2009) 'Improvised explosive devices: pathophysiology, injury profiles and current medical management.', *Journal of the Royal*

Army Medical Corps, 155(4), pp. 265–272.

Ramasamy, A., Hill, A. M., Hepper, A. E., Bull, A. M. and Clasper, J. C. (2009) ‘Blast mines: physics, injury mechanisms and vehicle protection.’, *Journal of the Royal Army Medical Corps*. British Medical Journal Publishing Group, pp. 258–264.

Ramasamy, A., Hill, A. M., Phillip, R., Gibb, I., Bull, A. M. J. and Clasper, J. C. (2011) ‘The Modern “Deck-Slap” Injury—Calcaneal Blast Fractures From Vehicle Explosions’, *The Journal of Trauma: Injury, Infection, and Critical Care*, 71(6), pp. 1694–1698.

Ramasamy, A., Hill, A., Masouros, S., Gibb, I., Bull, A. M. J. and Clasper, J. C. (2011) ‘Blast-related fracture patterns: A forensic biomechanical approach’, *Journal of the Royal Society Interface*, 8(58), pp. 689–698.

Randjbaran, E. (2013) ‘The Effects of Stacking Sequence Layers of Hybrid Composite Materials in Energy Absorption under the High Velocity Ballistic Impact Conditions: An Experimental Investigation’, *Journal of Material Science & Engineering*. OMICS Publishing Group, 02(04).

Rankin, I. A., Nguyen, T. T., Carpanen, D., Clasper, J. C. and Masouros, S. D. (2019) ‘Restricting Lower Limb Flail is Key to Preventing Fatal Pelvic Blast Injury’, *Annals of Biomedical Engineering*, 47(11), pp. 2232–2240.

Rankin, I. A., Webster, C. E., Gibb, I., Clasper, J. C. and Masouros, S. D. (2020) ‘Pelvic injury patterns in blast’, *Journal of Trauma and Acute Care Surgery*. Ovid Technologies (Wolters Kluwer Health), 88(6), pp. 832–838.

Rappold, J. F. and Bochicchio, G. V. (2016) ‘Surgical adjuncts to noncompressible torso hemorrhage as tools for patient blood management’, *Transfusion*, 56(April), pp. S203–S207.

Redlich, K., Görtz, B., Hayer, S., Zwerina, J., Kollias, G., Steiner, G., Smolen, J. S. and Schett, G. (2004) ‘Overexpression of tumor necrosis factor causes bilateral sacroiliitis’,

Arthritis & Rheumatism. Wiley-Blackwell, 50(3), pp. 1001–1005.

Report of the Army Dismounted Complex Blast Injury Task Force (2011) ‘Dismounted Complex Blast Injury. Report of the Army Dismounted Complex Blast Injury Task Force’, Available at <http://www.dtic.mil/docs/citations/ADA550676>; accessed October 10th 2018.

Available at: <http://www.dtic.mil/docs/citations/ADA550676> (Accessed: 10 October 2018).

Richmond, D., Glare, V., Goldizen, V. and Pratt, D. (1961) ‘A shock tube utilized to produce sharp-rising overpressures of 400 milliseconds duration and its employment in biomedical experimentation’, *Aerospace Med*, 32, pp. 997–1008. Available at:

<https://apps.dtic.mil/dtic/tr/fulltext/u2/279670.pdf> (Accessed: 15 May 2019).

Richmond, D., Goldizen, V., Clare, V. and White, C. (1962) ‘The overpressure-duration relationship and lethality in small animals’, *Technical Progress Report DASA-1325, Defence Atomic Support Agency, Department of Defense, U.S. Government*. Available at:

<https://apps.dtic.mil/docs/citations/AD0403504>.

Richmond, D. R., Goldzien, V. C., Clare, V. R., Pratt, D. E., Shering, F., SANCHEZ, R. T., Fischer, C. C. and White, C. S. (1962) ‘The biologic response to overpressure. III. Mortality in small animals exposed in a shock tube to sharp-rising overpressures of 3 to 4 msec duration.’, *Aerospace medicine*, 33, pp. 1–27. Available at:

<http://www.ncbi.nlm.nih.gov/pubmed/14492014>.

Richmond, D., Wetherbe, M. and Tadorelli, R. (1959) ‘Shock tube studies of the effects of sharp-rising, long-duration overpressures on biological systems’, *USAEC Report, TID6056, Office of Technical Services, Department of Commerce*. Available at:

<https://apps.dtic.mil/docs/citations/ADA385368> (Accessed: 15 May 2019).

Ring, W., JW, B. and FR, N. (1975) ‘USAF noncombat ejection experience 1968-1973: incidence, distribution, significance and mechanism of flail injury’, *In: Glaister DH, editor. Biodynamic response to windblast. Toronto/London: NATO Advisory Group for Aerospace*

Research and Development (AGARD); pp. B1–8.

Risling, M., Davidsson, J., Long, J., Reed Army, W., Laura Schaefer, M. and Wester, B. (2012) ‘Experimental animal models for studies on the mechanisms of blast-induced neurotrauma’.

Rodriguez, C. J., Weintrob, A. C., Shah, J., Malone, D., Dunne, J. R., Weisbrod, A. B., Lloyd, B. A., Warkentien, T. E., Murray, C. K., Wilkins, K., Shaikh, F., Carson, M. L., Aggarwal, D., Tribble, D. R. and Infectious Disease Clinical Research Program Trauma Infectious Disease Outcomes Study Group (2014) ‘Risk Factors Associated with Invasive Fungal Infections in Combat Trauma’, *Surgical Infections*, 15(5), pp. 521–526.

Rodriguez, C., Weintrob, A. C., Dunne, J. R., Weisbrod, A. B., Lloyd, B., Warkentien, T., Malone, D., Wells, J., Murray, C. K., Bradley, W., Shaikh, F., Shah, J., Carson, M. L., Aggarwal, D. and Tribble, D. R. (2014) ‘Clinical relevance of mold culture positivity with and without recurrent wound necrosis following combat-related injuries’, *Journal of Trauma and Acute Care Surgery*, 77(5), pp. 769–773.

Rosenberg, K. R. (1992) ‘The Evolution of Modern Human Childbirth’, *YEARBOOK OF PHYSICAL ANTHROPOLOGY*, 3589124. Available at:
<https://onlinelibrary.wiley.com/doi/pdf/10.1002/ajpa.1330350605> (Accessed: 28 March 2018).

Russell, R., Hunt, N. and Delaney, R. (2014) ‘The Mortality Peer Review Panel: a report on the deaths on operations of UK Service personnel 2002-2013.’, *Journal of the Royal Army Medical Corps*. British Medical Journal Publishing Group, 160(2), pp. 150–4.

Ruth, E. (1932) ‘A study of the development of the mammalian pelvis.pdf’.

Sathy, A. K., Starr, A. J., Smith, W. R., Elliott, A., Agudelo, J., Reinert, C. M. and Minei, J. P. (2009) ‘The effect of pelvic fracture on mortality after trauma: An analysis of 63,000 trauma patients’, *Journal of Bone and Joint Surgery - Series A*.

- Satoh, Y., Sato, S., Saitoh, D., Tokuno, S., Hatano, B., Shimokawaji, T., Kobayashi, H. and Takishima, K. (2010) 'Pulmonary blast injury in mice: A novel model for studying blast injury in the laboratory using laser-induced stress waves', *Lasers in Surgery and Medicine*, 42(4), pp. 313–318.
- Saunders, C. and Carr, D. (2018) 'Towards developing a test method for military pelvic protection', *The Journal of The Textile Institute*. Taylor & Francis, pp. 1–7.
- Schmal, H., Markmiller, M., Mehlhorn, A. T. and Sudkamp, N. P. (2005) 'Epidemiology and outcome of complex pelvic injury.', *Acta orthopaedica Belgica*, 71(1), pp. 41–7. Available at: <http://www.ncbi.nlm.nih.gov/pubmed/15792206> (Accessed: 14 February 2019).
- Schultz, A. H. (1949) 'Sex differences in the pelves of primates', *American Journal of Physical Anthropology*. Wiley-Blackwell, 7(3), pp. 401–424.
- Shi, S., Ciurli, C., Cartman, A., Pidoux, I., Poole, A. R. and Zhang, Y. (2003) 'Experimental immunity to the G1 domain of the proteoglycan versican induces spondylitis and sacroiliitis, of a kind seen in human spondylarthropathies.', *Arthritis and rheumatism*, 48(10), pp. 2903–15.
- Simpson, S. W., Quade, J., Levin, N. E., Butler, R., Dupont-Nivet, G. and Everett, M. (2008) 'A Female Homo erectus Pelvis from Gona, Ethiopia'. Available at: <http://science.sciencemag.org/content/sci/322/5904/1089.full.pdf> (Accessed: 28 March 2018).
- Singleton, J. A. G., Gibb, I. E., Bull, A. M. J. and Clasper, J. C. (2014) 'Blast-mediated traumatic amputation: evidence for a revised, multiple injury mechanism theory.', *Journal of the Royal Army Medical Corps*. British Medical Journal Publishing Group, 160(2), pp. 175–9.
- Singleton, J. A. G., Gibb, I. E., Hunt, N. C. A., Bull, A. M. J. and Clasper, J. C. (2013) 'Identifying future “unexpected” survivors: a retrospective cohort study of fatal injury patterns in victims of improvised explosive devices.', *BMJ open*. British Medical Journal

Publishing Group, 3(8), p. e003130.

Sinha, R., Van Den Heuvel, W. J. A. and Arokiasamy, P. (2011) 'Factors affecting quality of life in lower limb amputees', *Prosthetics and Orthotics International*. Prosthet Orthot Int, 35(1), pp. 90–96.

Smith, S., White, J., Wanis, K. N., Beckett, A., McAlister, V. C. and Hilsden, R. (2018) *The effectiveness of junctional tourniquets*, *Journal of Trauma and Acute Care Surgery*.

Smith, W., Williams, A., Agudelo, J., Shannon, M., Morgan, S., Stahel, P. and Moore, E. (2007) 'Early predictors of mortality in hemodynamically unstable pelvis fractures.', *Journal of orthopaedic trauma*, 21(1), pp. 31–7.

Standring, S. (2016) *Gray's anatomy : the anatomical basis of clinical practice*. Elsevier Inc.

Stannard, A., Morrison, J. J., Scott, D. J., Ivatury, R. A., Ross, J. D. and Rasmussen, T. E. (2013) 'The epidemiology of noncompressible torso hemorrhage in the wars in Iraq and Afghanistan', *Journal of Trauma and Acute Care Surgery*. J Trauma Acute Care Surg, 74(3), pp. 830–834.

Steinetz, B. G., O'Byrne, E. M., Butlet, M. C. and Hickman, L. B. (1983) 'Hormonal regulation of the connective tissue of the symphysis pubis', in *Biology of relaxin and its role in the human*, pp. 71–92.

Stemper, B. D., Yoganandan, N., Baisden, J. L., Umale, S., Shah, A. S., Shender, B. S. and Paskoff, G. R. (2015) 'Rate-dependent fracture characteristics of lumbar vertebral bodies', *Journal of the Mechanical Behavior of Biomedical Materials*. Elsevier Ltd, 41, pp. 271–279.

Stuhmiller, J. H., Phillips, Y. Y. and Richmond, D. R. (1991) 'The Physics and Mechanisms of Primary Blast Injury', *Conventional Warfare Ballistic, Blast and Burn Injuries*, p. pp.241 – 270.

Sundaramurthy, A., Alai, A., Ganpule, S., Holmberg, A., Plougouven, E. and Chandra, N.

(2012) ‘Blast-Induced Biomechanical Loading of the Rat: An Experimental and Anatomically Accurate Computational Blast Injury Model’, *Journal of Neurotrauma*. Mary Ann Liebert, Inc. 140 Huguenot Street, 3rd Floor New Rochelle, NY 10801 USA , 29(13), pp. 2352–2364.

Taylor, C., Hettiaratchy, S., Jeffery, S. L., Evriviades, D. and Kay, A. (2009) ‘Contemporary Approaches To Definitive Extremity Reconstruction Of Military Wounds’, *Article in Journal of the Royal Army Medical Corps*.

Thurman, J. T. (2017) *Practical Bomb Scene Investigation, Third Edition*. CRC Press.

Tile, M. (1996) ‘Acute Pelvic Fractures: I. Causation and Classification’, *Journal of the American Academy of Orthopaedic Surgeons*, 4(3), pp. 143–151.

TNO Defence Security and Safety, T. (2020) *Blast Testing and Data Acquisition | TNO*. Available at: <https://www.tno.nl/en/focus-areas/defence-safety-security/roadmaps/protection-munitions-weapons/world-class-ballistics-research/blast-testing-and-data-acquisition/> (Accessed: 3 April 2020).

Tremblay, J., Bergeron, D. and Gonzalez, R. (1998) ‘KTA1-29: Protection of Soft-Skinned Vehicle Occupants from Landmine Effects. In: Program TTCP, editor’, *Val- Belair, Canada: Defence Research Establishment Valcartier, Quebec, Canada*.

Treuting, P. M., Dintzis, S. M. and Montine, K. S. (2018) *Comparative anatomy and histology : a mouse, rat, and human atlas*. 2nd edn.

Trevathan, W. (2015) ‘Primate pelvic anatomy and implications for birth’, *Philosophical Transactions of the Royal Society B: Biological Sciences*, 370(1663), pp. 20140065–20140065.

Tully, C. C., Romanelli, A. M., Sutton, D. A., Wickes, B. L. and Hospenthal, D. R. (2009) ‘Fatal *Actinomucor elegans* var. *kuwaitiensis* Infection following Combat Trauma’, *Journal*

of Clinical Microbiology, 47(10), pp. 3394–3399.

Turégano-Fuentes, F., Caba-Doussoux, P., Jover-Navalón, J. M., Martín-Pérez, E., Fernández-Luengas, D., Díez-Valladares, L., Pérez-Díaz, D., Yuste-García, P., Guadalajara Labajo, H., Ríos-Blanco, R., Hernando-Trancho, F., García-Moreno Nisa, F., Sanz-Sánchez, M., García-Fuentes, C., Martínez-Virto, A., León-Baltasar, J. L. and Vazquez-Estévez, J. (2008) ‘Injury Patterns from Major Urban Terrorist Bombings in Trains: The Madrid Experience’, *World Journal of Surgery*, 32(6), pp. 1168–1175.

Uderhardt, S., Diarra, D., Katzenbeisser, J., David, J.-P., Zwerina, J., Richards, W., Kronke, G. and Schett, G. (2010) ‘Blockade of Dickkopf (DKK)-1 induces fusion of sacroiliac joints.’, *Annals of the rheumatic diseases*. BMJ Publishing Group Ltd, 69(3), pp. 592–7.

Valerio, I. L., Sabino, P. J., Mundinger, G. S. and Kumar, A. (2014) ‘From Battleside to Stateside The Reconstructive Journey of Our Wounded Warriors’, 72(May), pp. 38–45.

Vogel, E. W., Panzer, M. B., Morales, F. N., Varghese, N., Bass, C. R., Meaney, D. F. and Morrison, B. (2019) ‘Direct Observation of Low Strain, High Rate Deformation of Cultured Brain Tissue During Primary Blast’, *Annals of Biomedical Engineering*. Springer, 48(4), pp. 1196–1206.

Webster, C. E. (2017) *The Blast Pelvis (Doctoral dissertation)*. Imperial College London. Available at: <https://spiral.imperial.ac.uk/handle/10044/1/65755>.

Webster, C. E., Clasper, J., Gibb, I. and Masouros, S. D. (2018) ‘Environment at the time of injury determines injury patterns in pelvic blast.’, *Journal of the Royal Army Medical Corps*. British Medical Journal Publishing Group, p. jramc-2018-000977.

Webster, Clasper, J., Stinner, D. J., Eliahoo, J. and Masouros, S. D. (2018) ‘Characterization of Lower Extremity Blast Injury’, *Military Medicine*. Oxford University Press, 183(9–10), pp. e448–e453.

Wedmore, I., McManus, J. G., Pusateri, A. E. and Holcomb, J. B. (2006) 'A Special Report on the Chitosan-based Hemostatic Dressing: Experience in Current Combat Operations', *The Journal of Trauma: Injury, Infection, and Critical Care*, 60(3), pp. 655–658.

White, R. and Churchill, E. (1971) 'The Body Size of Soldiers U.S. Army Anthropometry. Report Number 72-51-CE (CPLSEL-94), U.S. Army Natick Laboratories, Natick, MA.'

Williams, M. and Jezior, J. (2013) 'Management of combat-related urological trauma in the modern era', *Nature Reviews Urology*. Nature Publishing Group, 10(9), pp. 504–512.

Wisner, D. H., Victor, N. S. and Holcroft, J. W. (1993) 'Priorities in the management of multiple trauma: intracranial versus intra-abdominal injury.', *The Journal of trauma*, 35(2), pp. 271–6; discussion 276-8. Available at: <http://www.ncbi.nlm.nih.gov/pubmed/8355308> (Accessed: 8 February 2019).

Yoganandan, N., Banerjee, A., Hsu, F.-C., Bass, C. R., Voo, L., Pintar, F. A. and Gayzik, F. S. (2016) 'Deriving injury risk curves using survival analysis from biomechanical experiments', *Journal of Biomechanics*. Elsevier, 49(14), pp. 3260–3267.

Yoganandan, N., Pintar, F. A., Boynton, M., Begeman, P., Prasad, P., Kuppa, S., Morgan, R. M. and Eppinger, R. (1996) 'Dynamic Axial Tolerance of the Human Foot-Ankle Complex', in *40th Stapp Car Crash Conference*, pp. 207–218.

Yoganandan, N., Stemper, B. D., Baisden, J. L., Pintar, F. A., Paskoff, G. R. and Shender, B. S. (2015) 'Effects of acceleration level on lumbar spine injuries in military populations', *Spine Journal*. Elsevier Inc., 15(6), pp. 1318–1324.

Zhang, Y. (2003) 'Animal models of inflammatory spinal and sacroiliac joint diseases.', *Rheumatic diseases clinics of North America*. Elsevier, 29(3), pp. 631–45.

Zuckerman, S. (1941) *DISCUSSION ON THE PROBLEM OF BLAST INJURIES*, *Proceedings of the Royal Society of Medicine*. Available at:

<http://journals.sagepub.com/doi/pdf/10.1177/003591574103400305> (Accessed: 29 July 2018).